The role of the Arabidopsis AHL15/REJUVENATOR gene in developmental phase transitions

Karami, O.; Karami O.

The role of the *Arabidopsis AHL15*/*REJUVENATOR* gene in developmental phase transitions

Omid Karami

Omid Karami

The role of the *Arabidopsis AHL15*/*REJUVENATOR* gene in developmental phase transitions

PhD Thesis, Leiden University, 2017

This work was performed in the Molecular and Developmental Genetics department at the Institute of Biology Leiden of Leiden University, The Netherlands, and was partially supported by Iranian Ministry of Science, Research, and Technology (Grant MSRT 89100156 to O.K.).

Cover designed by Omid Karami

Printed by Gildeprint, Enschede, The Netherlands

The role of the *Arabidopsis AHL15*/*REJUVENATOR* gene in developmental phase transitions

Proefschrift

Ter verkrijging van
de graad van Doctor aan de Universiteit Leiden,
op gezag van de Rector Magnificus Prof. Mr. C.J.J.M. Stolker,
volgens besluit van het College voor Promoties
te verdedigen op dinsdag 5 september 2017
klokke 12.30 uur

door

Omid Karami
Geboren te Divandareh, Iran
23th September 1977

Promotiecommissie

Promotor:	Prof. dr. R. Offringa
Overige leden:	Prof. dr. H.P. Spaink
	Prof. dr. P.J.J. Hooykaas
	Prof. dr. V. van Noort (KU Leuven)
	Dr. M.C.G. Proveniers (Utrecht University)
	Dr. P. Fransz (University of Amsterdam)

To my dear wife

Contents

Chapter 1

General introduction

The genetic basis of developmental phase transitions in plants

Omid Karami[1] and Remko Offringa[1]

[1]Plant Developmental Genetics, Institute of Biology Leiden, Leiden University, Sylviusweg 72, 2333 BE Leiden, Netherlands

Summary

Flowering plants display a wide range of life spans, varying from a few weeks for some annual species up to several thousand years for some perennial species, such as the sequoia trees. Related to their life span, they have evolved two opposing growth habits. Many species are monocarpic, as their life cycle is completed after flowering and producing offspring once, even under optimal growth conditions. By contrast, polycarpic plants flower and reproduce more than once during their life history and are able to survive multiple successful offspring production events. All annual plants are monocarpic, but not all perennial plants are polycarpic. Some perennial plants grow for several years, but as they still die after flowering and seed set these plants are in fact monocarpic.

Both annual and perennial plants undergo several distinct developmental phases during their life history. Studies in annual and perennial species have shown that these developmental phase transitions are tightly linked to orchestration of gene expression in response to environmental cues such as light intensity and quality, day length, nutrient availability, and temperature. Recent advances in plant molecular biology have provided new insights in genetic pathways and molecular mechanisms that trigger or modulate developmental phase transitions in plants. In this chapter we will present and discuss our current knowledge these mechanisms with a focus on those pathways that distinguish monocarpic from the polycarpic life history strategy.

Introduction

Like all multicellular organisms, plants undergo several distinct developmental phase transitions, starting with embryogenesis, and subsequently progressing from the juvenile vegetative and the adult vegetative to the adult reproductive and the gametophyte phase (Fig. 1). During this last phase, the male and female gametophytes are produced, respectively pollen grains carrying two sperm cells and the embryo sac containing the egg cell and two polar nuclei. Fertilization of the egg cell by one of the sperm cells forms a diploid zygote, and fusion of the other sperm cell with the polar nuclei forms a triploid nucleus. The zygotic cell will undergo multiple rounds of cell division, eventually forming the embryo in which the basic body plan of a plant is laid down, comprising a root apical meristem (RAM), a shoot apical meristem (SAM), a hypocotyl, cotyledons and vascular tissue (Fig. 1). By simultaneous nuclear divisions of the triploid nucleus the endosperm is formed, which is important for seed growth as it generates space and is a source of hormones and nutrients for the growing embryo (Baroux et al., 2007; Locascio et al., 2014). In *Arabidopsis*, the nutrients in the endosperm eventually become absorbed by the cotyledons during seed maturation, whereas in other plants the endosperm is maintained as energy provider during seed germination and the initial development of the seedling (Sabelli and Larkins, 2009). Postembryonic development of the plant starts with the vegetative phase, during which the SAM produces leaves and side branches and the RAM allows the root to grow and to subsequently branch by forming lateral roots. The vegetative growth is considered into two distinct phases, the juvenile phase during which the plant is not competent to flower, and the

adult phase in which plants have acquired the competence to flower (Huijser and Schmid, 2011). In some plants the transition between the juvenile and the adult phase, also referred to as the vegetative phase change, is marked by a distinguishable change in leaf morphology (heteroblasty) (Zotz et al., 2011). Upon acquisition of reproductive ability, the SAM becomes an inflorescence meristem that produces bract and flowers containing the reproductive organs. Below we will discuss the phases of plant development in more detail, with a focus on the changes that occur during the phase transitions (Bäurle and Dean, 2006; Huijser and Schmid, 2011; Poethig, 2013).

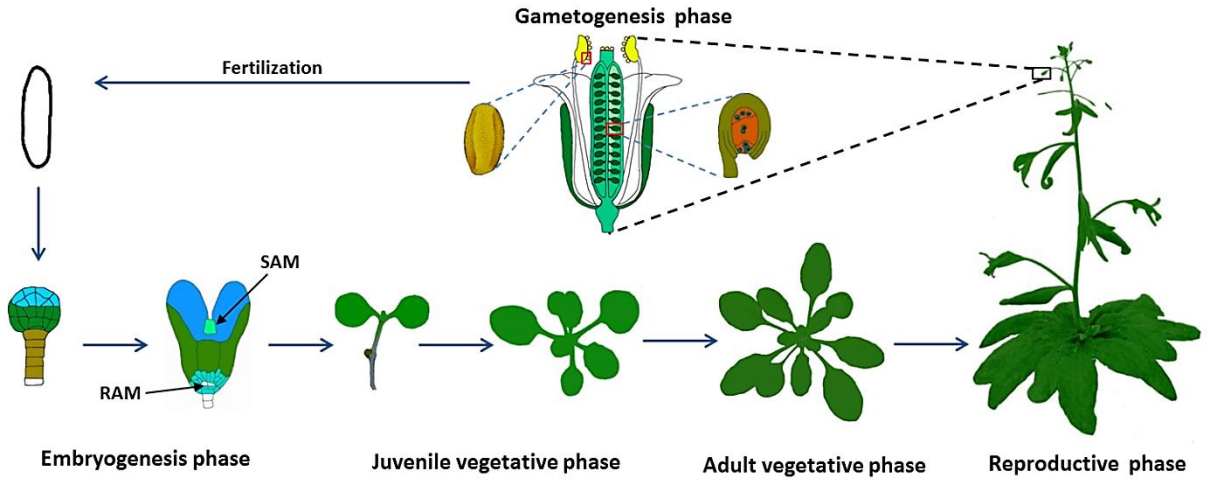

Figure 1. Developmental phase transitions during the life cycle of *Arabidopsis thaliana*. After fertilization, the basic body plan of the plant is laid down during embryogenesis, including the shoot and root apical meristem (resp. SAM and RAM). The subsequent germination of the seedling starts the vegetative phase, during which the SAM and RAM are responsible for organ formation, resulting in the shoot and root system. In the juvenile vegetative phase, plants are incompetent to flower, whereas plants in the adult vegetative phase have gained reproductive competency. *Arabidopsis* is a typical heteroblastic plant where juvenile and adult leaves show clear morphological differences. With the increasing number of leaves, the juvenile plant enters into the adult vegetative phase and acquires the competence to flower. During the change from the adult vegetative to the reproductive phase, the SAM becomes an inflorescence meristem that produces flowers and bracts instead of rosette leaves. As the flowers mature, the plant enters the gametogenesis phase, during which male and female gametes are formed within the flowers. The subsequent successful fusion of these gametes during fertilization starts the next life cycle with the development of the embryo from the zygote (for review see Bäurle and Dean, 2006; Huijser and Schmid, 2011; Poethig, 2013).

Embryogenesis

The first phase of a plant's life starts with the fusion of the male and female gametes during fertilization to generate the zygote. This developmental switch, which is defined as gametophyte-to-zygotic transition, coincides with one of the most complex cellular reprogramming events, transforming the highly specialized meiotically programmed egg cell into a totipotent mitotically active embryonic cell (Pillot et al., 2010; She and Baroux, 2014). The gametophyte-to-zygotic transition has been shown to be accompanied by erasing and re-establishment of genomic imprinting (Raissig et al., 2013), by reprogramming of epigenetic information (Jullien, 2010; Wollmann, 2012) and by rapid removal and replacement of gametic Histon3.3 variants (Ingouff et al., 2010). However, how the zygotic cell acquires totipotency remains largely unknown.

Plant embryogenesis has been best-studied in the model dicot *Arabidopsis thaliana*. The first division of the zygote is asymmetric, giving rise to a smaller apical and a larger basal cell. By a subsequent series of symmetric and asymmetric cell divisions, which in *Arabidopsis* occur in an extremely ordered fashion compared to other plant species, the apical cell gives rise to the embryo proper that develops through a morphological series from globular, heart, and torpedo to the final bent cotyledon stage. In *Arabidopsis*, embryogenesis ends by accumulation of proteins, starch, and lipids in the cotyledons and eventually by desiccation of the embryo. In contrast to the apical cell, the basal cell only undergoes a limited number of symmetric cell divisions forming the suspensor, a row of cells that connects the embryo to the maternal tissue. At the early globular stage, the most apical suspensor cell is recruited to the basal side of the embryo proper to become the hypophysis, the founder cell of the RAM. Simultaneously, the SAM is established at the apical side of the embryo, and the subsequent initiation of the cotyledon primordia induces a change in embryo morphology from globular-shaped with radial symmetry to heart-shaped with bilateral symmetry (Jenik et al., 2007). The highly organized cell divisions, cell fate specification, and cell-cell communication that lead to apical-basal and radial patterning during plant embryogenesis are controlled by embryo-specific transcription factors, hormonal gradients, and signaling components (Lau et al., 2012; Hove et al., 2015). Below we will discuss the role of several key transcription factors and the plant hormones auxin and cytokinin.

Genetic studies have revealed that the WUSCHEL RELATED HOMEOBOX (WOX) transcription factor family (van Der Graaff et al., 2009) plays an important role in determining cell identity during early embryo patterning (Jenik et al., 2007; Breuninger et al., 2008; Ueda et al., 2011). The asymmetric division of the zygote is critical for the formation of the apical-basal body axis, and the *WOX2/8/9* genes that are co-expressed in the zygote play an important role in this first step. After this asymmetric division, *WOX2* expression becomes restricted to the apical cell lineage, while *WOX8/9* remain expressed in the basal cell lineage (Breuninger et al., 2008; Ueda et al., 2011). The *Arabidopsis wox2/8/9* mutants display an abnormal asymmetric division of the zygote and distorted embryo development (Breuninger et al., 2008; Ueda et al., 2011).

The establishment of the RAM by hypophysis specification during early embryogenesis is first determined by a transient overlap of auxin and cytokinin signaling, which then separates into a distal auxin domain and a proximal cytokinin domain (Efroni et al., 2016). The auxin domain is required for hypophysis fate, as mutants in genes that cause defects in auxin biosynthesis, transport, perception or response are all impaired in hypophysis division and formation (Jenik et al., 2007; Mo and Weijers, 2009; Wabnik et al., 2013).

The SAM and RAM are established during early embryogenesis by small populations of cells, called the organizing-centers. The earliest genes expressed in these shoot and root organizing-centers are respectively *WUSCHEL* (*WUS*) and *WOX5* (Mayer et al., 1998; Sarkar et al., 2007). Both WUS and WOX5 homeodomain-like transcription factors have been implicated in shoot and root stem-cell maintenance, respectively (Mayer et al., 1998; Haecker et al., 2004). In addition, serval members of the APETALA2/Ethylene Responsive Factor (AP2/ERF) transcription factor family, such as *BABY BOOM* (*BBM*) and the *PLETHORA* (*PLT*) genes *PLT1* and *PLT2*, *PLT3* have been shown to be required for root stem cell formation and embryo development (Galinha et al., 2007). These genes are expressed during

early embryogenesis, where they are involved in maintaining cell division and preventing differentiation of embryogenic stem cells in a concentration-dependent manner (Boutilier et al., 2002; Galinha et al., 2007; Rybel et al., 2015). In *Arabidopsis*, mutations in these genes cause defects in root stem cell maintenance, leading to a severe rootless phenotype (Galinha et al., 2007).

The establishment of the protodermal cell layer during the transition from the 8- to the 16-cell embryo requires the expression of the homeodomain leucine zipper class IV (HD-ZIP IV) transcription factors ARABIDOPSIS THALIANA MERISTEM LAYER1 (ATML1) and its closest homologue PROTODERMAL FACTOR2 (PDF2) (Brambilla et al., 2014). The corresponding genes are specifically expressed in the protoderm and promote epidermal cell differentiation (Abe et al., 2003; Jenik et al., 2007; Takada and Jürgens, 2007). *atml1* and *pdf2* double mutants show severe embryo epidermal defects that lead to embryo lethality (Abe et al., 2003). *AtML1* expression is not restricted to early embryogenesis. The gene remains expressed in the developing epidermis of the embryo (Takada and Jürgens, 2007) and, subsequently, in the L1 layer of the SAM and leaf primordia (Takada et al., 2013). Both *AtML1* and *PDF2* maintain their expression in epidermal cells by binding to their own promoter (Takada and Jürgens, 2007).

Embryo morphogenesis and maturation is regulated by the B3 domain factors LEAFY COTYLEDON2 [LEC2], FUSCA3 [FUS3], and ABSCISIC ACID INSENSITIVE3 [ABI3]) and LEC1. B3 domain factors are related to the HAP3 subunit of the CCAAT binding factor family (Braybrook and Harada, 2008), and their corresponding genes are specifically expressed during embryogenesis (Santos-Mendoza et al., 2008). The *lec1, lec2,* and *fus3* loss-of-function mutants show defects in embryo identity, as embryos enter post-germination developmental programs such as the formation of trichomes on cotyledons. Moreover, *lec1* and *lec2* mutant embryos do not acquire dessication tolerance and have defects in accumulation of seed storage products (Santos-Mendoza et al., 2008). It has been shown that *LEC* genes control embryonic cell fate by modulating sucrose levels and auxin responses to promote cell division and embryonic maturation (Casson and Lindsey, 2006; Stone et al., 2008).

The plant hormone auxin contributes to a wide range of physiological and developmental processes (Teale et al., 2006; Vanneste and Friml, 2009), including most embryo pattern formation steps, such as embryonic axis formation, stem cell establishment, hypophysis establishment, and vascular patterning (Peer et al., 2011; Mo and Weijers, 2009; Wabnik et al., 2013; Hove et al., 2015). Auxin is not produced in all plant cells but after local biosynthesis in certain cells or tissues it is distributed to specific sites of the plant body by polar cell to cell transport by PIN-FORMED (PIN) auxin efflux carriers (Friml et al., 2003; Friml, 2010). PIN proteins determine the direction of polar auxin transport (PAT) through their asymmetric localization at the plasma membrane (Friml et al., 2003; Friml, 2010). In addition, the AUXIN1/LIKE-AUX1 (AUX/LAX) influx carriers are important drivers of PAT by mediating efficient uptake of auxin by cells and thus increasing the amount of auxin available for polar efflux by the PIN proteins (Bainbridge et al., 2008; Péret et al., 2012; Boot et al., 2016). The organized spatial expression and localization pattern of PIN and AUX/LAX carriers directs the differential accumulation of auxin in plant tissues (Kierzkowski et al.,

2013). It is well established now that PAT plays a crucial role in embryo pattern formation, (Jenik et al., 2007; Mo and Weijers, 2009; Wabnik et al., 2013).

Detailed insight toward understanding of the molecular basis of auxin signaling in embryogenesis has revealed several molecular pathways of auxin action (Rybel et al., 2015; Mironova et al., 2017), but the main auxin signaling pathway is through the TRANSPORT INHIBITOR RESPONSE1/AUXIN SIGNALING F-BOX (TIR1/AFB) proteins (Smit and Weijers, 2015; Mironova et al., 2017). The TIR1/AFB F-box proteins control the activity of AUXIN RESPONSE FACTORs (ARFs) that bind to cis-regulatory auxin response elements in target gene promoters (Guilfoyle and Hagen, 2007; Boer et al., 2014). Under low auxin levels, Auxin/INDOLE-3-ACETIC ACID (Aux/IAA) proteins bind and repress the activity of ARF proteins (Guilfoyle and Hagen, 2007). When auxin levels are increased, the TIR1/AFBs use auxin as molecular glue to recruit the Aux/IAA proteins to the Skp1-Cullin-F-box (SCF) E3 ubiquitin ligase complex. Following their ubiquitination, Aux/IAA proteins are degraded by the 26S proteasome, thereby allowing ARFs to activate transcription of their target genes (Dharmasiri et al., 2005; Kepinski and Leyser, 2005; dos Santos Maraschin et al., 2009; Mironova et al., 2017). The auxin signal transduction through ARFs/Aux/IAAs has been shown to play an important role in embryonic vascular tissue formation and the establishment of the embryonic RAM (Hove et al., 2015; Rybel et al., 2015). Embryogenesis ends with maturation and desiccation of the embryo, a phase during which in dicot species the endosperm is consumed and used as energy source for the final growth and maturation of the embryo (Lopes and Larkins, 1993). The hormone abscisic acid (ABA) plays an important role in this final phase of embryogenesis and it keeps the embryo dormant in the desiccated seed, whereas antagonistically acting gibberellins (GAs) promote embryo germination and development into a seedling (Santos-Mendoza et al., 2008; Rajjou et al., 2012). Embryo maturation and seed germination are developmental phase transitions involving complex regulatory mechanisms that have been extensively reviewed elsewhere (Rajjou et al., 2012), but are beyond the scope of this Chapter and will therefore not be discussed here.

The vegetative phase change

When seeds are germinated in the light, the seedling undergoes a developmental program referred to as photomorphogenesis, involving the production of chlorophyll and the onset of photosynthesis in the shoot part, the initiation of the first leaves by the SAM and the onset of root growth mediated by the RAM followed by the production of lateral roots (Weitbrecht et al., 2011). This first phase of post-embryonic plant development is referred to as the juvenile phase, and it is only after transition to the adult phase that the plant becomes competent to flower and to reproduce (Huijser and Schmid, 2011). The transition from juvenile-to-adult phase in plants is generally marked by morphological changes such as the position (phyllotaxis) and the timing (plastochron) between leaf initiation events, and the changes in leaf size and shape, trichome distribution and cell size, and internode length. This results in the appearance of both juvenile and adult leaves on the same plant, a situation also known as heteroblasty (Huijser and Schmid, 2011). Although a wide range of flowering plant species show morphological changes during their vegetative growth, the classical heteroblasty can be

most clearly observed in perennial woody plants that have a long juvenile period. In these plants, the heteroblastic changes can be simply followed, but limited genetic and molecular resources and the long generation time of such plants has for a long time limited our understanding of the molecular basis of heteroblasty (Zotz et al., 2011; Huijser and Schmid, 2011). Recently, some progress has been made in poplar (Hsu et al., 2011; Wang et al., 2011), but most biological studies on heteroblasty have focused on model annuals that show clear heteroblastic changes during the vegetative phase change. In *Arabidopsis* grown under 16 hours photoperiod, the vegetative phase change typically occurs following the production of six to eight juvenile leaves. Juvenile leaves in *Arabidopsis* are small and round, and have smooth margins, long petioles and they do not carry trichomes on their abaxial side. In contrast, the adult leaves are bigger and have short petioles, smaller cells and elongated blades with serrated margins (Telfer et al., 1997). The juvenile leaves in maize are short, covered with wax, and lack epidermal hairs, whereas the adult leaves are long and narrow, lack wax and have epidermal hairs (Usami et al., 2009a).

Like for all developmental phase transitions, environmental cues have a high impact on the juvenile-to-adult phase transition. The photoperiod, light intensity, and ambient temperature have all been shown to influence the juvenile phase, but the photoperiod is the most important environmental cue that determines the timing of the juvenile-to-adult transition (Huijser and Schmid, 2011).

Compared to the adult-to-reproductive phase transition, which is the most relevant trait in crops, much less is known about the molecular mechanisms that mediate the juvenile-to-adult transition. However, recent progress in *Arabidopsis* has demonstrated that several microRNAs (miRNAs) play an important role in this phase transition (Huijser and Schmid, 2011; Poethig, 2013). Below the miRNA-based regulation will be discussed in more detail.

miRNAs and gibberellic acid regulate the juvenile-to-adult transition

MiRNAs are gene-encoded small RNA molecules of 20 to 24 nucleotides in length that by translation suppression of the mRNAs of their target genes play a critical regulatory role in various developmental aspects of eukaryotic organisms. Regulation of developmental phase changes by miRNAs was first discovered in *Caenorhabditis elegans*. Recent studies show that two miRNAs, miR156 and miR172, are involved in the juvenile-to-adult transition in *Arabidopsis* and other plant species (Fig. 2) (Wu and Poethig, 2006; Xie et al., 2006; Saeteurn K, 2007; Wang et al., 2011; Zhang et al., 2011; Fu et al., 2012; Xie et al., 2012; Poethig, 2013). *Arabidopsis* plants overexpressing miR156 show a prolonged juvenile phase (Wu and Poethig, 2006; Wu et al., 2009; Xu et al., 2016), whereas miR156 knockdown lines have a significantly shortened juvenile phase (Wu et al., 2009; Yang et al., 2013), suggesting that miR156 is a master regulator of the vegetative phase change in plants.

The regulation of the juvenile-to-adult transition by miR156 was shown to be mediated by translation suppression of the plant-specific SQUAMOSA PROMOTER BINDING PROTEIN-LIKE (SPL) transcription factors (Cardon et al., 1999; Xie et al., 2006; Axtell et al., 2007; Preston and Hileman, 2013). In the juvenile shoot miR156 levels are high, resulting in low SPL levels, but the gradual down-regulation of miR156 expression during shoot

development results in up-regulation of SPL expression, thereby inducing the juvenile to adult phase change (Wu and Poethig, 2006; Wu et al., 2009). Like *miR156* loss-of-function mutants, transgenic plants expressing a miR156-insensitive *SPL* gene display a short juvenile phase (Wang et al., 2008; Wu et al., 2009). In *Arabidopsis*, 11 of the 17 members of *SPL* gene family are targeted by miR156 (Gandikota et al., 2007), but only 6 of these genes (*SPL2/9/10/11/13/15*) contribute to the juvenile-to-adult transition. Consistent with the high degree of functional redundancy among the *Arabidopsis SPL* genes, loss-of-function mutations in single genes have no significant effect on the juvenile phase (Wu and Poethig, 2006; Wang et al., 2008; Usami et al., 2009; Wu et al., 2009). Only in *spl2/9/10//11/13/15* sextuple mutant plants prolonged juvenile phase phenotypes are observed, similar to those in plants overexpressing miR156 (Xu et al., 2016).

The gradual decrease of *miR156* expression during shoot maturation is accompanied by an SPL-induced gradual increase in *miR172* expression. miR172 promotes the development of trichomes on the abaxial side of leaves by repressing the expression of the APETALA2-LIKE (AP2-like) transcription factors TARGET OF EARLY ACTIVATION TAGGED1 (TOE1) and TOE2 (Aukerman and Sakai, 2003; Wu et al., 2009). In addition, SPLs promote the other adult leaf traits such as leaf elongation and leaf serration independent of miR172.

Besides miRNAs and SPL proteins, the phytohormone GA has a strong influence on the vegetative phase change in *Arabidopsis*. *Arabidopsis* mutants insensitive to GA or deficient in GA biosynthesis display a prolonged juvenile vegetative development (Telfer et al., 1997; Park et al., 2017). In contrast, exogenous application of GA results in precocious appearance of adult vegetative traits in particular trichome initiation in *Arabidopsis* (Telfer et al., 1997; Park et al., 2017). GA has no effect on *miR156* expression in *Arabidopsis*, but promotes the expression of some *SPL* genes in the adult phase (Wang et al., 2009a; Galvão et al., 2012; Jung et al., 2012; Yu et al., 2012). On the other hand, the exogenous application of GA has nearly the same effect on the vegetative phase change in wild-type plants and plants over-expressing miR156 (Yu et al., 2012). Thus, the promotion of the vegetative phase change by GA does not seem to be mediated by activation of *SPL* genes. In addition, the formation of trichomes in *Arabidopsis* on the abaxial side of adult leaves is independently promoted by GA and SPL proteins (Yu et al., 2012), suggesting that the GA and SPL synergistically promote the vegetative-phase transition in *Arabidopsis*.

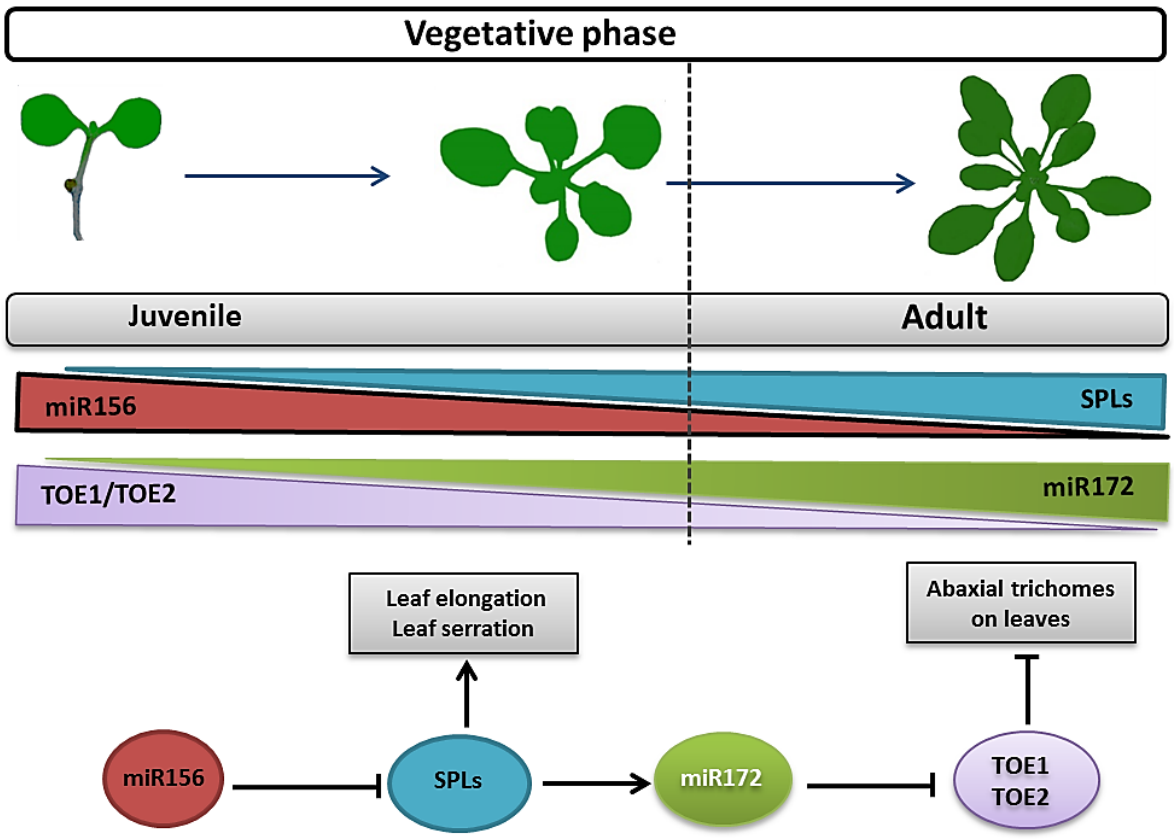

Figure 2. Regulation of the vegetative phase change in *Arabidopsis* by miR156 and miR172. miR156 is a master regulator of the vegetative phase change in plants. High expression of *miR156* maintains juvenility through translation suppression of *SPL* genes. A gradual decrease of the *miR156* transcription (brown bar) leads to enhanced production of SPLs proteins (turquoise bar), which promotes adult leaf morphology. SPLs directly induce *miR172* gene expression. Increased levels of miR172 (green bar) suppress the production of the TOE1 and TOE2 transcription factors (light purple bar), thereby allowing the development of trichomes on the abaxial side of leaves (for review see Huijser and Schmid, 2011; Poethig, 2013)

Vegetative-to-reproductive transition

The switch from vegetative growth to flowering is a major developmental transition in plants. For fruit and seed crops, the timing of vegetative-to-reproductive transition plays a crucial role in crop productivity, as flowering should take place in the correct season when the environmental conditions are suitable to ensure maximal reproductive success. Because of regional differences in the seasons, selection of the genotype with the correct timing for a region is part of the breeding process (Jung and Müller, 2009).

Acquisition of the reproductive competence in the SAM during vegetative growth is a key developmental switch in flowering. During the past two decades, genetic and physiological studies have led to the identification of a range of environmental cues that are involved in the acquisition of reproductive competence in plants (Amasino, 2010; Turnbull, 2011; Song et al., 2013). In *Arabidopsis*, four major flowering pathways have been identified: the photoperiod pathway, the vernalization pathway, the GA pathway, and the age pathway (Fig. 3) (Turnbull, 2011; Matsoukas et al., 2012; Song et al., 2013). A large number of genes

acting within these pathways have been identified that either promote or inhibit flowering, and work in a complex genetic network. Central in this network are genes such as *CONSTANS* (*CO*), *FLOWERING LOCUS T* (*FT*), *SUPRESSOR OF CONSTANS 1* (*SOC1*), the *SPLs*, and *FLOWERING LOCUS C* (*FLC*) that are considered as floral integrators (Fig. 3), as they integrate the different environmental and endogenous signaling pathways that influence flowering (Amasino, 2010; Amasino and Michaels, 2010; Andrés and Coupland, 2012; Matsoukas et al., 2012).

In *Arabidopsis*, *CO* plays a key role in the photoperiod flowering pathway (Fig. 3), as its expression is up-regulated by light signaling in leaves (Turnbull, 2011; Song et al., 2013). CO promotes flowering by activation of *FT* transcription. *FT* encodes a florigen signal that is transported from the leaf through the phloem to the SAM. In the SAM, FT interacts with transcription factor FD, and the FT-FD complex activates the transcription of several flowering-promoting genes (Fig. 3) (Turnbull, 2011; Song et al., 2013).

A central node in the vernalization pathway is the MADS box transcription factor FLC (Fig. 3), which acts as a potent repressor of flowering (Amasino, 2010; Kim and Sung, 2014). FLC affects flowering by suppressing the *FT* and *SPL* genes in leaves and the *FD* and *SOC1* genes in the shoot apex (Deng et al., 2011; Matsoukas et al., 2012). Prolonged exposure to low temperatures leads to silencing of *FLC* expression by local chromatin modification and subsequently to induction of flowering (Kim and Sung, 2014).

The key components of the age pathway are miR156 and its *SPL* target genes (Matsoukas et al., 2012; Wang, 2014; Wang and Wang, 2015). Like for the vegetative phase change, the age-related reduction of *miR156* expression leads to increasing levels of SPL proteins, which subsequently induce flowering by activating the transcription of *SOC1* and several other floral-promoting genes in the shoot apex. Activation of *miR172* by SPL proteins in leaves leads to repression of a sub-family of *APATELA2* (AP2)-like target genes that are repressors of flowering (Aukerman and Sakai, 2003; Huijser and Schmid, 2011; Poethig, 2013). Molecular genetic studies have shown that the age pathway is highly integrated into other flowering time pathways (Wang, 2014).

The GA pathway is a photoperiod independent pathway that also plays an important role in the promotion of flowering through activation of the *SOC1* and *SPL* genes (Yu et al., 2012; Wang, 2014). Mutations that decrease the GA concentration or increase the degradation of GA delay flowering (Jung et al., 2012; Yu et al., 2012). The GA pathway is activated by GA signaling-induced degradation of the DELLA repressor proteins, (Sun, 2010; Davière and Achard, 2013).

Downstream of the floral integrators are the floral meristem identity genes, such as *APETALA1* (*AP1*) and *LEAFY* (*LFY*), that promote the transition of the vegetative to inflorescence meristem (Andrés and Coupland, 2012; Matsoukas et al., 2012; Blümel et al., 2015). The photoperiod-regulated FT-FD complex is directly involved transcriptional activation of *AP1*, whereas the central floral integrator SOC1 in the SAM promotes flowering through activation of both floral meristem genes *AP1* and *LFY* (Turnbull, 2011; Song et al., 2013).

The important advances in the understanding of the molecular control of reproductive development in *Arabidopsis* have subsequently facilitated the discovery of the similar mechanisms in other flowering plants.

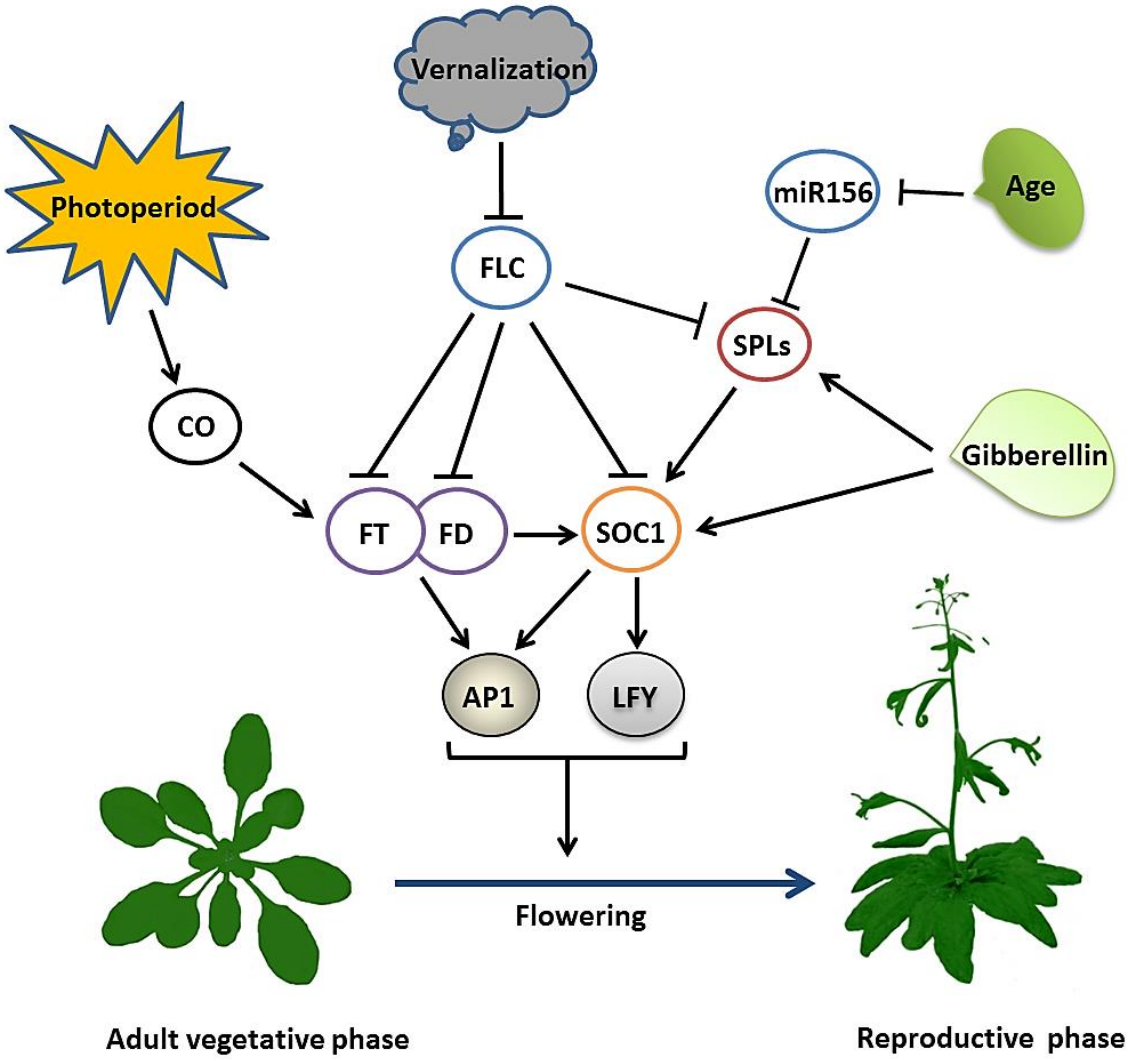

Figure 3. A simplified regulatory network of the different pathways controlling flowering in *Arabidopsis*. In the vernalization pathway cold treatment leads to stable repression of *FLC* transcription. The MADS box protein FLC determines the cold-period-dependent timing of flowering in *Arabidopsis* by repressing the expression of the floral integrator genes *FT*, *FD*, the *SPLs* and *SOC1*. *FT* expression is induced in the leaves by the photoperiod pathway through the accumulation of CO under long days. The FT protein subsequently travels to the SAM, where it physically interacts with FD to activate *SOC1* and *AP1*. In the age pathway, an age-dependent decline in the miR156 level allows an increased production of SPL proteins, which activate the transcription of *SOC1* and other floral integrators (not shown). The phytohormone GA independently promotes flowering through activation of *SOC1* (and *SPL* expression). The subsequent activation of the downstream floral meristem identity genes, such as *LFY* and *AP1*, completes the floral transition (for review see Turnbull, 2011; Andrés and Coupland, 2012; Song et al., 2013; Wang, 2014).

Mechanisms that differentiate between monocarpic or polycarpic plant growth habit

In annual or monocarpic plants, the whole plant body will senesce and die following a single reproductive phase, while polycarpic or perennial plants have more than one reproductive phase during their life history (Munné-Bosch, 2008; Thomas, 2013). For polycarpic plant growth it is critical that the plant maintains underground root stocks or axillary meristems in

the vegetative state, allowing them to produce new shoots after seed set and during the next growing season (Munné-Bosch, 2008; Amasino, 2009).
The fact that monocarpic and polycarpic species occur within the same plant family implies that that the transition between polycarpic and monocarpic growth habit is based on relatively small genetic changes. In fact, the switch between poly- and monocarpy is considered as the most common growth form transition in angiosperms (Amasino, 2009). However, despite considerable interest in the molecular basis of these two main growth habits in flowering plants, only few genes have yet been identified that differentiate between the seed set-linked death in monocarpic plants and the survival of polycarpic plants even after multiple rounds of flowering and seed set.

In monocarpic plants, the vegetative development from axillary shoot meristems is suppressed (Amasino, 2009; Davies and Gan, 2012) and all energy is funneled toward reproductive activities (Thomas, 2013).The remobilization of nutrients from leaves to flowers and fruits is well-known as major cause of leaf senescence in monocarpic plants (Avila-Ospina et al., 2014; Distelfeld et al., 2014). Leaf senescence is an age-dependent mechanism that is directly connected to plant body senescence and death, and therefore this mechanism is likely to contribute to the diversity of plant growth habits among different plant species. It is a complex process that is affected by an extensive range of developmental and environmental signals (Fischer and Fischer, 2017). Recent molecular genetic studies have uncovered that the leaf senescence process strongly depends on a major reprogramming of gene expression (Pujol, 2015; Fischer and Fischer, 2017), involving transcription factors of the NAC-, WRKY-, C2H2- zinc finger-, AP2/EREBP, - and MYB-class (Schippers, 2015; Fischer and Fischer, 2017). In addition, histone- and DNA modifications have been implicated in the senescence process (Ay et al., 2014), and overexpression of an AT-hook protein was shown to delay leaf senescence in *Arabidopsis* (Lim et al., 2007). Plant hormones such as ethylene, jasmonic acid, salicylic acid, cytokinin and ABA have also been shown to play important roles in leaf senescence (Jibran et al., 2013; Fischer and Fischer, 2017). Of these hormones, cytokinin and ethylene seem most effective in controlling leaf senescence, as up-regulation of cytokinin signaling or impaired ethylene signaling was shown to delay leaf senescence (Jibran et al., 2013). Based on recent multi-omics approaches, a picture is now beginning to emerge on the leaf senescence programme that reveals clear cross-talk between the transcriptional regulatory networks and plant hormone signaling (Penfold and Buchanan-wollaston, 2014; Schippers, 2015; Kim et al., 2016). Nonetheless, many of the regulatory mechanisms remain elusive.

Besides senescence, the phase identity of (axillary) shoot meristems plays an important role in determining the plant growth habit. The ability to maintain axillary meristems in the vegetative state after a successful round of offspring production is a key feature of polycarpic behavior. In annual monocarpic plants, the near simultaneous transition of all shoot meristems into the reproductive phase prevents vegetative development after seed set, and eventually leads to death of the plant body (Fig. 4). In contrast, many polycarpic plants prolong their life span by maintaining a number of axillary meristems in the vegetative phase (Fig. 4), thereby allowing subsequent cycles of reproductive development during the next growth season (Amasino, 2009). In some polycarpic plants, however, all axillary meristems do change to the reproductive phase, but vegetative development is maintained by the

reversion of some inflorescence meristems to the vegetative state under specific environmental conditions (Tooke et al., 2005).

Consistent with the central position of the vegetative-to-reproductive phase transition in determining the life history of a plant, the key regulators of this phase transition play an important role in regulating the vegetative activity of axillary shoot meristems during the reproductive phase. Studies in Brassicaceae have recently started to reveal the genetic basis that differentiates between the monocarpic and polycarpic growth habit. The *Arabidopsis FLC* MADS box gene ortholog *PERPETUAL FLOWERING1* (*PEP1*) (Michaels and Amasino, 1999) controls the temperature-dependent switch from polycarpic to monocarpic growth in the conditionally polycarpic *Arabis alpine* and *Cardamine flexuosa* (Wang et al., 2009b; Zhou et al., 2013a). PEP1 blocks the vegetative to reproductive transition of meristems, leading to vegetative development, but low temperature-induced chromatin modifications (during winter) lead to repression of *PEP1* transcription and subsequently to flowering (in spring), explaining the temperature-dependent polycarpic life history of *A. alpine* and *C. flexuosa* (Wang et al., 2009b; Zhou et al., 2013a).

It has been shown that the *Arabidopsis* double mutant in the flowering genes *SOC1* and *FRUITFULL* (*FUL*) shows a perennial-like lifestyle (Melzer et al., 2008). Interestingly, the PEP1-induced polycarpic behavior of *A. alpine* and *C.* flexuosa was also shown to be caused by suppression of *AaSOC1* and *CfSOC1* expression (Bergonzi et al., 2013; Zhou et al., 2013a). This indicates that advances in the understanding of molecular mechanisms that control monocarpic life strategies can help to elucidate the molecular basis of the capacity of polycarpic plants to survive after multiple rounds of flowering.

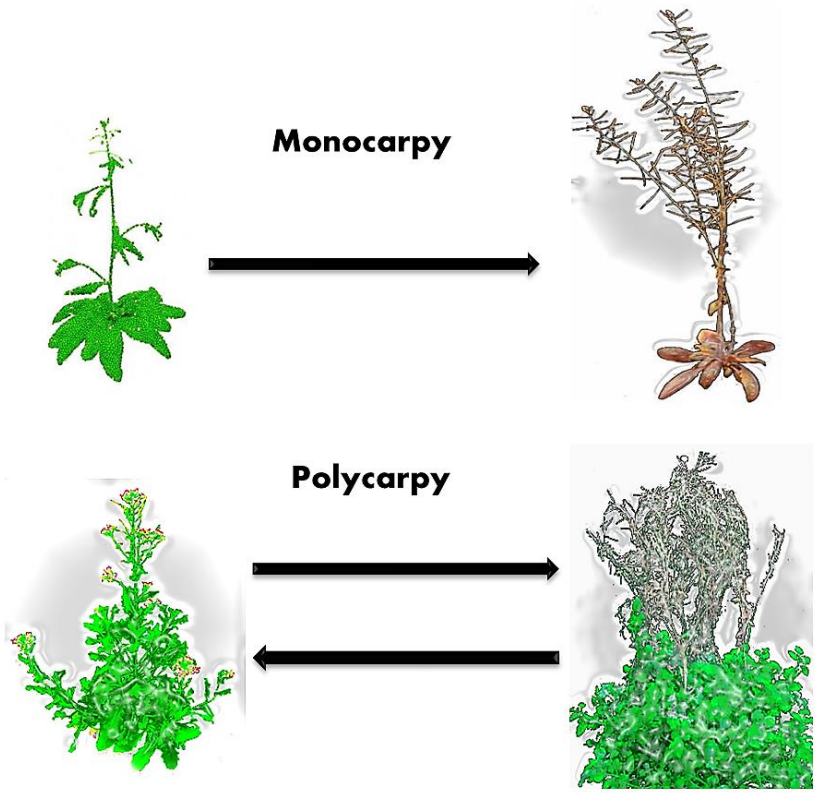

Figure 4. Schematic comparison of the monocarpic and polycarpic plant growth habit

Chromatin remodeling and AT-Hook motif nuclear proteins in plant developmental phase transitions

In the nucleus of multi-cellular organisms, the genomic DNA is packed into highly condensed chromatin, the complex of DNA with histone and non-histone proteins. The genomic studies in multicellular organisms have demonstrated that the structure and organization of chromatin determines the accessibility of the transcriptional machinery to the DNA, thereby dictating the transcriptome pattern (Ho and Crabtree, 2010). Similar to other multi-cellular organisms, remodeling of the chromatin structure plays a crucial role in temporal and spatial gene expression patterns during developmental processes in plants (Reyes, 2006; Exner and Hennig, 2008; Jarillo et al., 2009; Kaufmann et al., 2010). Large scale chromatin remodeling leading to global transcriptome reprogramming has been observed during embryonic-to-postembryonic and vegetative-to-reproductive phase transitions (Exner and Hennig, 2008; Holec and Berger, 2012; Han et al., 2015), thereby uncovering the role of chromatin remodeling in plant developmental phase transitions. During the past few years, molecular genetic studies have discovered histone modifications and DNA methylations play an important role in the regulation of developmental processes of plants (Reyes, 2006; Jarillo et al., 2009; Holec and Berger, 2012). Unlike animals, where the major epigenetic marks are established during embryo development, such epigenetic mechanisms operate throughout plant development (Jarillo et al., 2009). Therefore, the high level of developmental plasticity in plants is associated with differential regulation of epigenetic information. Recent studies have shown that the molecular memory of gene expression that is stored by epigenetic mechanisms is likely to be crucial for the plant growth behavior. For example, the expressions of the key floral transition genes including *FT*, *SOC1*, and *FLC*, are epigenetically regulated (Bratzel and Turck, 2015). A critical step for the perennial life history of *A. alpine* is the return of *PEP1* expression to its original levels a few weeks after the cold period, which is correlated with removal of the repressive trimethylation of histone H3 (H3K27me3) in the *PEP1* promotor (Wang et al., 2009b). Moreover, several other studies have shown an age-dependent increase in DNA methylation levels in plants, which might lead to repression of *miR156* expression (Hasbu et al., 2010; Saya et al., 2011; Huang et al., 2012; Yuan et al., 2014; Dubrovina and Kiselev, 2016).

Besides such epigenetic marks, many putative chromatin-remodelling proteins have been identified that are involved in plant developmental processes (Reyes, 2006; Jarillo et al., 2009; Holec and Berger, 2012). In many cases, however, the possible involvement of these proteins with remodeling of chromatin is only based on sequence homology with chromatin remodelers in other organisms.

A wide range of non-histone nuclear proteins, also known as high-mobility-group (HMG) proteins, have been found in eukaryotic cells to regulate functions of the complex eukaryotic genome (Bianchi and Agresti, 2005; Reeves, 2010). Three main families of HMG proteins have been identified, of which the HMGA proteins are considered as chromatin architectural factors involved in a diverse array of crucial cellular processes, including cell

growth, differentiation, transformation, proliferation, death, and DNA replication and repair, chromatin remodeling, and gene transcription (Reeves, 2010; Sgarra et al., 2010; Ozturk et al., 2014). These proteins preferentially bind to the narrow minor groove of DNA at AT-rich stretches using a highly conserved small DNA-binding motif, called AT-hook (Aravind and Landsman, 1998). The AT-hook motif is not unique to HMGA proteins and has also been found in a large number of non-HMGA proteins, such as chromatin remodeling proteins, transcription factors, and ATP-dependent chromatin remodeling complexes (Aravind and Landsman, 1998;Cairns et al., 1999; Xiao et al., 2001; Singh et al., 2006; Su et al., 2006; Maffini et al., 2008; Lucas et al., 2009).

The *Arabidopsis thaliana* genome encodes 29 AT-HOOK MOTIF CONTAINING NUCLEAR LOCALIZED (AHL) proteins that have either one or two AT-Hook DNA binding domains (Fujimoto et al., 2004; Matsushita et al., 2007; Ng et al., 2009; Zhao et al., 2013). AHL proteins also contain a Plant and Prokaryote Conserved (PPC) domain that is involved in the physical interaction between AHL proteins or with histones or other nuclear transcription factors (Fujimoto et al., 2004; Matsushita et al., 2007; Street et al., 2008; Zhao et al., 2013). *AHL* gene families seem to be land plant-specific, as they have been found in early diverging land plants such as *Physcomitrella patens* and *Selaginella moellendorffii*, but not in water dwelling uni- or multicellular algae (Gallavotti et al., 2011; Zhao et al., 2014).

Molecular genetic studies in *Arabidopsis* have revealed that AHL proteins are involved in multiple aspects of plant growth and development, including flowering time (Weigel et al., 2000; Street et al., 2008; Xiao et al., 2009; Jin et al., 2011), flower development (Ng et al., 2009; Gallavotti et al., 2011; Jin et al., 2011), hypocotyl growth (Street et al., 2008; Xiao et al., 2009; Zhao et al., 2013), vascular tissue differentiation (Zhou et al., 2013b), and hormonal response (Matsushita et al., 2007; Ng et al., 2009). Consistent with the lack of phenotypes in the single or double mutants of *Arabidopsis AHL* genes, a high degree of functional redundancy has been suggested among these genes, and therefore most information on the function *AHL* genes has come from phenotypic changes induced by overexpression of these genes in *Arabidopsis* (Street et al., 2008; Xiao et al., 2009; Zhao et al., 2013).

Based on the detection of epigenetic modifications around the DNA-binding sites of *AHL22*, *AHL16*, and *AHL21* (Ng et al., 2009; Yun et al., 2012; Xu et al., 2013), AHL proteins have been considered to act through chromatin modification. In addition, AHL proteins have been shown to preferably bind to Matrix Attachment Regions (MARs) (Fujimoto et al., 2004; Lim et al., 2007; Ng et al., 2009; Xu et al., 2013). MARs are AT-rich short DNA sequences (about 200-300 bp) that bind to the nuclear matrix and organize the chromatin into distinct loop domains (Heng et al., 2004; Girod et al., 2007; Chavali et al., 2011; Wilson and Coverley, 2013). In animals, several MAR-binding proteins have been identified (Wang et al., 2010), among which the AT-hook motif-containing special AT-rich sequence-binding protein 1 (SATB1) that is implicated in several cellular processes such as gene expression regulation, chromatin organization, and histone modification (Yasui et al., 2002; Cai et al., 2003; Kumar et al., 2007; Han et al., 2008; Kohwi-Shigematsu et al., 2012). However, the exact molecular mode of plant AHL proteins in the regulation of plant developmental aspects remains unknown yet.

Somatic embryogenesis: reversing a developmental phase transition

The ability of a plant cell to acquire totipotency and enter the embryogenesis programme is not restricted to the zygotic cell, as in specific (apomictic) plant species embryos are derived from diploid ovule cells or from unreduced gametophytes by asexual reproduction (without fertilization) (Ozias-Akins, 2006). In many flowering plants, however, vegetative somatic cells can be reprogrammed to a pluripotent state under appropriate *in vitro* conditions. This developmental pathway, which involves reversion of the transition from the embryonic to post-embryonic phase, is called somatic embryogenesis (SE) and considerably resembles ZE. Similar to ZE, distinct morphological and physiological stages can be recognized during SE, such as the transition from globular to cotyledon stages and finally the accumulation/storage of nutrients in the maturing embryo required for subsequent germination and seedling development (Arnold et al., 2002). Because of these similarities, SE is considered as a more easily accessible model system to study the biochemical and molecular processes in ZE (Zimmerman, 1993; Mordhorst et al., 1998).

More than 50 years ago, the induction of somatic embryos from differentiated plant cells was first demonstrated in carrot cell suspension cultures (Steward et al., 1958). Since then, SE has been reported in a wide range of dicot and monocot plant species. Besides providing an excellent tool for a better mechanistic understanding of embryogenesis and totipotency in plants, SE has offered great potential for applications in plant biotechnology and plant breeding, including genetic transformation, somatic hybridization, clonal propagation, synthetic seed technologies, cryopreservation, and somaclonal variation (Imin et al., 2005; Wang et al., 2012).

SE is typically achieved by exogenous application of plant hormones, and in 65% of the recent protocols the herbicide 2,4-dichlorophenoxyacetic acid (2,4-D), a synthetic analog of the natural auxin IAA, has been employed for SE induction. Therefore, auxin is considered as a key trigger of SE in most plants (Stone et al., 2008; Elhiti et al., 2013a; Wójcikowska et al., 2013), which is in line with its crucial role in the regulation of ZE (Friml et al., 2003; Jenik and Barton, 2005; Jenik et al., 2007; Lau et al., 2012; Robert et al., 2013). In line with the important role of PIN proteins in establishing of polar auxin transport-mediated patterning of the early ZE (Friml et al., 2003), PIN-driven auxin gradients have also been shown to be important during SE, not for the initiation of SE, but rather for the later development of somatic embryos (Philipsen, 2017).

Upregulation of several ARF genes, *ARF5/6/8/16/17*, that either promote or inhibit of auxin-responsive genes (Guilfoyle and Hagen, 2007; Boer et al., 2014) has been reported in embryogenic cultures of *Arabidopsis* (Gliwicka et al., 2013) and other plants (Shealy et al., 2003; Legrand et al., 2007; Singla et al., 2007; Sharma et al., 2008). Recently, mutations in the *ARF6* and *ARF8* genes were shown to arrest SE in *Arabidopsis* (Su et al., 2016). These data indicate that ARFs are required for SE. Other studies have shown that members of the *YUCCA* (*YUC*) gene family, encoding enzymes in the key tryptophan-dependent auxin biosynthesis pathway, are important for SE (Zhao, 2012). *YUC1/4/6/10* genes are upregulated (Bai et al., 2013; Elhiti et al., 2013a) and auxin biosynthesis is enhanced in 2,4-D-induced embryogenic cultures (Jiménez, 2005; Elhiti et al., 2013a). Moreover, quadruple mutants in the *YUC1/2/4/6* genes cause defects in SE (Bai et al., 2013), indicating that IAA biosynthesis

is required for SE and suggesting that not the exogenously applied 2,4-D but rather the endogenous YUC-mediated IAA biosynthesis provides the auxin signal required for proper SE.

The effectiveness of 2,4-D in inducing SE has been attributed on the one hand to its stability as auxin analog. On the other hand, however, at the high concentrations used during SE induction, 2,4-D might rather act as a stress-inducing herbicide, and the involvement of this stress in acquiring embryonic cell identity has been proposed as well. In several studies indicate that 2,4-D indeed induces many stress-related genes during 2,4-D-induced SE (Zavattieri et al., 2010; Gliwicka et al., 2013; Fehér, 2015). Consistent with the observed acquisition of embryogenic ability in somatic cells following stress treatments, such as heavy metal-, ultraviolet radiation-, osmotic-, temperature- or hypoxia stress in many plant species (Zavattieri et al., 2010), the stressor effect of 2,4-D may be more important than its auxin activity in the induction of SE.

With respect to importance of SE for plant breeding and propagation, many attempts have been made to understand the molecular basis of this phenomena in different plant species such as *Arabidopsis*, carrot, alfalfa, and conifers (Rose and Nolan, 2006; Namasivayam, 2007; Yang and Zhang, 2010a; Elhiti et al., 2013b; Smertenko and Bozhkov, 2014). So far, many genes have been identified that are involved in SE (Imin et al., 2008; Lucau-Danila et al., 2010; Yang and Zhang, 2010; Elhiti et al., 2013b; Gliwicka et al., 2013; Nic-Can et al., 2013; Smertenko and Bozhkov, 2014). Most of these genes have been identified as being up-regulated during SE, but their exact function in acquisition of embryogenic ability and embryo development has not been determined yet. Some of these genes, however, encode transcription factors that have been found to promote SE in the absence of exogenous 2,4-D or other plant growth regulators. For genes such as *BBM/PLT4* (Boutilier et al., 2002), *WUS* (Zuo et al., 2002), *(LEC1* (Lotan et al., 1998), and *LEC2* (Stone et al., 2001) it was shown that overexpression of a single gene can induce the pluripotent state in plant cells leading to SE. In addition, they also appeared to be key regulators of ZE.

The *BBM/PLT4* gene, for example is expressed during early stages of ZE in *Arabidopsis* (Boutilier et al., 2002; Galinha et al., 2007). *BBM/PLT4* overexpression is sufficient to induce SE from vegetative organs in *Arabidopsis* (Boutilier et al., 2002), tobacco (Srinivasan et al., 2007), chinese white poplar (Deng et al., 2009), and sweet pepper (Heidmann et al., 2011) in the absence of exogenous auxin. It was also found that overexpression of the *BBM* ortholog from Glycine max (*GmBBM1*) or of a close homolog of *BBM/PLT4* in *Arabidopsis*, *PLT5*, induce embryonic callus on *Arabidopsis* seedlings (El Ouakfaoui et al., 2010; Tsuwamoto et al., 2010), suggesting that the BBM function is probably conserved among family members and throughout higher plants. Up-regulation of two auxin biosynthesis genes, *YUC3* and *YUC8*, in *Arabidopsis* seedlings overexpressing BBM (Horstman, 2015) indicates that, similar to 2,4-D-induced SE, auxin biosynthesis is also important for BBM-induced SE.

The *WUS* transcription factor is well-known for its role in maintaining the pool of stem cells in the SAM (Mayer et al., 1998). Ectopic expression of *WUS* promotes SE in *Arabidopsis* root tissues without hormonal treatment (Zuo et al., 2002). *WUS* overexpression was also reported to significantly increase the SE efficiency in *Coffea canephora* (Arroyo-Herreraet al., 2008), whereas *WUS* knockdown in *Brassica napus* results in a reduced SE efficiency (Elhiti et al., 2010). Maintenance of cells in a relatively undifferentiated state by

WUS (Mayer et al., 1998) and the prevention of cell differentiation by *BBM* (Srinivasan et al., 2007; Horstman et al., 2015) indicates that repression of cellular differentiation might be essential for SE initiation.

Despite the fact that the *LEC1* and *LEC2* genes control distinct aspects of ZE such as embryo growth, embryo organ identity, and seed maturation (Stone et al., 2001; Braybrook and Harada, 2008), the SE induction by their overexpression in *Arabidopsis* indicated that these genes also promote embryonic cell identity (Lotan et al., 1998; Stone et al., 2001). Both *LEC* genes have been reported to be significantly up-regulated during 2,4-D-induced SE in *Arabidopsis* (Ledwoń and Gaj, 2011) and *Picea abies* (Uddenberg et al., 2011), whereas *Arabidopsis lec* mutants are impaired in 2,4-D-induced SE (Gaj et al., 2005).Moreover, the improved SE by ectopic expression of *LEC1* and *LEC2* in tobacco (Guo et al., 2013) and cacao (Zhang et al., 2014) shows the ability of these genes to promote SE in other plant species. The *LEC* genes seem to play a role in maintaining embryonic identity in somatic cells.

Recent studies have shown that *LEC2*-induced SE is accompanied by elevation of endogenous auxin levels in embryonic tissues. Like for BBM overexpression, several member of the *YUC* gene family, were shown to be significantly upregulated in *Arabidopsis* seedling-overexpressing *LEC2*. The rapid activation of *YUC2*, and *YUC4* expression by LEC2 (within 1 h after induction of LEC2 activity) suggests that LEC2 is a master regulator of auxin biosynthesis during SE-induction (Stone et al., 2008). In animals, the essential role of chromatin modification in the pluripotent stem cells establishment has been demonstrated (Gaspar-Maia et al., 2011; Apostolou and Hochedlinger, 2013; Buganim et al., 2013). The current genetic studies in plants also have indicated that the SE processes is accompanied by global modification of chromatin (Nic-Can et al., 2013; Fehér, 2015). Moreover, the SE potential of several *Arabidopsis* tissues was enhanced by down regulation of the H3K27me3 activity of Polycomb repressive complex 2 (PRC2) (Mozgova et al., 2017). However, the detailed contribution of chromatin modifications in SE is largely unknown.

Although several studies have predicted possible molecular pathways controlling SE (Radoeva and Weijers, 2014; Smertenko and Bozhkov, 2014), SE is a complex phenomenon and the exact molecular mechanisms or signaling pathways that lead to the induction of SE are one of the challenges to be solved with modern molecular biology.

Outline of the thesis

This thesis describes the functional analysis of the *AHL15* gene encoding an AT-Hook motif protein that was originally identified by a yeast one-hybrid screen. Functional analysis of this gene revealed that overexpression leads to the formation of somatic embryos on *Arabidopsis* seedlings in the absence of hormone treatment (van der Zaal and Hooykaas, 2004).

In **Chapter 2**, we focused on the initiation of SE by *AHL15* overexpression on *Arabidopsis* seedlings and the role of this gene in zygotic embryogenesis (ZE). *ahl15* loss-of-function mutants showed reduced somatic embryo induction in response to 2,4-D treatment or overexpression of the SE-inducing BBM transcription factor. The *AHL15* gene appeared to

be bound and transcriptionally-regulated by BBM during SE. During zygotic embryogenesis *AHL15* was found to be expressed in early embryos, where it is required for proper patterning and for development beyond the heart stage. Morphological and cellular analyses showed that a significant number of plants derived from *35S::AHL15* somatic embryos were polyploid. Chromatin staining with fluorescent reporters suggested that AHL15 induces chromatin decondensation, which might lead to chromosome missegregation and thus to the occurrence of polyploid cells. Using centromere-specific markers we demonstrated that polyploidisation was caused by endomitotic events that specifically occurred during the initiation of SE. Our findings indicate that AHL15 is an important driver of plant cell totipotency acquisition, and based on our results, we suggest that opening of the chromatin structure is required for the acquisition of embryonic competency in somatic plant cells.

More detailed analyses revealed that AHL15 is not specifically involved in the embryogenesis program, but that, surprisingly, the protein rather is involved in post embryonic development. The research described in **Chapter 3** focused on the role of *AHL15* and its close homologs, *AHL19* and *AHL20,* in the vegetative phase change, flowering and plant longevity. Because plants overexpressing *AHL15* reverse adult meristems to a juvenile state, AHL15 was named REJUVENATOR (RJV). In this chapter we showed that the AHL15/RJV is a suppressor of developmental phase changes. Loss of *RJV* gene function accelerated plant aging, whereas *RJV* overexpression converted monocarpic *Arabidopsis thaliana* and *Nicotiana tabacum* plants into polycarpic plants with enhanced seed and biomass production. Our results show that *AHL15/RJV* acts downstream of aging (*miR156*, *SPL*) and flowering (*SOC1*, *FUL*) genes as a molecular switch between monocarpic and polycarpic life history strategy. *RJV* expression acts as a molecular switch for life history strategies in plants, and can be used as a breeding tool to promote sustainable plant production by converting annual crops into perennial plants.

In **Chapter 4** we analysed our observation that transient (4 hours) activation of overexpressed AHL15-GR in *Arabidopsis* seedlings leads to long term effects on plant development. RNA sequencing analysis detected an extensive reprogramming of the transcriptome 4 hours after AHL15-GR activation. AHL15 seemed to act in a transcription level-dependent manner, activating predominantly low expressed genes and repressing mostly highly expressed genes. Rapid decondensation of heterochromatin was observed after AHL15 activation in leaf primordia and axillary meristems, indicating that the global reprogramming of the transcriptome by AHL15 might at least in part be caused by extensive modulation of the chromatin configuration. Co-activated or co-repressed genes were often physically linked in small chromosomal clusters, which is in line with regulation at the chromatin level. More detailed analysis of down-regulated genes indicated that AHL15 represses plant ageing by targeting several components of the ageing pathway, including the *SQUAMOSA-PROMOTER BINDING PROTEIN-LIKE* (*SPL*) genes, GA biosynthesis and photosynthesis-dependent sugar production.

References

Abe, M., Katsumata, H., Komeda, Y., and Takahashi, T. (2003). Regulation of shoot epidermal cell differentiation by a pair of homeodomain proteins in *Arabidopsis*. Development **130**: 635–643.

Amasino, R. (2009). Floral induction and monocarpic versus polycarpic life histories. Genome Biol. **10**: 228.

Amasino, R. (2010). Seasonal and developmental timing of flowering. Plant J. **61**: 1001–1013.

Amasino, R.M. and Michaels, S.D. (2010). The timing of flowering. Plant Physiol. **154**: 516–520.

Andrés, F. and Coupland, G. (2012). The genetic basis of flowering responses to seasonal cues. Nat. Rev. Genet. **13**: 627–639.

Apostolou, E. and Hochedlinger, K. (2013). Chromatin dynamics during cellular reprogramming. Nature **502**: 462–471.

Aravind, L. and Landsman, D. (1998). AT-hook motifs identified in a wide variety of DNA-binding proteins. Nucleic Acids Res. **26**: 4413–4421.

Arnold, S. Von, Sabala, I., Bozhkov, P., Dyachok, J., and Filonova, L. (2002). Developmental pathways of somatic embryogenesis. Plant Cell. Tissue Organ Cult. **69**: 233–249.

Arroyo-Herrera, A., Ku Gonzalez, A., Canche Moo, R., Quiroz-Figueroa, F.R., Loyola-Vargas, V.M., Rodriguez-Zapata, L.C., Burgeff D'Hondt, C., Suárez-Solís, V.M., and Castaño, E. (2008). Expression of *WUSCHEL* in *Coffea canephora* causes ectopic morphogenesis and increases somatic embryogenesis. Plant Cell Tissue Organ Cult. **94**: 171–180.

Aukerman, M.J. and Sakai, H. (2003). Regulation of flowering time and foral organ identity by a microRNA and its *APETALA2 -like* target genes. Genetics **15**: 2730–2741.

Avila-Ospina, L., Moison, M., Yoshimoto, K., and Masclaux-Daubresse, C. (2014). Autophagy, plant senescence, and nutrient recycling. J. Exp. Bot. **65**: 3799–3811.

Ay, N., Janack, B., and Humbeck, K. (2014). Epigenetic control of plant senescence and linked processes. J. Exp. Bot. **65**: 3875–3887.

Bai, B., Su, Y.H., Yuan, J., and Zhang, X.S. (2013). Induction of somatic embryos in *Arabidopsis* requires local *YUCCA* expression mediated by the down-regulation of ethylene biosynthesis. Mol. Plant **6**: 1247–1260.

Bainbridge, K., Guyomarc, S., Bayer, E., Swarup, R., Bennett, M., Mandel, T., and Kuhlemeier, C. (2008). Auxin influx carriers stabilize phyllotactic patterning. Genes Dev. **22**: 810–823.

Baroux, C., Pecinka, A., Fuchs, J., Schubert, I., and Grossniklaus, U. (2007). The triploid endosperm genome of *Arabidopsis* adopts a peculiar, parental-dosage-dependent chromatin organization. Plant Cell **19**: 1782–1794.

Bäurle, I. and Dean, C. (2006). The timing of developmental transitions in plants. Cell **125**: 655–664.

Bergonzi, S., Albani, M.C., Ver Loren van Themaat, E., Nordström, K.J. V, Wang, R., Schneeberger, K., Moerland, P.D., and Coupland, G. (2013). Mechanisms of age-dependent response to winter temperature in perennial flowering of *Arabis alpina*. Science **340**: 1094–1097.

Bianchi, M.E. and Agresti, A. (2005). HMG proteins: dynamic players in gene regulation and differentiation. Curr. Opin. Genet. Dev. **15**: 496–506.

Blümel, M., Dally, N., and Jung, C. (2015). Flowering time regulation in crops—what did we learn from *Arabidopsis*? Curr. Opin. Biotechnol. **32**: 121–129.

Boer, D.R., Freire-Rios, A., van Den Berg, W.A.M., Saaki, T., Manfield, I.W., Kepinski, S., López-Vidrieo, I., Franco-Zorrilla, J.M., De Vries, S.C., Solano, R., Weijers, D., and Coll, M. (2014). Structural basis for DNA binding specificity by the auxin-dependent ARF transcription factors.

Cell: 577–589.

Boot, K.J.M., Hille, S.C., Libbenga, K.R., Peletier, L.A., Van Spronsen, P.C., Van Duijn, B., and Offringa, R. (2016). Modelling the dynamics of polar auxin transport in inflorescence stems of *Arabidopsis thaliana*. J. Exp. Bot. **67**: 649–666.

Boutilier, K., Offringa, R., Sharma, V.K., Kieft, H., Ouellet, T., Zhang, L., Hattori, J., Liu, C., van Lammeren, A.A.M., Miki, B.L.A., and van Custers, L.C.M. (2002). Ectopic expression of *BABY BOOM* triggers a conversion from vegetative to embryonic growth. Plant Cell **14**: 1737–1749.

Brambilla, V., Fornara, F., Shrestha, R., and Go, J. (2014). Molecular control of seasonal flowering in rice , *Arabidopsis* and temperate cereals. Ann. Bot. **114**: 1445–1458.

Bratzel, F. and Turck, F. (2015). Molecular memories in the regulation of seasonal flowering: from competence to cessation. Genome Biol. **16**: 192.

Braybrook, S. A., and Harada, J.J. (2008). LECs go crazy in embryo development. Trends Plant Sci. **13**: 624–630.

Breuninger, H., Rikirsch, E., Hermann, M., Ueda, M., and Laux, T. (2008). Differential expression of *WOX* genes mediates apical-basal axis formation in the *Arabidopsis* embryo. Dev. Cell **14**: 867–876.

Buganim, Y., Faddah, D. a, and Jaenisch, R. (2013). Mechanisms and models of somatic cell reprogramming. Nat. Rev. Genet. **14**: 427–439.

Cai, S., Han, H.-J., and Kohwi-Shigematsu, T. (2003). Tissue-specific nuclear architecture and gene expression regulated by SATB1. Nat. Genet. **34**: 42–51.

Cairns, B.R., Schlichter, A., Erdjument-Bromage, H., Tempst, P., Kornberg, R.D., and Winston, F. (1999). Two functionally distinct forms of the RSC nucleosome-remodeling complex, containing essential AT hook, BAH, and bromodomains. Mol. Cell **4**: 715–723.

Cardon, G., Höhmann, S., Klein, J., Nettesheim, K., Saedler, H., and Huijser, P. (1999). Molecular characterisation of the *Arabidopsis SBP-box* genes. Gene **237**: 91–104.

Casson, S.A. and Lindsey, K. (2006). The turnip mutant of *Arabidopsis* reveals that *LEAFY COTYLEDON1* expression mediates the effects of auxin and sugars to promote embryonic cell identity. Plant Physiol. **142**: 526–541.

Chavali, P.L., Funa, K., and Chavali, S. (2011). Cis-regulation of *microRNA* expression by scaffold/matrix-attachment regions. Nucleic Acids Res. **39**: 6908–6918.

Davière, J.-M. and Achard, P. (2013). Gibberellin signaling in plants. Development **140**: 1147–1151.

Davies, P.J. and Gan, S. (2012). Towards an integrated view of monocarpic plant senescence. Russ. J. Plant Physiol. **59**: 467–478.

Deng, W., Luo, K., Li, Z., and Yang, Y. (2009). A novel method for induction of plant regeneration via somatic embryogenesis. Plant Sci. **177**: 43–48.

Deng, W., Ying, H., Helliwell, C.A., Taylor, J.M., Peacock, W.J., and Dennis, E.S. (2011). FLOWERING LOCUS C (FLC) regulates development pathways throughout the life cycle of *Arabidopsis*. Proc. Natl. Acad. Sci. **2011**: 1–6.

Dharmasiri, N., Dharmasiri, S., and Estelle, M. (2005). The F-box protein TIR1 is an auxin receptor. Nature **435**: 441–445.

Distelfeld, A., Avni, R., and Fischer, A.M. (2014). Senescence , nutrient remobilization , and yield in wheat and barley. J. Exp. Bot. **65**: 3783–3798.

Dubrovina, A.S. and Kiselev, K. V (2016). Age-associated alterations in the somatic mutation and DNA methylation levels in plants. Plant Biol. **18**: 185–196.

Efroni, I. et al. (2016). Root regeneration triggers an embryo-like sequence guided by hormonal

interactions. Cell: 1–13.

Elhiti, M., Hebelstrup, K.H., Wang, A., Li, C., Cui, Y., Hill, R.D., and Stasolla, C. (2013a). Function of type-2 *Arabidopsis* hemoglobin in the auxin-mediated formation of embryogenic cells during morphogenesis. Plant J. **74**: 946–958.

Elhiti, M., Stasolla, C., and Wang, A. (2013b). Molecular regulation of plant somatic embryogenesis. Vitr. Cell. Dev. Biol. - Plant **49**: 631–642.

Elhiti, M., Tahir, M., Gulden, R.H., Khamiss, K., and Stasolla, C. (2010). Modulation of embryo-forming capacity in culture through the expression of *Brassica* genes involved in the regulation of the shoot apical meristem. J. Exp. Bot. **61**: 4069–4085.

Exner, V. and Hennig, L. (2008). Chromatin rearrangements in development. Curr. Opin. Plant Biol.: 64–69.

Feher, Attila, Taras P. Pasternak, and D.D. (2003). Transition of somatic plant cells to an embryogenic state. Plant Cell. Tissue Organ Cult. **74**: 201–228.

Fehér, A. (2015). Somatic embryogenesis - Stress-induced remodeling of plant cell fate. Biochim. Biophys. Acta **1849**: 385–402.

Fischer, A.M. and Fischer, A.M. (2017). The complex regulation of senescence. CRC. Crit. Rev. Plant Sci. **2689**: 124–147.

Friml, J. (2010). Subcellular trafficking of PIN auxin efflux carriers in auxin transport. Eur. J. Cell Biol. **89**: 231–235.

Friml, J., Vieten, A., Sauer, M., Weijers, D., Schwarz, H., Hamann, T., Offringa, R., and Jürgens, G. (2003). Efflux-dependent auxin gradients establish the apical-basal axis of *Arabidopsis*. Nature **426**: 147–153.

Fu, C., Sunkar, R., Zhou, C., Shen, H., Zhang, J.-Y., Matts, J., Wolf, J., Mann, D.G.J., Stewart, C.N., Tang, Y., and Wang, Z.-Y. (2012). Overexpression of miR156 in switchgrass (Panicum virgatum L.) results in various morphological alterations and leads to improved biomass production. Plant Biotechnol. J. **10**: 443–452.

Fujimoto, S., Matsunaga, S., Yonemura, M., Uchiyama, S., Azuma, T., and Fukui, K. (2004). Identification of a novel plant MAR DNA binding protein localized on chromosomal surfaces. Plant Mol. Biol. **56**: 225–239.

Gaj, M.D., Zhang, S., Harada, J.J., and Lemaux, P.G. (2005). *Leafy cotyledon* genes are essential for induction of somatic embryogenesis of *Arabidopsis*. Planta **222**: 9779–9788.

Galinha, C., Hofhuis, H., Luijten, M., Willemsen, V., Blilou, I., Heidstra, R., and Scheres, B. (2007). PLETHORA proteins as dose-dependent master regulators of *Arabidopsis* root development. Nature **449**: 1053–1057.

Gallavotti, A., Malcomber, S., Gaines, C., Stanfield, S., Whipple, C., Kellogg, E., and Schmidt, R.J. (2011). BARREN STALK FASTIGIATE1 is an AT-hook protein required for the formation of maize ears. Plant Cell **23**: 1756–1771.

Galvão, V.C., Horrer, D., Küttner, F., and Schmid, M. (2012). Spatial control of flowering by DELLA proteins in *Arabidopsis thaliana*. Development **4082**: 4072–4082.

Gandikota, M., Birkenbihl, R.P., Höhmann, S., Cardon, G.H., Saedler, H., and Huijser, P. (2007). The *miRNA156/157* recognition element in the 3' UTR of the *Arabidopsis SBP* box gene *SPL3* prevents early flowering by translational inhibition in seedlings. Plant J. **49**: 683–693.

Gaspar-Maia, A., Alajem, A., Meshorer, E., and Ramalho-Santos, M. (2011). Open chromatin in pluripotency and reprogramming. Nat. Rev. Mol. Cell Biol. **12**: 36–47.

Girod, P., Nguyen, D., Calabrese, D., Puttini, S., Martinet, D., Regamey, A., Saugy, D., Beckmann, J.S., Bucher, P., and Mermod, N. (2007). Genome-wide prediction of matrix attachment

regions that increase gene expression in mammalian cells. Nat. Methods **4**: 747–753.

Gliwicka, M., Nowak, K., Balazadeh, S., Mueller-Roeber, B., and Gaj, M.D. (2013). Extensive modulation of the transcription factor transcriptome during somatic embryogenesis in *Arabidopsis thaliana*. PLoS One **8**: e69261.

van Der Graaff, E., Laux, T., and Rensing, S.A. (2009). The WUS homeobox-containing (WOX) protein family. Genome Biol. **10**: 248.

Guilfoyle, T.J. and Hagen, G. (2007). Auxin response factors. Curr. Opin. Plant Biol. **10**: 453–460.

Guo, F., Liu, C., Xia, H., Bi, Y., Zhao, C., Zhao, S., Hou, L., Li, F., and Wang, X. (2013). Induced expression of *AtLEC1* and *AtLEC2* differentially promotes somatic embryogenesis in transgenic tobacco plants. PLoS One **8**: e71714.

Haecker, A., Gross-Hardt, R., Geiges, B., Sarkar, A., Breuninger, H., Herrmann, M., and Laux, T. (2004). Expression dynamics of *WOX* genes mark cell fate decisions during early embryonic patterning in *Arabidopsis thaliana*. Development **131**: 657–68.

Han, H.-J., Russo, J., Kohwi, Y., and Kohwi-Shigematsu, T. (2008). SATB1 reprogrammes gene expression to promote breast tumour growth and metastasis. Nature **452**: 187–193.

Han, S.-K., Wu, M.-F., Cui, S., and Wagner, D. (2015). Roles and activities of chromatin remodeling ATPases in plants. Plant J. **83**: 62–77.

Hasbu, R., Rodrı, R., and Valledor, L. (2010). Variations in DNA methylation, acetylated histone H4, and methylated histone H3 during Pinus radiata needle maturation in relation to the loss of in vitro organogenic capability. J. Plant Physiol. **167**: 351–357.

Heidmann, I., de Lange, B., Lambalk, J., Angenent, G.C., and Boutilier, K. (2011). Efficient sweet pepper transformation mediated by the *BABY BOOM* transcription factor. Plant Cell Rep. **30**: 1107–1015.

Heng, H.H.Q., Goetze, S., Ye, C.J., Liu, G., Stevens, J.B., Bremer, S.W., Wykes, S.M., Bode, J., and Krawetz, S. (2004). Chromatin loops are selectively anchored using scaffold/matrix-attachment regions. J. Cell Sci. **117**: 999–1008.

Ho, L. and Crabtree, G.R. (2010). Chromatin remodelling during development. Nature **463**: 474–484.

Holec, S. and Berger, F. (2012). Polycomb group complexes mediate developmental transitions in plants. Plant Physiol. **158**: 35–43.

Horstman, A. (2015). BBM-induced somatic embryogenesis in *Arabidopsi*. phD Thesis, Wageningen University.

Horstman, A., Fukuoka, H., Muino, J.M., Nitsch, L., Guo, C., Passarinho, P., Sanchez-Perez, G., Immink, R., Angenent, G., and Boutilier, K. (2015). AIL and HDG proteins act antagonistically to control cell proliferation. Development **142**: 454–464.

Hove, C.A., Lu, K., and Weijers, D. (2015). Building a plant : cell fate specification in the early *Arabidopsis* embryo. Development **142**: 420–430.

Hsu, C.-Y. et al. (2011). *FLOWERING LOCUS T* duplication coordinates reproductive and vegetative growth in perennial poplar. Proc. Natl. Acad. Sci. **108**: 10756–10761.

Huang, L.-C., Hsiao, L.-J., Pu, S.-Y., Kuo, C.-I., Huang, B.-L., Tseng, T.-C., Huang, H.-J., and Chen, Y.-T. (2012). DNA methylation and genome rearrangement characteristics of phase change in cultured shoots of *Sequoia sempervirens*. Physiol. Plant. **145**: 360–368.

Huijser, P. and Schmid, M. (2011). The control of developmental phase transitions in plants. Development **138**: 4117–4129.

Imin, N., Goffard, N., Nizamidin, M., and Rolfe, B.G. (2008). Genome-wide transcriptional analysis of super-embryogenic *Medicago truncatula* explant cultures. BMC Plant Biol. **8**: 110.

Ingouff, M., Rademacher, S., Holec, S., Xin, N., Readshaw, A., and Foo, S.H. (2010). Report zygotic resetting of the HISTONE 3 variant repertoire participates in epigenetic reprogramming in *Arabidopsis*. Curr. Biol. **23**: 2137–2143.

Jarillo, J.A., Piñeiro, M., Cubas, P., and Martínez-zapater, J. (2009). Chromatin remodeling in plant development. Int. J. Dev. Biol. **1596**: 1581–1596.

Jenik, P.D. and Barton, M.K. (2005). Surge and destroy: the role of auxin in plant embryogenesis. Development **132**: 3577–3585.

Jenik, P.D., Gillmor, C.S., and Lukowitz, W. (2007). Embryonic patterning in *Arabidopsis thaliana*. Annu. Rev. Cell Dev. Biol. **23**: 207–236.

Jibran, R., Hunter, D.A., and Dijkwel, P.P. (2013). Hormonal regulation of leaf senescence through integration of developmental and stress signals. Plant Mol. Biol. **82**: 547–561.

Jiménez, V.M. (2005). Involvement of plant hormones and plant growth regulators on *in vitro* somatic embryogenesis. Plant Growth Regul. **47**: 91–110.

Jin, Y. et al. (2011). An *AT-hook* gene is required for palea formation and floral organ number control in rice. Dev. Biol. **359**: 277–88.

Jullien, P.E. (2010). DNA methylation reprogramming during plant sexual reproduction ? Trends Genet. **26**: 394–399.

Jung, C. and Müller, A.E. (2009). Flowering time control and applications in plant breeding. Trends Plant Sci. **14**: 563–573.

Jung, J., Ju, Y., Seo, P.J., Lee, J., Park, C., and Genomics, P. (2012). The SOC1-SPL module integrates photoperiod and gibberellic acid signals to control flowering time in *Arabidopsis*. Plant J.: 577–588.

Kaufmann, K., Pajoro, A., and Angenent, G.C. (2010). Regulation of transcription in plants: mechanisms controlling developmental switches. Nat. Rev. Genet. **11**: 830–842.

Kepinski, S. and Leyser, O. (2005). The Arabidopsis F-box protein TIR1 is an auxin receptor. Nature **435**: 1–6.

Kierzkowski, D., Lenhard, M., Smith, R., and Kuhlemeier, C. (2013). Interaction between meristem tissue layers controls phyllotaxis. Dev. Cell **26**: 616–628.

Kim, D.-H. and Sung, S. (2014). Genetic and epigenetic mechanisms underlying vernalization. *Arabidopsis* Book **12**: e0171.

Kim, J., Woo, H.R., and Nam, H.G. (2016). Toward systems understanding of leaf senescence : An integrated multi-omics perspective on leaf senescence research. Mol. Plant **9**: 813–825.

Kohwi-Shigematsu, T., Kohwi, Y., Takahashi, K., Richards, H.W., Ayers, S.D., Han, H.-J., and Cai, S. (2012). SATB1-mediated functional packaging of chromatin into loops. Methods **58**: 243–254.

Kumar, P.P., Bischof, O., Purbey, P.K., Notani, D., Urlaub, H., Dejean, A., and Galande, S. (2007). Functional interaction between PML and SATB1 regulates chromatin-loop architecture and transcription of the MHC class I locus. Nat. Cell Biol. **9**: 45–56.

Lau, S., Slane, D., Herud, O., Kong, J., and Jürgens, G. (2012). Early embryogenesis in flowering plants: setting up the basic body pattern. Annu. Rev. Plant Biol. **63**: 483–506.

Ledwoń, A. and Gaj, M.D. (2011). L*EAFY COTYLEDON1, FUSCA3* expression and auxin treatment in relation to somatic embryogenesis induction in *Arabidopsis*. Plant Growth Regul. **65**: 157–167.

Legrand, S., Hendriks, T., Hilbert, J.-L., and Quillet, M.-C. (2007). Characterization of expressed sequence tags obtained by SSH during somatic embryogenesis in *Cichorium intybus* L. BMC Plant Biol. **7**: 27.

Lim, P.O., Kim, Y., Breeze, E., Koo, J.C., Woo, H.R., Ryu, J.S., Park, D.H., Beynon, J., Tabrett, A.,

Buchanan-Wollaston, V., and Nam, H.G. (2007). Overexpression of a chromatin architecture-controlling AT-hook protein extends leaf longevity and increases the post-harvest storage life of plants. Plant J. **52**: 1140–1153.

Locascio, A., Roig-villanova, I., Bernardi, J., and Varotto, S. (2014). Current perspectives on the hormonal control of seed development in *Arabidopsis* and maize : a focus on auxin. Front. Plant Sci. **5**: 1–22.

Lopes, M.A. and Larkins, B.A. (1993). Endosperm Origin , Development , and Function. Plant Cell **5**: 1383–1399.

Lotan, T., Ohto, M., Yee, K.M., West, M. a, Lo, R., Kwong, R.W., Yamagishi, K., Fischer, R.L., Goldberg, R.B., and Harada, J.J. (1998). *Arabidopsis* LEAFY COTYLEDON1 is sufficient to induce embryo development in vegetative cells. Cell **93**: 1195–1205.

Lucas, J., Bilzer, A., Moll, L., Zündorf, I., Dingermann, T., Eichinger, L., Siol, O., and Winckler, T. (2009). The carboxy-terminal domain of dictyostelium C-module-binding factor is an independent gene regulatory entity. PLoS One **4**: e5012.

Lucau-Danila, A., Laborde, L., Legrand, S., Huot, L., Hot, D., Lemoine, Y., Hilbert, J.-L., Hawkins, S., Quillet, M.-C., Hendriks, T., and Blervacq, A.-S. (2010). Identification of novel genes potentially involved in somatic embryogenesis in chicory (*Cichorium intybus* L.). BMC Plant Biol. **10**: 122.

Maffini, M., Denes, V., Sonnenschein, C., Soto, A., and Geck, P. (2008). *APRIN* is a unique *Pds5* paralog with features of a chromatin regulator in hormonal differentiation. J. Steroid Biochem. Mol. Biol. **108**: 32–43.

Matsoukas, I.G., Massiah, A.J., and Thomas, B. (2012). Florigenic and antiflorigenic signaling in plants. Plant Cell Physiol. **53**: 1827–1842.

Matsushita, A., Furumoto, T., Ishida, S., and Takahashi, Y. (2007). AGF1, an AT-hook protein, is necessary for the negative feedback of *AtGA3ox1* encoding GA 3-oxidase. Plant Physiol. **143**: 1152–1162.

Mayer, K.F., Schoof, H., Haecker, A., Lenhard, M., Jürgens, G., and Laux, T. (1998). Role of WUSCHEL in regulating stem cell fate in the *Arabidopsis* shoot meristem. Cell **95**: 805–815.

Melzer, S., Lens, F., Gennen, J., Vanneste, S., Rohde, A., and Beeckman, T. (2008). Flowering-time genes modulate meristem determinacy and growth form in *Arabidopsis thaliana*. Nat. Genet. **40**: 1489–1492.

Michaels, S.D. and Amasino, R.M. (1999). *FLOWERING LOCUS C* encodes a novel MADS domain protein that acts as a repressor of flowering. Plant Cell **11**: 949–956.

Mironova, V., Teale, W., Shahriari, M., Dawson, J., and Palme, K. (2017). The systems biology of auxin in developing embryos. Trends Plant Sci. **22**: 225–235.

Mo, B. and Weijers, D. (2009). Auxin control of embryo patterning. Cold Spring Harb. Perspect. Biol. **1**: 1–14.

Mordhorst, A. P., Voerman, K. J., Hartog, M. V., Meijer, E. A., Van Went, J., Koornneef, M., and De Vries, S.C. (1998). Somatic embryogenesis in *Arabidopsis* thaliana is facilitated by mutations in genes repressing meristematic cell divisions. Genetics **149**: 549–563.

Mozgová, I., Muñoz-Viana, R., and Hennig, L. (2017). PRC2 represses hormone-induced somatic embryogenesis in vegetative tissue of *Arabidopsis thaliana*. PLoS genetics, **13**, e1006562.

Munné-Bosch, S. (2008). Do perennials really senesce? Trends Plant Sci. **13**: 216–220.

Namasivayam, P. (2007). Acquisition of embryogenic competence during somatic embryogenesis. Plant Cell. Tissue Organ Cult. **90**: 1–8.

Ng, K.-H., Yu, H., and Ito, T. (2009). AGAMOUS controls *GIANT KILLER*, a multifunctional chromatin modifier in reproductive organ patterning and differentiation. PLoS Biol. **7**: e1000251.

Nic-Can, G.I., López-Torres, A., Barredo-Pool, F., Wrobel, K., Loyola-Vargas, V.M., Rojas-Herrera, R., and De-la-Peña, C. (2013). New insights into somatic embryogenesis: *leafy cotyledon1*, *baby boom1* and *WUSCHEL-related homeobox4* are epigenetically regulated in *Coffea canephora*. PLoS One **8**: e72160.

El Ouakfaoui, S., Schnell, J., Abdeen, A., Colville, A., Labbé, H., Han, S., Baum, B., Laberge, S., and Miki, B. (2010). Control of somatic embryogenesis and embryo development by *AP2* transcription factors. Plant Mol. Biol. **74**: 313–326.

Ozias-Akins, P. (2006). Apomixis: developmental characteristics and genetics. CRC. Crit. Rev. Plant Sci. **25**: 199–214.

Ozturk, N., Singh, I., Mehta, A., Braun, T., and Barreto, G. (2014). HMGA proteins as modulators of chromatin structure during transcriptional activation. Front. Cell Dev. Biol. **2**: 1–9.

Park, J., Oh, D., Dassanayake, M., Nguyen, K.T., Ogas, J., and Choi, G. (2017). Gibberellin signaling requires chromatin remodeler PICKLE to promote vegetative growth and phase transitions. Plant Physiol. **173**: 1463–1474.

Peer, W.A., Blakeslee, J.J., Yang, H., and Murphy, A.S. (2011). Seven things we think we know about auxin transport. Mol. Plant **4**: 487–504.

Penfold, C.A. and Buchanan-wollaston, V. (2014). Modelling transcriptional networks in leaf senescence. J. Exp. Bot. **65**: 3859–3873.

Péret, B. et al. (2012). *AUX/LAX* genes encode a family of auxin influx transporters that perform distinct functions during *Arabidopsis* development. Plant Cell **24**: 2874–2885.

Philipsen, C. (2017). Unraveling the auxin mechanism in 2,4-D induced somatic embryogenesis in *Arabidopsis Thaliana*. phD Thesis, Leiden University.

Pillot, M., Baroux, C., Vazquez, M.A., Autran, D., Leblanc, O., Vielle-Calzada, J.P., Grossniklaus, U., and Grimanelli, D. (2010). Embryo and endosperm inherit distinct chromatin and transcriptional states from the female gametes in *Arabidopsis*. Plant Cell **22**: 307–320.

Poethig, R.S. (2013). Vegetative phase change and shoot maturation in plants. Curr. Top. Dev. Biol. **105**: 125–152.

Pujol, B. (2015). Genes and quantitative genetic variation involved with senescence in cells, organs, and the whole plant. Front. Genet. **6**: 1–10.

Radoeva, T. and Weijers, D. (2014). A roadmap to embryo identity in plants. Trends Plant Sci. **19**: 709–716.

Raissig, M. T., Bemer, M., Baroux, C., and Grossniklaus, U. (2013). Genomic imprinting in the *Arabidopsis* embryo is partly regulated by PRC2. PLoS Genet. **9**: 21–23.

Rajjou, L., Duval, M., Gallardo, K., Catusse, J., Bally, J., Job, C., and Job, D. (2012). Seed germination and vigor. Annu. Rev. Plant Biol. **63**: 507–533.

Reeves, R. (2010). Nuclear functions of the HMG proteins. Biochim. Biophys. Acta - Gene Regul. Mech. **1799**: 3–14.

Reyes, C. (2006). Chromatin modifiers that control plant development. Curr. Opin. Plant Biol. **9**: 21–27.

Robert, H.S., Grones, P., Stepanova, A.N., Robles, L.M., Lokerse, A.S., Alonso, J.M., Weijers, D., and Friml, J. (2013). Local auxin sources orient the apical-basal axis in *Arabidopsis* embryos. Curr. Biol. **23**: 2506–2512.

Rose, R.J. and Nolan, K.E. (2006). Invited review: Genetic regulation of somatic embryogenesis with particular reference to *Arabidopsis thaliana* and *Medicago truncatula*. Vitr. Cell. Dev. Biol. Plant **42**: 473–481.

Rybel, B.D., Mähönen, A.P., Helariutta, Y., and Weijers, D. (2015). Plant vascular development : from early specification to differentiation. Nat. Rev. Mol. Cell Biol. **17**: 30–40.

Sabelli, P.A. and Larkins, B.A. (2009). The Development of endosperm in grasses. Plant Physiol. **149**: 14–26.

Saeteurn, K.H.S. , and huck G.C.A. (2007). The heterochronic maize mutant *Corngrass1* results from overexpression of a tandem microRNA. Nat. Genet. **39**: 544–549.

Santos-Mendoza, M., Dubreucq, B., Baud, S., Parcy, F., Caboche, M. & Lepiniec, L.((2008). Deciphering gene regulatory networks that control seed development and maturation in *Arabidopsis*. Plant J. **54**: 608–620.

dos Santos Maraschin, F., Memelink, J., and Offringa, R. (2009). Auxin-induced, SCFTIR1-mediated poly-ubiquitination marks AUX/IAA proteins for degradation. Plant J. **59**: 100–109.

Sarkar, A.K., Luijten, M., Miyashima, S., Lenhard, M., Hashimoto, T., Nakajima, K., Scheres, B., Heidstra, R., and Laux, T. (2007). Conserved factors regulate signalling in *Arabidopsis thaliana* shoot and root stem cell organizers. Nature **446**: 811–814.

Saya, A.R., Doulbeau, S., Lartaud, M., Verdeil, J., and Monteuuis, O. (2011). Variations of DNA methylation in *Eucalyptus urophylla* × *Eucalyptus grandis* shoot tips and apical meristems of different physiological ages. Physiol. Plant. **143**: 178–187.

Schippers, J.H.M. (2015). Transcriptional networks in leaf senescence. Curr. Opin. Plant Biol. **27**: 77–83.

Sgarra, R., Zammitti, S., Lo Sardo, A., Maurizio, E., Arnoldo, L., Pegoraro, S., Giancotti, V., and Manfioletti, G. (2010). HMGA molecular network: From transcriptional regulation to chromatin remodeling. Biochim. Biophys. Acta **1799**: 37–47.

Sharma, S.K., Millam, S., Hedley, P.E., McNicol, J., and Bryan, G.J. (2008). Molecular regulation of somatic embryogenesis in potato: An auxin led perspective. Plant Mol. Biol. **68**: 185–201.

She, W. and Baroux, C. (2014). Chromatin dynamics during plant sexual reproduction. Front. Plant Sci. **5**: 354.

Shealy, R.T., Khanna, A., and Vodkin, L.O. (2003). Clustering of microarray data reveals transcript patterns associated with somatic embryogenesis in soybean. Plant Physiol. **132**: 118–136.

Singh, M., D'Silva, L., and Holak, T. a (2006). DNA-binding properties of the recombinant high-mobility-group-like AT-hook-containing region from human BRG1 protein. Biol. Chem. **387**: 1469–1478.

Singla, B., Tyagi, A.K., Khurana, J.P., and Khurana, P. (2007). Analysis of expression profile of selected genes expressed during auxin-induced somatic embryogenesis in leaf base system of wheat (*Triticum aestivum*) and their possible interactions. Plant Mol. Biol. **65**: 677–692.

Smertenko, A. and Bozhkov, P. V (2014). Somatic embryogenesis: life and death processes during apical-basal patterning. J. Exp. Bot. **65**: 1343–1360.

Smit, M.E. and Weijers, D. (2015). The role of auxin signaling in early embryo pattern formation. Curr. Opin. Plant Biol. **28**: 99–105.

Song, Y.H., Ito, S., and Imaizumi, T. (2013). Flowering time regulation: photoperiod- and temperature-sensing in leaves. Trends Plant Sci. **18**: 575–583.

Srinivasan, C., Liu, Z., Heidmann, I., Supena, E.D.J., Fukuoka, H., Joosen, R., Lambalk, J., Angenent, G., Scorza, R., Custers, J.B.M., and Boutilier, K. (2007). Heterologous expression of the *BABY BOOM AP2*/*ERF* transcription factor enhances the regeneration capacity of tobacco (*Nicotiana tabacum* L.). Planta **225**: 341–351.

Steward, F.C., Mapes, M.O., and Mears, K. (1958). Growth and organized development of cultured cells. II. organization in cultures grown from freely suspended cells. Am. J. Bot. **45**: 705–708.

Stone, S.L., Braybrook, S.A., Paula, S.L., Kwong, L.W., Meuser, J., Pelletier, J., Hsieh, T.-F., Fischer, R.L., Goldberg, R.B., and Harada, J.J. (2008). Arabidopsis *LEAFY COTYLEDON2* induces maturation traits and auxin activity: Implications for somatic embryogenesis. Proc. Natl. Acad. Sci. **105**: 3151–3156.

Stone, S.L., Kwong, L.W., Yee, K.M., Pelletier, J., Lepiniec, L., Fischer, R.L., Goldberg, R.B., and Harada, J.J. (2001). *LEAFY COTYLEDON2* encodes a B3 domain transcription factor that induces embryo development. Proc. Natl. Acad. Sci. **98**: 11806–11811.

Street, I.H., Shah, P.K., Smith, A.M., Avery, N., and Neff, M.M. (2008). The AT-hook-containing proteins SOB3/AHL29 and ESC/AHL27 are negative modulators of hypocotyl growth in *Arabidopsis*. Plant J. **54**: 1–14.

Su, Y., Kwon, C.S., Bezhani, S., Huvermann, B., Chen, C., Peragine, A., Kennedy, J.F., and Wagner, D. (2006). The N-terminal ATPase AT-hook-containing region of the *Arabidopsis* chromatin-remodeling protein SPLAYED is sufficient for biological activity. Plant J. **46**: 685–699.

Su, Y.H., Liu, Y.B., Zhou, C., Li, X.M., and Zhang, X.S. (2016). The microRNA167 controls somatic embryogenesis in *Arabidopsis* through regulating its target genes *ARF6* and *ARF8*. Plant Cell. Tissue Organ Cult. **124**: 405–417.

Sun, T. -p. (2010). Gibberellin-GID1-DELLA: A pivotal regulatory module for plant growth and development. Plant Physiol. **154**: 567–570.

Takada, S. and Jürgens, G. (2007). Transcriptional regulation of epidermal cell fate in the *Arabidopsis* embryo. Development **134**: 1141–1150.

Takada, S., Takada, N., and Yoshida, A. (2013). *ATML1* promotes epidermal cell differentiation in *Arabidopsis* shoots. Development **140**: 1919–1923.

Teale, W.D., Paponov, I.A., and Palme, K. (2006). Auxin in action: signalling, transport and the control of plant growth and development. Nat. Rev. Mol. Cell Biol. **7**: 847–859.

Telfer, A., Bollman, K.M., and Poethig, R.S. (1997). Phase change and the regulation of trichome distribution in *Arabidopsis thaliana*. Development **124**: 645–654.

Thomas, H. (2013). Senescence , ageing and death of the whole plant. New Phytol.: 696–711.

Tooke, F., Ordidge, M., Chiurugwi, T., and Battey, N. (2005). Mechanisms and function of flower and inflorescence reversion. J. Exp. Bot. **56**: 2587–2599.

Tsuwamoto, R., Yokoi, S., and Takahata, Y. (2010). *Arabidopsis EMBRYOMAKER* encoding an *AP2* domain transcription factor plays a key role in developmental change from vegetative to embryonic phase. Plant Mol. Biol. **73**: 481–492.

Turnbull, C. (2011). Long-distance regulation of flowering time. J. Exp. Bot. **62**: 4399–43413.

Uddenberg, D., Valladares, S., Abrahamsson, M., Sundström, J.F., Sundås-Larsson, A., and von Arnold, S. (2011). Embryogenic potential and expression of embryogenesis-related genes in conifers are affected by treatment with a histone deacetylase inhibitor. Planta **234**: 527–539.

Ueda, M., Zhang, Z., and Laux, T. (2011). Transcriptional activation of *Arabidopsis* axis patterning genes *WOX8*/*9* links zygote polarity to embryo development. Dev. Cell **20**: 264–2670.

Usami, T., Horiguchi, G., Yano, S., and Tsukaya, H. (2009). The more and smaller cells mutants of *Arabidopsis thaliana* identify novel roles for *SQUAMOSA PROMOTER BINDING PROTEIN-LIKE* genes in the control of heteroblasty. Development **136**: 955–964.

Vanneste, S. and Friml, J. (2009). Auxin: a trigger for change in plant development. Cell **136**: 1005–1016.

Wabnik, K., Robert, H.S., Smith, R.S., and Friml, J. (2013). Modeling framework for the establishment of the apical-basal embryonic axis in plants. Curr. Biol. **23**: 2513–2518.

Wang, B., Zhang, Z., Yin, Z., Feng, C., and Wang, Q. (2012). Novel and potential application of cryopreservation to plant genetic transformation. Biotechnol. Adv. **30**: 604–612.

Wang, H. and Wang, H. (2015). The miR156/SPL module, a regulatory hub and versatile toolbox, gears up crops for enhanced agronomic traits. Mol. Plant **8**: 677–688.

Wang, J.-W. (2014). Regulation of flowering time by the miR156-mediated age pathway. J. Exp. Bot. **65**: 4723–4730.

Wang, J.-W., Czech, B., and Weigel, D. (2009a). miR156-regulated *SPL* transcription factors define an endogenous flowering pathway in *Arabidopsis thaliana*. Cell **138**: 738–749.

Wang, J.-W., Park, M.Y., Wang, L.-J., Koo, Y., Chen, X.-Y., Weigel, D., and Poethig, R.S. (2011). miRNA control of vegetative phase change in trees. PLoS Genet. **7**: e1002012.

Wang, J.-W., Schwab, R., Czech, B., Mica, E., and Weigel, D. (2008). Dual effects of miR156-targeted *SPL* genes and *CYP78A5*/*KLUH* on plastochron length and organ size in *Arabidopsis thaliana*. Plant Cell **20**: 1231–1243.

Wang, R., Farrona, S., Vincent, C., Joecker, A., Schoof, H., Turck, F., Alonso-Blanco, C., Coupland, G., and Albani, M.C. (2009b). PEP1 regulates perennial flowering in *Arabis alpina*. Nature **459**: 423–427.

Wang, T.-Y., Han, Z.-M., Chai, Y.-R., and Zhang, J.-H. (2010). A mini review of MAR-binding proteins. Mol. Biol. Rep. **37**: 3553–3560.

Weigel, D. et al. (2000). Activation tagging in *Arabidopsis*. Plant Physiol. **122**: 1003–1013.

Weitbrecht, K., Müller, K., and Leubner-Metzger, G. (2011). First off the mark: Early seed germination. J. Exp. Bot. **62**: 3289–3309.

Wilson, R.H.C. and Coverley, D. (2013). Relationship between DNA replication and the nuclear matrix. Genes Cells **18**: 17–31.

Wójcikowska, B., Jaskóła, K., Gąsiorek, P., Meus, M., Nowak, K., and Gaj, M.D. (2013). *LEAFY COTYLEDON2* (*LEC2*) promotes embryogenic induction in somatic tissues of *Arabidopsis*, via YUCCA-mediated auxin biosynthesis. Planta **238**: 425–440.

Wollmann, H. (2012). Epigenetic reprogramming during plant reproduction and seed development. Curr. Opin. Plant Biol. **15**: 63–69.

Wu, G., Park, M.Y., Conway, S.R., Wang, J.-W., Weigel, D., and Poethig, R.S. (2009). The sequential action of miR156 and miR172 regulates developmental timing in *Arabidopsis*. Cell **138**: 750–759.

Wu, G. and Poethig, R.S. (2006). Temporal regulation of shoot development in *Arabidopsis* thaliana by miR156 and its target SPL3. Development **133**: 3539–3547.

Xiao, C., Chen, F., Yu, X., Lin, C., and Fu, Y.-F. (2009). Over-expression of an AT-hook gene, *AHL22*, delays flowering and inhibits the elongation of the hypocotyl in *Arabidopsis thaliana*. Plant Mol. Biol. **71**: 39–50.

Xiao, H., Sandaltzopoulos, R., Wang, H.M., Hamiche, A., Ranallo, R., Lee, K.M., Fu, D., and Wu, C. (2001). Dual functions of largest NURF subunit NURF301 in nucleosome sliding and transcription factor interactions. Mol. Cell **8**: 531–543.

Xie, K., Shen, J., Hou, X., Yao, J., Li, X., Xiao, J., and Xiong, L. (2012). Gradual increase of *miR156* regulates temporal expression changes of numerous genes during leaf development in rice. Plant Physiol. **158**: 1382–1394.

Xie, K., Wu, C., and Xiong, L. (2006). Genomic organization, differential expression, and interaction of S*QUAMOSA Promoter-Binding-Like* transcription factors and *microRNA156* in rice. Plant Physiol. **142**: 280–293.

Xu, M., Hu, T., Zhao, J., Park, M.-Y., Earley, K.W., Wu, G., Yang, L., and Poethig, R.S. (2016). Developmental functions of miR156-regulated *SQUAMOSA PROMOTER BINDING PROTEIN-LIKE* (*SPL*) genes in *Arabidopsis thaliana*. PLoS Genet. **12**: e1006263.

Xu, Y., Wang, Y., Stroud, H., Gu, X., Sun, B., Gan, E.-S., Ng, K.-H., Jacobsen, S.E., He, Y., and Ito, T. (2013). A matrix protein silences transposons and repeats through interaction with retinoblastoma-associated proteins. Curr. Biol. **23**: 345–350.

Yang, L., Xu, M., Koo, Y., He, J., and Poethig, R.S. (2013). Sugar promotes vegetative phase change in *Arabidopsis thaliana* by repressing the expression of *MIR156A* and *MIR156C*. Elife **2**: e00260.

Yang, X. and Zhang, X. (2010). Regulation of somatic embryogenesis in higher plants. CRC. Crit. Rev. Plant Sci. **29**: 36–57.

Yasui, D., Miyano, M., Cai, S., Varga-Weisz, P., and Kohwi-Shigematsu, T. (2002). SATB1 targets chromatin remodelling to regulate genes over long distances. Nature **419**: 641–645.

Yu, S., Galvão, V.C., Zhang, Y.-C., Horrer, D., Zhang, T.-Q., Hao, Y.-H., Feng, Y.-Q., Wang, S., Schmid, M., and Wang, J.-W. (2012). Gibberellin regulates the *Arabidopsis* floral transition through miR156-targeted *SQUAMOSA promoter binding-like transcription factors*. Plant Cell **24**: 3320–32.

Yuan, J., Sun, H., Guo, G., Yue, J., and Gu, X. (2014). Correlation between DNA methylation and chronological age of *Moso bamboo* (*Phyllostachys heterocycla* var . pubescens). Bot. Stud. **55**: 1–7.

Yun, J., Kim, Y.-S., Jung, J.-H., Seo, P.J., and Park, C.-M. (2012). The AT-hook motif-containing protein AHL22 regulates flowering initiation by modifying *FLOWERING LOCUS T* chromatin in *Arabidopsis*. J. Biol. Chem. **287**: 15307–16.

van der Zaal, B., and Hooykaas, P.J.J (2004). US Patet nr:Control of plant growth and developmental processe.WO2004/066985.

Zavattieri, M.A., Frederico, A.M., Lima, M., Sabino, R., and Arnholdt-Schmitt, B. (2010). Induction of somatic embryogenesis as an example of stress-related plant reactions. Electron. J. Biotechnol. **13**: 1–9.

Zhang, X., Zou, Z., Zhang, J., Zhang, Y., Han, Q., Hu, T., Xu, X., Liu, H., Li, H., and Ye, Z. (2011). Over-expression of *sly-miR156a* in tomato results in multiple vegetative and reproductive trait alterations and partial phenocopy of the *sft* mutant. FEBS Lett. **585**: 435–439.

Zhang, Y., Clemens, A., Maximova, S.N., and Guiltinan, M.J. (2014). The *Theobroma cacao B3 domain* transcription factor *TcLEC2* plays a duel role in control of embryo development and maturation. BMC Plant Biol. **14**: 1–16.

Zhao, J., Favero, D.S., Peng, H., and Neff, M.M. (2013). *Arabidopsis thaliana* AHL family modulates hypocotyl growth redundantly by interacting with each other via the PPC/DUF296 domain. Proc. Natl. Acad. Sci. **110**: 4688–4697.

Zhao, J., Favero, D.S., Qiu, J., Roalson, E.H., and Neff, M.M. (2014). Insights into the evolution and diversification of the AT-hook Motif Nuclear Localized gene family in land plants. BMC Plant Biol. **14**: 266.

Zhao, Y. (2012). Auxin biosynthesis and its role in plant development. Annu Rev Plant Biol **61**: 49–64.

Zhou, C.-M., Zhang, T.-Q., Wang, X., Yu, S., Lian, H., Tang, H., Feng, Z.-Y., Zozomova-Lihová, J., and Wang, J.-W. (2013a). Molecular basis of age-dependent vernalization in *Cardamine flexuosa*. Science **340**: 1097–1100.

Zhou, J., Wang, X., Lee, J.-Y., and Lee, J.-Y. (2013b). Cell-to-cell movement of two interacting AT-hook factors in *Arabidopsis* root vascular tissue patterning. Plant Cell **25**: 187–201.

Zimmerman, J.L. (1993). Somatic embryogenesis: A model for early development in higher Plants.

Plant Cell **5**: 1411–1423.

Zotz, G., Wilhelm, K., and Becker, A. (2011). Heteroblasty—A Review. Bot. Rev. **77**: 109–151.

Zuo, J., Niu, Q.-W., Frugis, G., and Chua, N.-H. (2002). The *WUSCHEL* gene promotes vegetative-to-embryonic transition in *Arabidopsis*. Plant J. **30**: 349–359.

Chapter 2

An Arabidopsis AT-hook motif nuclear protein mediates somatic-to-embryonic cell fate conversion coinciding with genome duplication

Omid Karami[1], Arezoo Rahimi[1], Patrick Mak[2,3], Anneke Horstman[4], Kim Boutilier[4], Monique Compier[2,5], Bert van der Zaal[1] and Remko Offringa[1]

[1]Plant Developmental Genetics, Institute of Biology Leiden, Leiden University, Sylviusweg 72, 2333 BE Leiden, Netherlands

[2]Add2X Biosciences BV, Sylviusweg 72, 2333 CB Leiden, Netherlands.

[3]Current address: Sanquin Plasma Products B.V., Plesmanlaan 125, P.O. Box 26, 1066 CX Amsterdam, the Netherlands

[4]Bioscience, Wageningen University and Research, Droevendaalsesteeg 1, 6708 PB Wageningen, Netherlands

[5] Molecular Biology, Wageningen University and Research, Droevendaalsesteeg 1, 6708 PB Wageningen, Netherlands

[6]Current address: Rijk Zwaan Netherlands B.V., Burgemeester Crezéelaan 40, P.O. Box 40, 2678 ZG De Lier, The Netherlands

Abstract

The ability of plants to undergo embryogenesis is not restricted to fertilized egg cells, as somatic cells can be reprogrammed to totipotent embryonic cells that are able to form differentiated embryos in a process called somatic embryogenesis (SE). SE is induced after treatment with plant hormones, usually the synthetic auxin, 2,4-dichlorophenoxyacetic acid (2,4-D), or through overexpression of certain transcription factor genes. Here we show that the AT-HOOK MOTIF CONTAINING NUCLEAR LOCALIZED 15 (AHL15) protein plays an important role in the acquisition of plant cell totipotency and embryogenesis. *AHL15* overexpression induces formation of somatic embryos on *Arabidopsis thaliana* seedlings in the absence of hormone treatment. By contrast, *ahl15* loss-of-function mutants showed reduced somatic embryo induction in response to 2,4-D treatment or overexpression of the SE-inducing *BABY BOOM* (*BBM*) transcription factor. The *AHL15* gene is bound and transcriptionally-regulated by BBM during SE. During zygotic embryogenesis *AHL15* is expressed in early embryos, where it is required for proper patterning and for development beyond the heart stage. Morphological and cellular analyses showed that a significant number of plants derived from *35S::AHL15* SEs are polyploid. Chromatin staining with fluorescent reporters suggests that AHL15 induces chromatin decondensation which might lead to chromosome missegregation and thus to the occurrence of polyploid cells. Using centromere-specific markers we demonstrated that polyploidisation was caused by endomitotic events that specifically occurred during the initiation of SE. Our findings indicate that *AHL15* is an important driver of plant cell totipotency acquisition, and based on our results, we suggest that opening of the chromatin structure is required for the acquisition of embryonic competency in somatic plant cells.

Keywords: Somatic embryogenesis, AT-HOOK MOTIF CONTAINING NUCLEAR LOCALIZED 15, 2,4-D, BABY BOOM, chromatin decondensation, polyploidy, *Arabidopsis thaliana*

Introduction

The conversion of differentiated somatic cells into embryonic stem cells is a process that occurs in only a few plant species in nature, for example on the leaf margins of *Bryophyllum calycinum* (Yarbrough, 1932) or *Malaxis paludosa* (Taylor, 1967), or from the unfertilized egg cell or ovule cells of apomictic plants (Ozias-Akins and van Dijk, 2007; Hand and Koltunow, 2014). By contrast, for many more plant species, differentiated cells can be converted into embryonic cells under specific laboratory conditions (Birnbaum and Alvarado, 2008; Smertenko and Bozhkov, 2014). The process of inducing embryonic cell fate in differentiated somatic plant tissues is referred to as somatic embryogenesis (SE). Apart from being a tool to study and understand early embryo development, SE is also an important tool in plant biotechnology, where it is used for asexual propagation of (hybrid) crops or for the regeneration of genetically modified plants during transformation (Bhojwani, 2012).

SE is usually induced in *in vitro* cultured tissues by exogenous application of plant growth regulators. The synthetic analog of the plant hormone auxin 2,4-dichlorophenoxyacetic acid (2,4-D) is the most commonly used plant growth regulator for the induction of SE (Gaj, 2001; Jiménez, 2005). During the past two decades, several genes have been identified that can induce SE on cultured immature zygotic embryos or seedlings when overexpressed in the model plant *Arabidopsis thaliana* (Radoeva and Weijers, 2014; Smertenko and Bozhkov, 2014). Several of these genes, including *BABY BOOM* (*BBM*), *WUSCHEL*, and *LEAFY COTYLEDON 1* (*LEC1*) and *LEC2*, have now been recognized as key regulators of SE (Lotan et al., 1998; Stone et al., 2001; Boutilier et al., 2002; Zuo et al., 2002). Recent studies have shown that *LEC2*-induced SE is accompanied by activation of *YUCCA* genes that mediate auxin biosynthesis (Wójcikowska et al., 2013; Stone et al., 2008). However, the molecular mechanisms and key genetic factors that result in the somatic- to embryonic cell fate conversion are still largely unknown.

Here we show that overexpression of *Arabidopsis AT-HOOK MOTIF CONTAINING NUCLEAR LOCALIZED 15* (*AHL15*) can also induce somatic embryos (SEs) on germinating seedlings in the absence of plant growth regulators. AT-hook motifs exist in a wide range of eukaryotic nuclear proteins, and are known to bind to the narrow minor groove of DNA at short AT-rich stretches (Aravind and Landsman, 1998; Reeves, 2010). In mammals, AT-hook motif proteins are chromatin remodelling factors that participate in a wide array of cellular processes, including DNA replication and repair, and gene transcription leading to cell growth, -differentiation, -transformation, -proliferation, and -death (Sgarra et al., 2010). The *Arabidopsis* genome encodes 29 AHL proteins that contain one or two AT-hook motifs and a PPC domain that promotes/directs nuclear localization (Fujimoto et al., 2004; Zhao et al., 2013). *AHL* gene families are found in angiosperms and also in early diverging land plants such as *Physcomitrella patens* and *Selaginella moellendorffii* (Gallavotti et al., 2011; Zhao et al., 2014). *Arabidopsis* AHL proteins have roles in several aspects of plant growth and development, including flowering time, hypocotyl growth (Street et al., 2008; Xiao et al., 2009), flower development (Ng et al., 2009), vascular tissue differentiation (Zhou et al., 2013), and gibberellin biosynthesis (Matsushita et al., 2007). How plant AHL proteins regulate these underlying biological events is largely unknown. Here we show that *AHL15*

and its close homologs (*AHL19*, *AHL20* and *AHL29*) play major roles in directing plant cell totipotency during both zygotic embryogenesis and 2,4-D and BBM-mediated SE. Furthermore, our data show that AHL15 has a role in opening of chromatin, leading to endomitosis and polyploidy in embryonic cells and that *AHL15* overexpression can lead to polyploid SEs and plants, probable by endomitotic events caused by incomplete chromatin condensation during cell division.

Results

AHL genes are sufficient and required for SE induction

To characterize the function of *AHL15*, we generated *Arabidopsis* lines overexpressing *AHL15* under control of the *35S* promoter (*35S::AHL15*). Overexpression seedlings initially remained small and pale and developed very slowly (Fig. S1A,B). Three to four weeks after germination, seedlings from the majority of the transgenic lines (41 of 50 lines) recovered from this growth retardation (Fig. S1C) and continued a relatively normal development, producing rosettes, flowers and finally seeds. However, one- to two weeks after germination, globular structures could be observed on cotyledons of the remaining *35S::AHL15* lines (9 of 50 lines) (Fig. 1A). These structures developed into heart- or torpedo-shaped SEs (Fig. 1B) that could be germinated to produce fertile plants.

In *Arabidopsis*, the cotyledons of immature zygotic embryos (IZEs) are the most competent tissues for SE in response to the synthetic auxin 2,4-D (Gaj, 2001). Remarkably, IZEs from almost all *35S::AHL15* lines were able to produce somatic embryos when cultured on medium lacking 2,4-D. When left on this medium for a longer time, these primary *35S::AHL15* SEs produced secondary SEs (Fig. S2A, B), and in about 20% of *35S::AHL15* lines, this repetitive induction of SEs resulted in the formation of embryonic masses (Fig. S1C). Overexpression of several *Arabidopsis AHL* genes encoding proteins with a single AT-hook motif (the close homologs *AHL19*, *AHL20* and *AHL29* (Fig. S3)), did not induce SEs on germinating seedlings, but did induce SE on low percentage of IZEs in the absence of 2,4-D (not shown). These results suggest that the single AT-hook motif AHL proteins can enhance the embryonic competence of plant tissues, with AHL15 being able to induce a totipotent state already without extra addition of 2,4-D,, the others less so.

Next we investigated the contribution of *AHL* genes to 2,4-D-induced SE, by culturing IZEs from *ahl* loss-of-function mutants on medium containing 2,4-D. Only a slight reduction in SE induction efficiency was observed in the single *ahl15* loss-of-function mutant (Fig. 1C), which stimulated us to examine the contribution of other *AHL* genes in this process. qRT-PCR analysis showed that *AHL15*, *AHL19* and *AHL20* expression was significantly upregulated in IZEs following seven days of 2,4-D treatment (Fig. 1F). Moreover, GUS staining of *AHL15*::*AHL15-GUS* IZEs showed that *AHL15* expression was specifically enhanced in the cotyledon regions where somatic embryos were initiated (Fig. 1D,E). When assessing SE induction, IZEs from double *ahl15 ahl19* loss-of-function mutants carrying an artificial microRNA targeting *AHL20* (*amiRAHL20*; *ahl15 ahl19 amiRAHL20*) produced significantly less SEs (Fig. 1C) and also led to a relative increase in the number of abnormal

SEs or "hairy callus" (Fig.1G). These results indicated that *AHL15* and several homologs are required for 2,4-D-induced somatic embryo formation starting from IZEs.

We noticed that *AHL15::AHL15-GUS* IZEs showed a slightly decreased capacity to form somatic embryos in the presence of 2,4-D (Fig. 1C). Crossing of the *AHL15::AHL15-GUS* reporter into the *ahl15* mutant background induced a strong decrease in the embryogenic capacity of the *ahl15/+ AHL15::AHL15-GUS* IZEs (Fig. 1C). The majority of the IZEs were converted into non-embryogenic calli that were not observed in the other genotypes (Fig. 1G). These results suggest that the chimeric AHL15-GUS protein is inactive and has a dominant negative effect on the other, redundantly acting AHL proteins. This effect is stronger in the *ahl15* loss-of-function mutant, which is in line with the report that AHL proteins form hetero-multimeric complexes with their homologous proteins (Zhao et al., 2013).

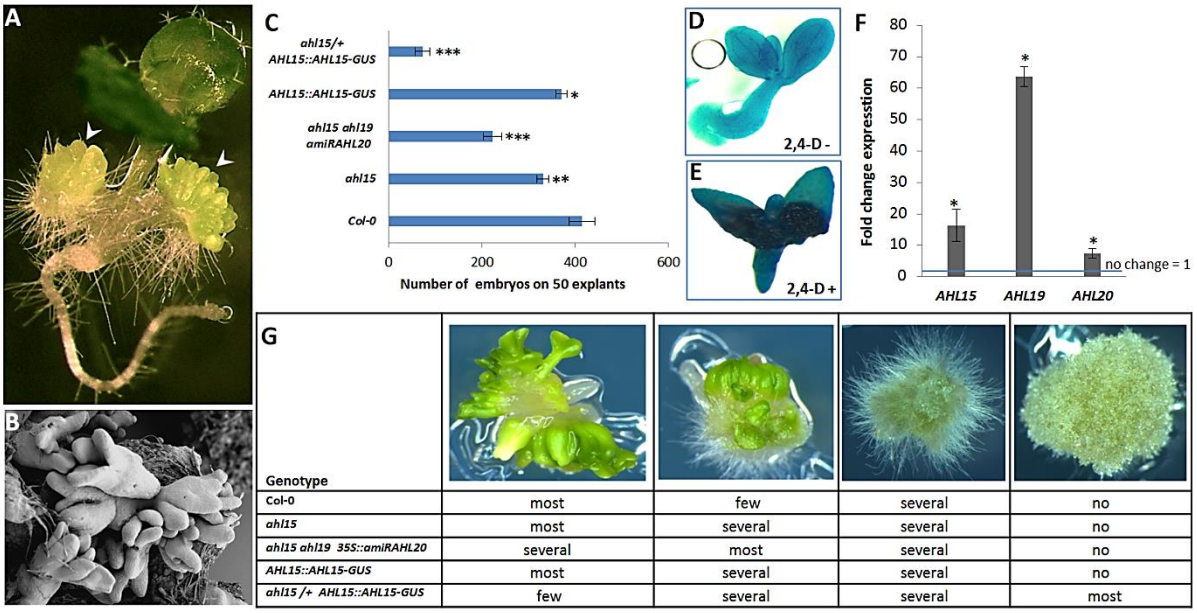

Figure 1 *AHL15* and close homologs are required for SE in *Arabidopsis*. (A) Two-week-old *35S::AHL15 Arabidopsis* seedling with somatic embryossomatic embryos on the cotyledons (arrowheads). (B) Scanning electron micrograph showing torpedo stage somatic embryossomatic embryos on *35S::AHL15* cotyledons. (C) Effects of *ahl* loss-of-function mutations or the presence of the dominant negative *AHL15::AHL15-GUS* fusion construct on the capacity to induce somatic embryossomatic embryos on IZEs by 2,4–D. Asterisks indicate statistically significant differences between the wild type and *ahl* mutant lines, as determined by the Student's *t*-test (* $p<0.05$, ** $p<0.01$, *** $p<0.001$). Error bars indicate standard error of the mean of three biological replicates, with 50 IZEs per replicate. (D, E) Expression of *AHL15::AHL15-GUS* in IZEs cultured for 8 days in the absence (D) or presence (E) of 5 µM 2,4-D. (F) qRT-PCR analysis of *AHL15*, *AHL19*, *AHL20* expression in IZEs cultured for 7 days on medium without and with 5 µM 2,4-D. Asterisks indicate a significant enhancement of *AHL* gene expression in IZEs cultured on medium with 2,4-D compared to medium without 2,4-D (Student's *t*-test, $p < 0.01$). Error bars indicate the standard error of the mean of four biological replicates. (G) Type and proportion of embryo structures and non-embryonic calli on IZEs obtained from wild-type, *ahl15*, *ahl15 ahl19 35S::amiRAHL20*, *AHL15::AHL15-GUS*, and *ahl15/+ AHL15::AHL15-GUS* plants cultured for 2 weeks on 2,4-D medium. The genotype of *ahl15/+ AHL15::AHL15-GUS* calli was verified by PCR analysis.

AHL15 is important during zygotic embryogenesis

Consistent with the critical role of *AHL15* and its close homologs in SE, the involvement of these genes in controlling zygotic embryogenesis was examined. Single and triple *ahl15*, *ahl19* and *ahl20* loss-of-function mutants showed wild-type zygotic embryo (ZE) development. By contrast, siliques of *ahl15/+ AHL15::AHL15-GUS* plants contained brown shrunken seeds (Fig. 2A) that were unable to germinate. The defects could be traced back to abnormal patterns of cell division in globular embryos and arrest at the heart stage in the *ahl15/+ AHL15::AHL15-GUS* ovules (Fig. 2E). We were unable to obtain *ahl15 AHL15::AHL15-GUS* seedlings among 50 F2 plants that we genotyped, suggesting that these patterning defects finally lead to the observed embryo arrest in the homozygous *ahl15 AHL15::AHL15-GUS* embryos. *AHL15::AHL15-GUS* plants produced wild-type embryos (Fig. 2F) and seeds (Fig. 2B), providing additional support for the hypothesis that the dominant negative effect of the AHL15-GUS fusion protein is only observed in the absence of the wild-type AHL15 protein. To confirm that the mutant phenotypes were caused by the dominant negative effect of the chimeric AHL15-GUS fusion protein, an *AHL15::AHL15-GUS* plant line was crossed with an *ahl15 pAHL15::AHL15-TagRFP* line. Unlike *AHL15::AHL15-GUS* lines, *pAHL15::AHL15-tagRFP* lines do not show defects in ZE in *ahl15* background (Fig. 2C). The resulting *ahl15 AHL15::AHL15-GUS AHL15::AHL15-TagRFP* siliques contained WT embryos, indicating that the functional AHL15-TagRFP protein is able to complement the dominant negative effect of the AHL15-GUS fusion (Fig. 2D).

Expression analysis using the *AHL15::AHL15-GUS* and *AHL15::AHL15-tagRFP* lines, both in the wild-type background, showed that *AHL15* is expressed in ZEs from the globular stage onward, with its expression peaking at the bent-cotyledon stage (Fig. 2G-N). In line with the previously reported nuclear localization of AHL proteins (Lim et al., 2007; Ng et al., 2009), the AHL15-TagRFP fusion protein was detected in the nucleus (Fig. 2O).

AHL genes are direct BABY BOOM targets

Overexpression of the AINTEGUMENTA-LIKE (AIL) transcription factor BBM efficiently induces SE in *Arabidopsis* in the absence of exogenous growth regulators (Boutilier et al., 2002). Genome-wide analysis of BBM binding sites using chromatin immunoprecipitation in 2,4-D and *35S::BBM*-induced somatic embryos (ChIP; Horstman et al., 2015) showed that BBM binds to the promoter regions of *AHL15*, *AHL19* and *AHL20* (Fig. 3A-C), suggesting that *AHL* genes are direct downstream BBM targets. To determine whether these genes are also transcriptionally regulated by BBM, we analyzed gene expression changes in *35S::BBM-GR* plants three hours after treatment with dexamethasone (DEX) and the translational inhibitor cycloheximide (CHX). These experiments showed that BBM activated mRNA expression of *AHL15* and *AHL20*, but not yet significantly so for *AHL19* (Fig.3D).

Next, we investigated the requirement for *AHL* genes in *BBM*-induced SE by transforming the *35S::BBM-GR* construct into the triple *ahl15 ahl19 amiRAHL20* and *AHL15::AHL15-GUS* plants. In wild-type Col-0, this construct induced SE in about 7% (40 of 554 transformants) of the primary transformants, which was reduced to 3% in the

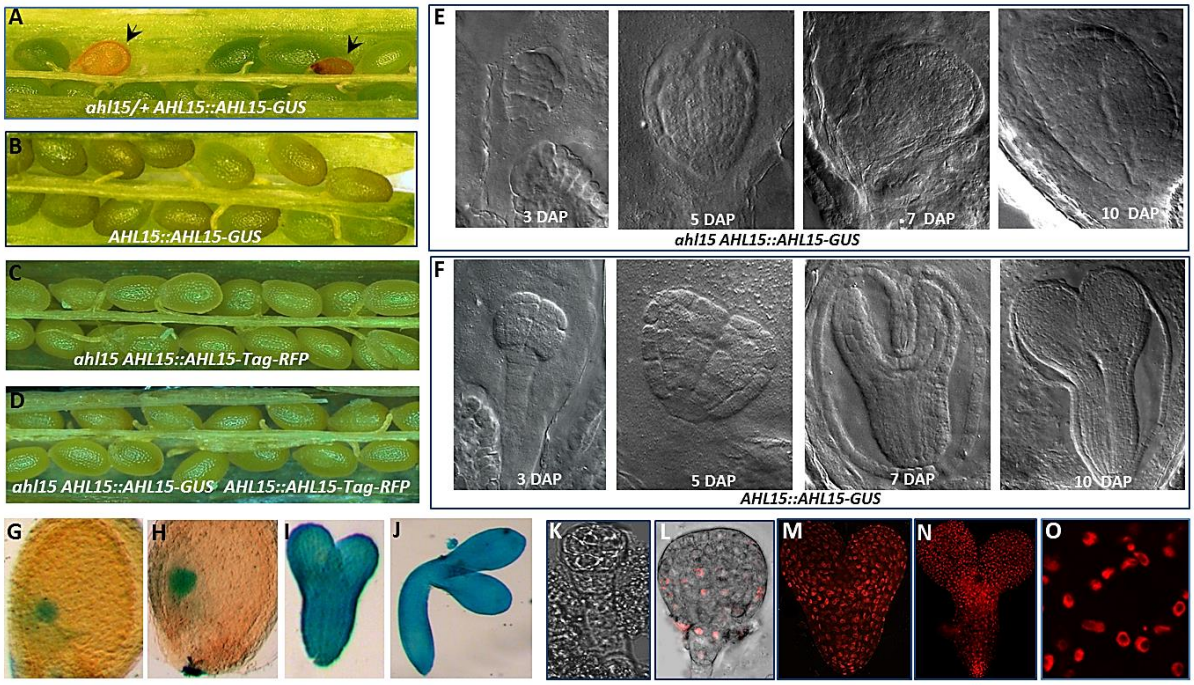

Figure 2 *AHL15* is expressed and essential during ZE. (A) Aberrant development of *ahl15/+ AHL15::AHL15-GUS* seeds (arrowheads). (B-D) Wild-type development of *AHL15::AHL15-GUS* seed (C), *ahl15 AHL15::AHL15-tag-RFP*, (D) and *ahl15 AHL15::AHL15-tag-RFP AHL15::AHL15-GUS* plants. (E,F) DIC images of abnormal zygotic embryo development in siliques of *ahl15/+ AHL15::AHL15-GUS* plants at 3, 5, 7 and 10 days after pollination (DAP, E), and normal zygotic embryo development in siliques of *AHL15::AHL15-GUS* plants at 3, 5, 7 and 10 DAP (F). (G-J) Expression pattern of *AHL15::AHL15-GUS* in globular- (G), heart- (H), torpedo- (I) and bent cotyledon (J) stage embryos. (K-N) Confocal microscopy images of *AHL15::AHL15-tagRFP* early globular- (K), late globular- (L), heart- (M), and torpedo (N) stage embryos. (O) Detail of a torpedo stage embryo showing nuclear localization of AHL15-TagRFP. (K-O) Images show a merge of the transmitted light and the RFP channel (K,L), or the RFP channel alone (M-O)

AHL15::AHL15-GUS background (26 of 801 transformants) and was completely abolished SE in the *ahl15 ahl19 amiRAHL20* background (0 of 351 transformants). These results together with the observation that *AHL15* overexpression, like *BBM* overexpression, induces spontaneous SE suggests that induction of *AHL* gene expression is a key regulatory component of the BBM signaling pathway.

Nuclear *AHL15* modulates the chromatin state in embryonic cells

Based on the observation in animal cells that AT-hook proteins are essential for the open chromatin in neural precursor cells (Catez et al., 2004; Kishi et al., 2012), we investigated whether AHL15 modulates the chromatin structure during SE initiation. Global chromatin structure is characterized by tightly condensed, transcriptionally-repressed regions, called heterochromatin, which can be visualized using fluorescent chromatin markers or DNA staining. Large-scale changes in heterochromatin in somatic plant cells are considered as a sign of cell identity reprogramming (Meister et al., 2011; Bourbousse et al., 2015). Propidium iodide (PI) staining of chromosomal DNA in cotyledon cells of *35S::AHL15* IZEs showed a remarkable disruption of heterochromatin at seven days after culture (Fig. 4A), when

compared to cotyledon cells 3 days after culture (Fig. 4A). In contrast, cotyledon cells of wild-type IZEs did not show a clear change in heterochromatin state between three and seven days (Fig 4A). The *Arabidopsis* HISTONE 2B-GFP protein is incorporated into nucleosomes, providing a marker for the chromatin state in living cells (Bourbousse et al., 2015). H2B-GFP fluorescence observations confirmed that the chromocenters in 7-day-old *35S::AHL15* cotyledon cells (Fig. 4B) were much more diffuse compared to 3-day-old cells (Fig. 4B). No significant differences in H2B-GFP signals were detected between cotyledon cells of three and seven day-incubated wild-type IZEs (Fig 4B). Quantification of the number of detectable chromocenters confirmed that that the number of chromocentres was significantly decreased in cotyledon cells of 7 days incubated *35S::AHL15* IZEs relative to wild-type IZEs (Fig. 4C). This result suggests that AHL15 promotes heterochromatin decondensation. Surprisingly, in cells expressing both *AHL15::AHL15-tagRFP* and *H2B::H2B-GFP* reporters, *AHL15-tagRFP* did not co-localize with the chromocenters (Fig. S4), but showed a more diffuse nuclear distribution, suggesting that the AHL15 regulates global chromatin decondensation.

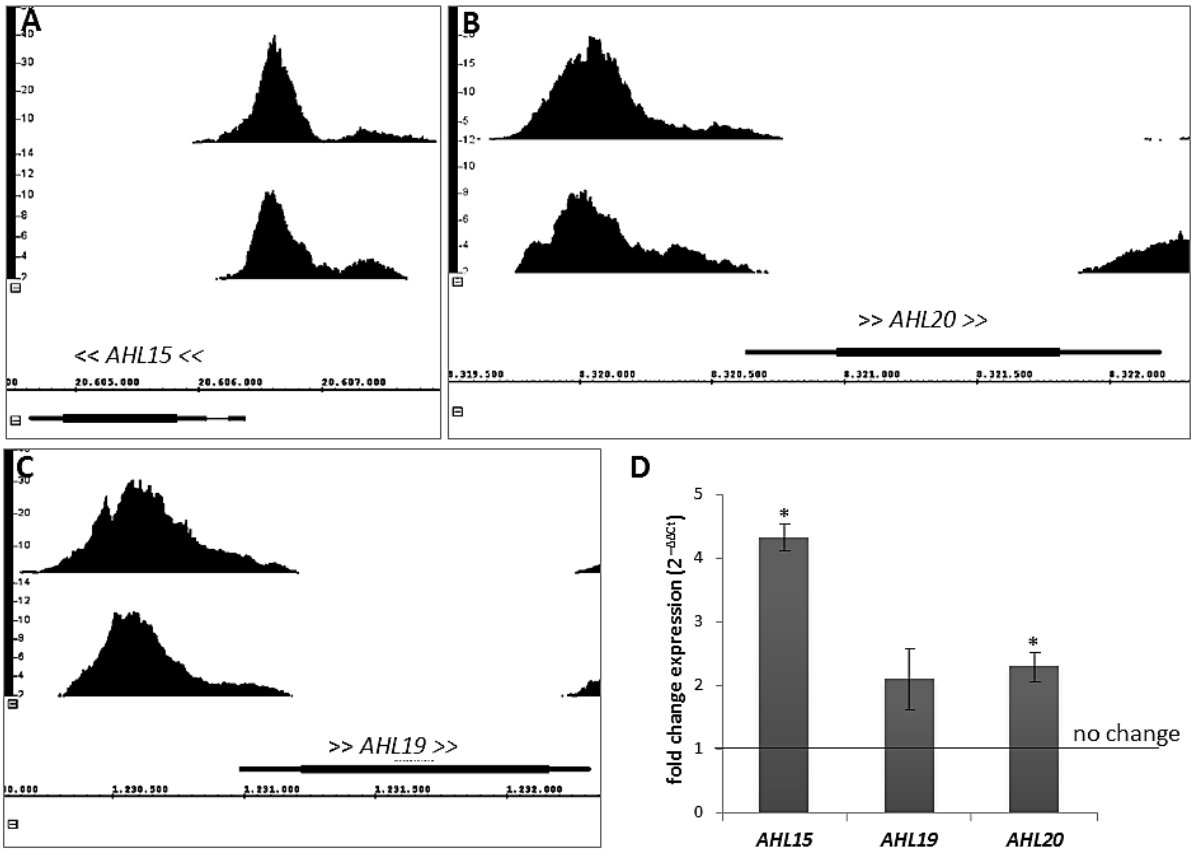

Figure 3 SE-promoting *AHL* genes are direct targets of BBM. (A-C) ChIP-seq BBM binding profiles for *AHL15* (A), *AHL20* (B) and *AHL19* (C). The binding profiles from the *35S::BBM-GFP* (upper profile) and *BBM::BBM-YFP* (lower profile) ChIP-seq experiments are shown. The x-axis shows the nucleotide position of DNA binding in the selected genes (TAIR 10 annotation), the y-axis shows the ChIP-seq score, and the arrow brackets around the gene name indicate the direction of gene transcription. (D) qRT-PCR analysis of the fold change in expression of *AHL* genes in DEX + CHX treated *35S::BBM-GR* seedlings relative to that in DEX + CHX treated Col-0 wild-type seedlings. Asterisks indicate a significant difference in expression levels in *35S::BBM-GR* plants compared to wild-type plants (Student's *t*-test, $p < 0.05$). Error bars indicate standard error of the mean of four biological replicates.

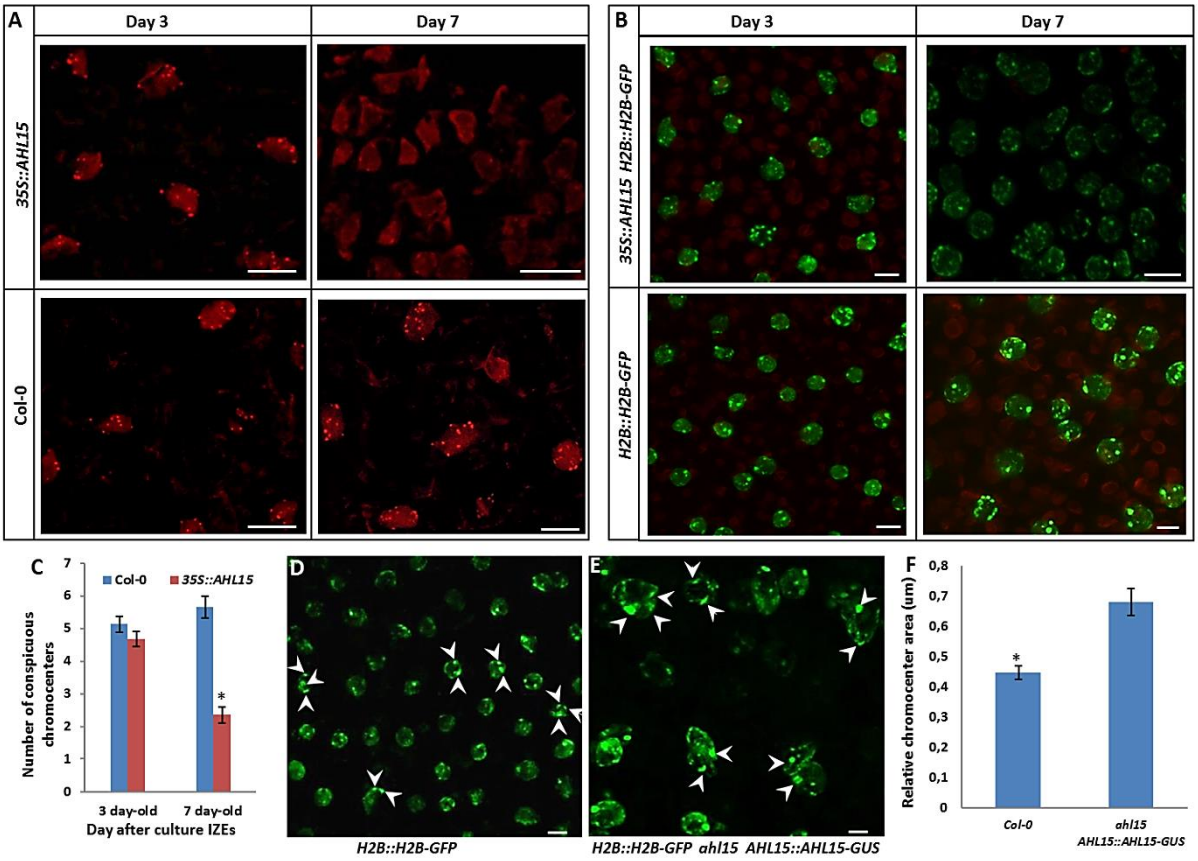

Figure 4 *AHL15* reduces heterochromatin condensation and chromocenter size. (A, B) Visualization of DNA compaction using propidium iodide (PI) staining (A) or H2B-GFP labelling (B) in cotyledon cell nuclei of wild-type and *35S::AHL15* IZEs 3- or 7 days after culture on B5 medium. Size bar indicates 6 µm in A and B. (C) Quantification of the number of conspicuous chromocenters labelled with PI in cotyledon cell nuclei of wild-type and *35S::AHL15* IZEs 3- or 7 days after culture on B5 medium. Error bars indicate standard error of the mean of 4 biological replicates. Statistically significant differences were determined using the Student's *t*-test (* $p<0.01$). (D, E) Visualization of chromocenters using the H2B-GFP reporter in wild-type (D) and defective *ahl15 AHL15::AHL15-GUS* ZEs (E) at 6 DAP. Size bar indicates 3.5 µm in D and E. (F) Quantification of the chromocenter area labelled with H2B-GFP in nuclei of wild-type and *ahl15 AHL15::AHL15-GUS* ZEs at 6 DAP. Error bars indicate standard error of the mean of 6 biological replicates. For each replicate 30 chromocenters were measured (2 or3 of the most clear chromocenters per nucleus), indicated with arrow heads in D and E). Statistically significant differences were determined using the Student's *t*-test (* $p<0.01$).

To obtain insight into the role of AHL15 in chromatin decondensation during zygotic embryogenesis, we introduced the *H2B::H2B-GFP* reporter into the *ahl15/+ AHL15::AHL15-GUS* background. In defective *ahl15 AHL15::AHL15-GUS* embryos, we observed irregular shaped chromocenters that were much larger than those in wild-type cells (Fig. 4D-F). This result together with the reduced heterochromatin condensation observed in cotyledon cells of *35S::AHL15* IZEs suggests that *AHL15* plays a role in regulating the chromatin architecture during embryogenesis.

AHL15 overexpression induces polyploidy during SE initiation

Plants regenerated from somatic embryos obtained from cotyledons of *35S*::*AHL15* IZEs without 2,4-D regularly developed large rosettes with dark green leaves and large flowers (Fig. S5A), phenotypes that were not observed in *35S::AHL15* progeny obtained through ZE. As these phenotypes are typical for polyploid plants, we investigated the ploidy level of the plants. The number of chloroplasts in guard cells (Finn et al., 2011) of plants showing large flowers was two times higher (8-12) than that of diploid wild-type plants (4-6) (Fig. S5B). Moreover, flow cytometry analysis on SE-derived plant lines confirmed that most of these lines were tetraploid, and two were even octoploid (Table 1). The frequency of SE-derived polyploidy varied per *35S::AHL15* line, ranging from 18 to 69% (Table 1). No polyploid plants were obtained from somatic embryos induced by 2,4-D on wild-type IZEs (Table 1), or by *BBM* overexpression (Boutilier et al., 2002) (Table 1), indicating that polyploidisation is specifically induced by *AHL15* overexpression.

Table1. Ploidy level of plants derived from SEs induced by *AHL15* overexpression, *BBM* overexpression or by 2,4-D treatment

Genotype	SE-derived plants	Ploidy level of plants*			ploidy percentage
		2n	4n	8n	
35S::AHL15-2	16	5	11	-	69
35S::AHL15-4	6	4	1	1	33
35S::AHL15-13	11	7	4	-	36
35S::AHL15-14	17	14	2	1	18
35S::AHL15-15	15	11	4	-	27
Col-0, 2,4-D	30	30	-	-	0
35S::BBM	20	20	-	-	0

* The ploidy level was analyzed by counting the chloroplast number in guard cells. For plants derived from *35S::AHL15*-induced SEs, the ploidy level was confirmed using flow cytometry.

Polyploidisation is typically correlated with an increase in cell- and nuclear size in *Arabidopsis* and many other organisms (Tsukaya, 2013). Indeed root cells of tetraploid *35S::AHL15* seedlings showed a larger nucleus and a larger cell volume than diploid control plants (Fig. S5C), explaining the larger organ size observed for these plants. We used the centromere-specific HISTONE3-GFP fusion protein (*CENH3-GFP*) (Fang and Spector, 2005; De Storme et al., 2013) to count the number of chromosomes per cell (Fang and Spector, 2005; De Storme et al., 2013). Seven to eight *CENH3-GFP*-marked centromeric dots could be detected in root cells of wild-type plants and diploid *35S::AHL15* SE-derived plants (Fig S5D). By contrast, around 12-16 centromeric dots were observed in the larger nuclei in root cells of tetraploid *35S::AHL15* plants (Fig S5D). This confirmed that the plants with large organs that were regenerated from *AHL15* overexpression-induced somatic embryos are polyploid.

The considerable frequency polyploid plants were regenerated from *35S::AHL15* somatic embryos posed the question as to when polyploidisation occurs, and whether it is correlated with, or is even promoted by SE induction. We observed a variable number of

CENH3-GFP labelled centromeric dots (6-8, 12-15 and 25-30) per cell in cotyledons of *35S::AHL15* IZEs seven to eight days after of the start of culture, reflecting the presence of diploid, tetraploid and octaploid cells (Fig 5A). No evidence was obtained for polyploidy in root meristems (Fig. S6A) or young leaves (Fig. S6B) of *35S::AHL15* plants propagated through ZE, nor was polyploidy observed in the 2,4-D-induced non-embryogenic calli found on leaf and root tissues of *35S::AHL15* plants (Fig. S6C, D). Based on these results, and in line with the observation that *35S::AHL15* polyploid plants were only obtained from *35S::AHL15* somatic embryos, we conclude that the *AHL15*-induced polyploidisation occurs specifically during in vitro embryogenesis.

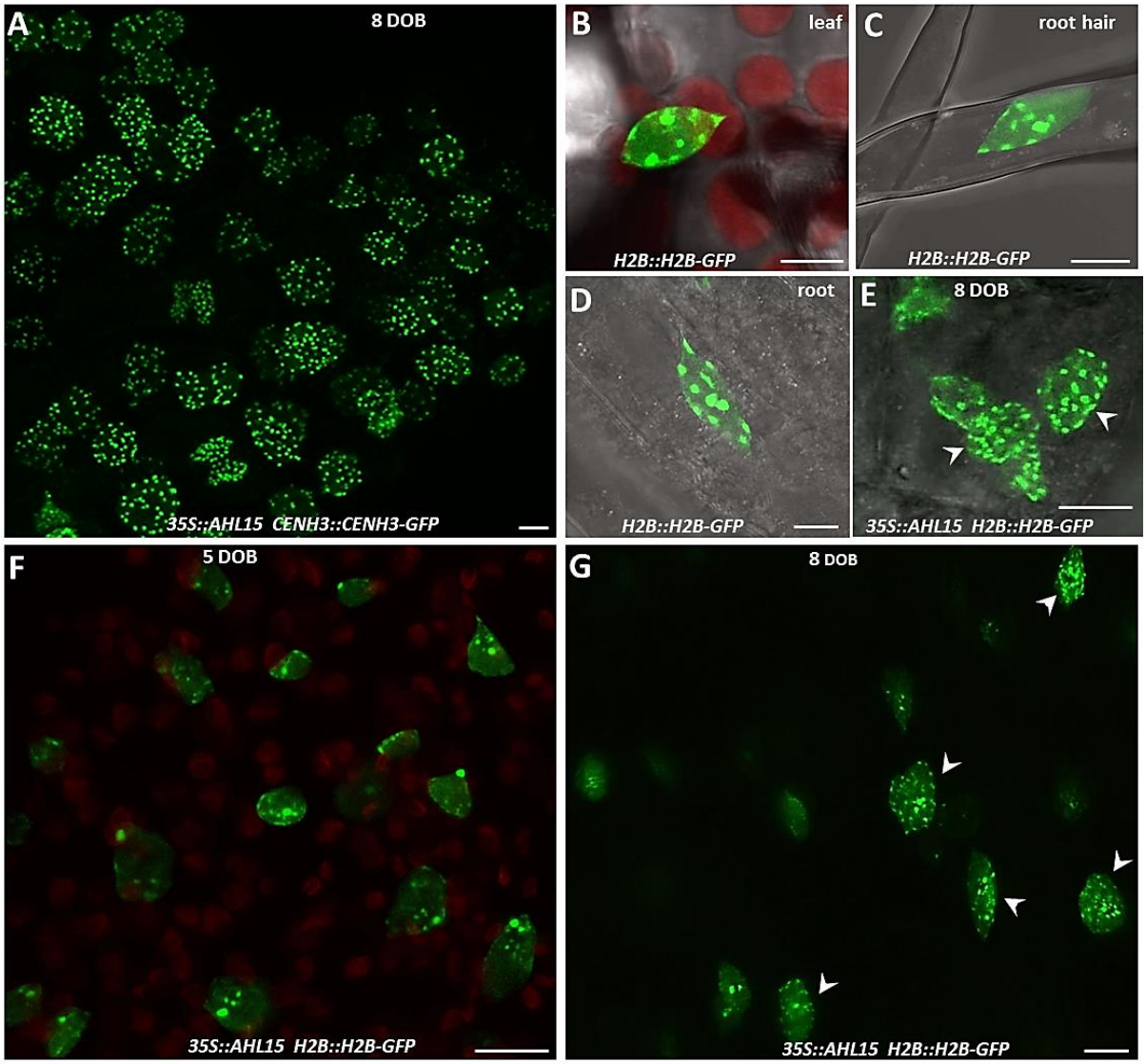

Figure 5 Polyploidy by endomitosis in nuclei of cotyledon cells of cultured *35S::AHL15* IZEs. (A) Confocal image of polyploid cells detected by CENH3-GFP-mediated centromere labeling in an embryonic structure developing on a cotyledon of a *35S::AHL15* IZE cultured for 8 days on B5 medium (DOB). (B-E) Confocal images of H2B-GFP labelled chromocenters in a endoreduplicated nucleus of wild-type cotyledon (B), root hair (C), or root epidermis (D) cell, or in nuclei of cotyledon cells of a *35S::AHL15* IZE cultured for 8 DOB (E). (F, G) H2B-GFP-labelled chromocenters in nuclei of cotyledon cells of *35S::AHL15* IZEs cultured for 5 (F) or 8 (G) DOB. White arrowheads indicate cells with a duplicated number of chromocenters in E and G. Size bars indicate 6 µm. Images show a merge of the transmitted light and the GFP channel (B-E), or the GFP channel alone (A,F,G).

AHL15 overexpression induces endomitosis specifically in somatic embryo progenitor cells

Endoreduplication normally occurs in expanding cells to facilitate cell growth. During endoreduplication duplicated chromosomes do not enter into mitosis and the number of chromocenters does not increase (Edgar and Orr-Weaver, 2001; Lermontova et al., 2006; Lee et al., 2009). We observed an increase in H2B-GFP-marked chromocenters in *35S::AHL15* cotyledon cells that coincided with polyploidisation events (Fig. 5E and G), but not in leaf, root or root hair cells (Fig. 5B-D), suggesting that these polyploid cells are not derived from endoreduplication. Thus duplication of segregated chromosomes in *35S::AHL15* cotyledons cells must be caused by endomitotis, during which mitosis is initiated and chromosomes are separated, but cytokinesis fails to occur. When we followed the H2B-GFP reporter in cotyledons of *35S::AHL15* IZEs, we did not observe any cells with an increased number of chromocenters during the first week of culture, indicating the absence of endomitosis during this period (Fig. 5F). At eight days of IZE culture, however, an increase in chromocenter number could be detected in proliferating *35S::AHL15* cotyledon cells (Fig. 5G). This result showed that cellular polyploidisation in *35S::AHL15* cotyledon cells is tightly associated with the induction of somatic embryos. Although ectopic overexpression of *AHL15* resulted in a high percentage of polyploid plants (Table 1), polyploidy of the embryo itself was no absolute prerequisite for further development of SEs into plants as the most of the *AHL15* expressing plants were still diploid.

Chromosome mis-segregation in *35S::AHL15* cotyledon cells

Disruption of heterochromatin in human mitotic cells leads to mis-segregation of chromosomes (Maison and Almouzni, 2004; Kondo et al., 2008; Carone and Lawrence, 2013; Hahn et al., 2013) and cellular polyploidization (Shi and King, 2005). We hypothesized that heterochromatin disruption and more global chromatin decondensation in dividing *35S::AHL15* cotyledon cells might contribute to endomitosis resulting in polyploid somatic embryo progenitor cells. Compared to normal chromosome segregation (Fig. 6A), chromosome segregation lagged behind (Fig. 6B) and binucleate cells (Fig. 6C-D) could be detected in dividing cotyledon cells of 7-day-old *35S::AHL15* explants. The observation of binucleate cotyledon cells expressing the *WOX2::NLS-YFP* embryo marker (Fig 6E) confirmed that such cells can adopt embryo identity and thus lead to polyploid somatic embryos. Taken together, we conclude that heterochromatin disruption in *35S::AHL15* induced embryonic cotyledon cells may lead to chromosome mis-segregation, the formation of binucleate cells and finally to cellular polyploidization coinciding with the development of polyploid somatic embryos.

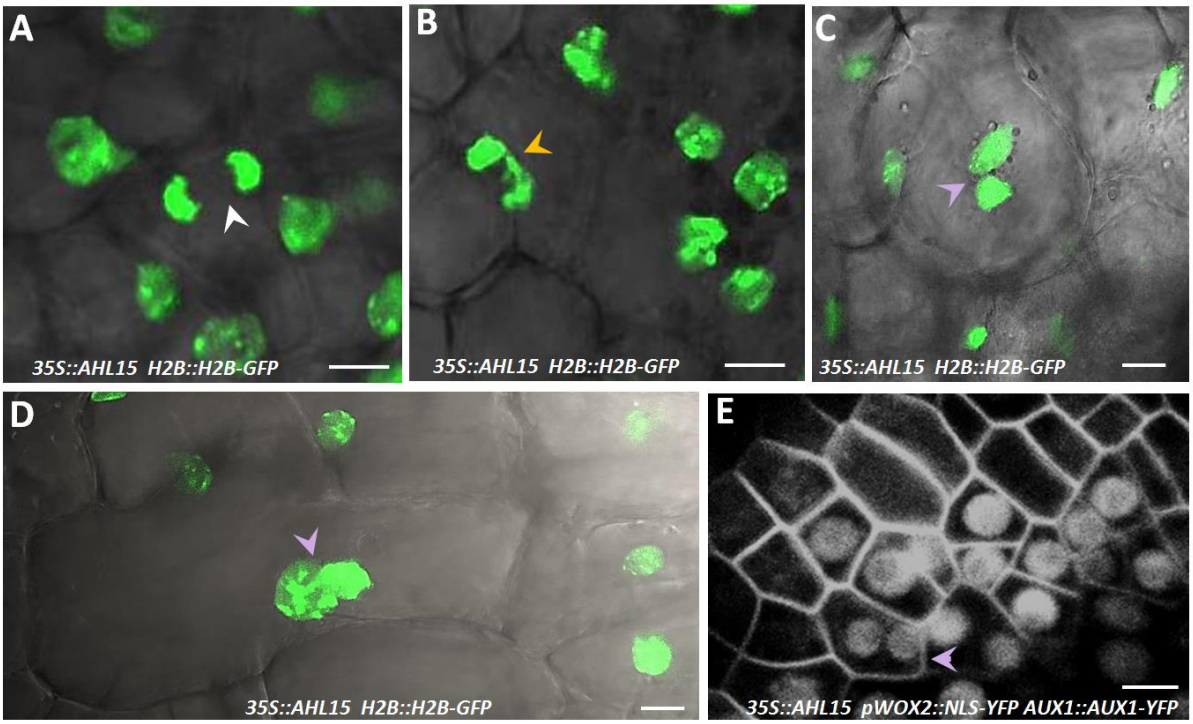

Figure 6 *AHL15* overexpression causes chromosome mis-segregation in IZE cotyledon cells. (A-D) Confocal microscopy analysis of chromosome segregation in cotyledons of *35S::AHL15* IZEs using the H2B-GFP reporter. The white arrowhead indicates normal chromosome segregation during anaphase (A), the yellow arrowhead indicates mis-segregation of chromosomes during anaphase (B), and the magenta arrowhead indicates a bi-nucleated cell (C,D) in cotyledons of *35S::AHL15* IZEs 8 DOB. (E) Confocal microscopy image of a cotyledon of a *35S::AHL15 pWOX2::NLS-YFP pAUX1::AUX1-YFP* IZE. *pWOX2::NLS-YFP* and *pAUX1::AUX1-YFP* reporters were used to mark embryonic nucleus and plasma membranes respectively. The magenta arrowhead indicates a bi-nucleated cell in an area of cells with WOX2-YFP- marked embryo cell fate. Images show a merge of the transmitted light and the GFP channel (A-D), or the YFP channel alone (E). Size bar indicates Size bars indicate 6 µm.

Discussion

The herbicide 2,4-D is extensively used for SE induction in *Arabidopsis* and a wide range of other plant species. In *Arabidopsis*, SE can also be induced on IZEs or seedlings in the absence of 2,4-D treatment by the overexpression of specific transcription factors, such as the AIL transcription factor BBM (Boutilier et al., 2002). In this study, we showed that AHL15 adds to the list of nuclear proteins whose overexpression induces somatic embryos on IZEs and seedlings in the absence of 2,4-D. In line with this observation, AHL15 and its close homologs are upregulated and required for proper SE induction upon 2,4-D treatment. Furthermore, we showed that *AHL15* and its close homologs are downstream targets of BBM, and that they are required for efficient *BBM* overexpression-induced SE.

AT-hook motif-containing proteins are generally considered to be chromatin architecture factors (Catez et al., 2004; Fusco and Fedele, 2007; Sgarra et al., 2010; Kishi et al., 2012). Studies in animals have shown that chromatin decondensation precedes the induction of pluripotent stem cells and their subsequent differentiation (Gaspar-Maia et al., 2011). In the *Arabidopsis* zygote, predominant decondensation of the heterochromatin configuration is

likely to contribute to the totipotency of this cell (Pillot et al., 2010). Our data indicate that *AHL15* overexpression induces a global reduction of the amount of heterochromatin in induced somatic embryonic cells, whereas *ahl* loss-of-function mutants show enhanced heterochromatin formation in *in vitro* cultured explants and also reduces the embryonic competence of these explants. Based on our results, we suggest a model in which chromatin opening is required for the acquisition of embryonic competence in somatic plant cells (Fig. 7). In this model chromatin opening is mediated by upregulation of *AHL* genes, which can be achieved by *35S* promotor-driven overexpression, by 2,4-D treatment or by *BBM* overexpression.

During cell division, eukaryotic cells duplicate their chromosomes after which the mitosis machinery ensures that the sister chromatids segregate equally over the two daughter cells. However, some cell types do not separate the duplicated chromosomes, leading to a polyploidy state known as endopolyploidy (Breuer et al., 2014). In plants, endopolyploidy is commonly classified either endomitosis or endoreduplication (Breuer et al., 2014). In endoreduplication, chromosomes are duplicated during cellular differentiation but do not segregate, leading to the formation of polytene chromosomes (Lermontova et al., 2006). By contrast, during endomitosis sister chromatids are separated, but the last steps of mitosis including nuclear division and cytokinesis are skipped, generally leading to a duplication of the chromosome number. In this work we showed that polyploid cells can be specifically detected during *35S::AHL15* induced SE. The lack of polytene chromosomes suggests that *35S::AHL15*-induced polyploidy is the result of endomitosis.

Previous studies have shown that defects in heterochromatin condensation in animal cells lead to mis-separation of chromosomes during mitosis (Maison and Almouzni, 2004; Kondo et al., 2008; Carone and Lawrence, 2013; Hahn et al., 2013), and that mis-segregation of chromosomes subsequently leads to cellular polyploidisation (Shi and King, 2005). In our experiments, we found a high reduction of heterochromatin coinciding with mis-segregation of chromosomes in in vitro-cultured *35S::AHL15* cotyledon cells. Consistent with the strong conservation of chromosome segregation mechanisms between animal and plant cells (Yanagida, 2005), we propose that cellular polyploidisation in *35S::AHL15* embryonic cells is caused by an AHL15-mediated reduction in chromosome condensation during mitosis, which results in chromosome mis-segregation. The observation that polyploid embryos and plants are not obtained after 2,4-D treatment or by *BBM* overexpression suggests that in these somatic embryos *AHL15* expression levels are not sufficiently elevated to induce a level of chromatin decondensation that leads to chromosome mis-segregation (Fig 7).

A low frequency of polyploid plants derived from somatic embryo culture has been reported (Winkelmann et al., 1998; Borchert et al., 2007; Orbović et al., 2007; Prado et al., 2010), but the molecular and cytological basis for this genetic instability in relation to *in vitro* embryogenesis has not been described. Our data suggest that *AHL15*-mediated polyploidisation could be one factor driving genome duplication events during SE in somatic embryo cultures. AHL15-mediated genome duplication might therefore provide a more efficient means for chromosome doubling of embryos derived from haploid explants such as egg cells or microspores (Soriano et al., 2013) and for the production of polyploid crops.

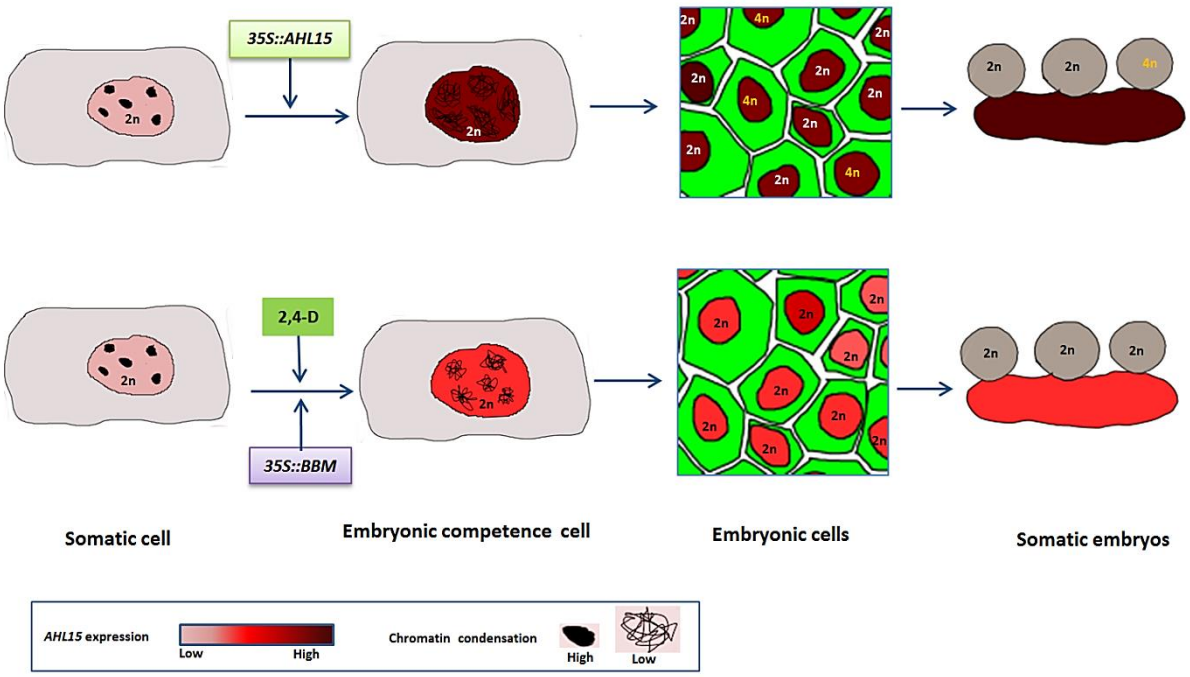

Figure 7 Model for somatic-to-embryonic reprogramming and cellular polyploidization by *AHL15* overexpression. *AHL15* or *BBM* overexpression, or 2,4-D treatment all induce the chromatin decondensation that is required to induce embryonic competence in somatic cells. The high level of chromatin decondensation obtained by *35S* promoter-driven *AHL15* overexpression prevents chromosome segregation in some cells, leading to endomitosis events that give rise to polyploid embryonic cells and subsequently to polyploid somatic embryos. *BBM* overexpression or 2,4-D treatment also lead to enhanced *AHL15* expression resulting in chromatin decondensation sufficient to induce embryonic cells and the resulting somatic embryos, but insufficient to lead to endomitosis, thus only giving rise to diploid somatic embryos.

Methods

Plant material and growth conditions

T-DNA insertion mutants *ahl15* (SALK_040729) and *ahl19* (SALK_070123) were obtained from the European Arabidopsis Stock Centre (http://arabidopsis.info/). Primers used for genotyping are described in Table S1. The reporter lines *CENH3::CENH3-GFP* (Fang and Spector, 2005) and *H2B::H2B-GFP* (Fang and Spector, 2005), *pWOX2::NLS-YFP* (Breuninger et al., 2008), and pAUX1::AUX1-YFP (Swarup et al., 2005) have been described previously. For *in vitro* plant culture, seeds were sterilized in 10 % (v/v) sodium hypochlorite for 12 minutes and then washed four times in sterile water. Sterilized seeds were plated on MA medium (Masson and Paszkowski, 1992) containing 1 % (w/v) sucrose and 0.7 % agar. Seedlings, plants and explants were grown at 21°C, 70% relative humidity, and 16 hours photoperiod.

Plasmid construction and plant transformation

The *35S::AHL15* construct was generated by PCR amplification of the full-length *AHL15* cDNA of (AT3G55560) from ecotype Columbia (Col-0) using primers 35S::AHL15-F and -R (Table S1). The resulting PCR product was cloned as a *Sma*I/*Bgl*II fragment into the *p35S-3'OCS* expression cassette of plasmid pART7, which was subsequently cloned as *Not*I fragment into the binary vector pART27 (Gleave, 1992). To generate the other overexpression constructs, the full-length cDNA clones of *AHL19* (AT3G04570), *AHL20* (AT4G14465), and *AHL29* (AT1G76500) from *Arabidopsis* Col-0 were used to amplify the open reading frames (ORFs) using primers indicated in Table S1. The ORFs were cloned into plasmid pJET1/blunt (GeneJET™ PCR Cloning Kit, #K1221), and next transferred as *Not*I fragments to binary vector *pGPTV 35S::FLAG* (Becker et al., 1992). To generate the *AHL15::AHL15-GUS* and *pAHL15::AHL15-TagRFP* translational fusions, a 4 kb fragment containing the promoter and the full coding region of *AHL15* was amplified using PCR primers AHL15-GUS-F and -R (Table S1), and inserted into pDONR207 using a BP reaction (Gateway, Invitrogen). LR reactions were carried out to fuse the 4 kb fragment upstream of GUS and *tagRFP* in respectively destination vectors pMDC163 (Karimi et al., 2007) and pGD121 (Immink et al., 2012). The artificial microRNA (amiR) targeting *AHL20* was generated as described by Schwab and colleagues (Schwab et al., 2006) using oligonucleotides I-IV miR-a/s AHL20 (Table S1). The fragment of the *amiRAHL20* precursor was amplified using PCR primers amiRNA AHL20-F and –R (Table S1), and subsequently introduced into the entry vector pDONR207 via a BP reaction (Gateway, Invitrogen). The *amiRAHL20* precursor was recombined into destination vectors pMDC32 (Karimi et al., 2007) downstream of the *35S* promoter via an LR reaction (Gateway, Invitrogen). The *p35S::BBM-GR* construct has been described previously (Passarinho et al., 2008). All binary vectors were introduced into *Agrobacterium tumefaciens* strain AGL1 by electroporation (den Dulk-Ras and Hooykaas, 1995) and transgenic *Arabidopsis* Col-0 lines were obtained by the floral dip method (Clough and Bent, 1998).

Somatic embryogenesis

Immature zygotic embryos (IZEs) at the bent cotyledon stage of development (10-12 days after pollination) or germinating dry seeds were used as explants to induce SE using a previously described protocol (Gaj, 2001). In short, seeds and IZEs were cultured on solid B5 medium (Gamborg et al., 1968) supplemented with 5 μM 2,4-D, 2 % (w/v) sucrose and 0.7 % agar (Sigma). Control seeds or IZEs were cultured on solid B5 medium without 2,4-D. To allow further embryo development, explants were transferred to medium without 2,4-D. One week after subculture, the capacity to induce SE was scored under a stereomicroscope as the number of somatic embryos produced from 50 explants cultured on a plate. Three plates were scored for each line. The Student's *t*-test was used for statistical analysis of the data.

Quantitative real-time PCR (qRT-PCR) and ChIP seq analysis

To determine the expression of *AHL* genes during SE induction, RNA was isolated from 25 IZEs cultured for 7 days on B5 medium with or without 2,4-D in 4 biological replicates using a Qiagen RNeasy Plant Mini Kit. The RNA samples were treated with Ambion® TURBO DNA-free™ DNase. To determine the expression of *AHL* genes in 2,4-D treated Col-0 IZEs by qRT-PCR, 1 µg of total RNA was used for cDNA synthesis with the iScript™ cDNA Synthesis Kit (BioRad). PCR was performed using the SYBR-Green PCR Master mix (Biorad) and a CHOROMO 4 Peltier Thermal Cycler (MJ RESEARCH). The Pfaffl method was used to determine relative expression levels (Pfaffl, 2001). Expression was normalized using the *β-TUBULIN*-6 (At5g12250) gene. The gene-specific PCR primers used are described in Table S1.

The effect of *BBM* overexpression on *AHL* gene expression was examined by inducing five-day-old *Arabidopsis thaliana* Col-0 and *35S::BBM-GR* seedlings (four biological replicates for each line) for three hours with 10 µM dexamethasone (DEX) plus 10 µM cycloheximide (CHX). RNA was isolated using the Invitek kit, treated with DNAseI (Invitrogen) and then used for cDNA synthesis with the Taqman cDNA synthesis kit (Applied Biosystems). qRT-PCR was performed as described above. The relative expression level of *AHL* genes was calculated according to the $2^{-\Delta\Delta Ct}$ method (Livak and Schmittgen, 2001), using the wild-type Col-0 value to normalize and the *SAND* gene (At2g28390; (Czechowski et al., 2005) as a reference. The gene-specific PCR primers are listed in Table S1.

The ChIP-seq data and analysis was downloaded from GEO (GSE52400). Briefly, the experiments were performed using somatic embryos from either 2,4-D-induced *BBM::BBM-YFP* cultures (with *BBM::NLS-GFP* as a control) or a *35S::BBM-GFP* overexpression line (with *35S::BBM* as a control), as described in (Horstman et al., 2015).

Ploidy analysis

The ploidy level of plants derived from *35S::AHL15*-induced somatic embryos was determined by flow cytometry (Plant Cytometry Services, Schijndel, Netherlands), and confirmed by counting the total number of chloroplasts in stomatal guard cells and by comparing flower size and or the size of the nucleus in root epidermal cells. The number of chloroplasts in stomatal guard cells was counted for plants derived from 2,4-D- and BBM-induced somatic embryos.

Histological staining and microscopy

Histochemical β-glucuronidase (GUS) staining of *AHL15::AHL15-GUS* IZEs or ovules was performed as described previously (Anandalakshmi et al., 1998) for 4 hours at 37 °C, followed by rehydration in a graded ethanol series (75, 50, and 25 %) for 10 minutes each. GUS stained tissues were observed and photographed using a LEICA MZ12 microscopy (Switzerland) equipped with a LEICA DC500 camera.

DNA staining of wild-type and *35S::AHL15* seedlings was performed using propidium iodide (PI) according to the protocol described by Baroux *et al*. (Baroux et al., 2007). To

stain nuclei, the samples were incubated for 30 minutes in 4′,6-diamidino-2-phenylindole (DAPI) staining solution (1 μg/ml DAPI in phosphate-buffered saline (PBS) just before observation.

For scanning electron microscopy (SEM), seedlings were fixed in 0.1 M sodium cacodylate buffer (pH 7.2) containing 2.5% glutaraldehyde and 2% formaldehyde. After fixation, samples were dehydrated by a successive ethanol series (25, 50, 70, 95, and 100 %), and subsequently critical-point dried in liquid CO_2. Dried specimens were gold-coated and examined using a JEOL SEM-6400 (Japan).

For morphological studies of embryos, fertilized ovules were mounted in a clearing solution (glycerol:water:chloral hydrate = 1:3:8 v/v) and then incubated at 65 °C for 30 min and observed using a LEICA DC500 microscopy (Switzerland) equipped with differential interference contrast (DIC) optics.

The number of chloroplasts in leaf guard cells, the size of the DAPI stained nuclear area in root cells and the number of conspicuous heterochromatin regions of the PI stained nuclei of cotyledon cells were recorded using a confocal laser scanning microscope (ZEISS-003-18533), using a 633 laser, a 488 nm LP excitation and a 650-700 nm BP emission filters for chlorophyll signals in guard cells, a 405 laser, a 350 nm LP excitation and a 425-475 nm BP emission filters for DAPI signals in cotyledon cells, and a 633 laser, 488 nm LP excitation and 600-670 nm emission BP filters for PI signals in cotyledon cells. The relative size chromocenter spots were measured from confocal images by measuring of region of the spots using the measuring region tool of ImageJ software (Rasband).

Cellular and subcellular localization of AHL15-TagRFP and H2B- or CENH3-GFP protein fusions were visualized using the same laser scanning microscope with a 633 laser, and a 532 nm LP excitation and 580-600 nm BP emission filters for TagRFP signals and a 534 laser, 488 nm LP excitation and 500-525 nm BP emission filters for GFP signals.

Acknowledgements

This work is partially supported by Iranian Ministry of Science, Research, and Technology (Grant MSRT 89100156 to O.K.)

References

Anandalakshmi, R., Pruss, G.J., Ge, X., Marathe, R., Mallory, A.C., Smith, T.H., and Vance, V.B. (1998). A viral suppressor of gene silencing in plants. Proc. Natl. Acad. Sci. **95**: 13079-13084.

Aravind, L. and Landsman, D. (1998). AT-hook motifs identified in a wide variety of DNA-binding proteins. Nucleic Acids Res. **26**: 4413–4421.

Baroux, C., Pecinka, A., Fuchs, J., Schubert, I., and Grossniklaus, U. (2007). The triploid endosperm genome of *Arabidopsis* adopts a peculiar, parental-dosage-dependent chromatin organization. Plant Cell **19**: 1782–1794.

Becker, D., Kemper, E., Schell, J and Masterson. A. (1992). New plant binary vectors with selectable markers located proximal to the left T-DNA border. Plant Mol. Biol. **20**: 1195–1197.

Bhojwani, S.S. (2012). Plant tissue culture: applications and limitations (Elsevier B.V.).

Birnbaum, K.D. and Sánchez Alvarado, A. (2008). Slicing across kingdoms: regeneration in plants and animals. Cell **132**: 697–710.

Borchert, T., Fuchs, J., Winkelmann, T., and Hohe, A. (2007). Variable DNA content of Cyclamen persicum regenerated via somatic embryogenesis: rethinking the concept of long-term callus and suspension cultures. Plant Cell. Tissue Organ Cult. **90**: 255–263.

Bourbousse, C., Mestiri, I., Zabulon, G., Bourge, M., Formiggini, F., Koini, M. a, Brown, S.C., Fransz, P., Bowler, C., and Barneche, F. (2015). Light signaling controls nuclear architecture reorganization during seedling establishment. Proc. Natl. Acad. Sci. **112**: E2836–E2844.

Boutilier, K., Offringa, R., Sharma, V.K., Kieft, H., Ouellet, T., Zhang, L., Hattori, J., Liu, C., van Lammeren, A.A.M., Miki, B.L.A., Custers, J.B.M., and van Lookeren, M.M. (2002). Etopic expression of *BABY BOOM* triggers a conversion from vegetative to embryonic growth. Plant Cell **14**: 1737–1749.

Breuer, C., Braidwood, L., and Sugimoto, K. (2014). Endocycling in the path of plant development. Curr. Opin. Plant Biol. **17C**: 78–85.

Breuninger, H., Rikirsch, E., Hermann, M., Ueda, M., and Laux, T. (2008). Differential expression of *WOX* genes mediates apical-basal axis formation in the *Arabidopsis* embryo. Dev. Cell **14**: 867–76.

Carone, D.M. and Lawrence, J.B. (2013). Heterochromatin instability in cancer: from the Barr body to satellites and the nuclear periphery. Semin. Cancer Biol. **23**: 99–108.

Catez, F., Yang, H., Tracey, K.J., Reeves, R., Misteli, T., and Bustin, M. (2004). Network of dynamic interactions between histone h1 and high-mobility-group proteins in chromatin. Mol Cell Biol. **24**:4321-4328.

Clough, S.J. and Bent, F. (1998). Floral dip: a simplified method for *Agrobacterium*-mediated transformation of *Arabidopsis thaliana*. Plant J. **16**: 735–743.

Czechowski, T., Stitt, M., Altmann, T., and Udvardi, M.K. (2005). Genome-wide identification and testing of superior reference genes for transcript normalization in *Arabidopsis* . Plant Physil **139**: 5–17.

Den Dulk-Ras, A. and Hooykaas, P.J.J (1995). Electroporation of *Agrobacterium tumefaciens*. Plant Cell Electroporation Electrofusion Protoc.**55**: 63–72.

Edgar, B. a and Orr-Weaver, T.L. (2001). Endoreduplication cell cycles: more for less. Cell **105**: 297–306.

Fang, Y. and Spector, D.L. (2005). Centromere positioning and dynamics in living *Arabidopsis* plants. Mol Biol Cell. **16**: 5710–5718.

Finn, T.E., Wang, L., Smolilo, D., Smith, N. a, White, R., Chaudhury, A., Dennis, E.S., and Wang, M.-B. (2011). Transgene expression and transgene-induced silencing in diploid and autotetraploid *Arabidopsis*. Genetics **187**: 409–443.

Fujimoto, S., Matsunaga, S., Yonemura, M., Uchiyama, S., Azuma, T., and Fukui, K. (2004). Identification of a novel plant MAR DNA binding protein localized on chromosomal surfaces. Plant Mol. Biol. **56**: 225–239.

Gaj, M.D. (2001). Direct somatic embryogenesis as a rapid and efficient system for in vitro regeneration of *Arabidopsis thaliana*. Plant Cell. Tissue Organ Cult. **64**: 39–46.

Gallavotti, A., Malcomber, S., Gaines, C., Stanfield, S., Whipple, C., Kellogg, E., and Schmidt, R.J. (2011). BARREN STALK FASTIGIATE1 is an AT-hook protein required for the formation of maize ears. Plant Cell **23**: 1756–1771.

Gamborg, O. L., Miller, R., and Ojima, K. (1968). Nutrient requirements of suspension cultures of soybean root cells. Exp. Cell Res. **50**: 151–158.

Gleave, A.P. (1992). A versatile binary vector system with a T-DNA organisational structure conducive to efficient integration of cloned DNA into the plant genome. Plant Mol. Biol. **20**: 1203–1207.

Hahn, M. et al. (2013). Suv4-20h2 mediates chromatin compaction and is important for cohesin recruitment to heterochromatin. Genes Dev. **27**: 859–872.

Hand, M.L. and Koltunow, A.M.G. (2014). The genetic control of apomixis: asexual seed formation. Genetics **197**: 441–450.

Horstman, A., Fukuoka, H., Muino, J.M., Nitsch, L., Guo, C., Passarinho, P., Sanchez-Perez, G., Immink, R., Angenent, G., and Boutilier, K. (2015). AIL and HDG proteins act antagonistically to control cell proliferation. Development **142**: 454–464.

Immink, R.G.H., Posé, D., Ferrario, S., Ott, F., Kaufmann, K., Valentim, F.L., de Folter, S., van der Wal, F., van Dijk, A.D.J., Schmid, M., and Angenent, G.C. (2012). Characterization of SOC1's central role in flowering by the identification of its upstream and downstream regulators. Plant Physiol. **160**: 433–449.

Jiménez, V.M. (2005). Involvement of plant hormones and plant growth regulators on in vitro somatic embryogenesis. Plant Growth Regul. **47**: 91–110.

Karimi, M., Depicker, A., and Hilson, P. (2007). Recombinational cloning with plant gateway vectors. Plant Physiol. **145**: 1144–1154.

Kishi, Y., Fujii, Y., Hirabayashi, Y., and Gotoh, Y. (2012). HMGA regulates the global chromatin state and neurogenic potential in neocortical precursor cells. Nat. Neurosci. **15**: 1127–33.

Kondo, Y., Shen, L., Ahmed, S., Boumber, Y., Sekido, Y., Haddad, B.R., and Issa, J.-P.J. (2008). Downregulation of histone H3 lysine 9 methyltransferase G9a induces centrosome disruption and chromosome instability in cancer cells. PLoS One **3**: e2037.

Lee, H.O., Davidson, J.M., and Duronio, R.J. (2009). Endoreduplication : polyploidy with purpose. Genes Dev.**23**: 2461–2477.

Lermontova, I., Schubert, V., Fuchs, J., Klatte, S., Macas, J., and Schubert, I. (2006). Loading of *Arabidopsis* centromeric histone CENH3 occurs mainly during G2 and requires the presence of the histone fold domain. Plant Cell **18**: 2443–2451.

Lim, P.O., Kim, Y., Breeze, E., Koo, J.C., Woo, H.R., Ryu, J.S., Park, D.H., Beynon, J., Tabrett, A., Buchanan-Wollaston, V., and Nam, H.G. (2007). Overexpression of a chromatin architecture-controlling AT-hook protein extends leaf longevity and increases the post-harvest storage life of plants. Plant J. **52**: 1140–1153.

Livak, K.J. and Schmittgen, T.D. (2001). Analysis of relative gene expression data using real-time quantitative PCR and the 2(-Delta Delta C(T)) Method. Methods **25**: 402–408.

Lotan, T., Ohto, M., Yee, K.M., West, M. a, Lo, R., Kwong, R.W., Yamagishi, K., Fischer, R.L., Goldberg, R.B., and Harada, J.J. (1998). *Arabidopsis LEAFY COTYLEDON1* is sufficient to induce embryo development in vegetative cells. Cell **93**: 1195–1205.

Maison, C. and Almouzni, G. (2004). HP1 and the dynamics of heterochromatin maintenance. Nat. Rev. Mol. Cell Biol. **5**: 296–304.

Masson, Jean and Paszkowski, J. (1992). The culture response of *Arabidopsis thaliana* protoplasts is determined by the growth conditions of donor plants. Plant J. **2**: 829–833.

Matsushita, A., Furumoto, T., Ishida, S., and Takahashi, Y. (2007). AGF1, an AT-hook protein, is necessary for the negative feedback of *AtGA3ox1* encoding *GA 3-oxidas*e. Plant Physiol. **143**: 1152–1162.

Meister, P., Mango, S.E., and Gasser, S.M. (2011). Locking the genome: nuclear organization and cell fate. Curr. Opin. Genet. Dev. **21**: 167–174.

Ng, K.-H., Yu, H., and Ito, T. (2009). AGAMOUS controls *GIANT KILLER*, a multifunctional chromatin modifier in reproductive organ patterning and differentiation. PLoS Biol. **7**: e1000251.

Orbović, V., Ćalović, M., Viloria, Z., Nielsen, B., Gmitter, F.G., Castle, W.S., and Grosser, J.W. (2007). Analysis of genetic variability in various tissue culture-derived lemon plant populations using RAPD and flow cytometry. Euphytica **161**: 329–335.

Ozias-Akins, P. and van Dijk, P.J. (2007). Mendelian genetics of apomixis in plants. Annu. Rev. Genet. **41**: 509–537.

Passarinho, P., Ketelaar, T., Xing, M., van Arkel, J., Maliepaard, C., Hendriks, M.W., Joosen, R., Lammers, M., Herdies, L., den Boer, B., van der Geest, L., and Boutilier, K. (2008). BABY BOOM target genes provide diverse entry points into cell proliferation and cell growth pathways. Plant Mol. Biol. **68**: 225–237.

Pfaffl, M.W. (2001). A new mathematical model for relative quantification in real-time RT-PCR. Nucleic Acids Res. **29**: e45.

Pillot, M., Baroux, C., Vazquez, M.A., Autran, D., Leblanc, O., Vielle-Calzada, J.P., Grossniklaus, U., and Grimanelli, D. (2010). Embryo and endosperm inherit distinct chromatin and transcriptional states from the female gametes in *Arabidopsis*. Plant Cell **22**: 307–320.

Prado, M.J., Rodriguez, E., Rey, L., González, M.V., Santos, C., and Rey, M. (2010). Detection of somaclonal variants in somatic embryogenesis-regenerated plants of Vitis vinifera by flow cytometry and microsatellite markers. Plant Cell, Tissue Organ Cult. **103**: 49–59.

Radoeva, T. and Weijers, D. (2014). A roadmap to embryo identity in plants. Trends Plant Sci: **19**, 709–716.

Reeves, R. (2010). Nuclear functions of the HMG proteins. Biochim. Biophys. Acta - Gene Regul. Mech. **1799**: 3–14.

Schwab, R., Ossowski, S., Riester, M., Warthmann, N., and Weigel, D. (2006). Highly specific gene silencing by artificial microRNAs in *Arabidopsis*. Plant Cell **18**: 1121–1133.

Sgarra, R., Zammitti, S., Lo Sardo, A., Maurizio, E., Arnoldo, L., Pegoraro, S., Giancotti, V., and Manfioletti, G. (2010). HMGA molecular network: From transcriptional regulation to chromatin remodeling. Biochim. Biophys. Acta **1799**: 37–47.

Shi, Q. and King, R.W. (2005). Chromosome nondisjunction yields tetraploid rather than aneuploid cells in human cell lines. Nature **437**: 1038–1042.

Smertenko, A. and Bozhkov, P. V (2014). Somatic embryogenesis: life and death processes during apical-basal patterning. J. Exp. Bot. **65**: 1343–1360.

Soriano, M., Li, H., and Boutilier, K. (2013). Microspore embryogenesis : establishment of embryo identity and pattern in culture. Plant Reprod. **26**: 181–196.

Stone, S.L., Braybrook, S. A, Paula, S.L., Kwong, L.W., Meuser, J., Pelletier, J., Hsieh, T.-F., Fischer, R.L., Goldberg, R.B., and Harada, J.J. (2008). *Arabidopsis LEAFY COTYLEDON2* induces maturation traits and auxin activity: Implications for somatic embryogenesis. Proc. Natl. Acad. Sci. **105**: 3151–3156.

Stone, S.L., Kwong, L.W., Yee, K.M., Pelletier, J., Lepiniec, L., Fischer, R.L., Goldberg, R.B., and Harada, J.J. (2001). *LEAFY COTYLEDON2* encodes a B3 domain transcription factor that induces embryo development. Proc. Natl. Acad. Sci. **98**: 11806–11811.

De Storme, N., De Schrijver, J., Van Criekinge, W., Wewer, V., Dörmann, P., and Geelen, D. (2013). *GLUCAN SYNTHASE-LIKE8* and *STEROL METHYLTRANSFERASE2* are required for ploidy consistency of the sexual reproduction system in *Arabidopsis.* Plant Cell **25**: 387–403.

Street, I.H., Shah, P.K., Smith, A.M., Avery, N., and Neff, M.M. (2008). The AT-hook-containing proteins SOB3/AHL29 and ESC/AHL27 are negative modulators of hypocotyl growth in *Arabidopsis*. Plant J. **54**: 1–14.

Swarup, R., Kramer, E. M., Perry, P., Knox, K., Leyser, H. O., Haseloff, J., and Bennett, M.J. (2005). Root gravitropism requires lateral root cap and epidermal cells for transport and response to a mobile auxin signal. Nat. Cell Biol. **7**: 1057–1065.

Taylor, R.L. (1967). The foliar embryos of *Malaxis paludosa*. Can. J. Bot. **45**: 1553–1556.

Tsukaya, H. (2013). Does ploidy level directly control cell size? Counterevidence from *Arabidopsis* genetics. PLoS One **8**: e83729.

Winkelmann, T., Sangwan, R.S., and Schwenkel, H.-G. (1998). Flow cytometric analyses in embryogenic and non-embryogenic callus lines of *Cyclamen persicum Mill*.: relation between ploidy level and competence for somatic embryogenesis. Plant Cell Rep. **17**: 400–404.

Wójcikowska, B., Jaskóła, K., Gąsiorek, P., Meus, M., Nowak, K., and Gaj, M.D. (2013). *LEAFY COTYLEDON2* (*LEC2*) promotes embryogenic induction in somatic tissues of *Arabidopsis*, via YUCCA-mediated auxin biosynthesis. Planta **238**: 425–440.

Xiao, C., Chen, F., Yu, X., Lin, C., and Fu, Y.-F. (2009). Over-expression of an AT-hook gene, *AHL2*2, delays flowering and inhibits the elongation of the hypocotyl in *Arabidopsis thaliana*. Plant Mol. Biol. **71**: 39–50.

Yanagida, M. (2005). Basic mechanism of eukaryotic chromosome segregation. Phil. Trans. R. Soc. B **360**: 609–621.

Yarbrough, J.A. (1932). Anatomical and developmental studies of the foliar embryos of *Bryophyllum calycinum*. Am. J. Bot. **19**: 443–453.

Zhao, J., Favero, D.S., Peng, H., and Neff, M.M. (2013). *Arabidopsis thaliana* AHL family modulates hypocotyl growth redundantly by interacting with each other via the PPC/DUF296 domain. Proc. Natl. Acad. Sci. **110**: E4688–E4697

Zhao, J., Favero, D.S., Qiu, J., Roalson, E.H., and Neff, M.M. (2014). Insights into the evolution and diversification of the *AT-hook Motif Nuclear Localized* gene family in land plants. BMC Plant Biol. **14**: 2-19

Zhou, J., Wang, X., Lee, J.-Y., and Lee, J.-Y. (2013). Cell-to-cell movement of two interacting AT-hook factors in *Arabidopsis* root vascular tissue patterning. Plant Cell **25**: 187–201.

Zuo, J., Niu, Q.-W., Frugis, G., and Chua, N.-H. (2002). The *WUSCHEL* gene promotes vegetative-to-embryonic transition in *Arabidopsis*. Plant J. **30**: 349–359.

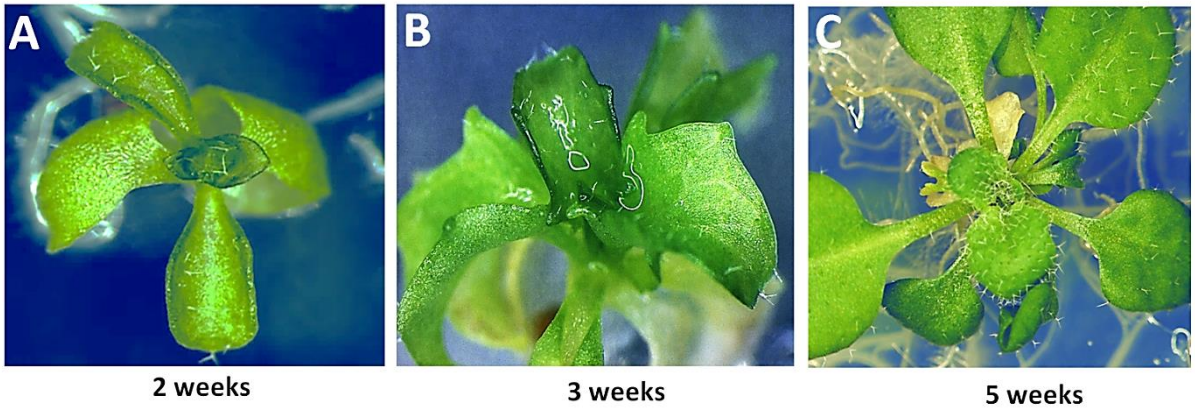

Supplementary figure 1 *AHL15* overexpression represses seedling development in *Arabidopsis*. (A-C) The morphology of 2 (A), 3 (B), and 5 (C)-week-old *35S::AHL15* plants were grown in long day conditions (16 hr light/ 8 hr dark).

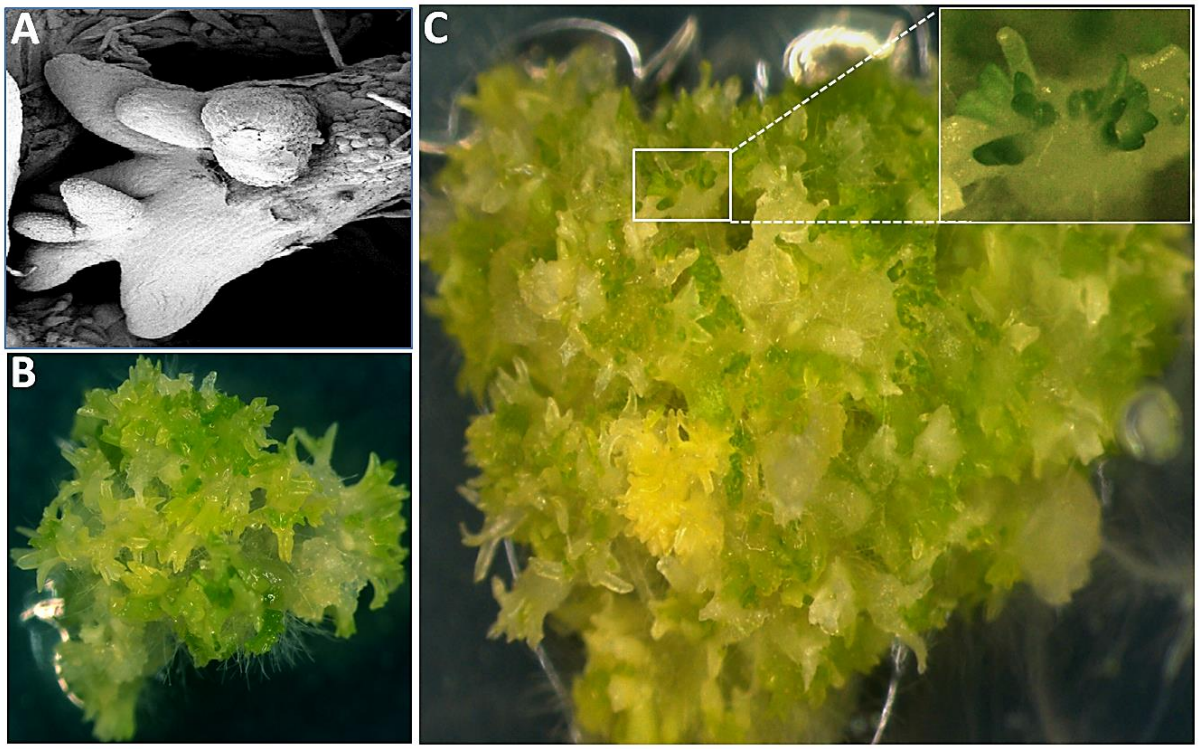

Supplementary figure 2 *AHL15* overexpression induces reiterative somatic embryo initiation resulting in embryonic masses. (A) Scanning electron micrograph showing the secondary somatic embryos formed on a 35S::AHL15 primary somatic embryo. (B) The morphology of a 3-week-old *AHL15*-induced embryonic mass following secondary SE. (C) The morphology of a 2-month-old embryonic mass formed from a *35S::AHL15* seedling.

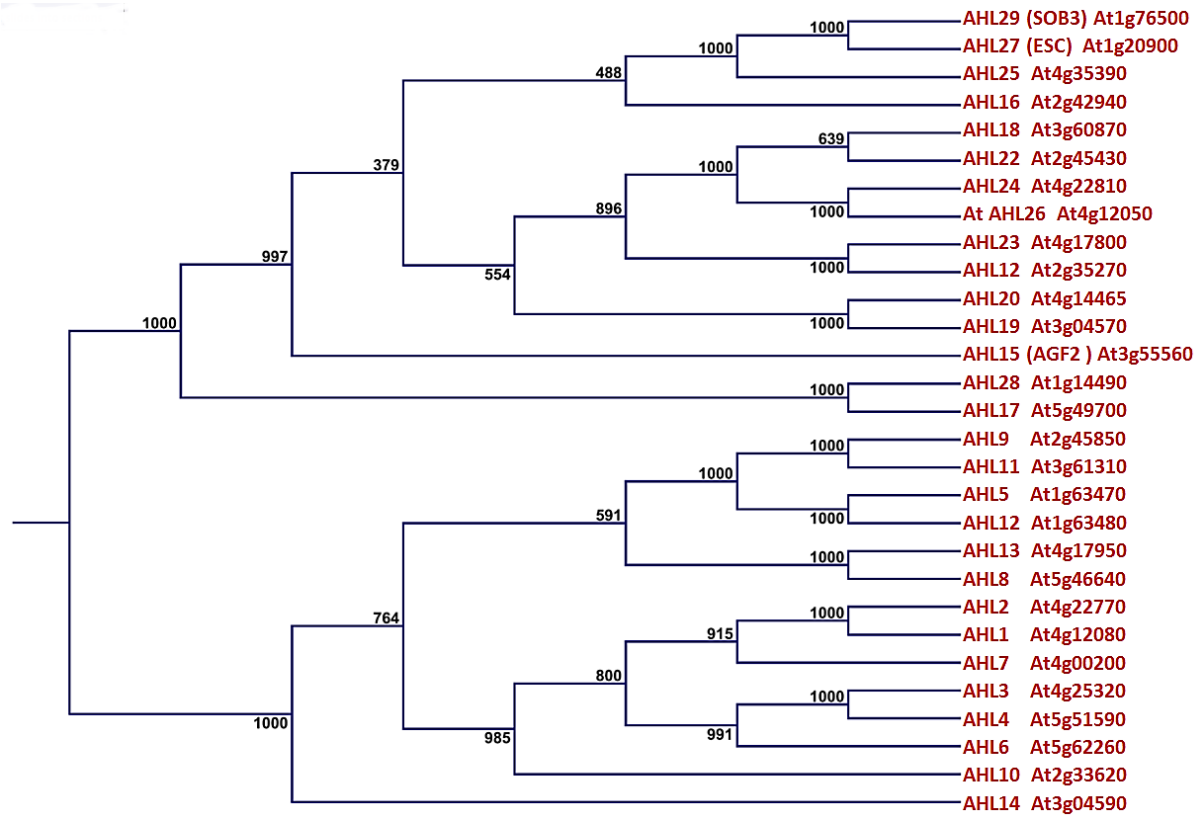

Supplementary figure 3 A phylogenetic tree of the *Arabidopsis AHL* gene family.

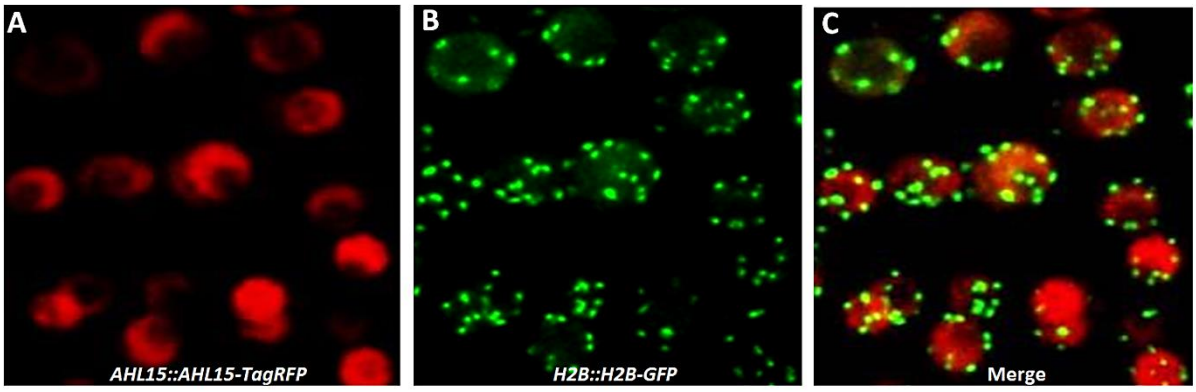

Supplementary figure 4 AHL15-TagRFP does not co-localize with H2B-GFP-marked heterochromatin. (A-C) Confocal images of root meristem cells. The RFP channel showing nuclear-localized AHL15-tagRFP (A), the GFP channel showing H2B-GFP marked heterochromatin (B), and the merged images (C).

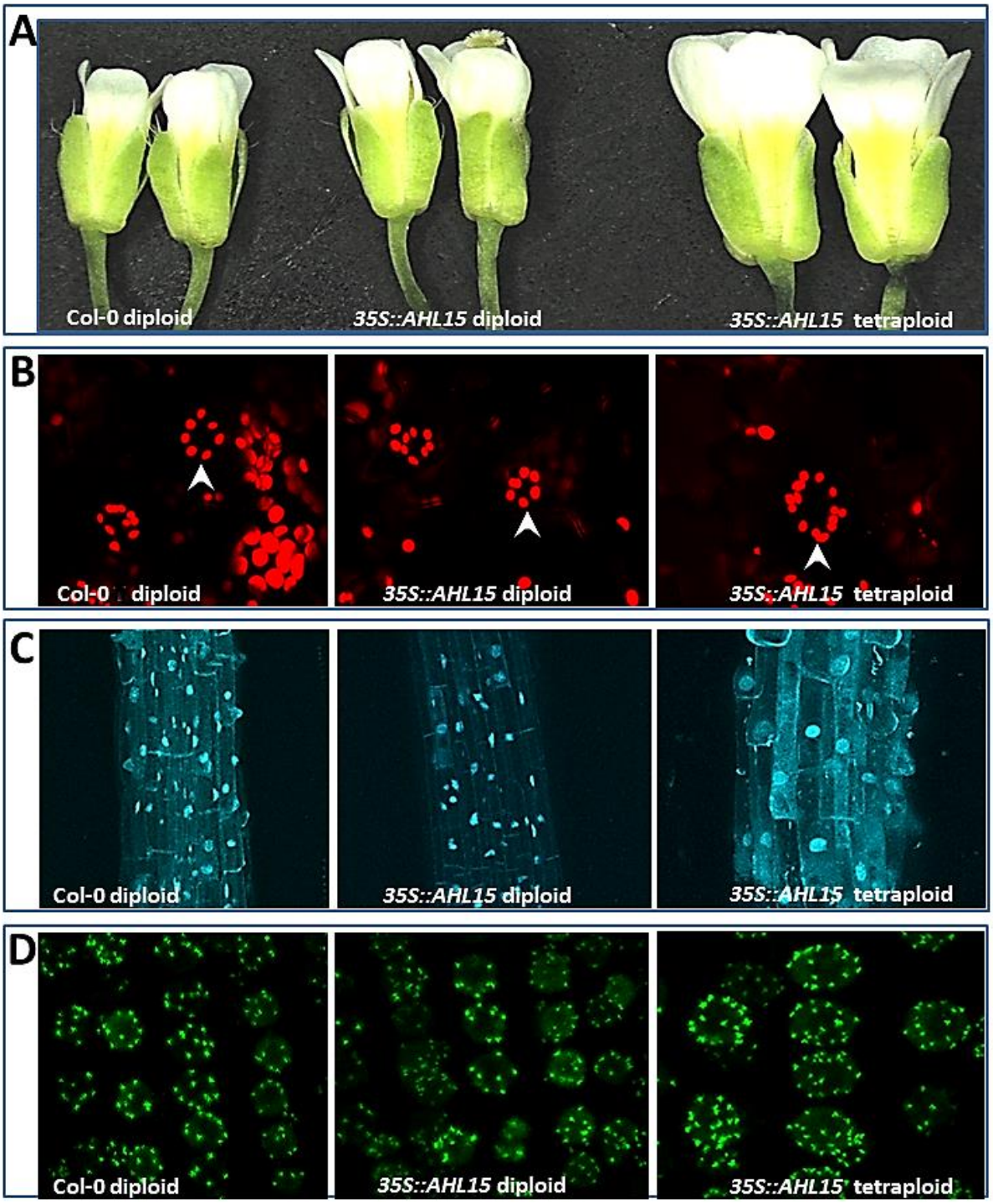

Supplementary figure 5 Plants regenerated from *35S::AHL15*-induced somatic embryos are frequently polyploid. (A-D) Analysis of wild-type *Arabidopsis* (left), and a diploid plant line (middle), and a tetraploid plant line (right) each regenerated from an *35S::AHL15*-induced somatic embryo. (A) Tetraploid *35S::AHL15* plants show increased organ size compared to the diploid control plants, as demonstrated by the size of the flower organs. (B-D) Tetraploid *35S::AHL15* plants have twice the number/a higher number of chloroplasts in guard cells (marked by arrow heads, B), show root cells with a larger nucleus and cell size (C), and show a duplication in the CENH3-GFP-labelled centromeres (D) compared to wild-type and diploid *35S::AHL15 Arabidopsis* plants.

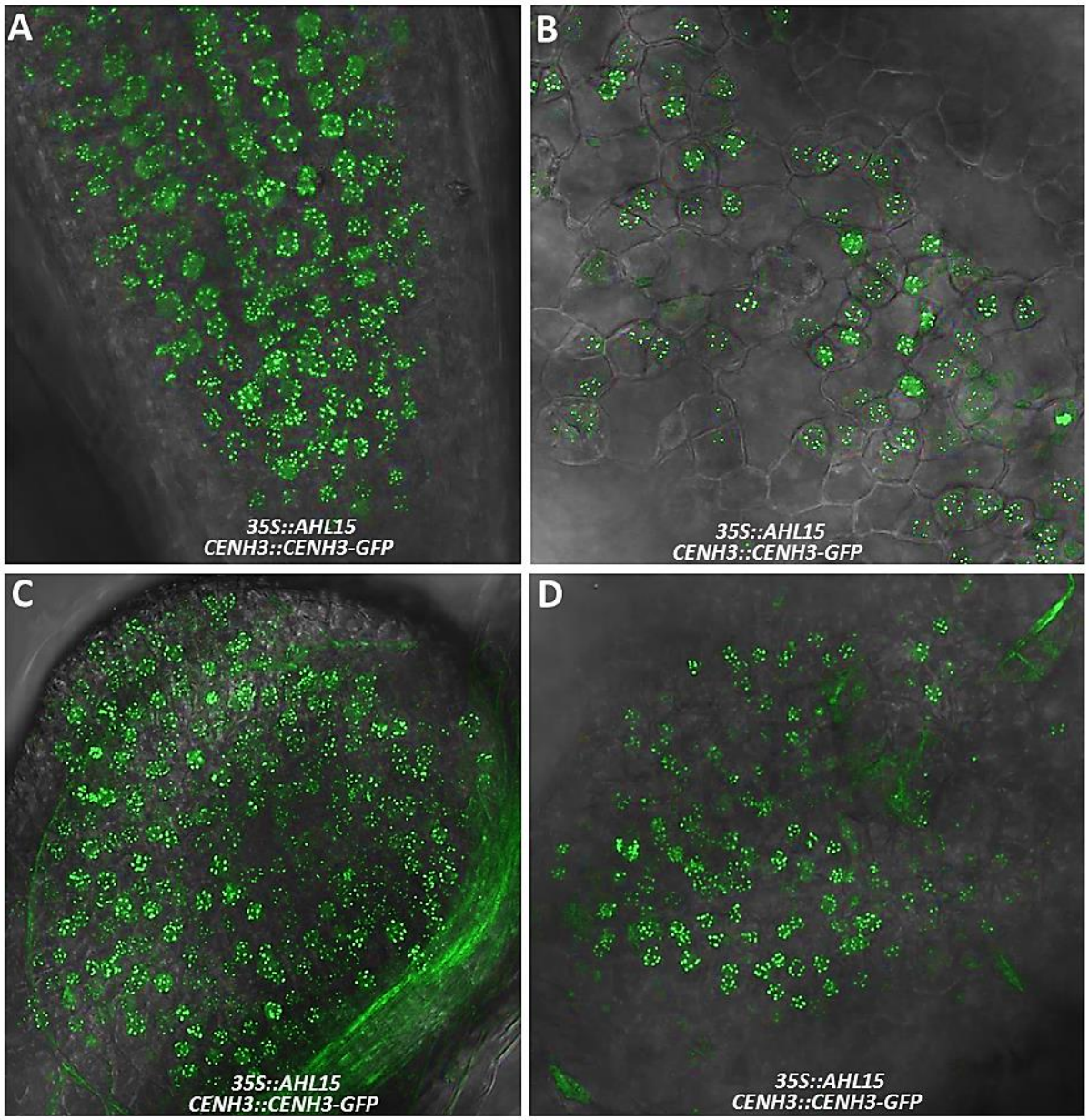

Supplementary figure 6 Endoploidy does not occur in *35S::AHL15* leaves and roots. (A-D) CENH3-GFP–mediated centromere labeling in cells of a root tip (A), a young leaf (B), or in cells of 2,4-D-induced callus on a root (C), or a young leaf (D).

Supplementary Table 1: Primers used for cloning, genotyping and qRT-PCR (F: forward; R: reverse)

Name	Sequence (5' to 3')	Purpose
35S::AHL15-F	CCCGGGATGGCGAATCCTTGGTGGGTAG	*35S::AHL15* construct
35S::AHL15-R	GGATCCTCAATACGAAGGAGGAGCACG	
35S::AHL29-F	ATAAGAATGCGGCCGCGACGGTGGTTACGATCAATC	*35S::AHL29* construct
35S::AHL29-R	ATAGTTTAGCGGCCGCCTAAAAGGCTGGTCTTGGTG	
35S::AHL20 –F	ATAAGAATGCGGCCGCGCAAACCCTTGGTGGACGAAC	*35S::AHL20* construct
35S::AHL20-R	ATAGTTTAGCGGCCGCTCAGTAAGGTGGTCTTGCGT	
35S::AHL19-F	GGGGACAAGTTTGTACAAAAAAGCAGGCTCGATGGCG AATCCATGGTGGAC	*35S::AHL19* construct
35S::AHL19-R	GGGGACCACTTTGTACAAGAAAGCTGGGTAAACAAGT AGCAACTGACTGG	
AHL15-GUS-F	GGGGACAAGTTTGTACAAAAAAGCAGGCTCGACACTCC TCTGTGCCACATT	*AHL15::AHL15-GUS* construct
AHL15-GUS-R	GGGGACCACTTTGTACAAGAAAGCTGGGTAATACGAAG GAGGAGCACGAG	*AHL15::AHL15-tagRFP*
I miR-s AHL20	GATTAGACTACCTCAAATTGCTATCTCTCTTTTGTATTCC	
II miR-a AHL20	GATAGCAATTTGAGGTAGTCTAATCAAAGAGAATCAATGA	
III miR*s AHL20	GATAACAATTTGAGGAAGTCTATTCACAGGTCGTGATATG	*35S::amiRAHL20* construct
IV miR*a AHL20	GAATAGACTTCCTCAAATTGTTATCTACATATATATTCCT	
amiRNA AHL20-F	GGGGACAAGTTTGTACAAAAAAGCAGGCTCGCGACGGT ATCGATAAGCTTG	
amiRNA AHL20-R	GGGGACCACTTTGTACAAGAAAGCTGGGTACCCATGGCG ATGCCTTAAAT	
SALK_040729-F	GTCGGAGAGCCATCAACACCA	ahl15 genotyping
SALK_040729-R	CGACGACCCGTAGACCCGGATC	
SALK_070123-F	GGCGAATCCATGGTGGACAGG	ahl19 genotyping
SALK_070123-R	GGCCGCTCATCTGTCCTCCTC	
qAHL15-F	AAGAGCAGCCGCTTCAACTA	qRT-PCR *AHL15*
qAHL15-R	TGTTGAGCCATTTGATGACC	
qAHL20-F	CAAGGCAGGTTTGAAATCTTATCT	qRT-PCR *AHL120*
qAHL20-R	TAGCGTTAGAGAAAGTAGCAGCAA	
qAHL19-F	CTCTAACGCGACTTACGAGAGATT	qRT-PCR *AHL19*
qAHL19-R	ATATTATACACCGGAAGTCCTTGGT	
qβ-TUBULIN-6-F	TGGGAACTCTGCTCATATCT	qRT-PCR *TUBULIN-6*
qβ-TUBULIN-6-R	GAAAGGAATGAG GTTCACTG	
qSAND-F	AACTCTATGCAGCATTTGATCCACT	qRT-PCR *SAND*
qSAND-R	TGATTGCATATCTTTATCGCCATC	

*, F: forward; R: reverse

Chapter 3

A molecular switch for juvenility and polycarpy in flowering plants

Omid Karami[1], Majid Khan[1], Arezoo Rahimi[1], Patrick Mak[2,3], Monique Compier[2,4] and Remko Offringa[1]

[1]Plant Developmental Genetics, Institute of Biology Leiden, Leiden University, Sylviusweg 72, 2333 BE Leiden, Netherlands
[2]Add2X Biosciences BV, Sylviusweg 72, 2333 CB Leiden, Netherlands
[3] Current address: Sanquin Plasma Products bv, Dept. Product Development, Plesmanlaan 125, 1066 CX Amsterdam, The Netherlands
[4] Current address: Rijk Zwaan, Burgemeester Crezeelaan 40, 2678 KX De Lier, Netherlands

Abstract

In flowering plants, Ageing is defined by a series of developmental phase transitions that start with vegetative growth, followed by flowering and culminating in seed production. Tissue senescence and plant death follow seed production in monocarpic plants while polycarpic plants prolong their life span by maintaining a number of vegetative axillary meristems, thereby allowing subsequent cycles of vegetative and reproductive development. Here we show that the AT-HOOK MOTIF CONTAINING NUCLEAR LOCALIZED protein AHL15/REJUVENATOR (RJV) is a suppressor of developmental phase transitions. Loss-of-function of *RJV* in *Arabidopsis* resulted in precocious appearance of adult vegetative traits and early flowering, whereas *RJV* overexpression prolonged the juvenile phase and delayed flowering in *Arabidopsis* and tobacco. We also show that RJV is a suppressor of axillary meristem maturation, with effects on plant shoot architecture and longevity. Expression of a dominant-negative *RJV-GUS* gene fusion accelerated axillary meristem maturation, whereas constitutive expression of *RJV* kept juvenile traits on axillary meristems during flowering and converted monocarpic *Arabidopsis* and tobacco plants into polycarpic plants with enhanced seed and biomass production. Our results show that *RJV* acts downstream of Ageing (*miR156*, *SPL*) and flowering (*SOC1*, *FUL*) genes as a molecular switch between monocarpic and polycarpic life history strategy, and can be used as a breeding tool to promote sustainable plant production by converting annual crops into perennial plants.

Keywords: developmental phase changes, *AHL* genes, *REJUVENATOR* gene, monocarpic, polycarpic, *Arabidopsis*, tobacco

Introduction

Plant development progresses through a fixed order of distinct phases, starting with embryogenesis and followed successively by the juvenile vegetative, adult vegetative, reproductive and gametophytic phases. During the juvenile vegetative phase the plant is usually not competent to flower. Flowering requires the transition from juvenile to adult vegetative development, which is referred to as the vegetative phase change, and is characterized by specific changes in leaf morphology (Wu and Poethig, 2006; Wu et al., 2009; Usami et al., 2009). The transition from the juvenile to the adult phase involves/requires considerable genetically pre-determined molecular and physiological changes that are also environmentally regulated (Jarillo et al., 2009; Kaufmann et al., 2010). Although all flowering plants go through the same developmental phases, there are major differences in the life span of individual plant species, which can vary from a few weeks up to several thousand years. Many flowering plant species are monocarpic: they produce seed but are unable to grow further as all their vegetative meristems are converted to reproductive meristems. Monocarpic plants are generally annual or biannual, i.e. they live one or two growing seasons, respectively. By contrast, many other flowering plant species are polycarpic: polycarpic plants generally live for more than two growing seasons (perennial), and do so by maintaining underground root stocks or axillary meristems in the vegetative state, allowing them to produce new shoots after seed set and during the next growing season (Munné-Bosch, 2008; Amasino, 2009).

The genetic basis for the monocarpic and polycarpic growth habits has been investigated in a number of cruciferous plants (Wang et al., 2009b; Zhou et al., 2013a). *Arabis alpine* and *Cardamine flexuosa* show temperature-dependent polycarpy that is regulated by the temperature sensitive repression of orthologs of the *Arabidopsis thaliana* MADS box gene *FLOWERING LOCUS C* (*FLC*), respectively *PEP1* and *CfFLC* (Wang et al., 2009b; Zhou et al., 2013a). Under higher ambient temperatures *PEP1* and *CfFLC* block the conversion of vegetative meristems into floral meristems to maintain vegetative development, but under low temperatures, during winter, cold-induced chromatin modifications repress *PEP1* and *CfFLC* expression, promoting conversion of vegetative meristems to floral mersitems and subsequent flowering in spring (Wang et al., 2009b; Zhou et al., 2013a). Despite these studies, the molecular basis for the difference between the mono- and polycarpic growth habit is still largely unknown.

Here we identify a role for the *Arabidopsis AT-HOOK MOTIF COINTAINING NUCLEAR LOCALIZED 15/REJUVENATOR* (*AHL15/RJV*) gene in the control of plant growth habit. Nuclear proteins containing one or more AT-hook motifs have been identified in all eukaryotes, where they contribute to a diverse array of crucial cellular processes (Reeves, 2010). The AT-hook motif binds to the minor groove of AT-rich DNA, and in animal cells these proteins have been found to induce changes in chromatin structure(Aravind and Landsman, 1998; Reeves, 2010). Besides the AT-hook motif, the plant-specific AHL proteins have a PPC domain that contributes to the physical interaction of AHL proteins with other nuclear proteins, such as transcription factors (Zhao et al., 2013). Other AHL proteins have been shown to be implicated in several aspects of plant growth and development in *Arabidopsis*, including hypocotyl growth (Street et al., 2008; Xiao et al., 2009; Zhao et al.,

2013), vascular tissue differentiation (Zhou et al., 2013b), flower development (Ng et al., 2009), and flowering time (Street et al., 2008; Xiao et al., 2009; Xu et al., 2013; Yun et al., 2012).

Our analyses in *Arabidopsis* and tobacco (*Nicotiana tabacum*) show that *AHL15/RJV* and its paralogs act as general suppressors of developmental phase changes. In the monocarpic plant species *Arabidopsis*, reduced A*HL15/RJV* expression coincided with a faster progression from the vegetative to the reproductive phase, during which all vegetative meristems were converted to reproductive meristems. By contrast, A*HL15/RJV* overexpression delayed the vegetative to reproductive phase change in both *Arabidopsis* and tobacco, causing some axillary meristems to be maintained in the vegetative phase, thereby allowing polycarpic development in these monocarpic annuals.

Results

Arabidopsis AHL15 and its close homologs delay the vegetative phase change and flowering

The *Arabidopsis AHL15* gene was identified in an unrelated yeast one-hybrid screen. Database analysis showed that it belonged to a large gene family of AT-hook motif nuclear proteins in *Arabidopsis*, where it grouped together with proteins containing a single AT-hook motif, among which the close paralogs *AHL19* and *AHL20* (Fig. S1A). To study the wild-type function of *AHL15*, we selected *ahl15* and *ahl19* single loss-of-function mutants (Fig. S1B), and generated a knock down for *AHL20* using an artificial microRNA (*amiRAHL20*), since a T-DNA insertion line was not available for this gene. In line with the previously reported functional redundancy between *AHL* genes (Street et al., 2008; Xiao et al., 2009; Zhao et al., 2013), *ahl15* and *ahl19* loss-of-function mutants (Fig. S1B) flowered at the same time as wild-type plants, as measured by the number of leaves at flowering (Table 1); however, an *ahl15 ahl19 amiRAHL20* triple mutant, and *ahl15/+* heterozygous mutant plants expressing a dominant negative *AHL15::AHL15-GUS* fusion (*ahl15/+ AHL15::AHL15-GUS*) showed a significant reduction in flowering time (Table 1 and Fig. S1C,D). All generated *pAHL15::AHL15-tagRFP* plant lines (n=20) showed a wild-type phenotype, but the majority of the *AHL15::AHL15-GUS* lines (n=25) flowered and senesced early (Fig. S1D). This phenotype was strongly enhanced when the *AHL15::AHL15-GUS* locus of 3 lines was combined with the heterozygous *ahl15* loss-of-function allele. In addition, approximately 25% of the seeds produced by *ahl15/+ AHL15::AHL15-GUS* plants were defective (Chapter 2, Fig. 2), and no progeny homozygous for the *ahl15* allele could be obtained, suggesting that this genetic combination is embryo lethal. In contrast, *ahl15 pAHL15::AHL15-tagRFP* plants were fertile and showed wild-type development. These results suggested that the AHL15-tagRFP fusion is functional, and that the AHL15-GUS fusion protein is inactive and has a dominant negative effect on the activity of other AHL proteins in the absence of sufficient wild-type AHL15 protein. Triple homozygous *ahl15 AHL15::AHL15-GUS AHL15::AHL15-tagRFP* plants developed normally and were fertile, corroborating that the AHL15-tagRFP protein is functional and can negate the dominant negative effect of the AHL15-GUS fusion in the *ahl15* loss-of-function mutant background.

Table 1: *AHL* genes redundantly maintain leaf juvenility and suppress flowering.

	Long days (LD)		Short days (SD)	
Genotype	# leaves w/o ab. trichom.[1]	# of rosette leaves[2]	# leaves w/o ab. trichom.[1]	# of rosette leaves[2]
Col-0	5.85 ± 0.08	16.5 ± 0.32	7.10 ± 0.10	34.02 ± 0.35
35S::AHL15-1	16.7 ± 0.42	44.35 ± 0.68 [c]	18.05 ± 0.46[c]	76.10 ± 1.19 [c]
35S::AHL15-2	14.9 ± 0.37[c]	40.55 ± 0.71 [c]	16.40 ± 0.42[c]	69.65 ± 1.18 [c]
ahl15	5.05 ± 0.05[b]	16.15 ± 0.27 [a]	5.65 ± 0.18[b]	31.40 ± 0.34[a]
ahl19	5.75 ± 0.09[a]	15.90 ± 0.33[a]	7.15 ± 0.1[a]	33.30 ± 0.36[a]
ahl15 ahl19	5.15 ± 0.08[b]	15.90 ± 0.19[a]	5.6 ± 0.21[b]	31.05 ± 0.38[a]
ahl15 ahl19 35S:amiRAHL20-1	4.90 ± 0.10[b]	13.80 ± 0.23[c]	5.10 ± 0.14[c]	25.85 ± 0.31[c]
ahl15 ahl19 35S:amiRAHL20-2	5.25 ± 0.14[b]	12.00 ± 0.16[c]	5. 30 ± 0.16[c]	22.04 ± 0.38[c]
AHL15::AHL15-GUS-1	3.90 ± 0.06[c]	10.40 ±0.24 [c]	4.25 ± 0.09 [c]	25.85 ± 0.33[c]
AHL15::AHL15-GUS-2	4.00 ± 0.06[c]	10.75 ± 0.23[c]	4.35 ± 0.13[c]	26.75 ± 0.42[c]
ahl15/+ AHL15::AHL15-GUS	3.95 ± 0.11[c]	9.20 ± 0.34[c]	4.10 ± 0.12 [c]	17.87 ± 0.46 [c]

[a] Not significantly different from wild type (Student's *t*-test, $p > 0.05$).
[b] Significantly different from wild type (Student's *t*-test, $p < 0.05$).
[c] Significantly different from wild type (Student's *t*-test, $p < 0.01$).
[1] Number of rosette leaves without abaxial trichomes.
[2] Total number of rosette leaves upon bolting. Shown is the mean ± SEM. n= 20 for all genotypes.

In *Arabidopsis*, leaf heteroblasty provides a clear indicator of the vegetative phase change. Juvenile leaves have smooth margins, are rounder (length/width ratio ca. 1) and lack abaxial trichomes, whereas adult leaves have serrated margins, are more elongated (length/width ratio ca. 1.7) and have abaxial trichomes (Telfer et al., 1997). The *ahl15* single and *ahl15 ahl19 amiRAHL20* triple loss-of-function mutants showed precocious development of adult traits, including elongated and serrated leaves (Fig. 1A,B). In wild-type *Arabidopsis*, only inflorescence meristems produced cauline leaves, whereas *ahl15 ahl19 amiRAHL20* triple mutant plants already formed cauline-like leaves during the vegetative phase (Fig. 1B, e.g. leaf number 10). Similar to *ahl15 ahl19 amiRAHL20* mutant plants, *AHL15::AHL15-GUS* rosette leaves developed a more elongated leaf blade (Fig. 1A,B), and under short day (SD) conditions abaxial trichome production was observed about three plastochrons (time between successive leaf initiation events) earlier than in wild-type plants (Table 1, under SD, in column number of leaves without abaxial trichomes). *ahl15/+ AHL15::AHL15-GUS* plants produced rosette leaves with the most strongly elongated leaf blade (Fig. 1A, B). Expression of *AHL15*, *AHL19*, and *AHL20* and of a more distantly related family member *AHL29* was negatively correlated with shoot age: expression of all four genes declined during the juvenile to adult transition (week three), when shoots and leaves started to show mature traits (Fig. 1C,D).

The above results indicate that besides their role in prolonging flowering time, *AHL* genes also function during early plant development to repress the vegetative phase change and maintain juvenile traits. Previous studies have shown that the competence to enter the reproductive phase in *Arabidopsis* is tightly associated with the vegetative phase change

(Weigel, 1995; Wu and Poethig, 2006), thus *AHL* genes might delay flowering through the maintenance of juvenile potential.

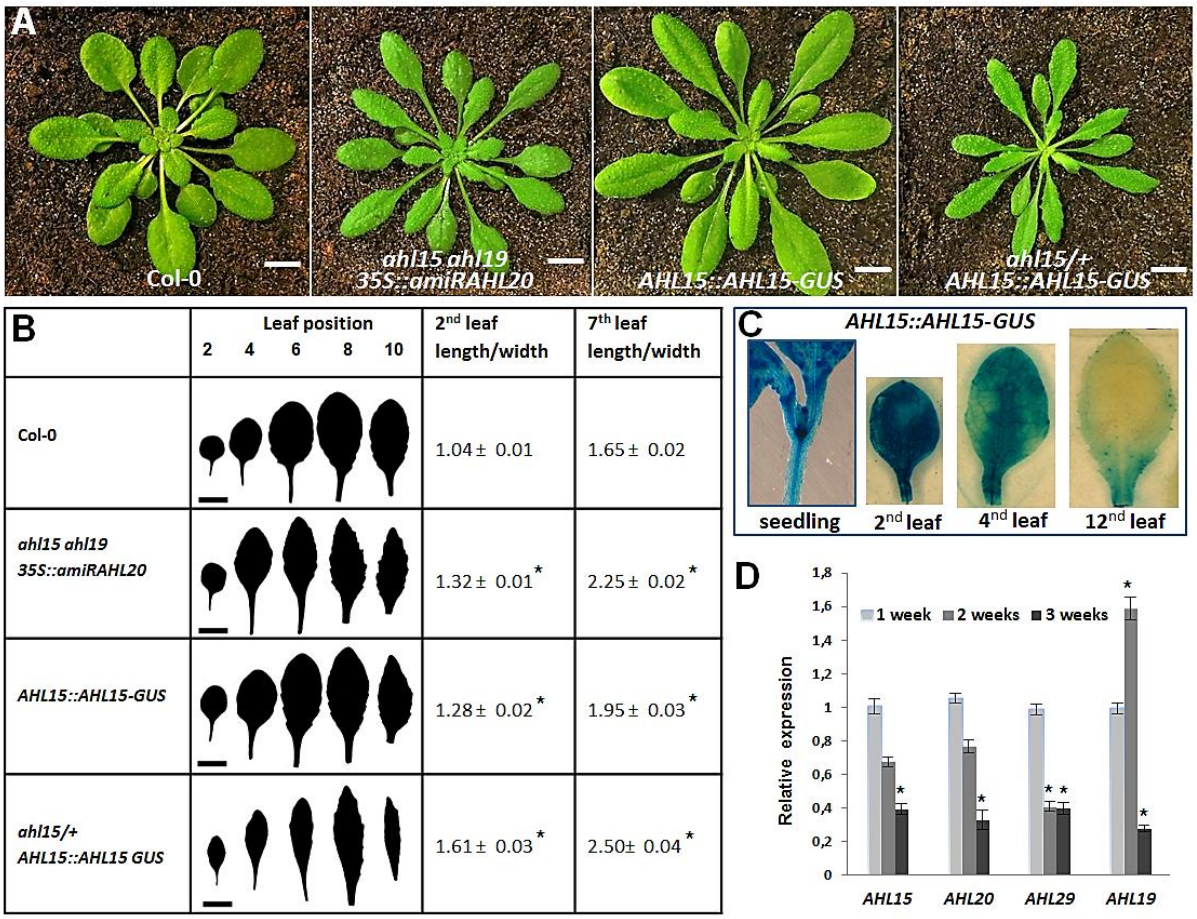

Figure 1 Arabidopsis AHL15 and close paralogs redundantly prolong leaf juvenility during vegetative development. (A) The rosette phenotype of 5-week-old wild-type (Col), *ahl15 ahl19 35S::amiRAHL20*, *AHL15::AHL15-GUS* and *ahl15/+ AHL15::AHL15-GUS* plants grown in short day (SD) conditions. (B) Overview and quantification of rosette leaf shape of wild-type, *ahl15 ahl19 35S::amiRAHL20*, *AHL15::AHL15-GUS* and *ahl15/+ AHL15::AHL15-GUS* plants grown under long day (LD) conditions. Asterisks indicate significant difference from wild-type (Student's *t*-test, $p < 0.01$) and error bars indicate standard error of the mean (n =20). (C) *AHL15::AHL15-GUS* expression in a six-day-old seedling and in juvenile and adult leaves of *AHL15::AHL15-GUS* plants under LD conditions. Leaves were harvested from one-month-old plants. (D) Quantitative RT-PCR analysis of *AHL15*, *AHL20*, *AHL29*, and *AHL19* expression in the shoot apices of one-, two-, or three-week-old seedlings grown under short day (SD) conditions. Asterisks indicate a significant difference in expression levels in one-week-old seedlings (Student's *t*-test, $p < 0.01$) and error bars indicate standard error of the mean of three biological replicates, each with three technical replicates. *β-TUBULIN-6* (At5g12250) was used as the reference gene. Size bars indicate 2 and 1 cm in A and B, respectively.

AHL15 and its paralogs promote vegetative activity of axillary meristems

The bottom nodes of wild-type *Arabidopsis* inflorescences contain an axillary meristem that produces a single cauline leaf and a lateral inflorescence. The first cauline leaves produced on wild-type primary inflorescences are phenotypically similar to rosette leaves (Fig. 2A), whereas the first cauline leaves on *ahl15/+ AHL15::AHL15-GUS* inflorescences were phenotypically more similar to the cauline leaves produced later on wild-type inflorescences (Fig. 2B). The early maturity of *ahl15/+ AHL15::AHL15-GUS* plants led to reduced cauline

leaf formation compared to wild-type plants (Fig. 2H). *AHL15::AHL15-GUS* and *ahl15/+ AHL15::AHL15-GUS* plants also senescenced earlier than wild-type plants (Fig. S2). Under SD conditions, in wild-type plants the most-basal meristems and some aerial axillary meristems continued producing rosette leaves during flowering, indicating that they were still in the vegetative phase (Fig. 3A,C). By contrast, the *ahl15/+ AHL15::AHL15-GUS* axillary meristems lost all vegetative activity after flowering under SD conditions (Fig. 3B,D). To examine whether *AHL15* expression contributed to the photoperiod-dependent fate of axillary meristems, we compered the *AHL15* expression at inflorescence nodes and axils of aerial leaves in plants grown under long day (LD) and SD conditions. GUS staining of *AHL15::AHL15-GUS* plants showed increased *AHL15* expression under SD compared to LD conditions (Fig. 3E). These data show that the *AHL15* gene acts in a photoperiod-dependent manner to promote vegetative development, and further support a role for *AHL15* and its paralogs in maintaining juvenile traits.

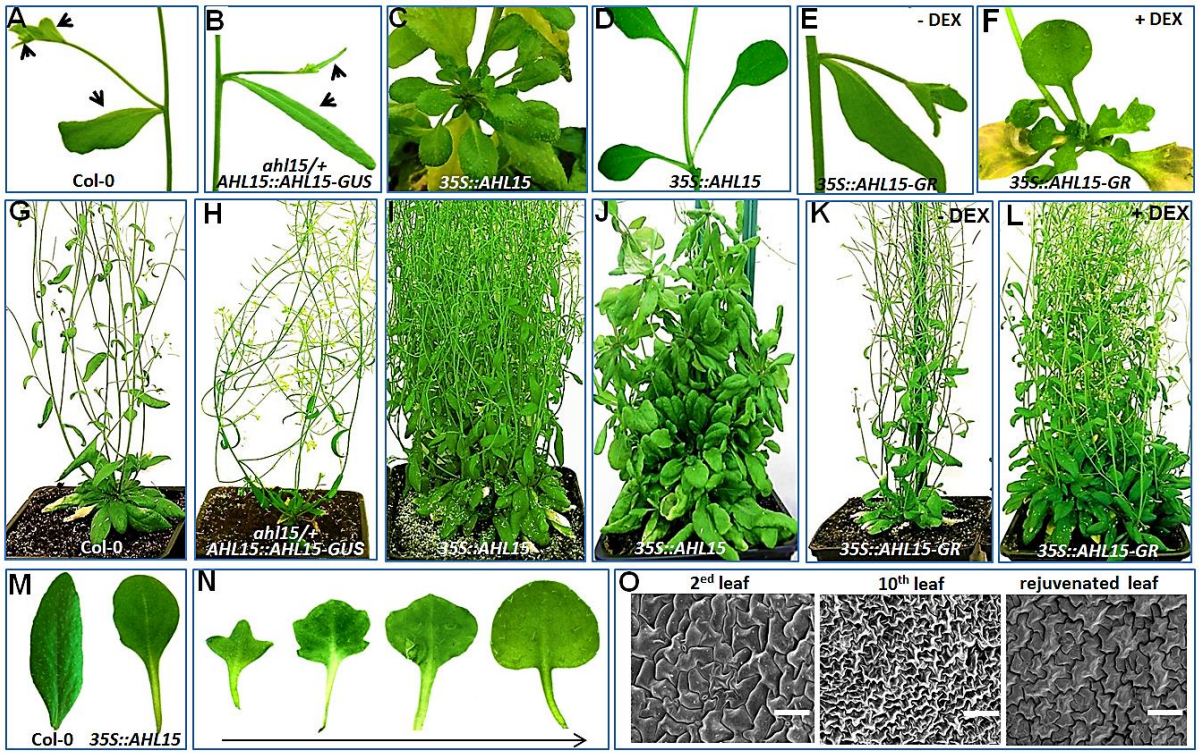

Figure 2 Ectopic *AHL15* expression in *Arabidopsis* rejuvenates axillary meristems. (A) A lateral inflorescence with fertilized flower and cauline leaves (arrow heads) formed on the first inflorescence node of a thirty five-day-old wild-type *Arabidopsis*. (B) A lateral inflorescence with fertilized flower and cauline leaf (arrow heads) formed on the first aerial node of a thirty-day-old *ahl15/+ AHL15::AHL15-GUS* plant. (C) An aerial rosette with juvenile leaves formed on the first inflorescence node of a three-month-old *35S::AHL15* plant. (D The juvenile-like cauline leaves produced on a lateral inflorescence of a 4-month-old *35S::AHL15* plant. (E) A lateral inflorescence and bract on the first inflorescence node of an untreated thirty five-day-old *35S::AHL15-GR* plant. (F) An aerial rosette with juvenile leaves developing from the first inflorescence node of a two- month-old *35S::AHL15-GR* plant two weeks after dexamethasone (DEX) application. (G-L) Mature shoot phenotypes of a flowering wild-type plant (G), a *ahl15/+ AHL15::AHL15-GUS* plant (H), a *35S::AHL15* plant (I), a *35S::AHL15* plant (J), an untreated *35S::AHL15-GR* plant (K), and a *35S::AHL15-GR* plant sprayed with DEX (L). Plants in A-I and K, L were grown under long day conditions, the plant in J under short day conditions. (M) Wild-type (Col-0) and the juvenile-like *35S::AHL15* cauline leaf. (N) Sequential leaves of an aerial rosette produced from an axillary meristem of a *35S::AHL15-GR* plant after DEX application. Leaves were harvested from two-month-old plants. (O) Scanning electron micrographs of *35S::AHL15-GR* epidermal leaf cells from respectively the 2nd rosette leaf, the 10th rosette leaf and a juvenile-like leaf produced from an axillary meristem on a two-month-old plant treated with DEX. Size bar indicates 50 μm.

Ectopic expression of *AHL15/REJUVENATOR* reverses developmental transitions in *Arabidopsis*

To substantiate the role of *AHL15* in repressing the vegetative phase change and flowering, we ectopically expressed the gene under control of the strong *CaMV 35S* promoter. *35S::AHL15* seedlings initially developed very slowly, but plants recovered three to four weeks after germination and produced rosettes and inflorescences. We noticed, however, that from the point of growth recovery these overexpression plants showed a significant delay in flowering. They produced more than twice the number of rosette leaves before bolting compared to wild-type plants, both under LD and SD conditions (Table 1 and Fig. S1D). The delay in flowering in *AHL15* overexpressing plants correlated with a significant increase in the production of juvenile leaves lacking abaxial trichomes (Table 1). These *35S::AHL15* early juvenile leaves showed a stronger reduction in adaxial trichome number and were significantly smaller than wild-type juvenile leaves up to the seventh leaf stage.

In contrast to the cauline leaf and lateral inflorescence formed at bottom nodes of wild-type *Arabidopsis* inflorescences (Fig 2A,G,M), the axillary meristems at the most basal and some aerial nodes of *35S::AHL15* inflorescences first produced a cauline leaf followed by several juvenile-like-leaves (Fig. 2C,D), eventually leading to the formation of aerial rosettes (Fig. 2I,J). Since the juvenile-like leaves and aerial rosettes (Fig. 2M) were produced after a wild-type looking cauline leaf (Fig. 2C), this suggested that ectopic *AHL15* expression induced rejuvenation of these meristems. To test the capacity of *AHL15* to rejuvenate plant tissues, we generated lines that express a fusion protein between AHL15 and the rat glucocorticoid receptor (GR) under control of the *CaMV 35S* promoter (*35S::AHL15-GR*), rendering the nuclear import and thus the activity of the ectopically expressed AHL15-GR fusion inducible by the glucocorticoid hormone dexamethasone (DEX). Untreated *35S::AHL15-GR* plants showed a wild-type phenotype (Fig. 2E,K). By contrast, after spraying forty five-day-old flowering *35S::AHL15-GR* plants with DEX, most of the basal and aerial axillary meristems produced small rosette leaves, initially resembling the small first leaves of *35S::AHL15* plants, and later producing normal juvenile leaves without abaxial trichomes (Fig. 2F,N). In these juvenile aerial rosettes the vegetative phase change occurred two to three weeks after DEX treatment, resulting in the production of adult rosette leaves. A second DEX application, four weeks after the first one, again reverted many axillary meristems to vegetative meristems, resulting in abundant production of aerial rosettes (Fig. 2L), whereas non-treated inflorescences only produced a few cauline leaves (Fig. 2K).

The vegetative phase change in *Arabidopsis* is accompanied by a decrease in leaf epidermal cell size (Usami et al., 2009). To confirm rejuvenation by ectopic *AHL15* expression, we compared the cell size of early juvenile, adult and rejuvenated leaves in *35S::AHL15-GR* plants before and after DEX treatment. The epidermis cells in DEX-treated *35S::AHL15-GR* aerial rosette leaves were significantly larger than those in adult leaves and strikingly similar in size to the second juvenile leaf produced after germination (Fig. 2O).

The above data provide evidence, both through loss-of-function and ectopic expression, that the AHL15 protein represses and can even reverse two major developmental phase transitions in plant development, the transition from vegetative to reproductive development, and the transition from juvenile to adult development. AHL15 was named REJUVENATOR (RJV) because of its generic capacity to rejuvenate plant tissues.

Overexpression of the *Arabidopsis AHL* family members *AHL19*, *AHL20*, *AHL27* and *AHL29*, and two possible *AHL15* orthologs from *Brassica oleracea* and *Medicago truncatula* in *Arabidopsis* resulted in similar morphological changes as observed for *35S::AHL15* plants, i.e. a shift from mono- to polycarpic life style/growth habit through the continuous production of aerial rosettes (Fig. S3). These results corroborated the previously observed co-regulation and functional redundancy among *Arabidopsis AHL* family members (Fig. 1, Table 1, and Fig. S1 in this paper, (Street et al., 2008; Xiao et al., 2009; Zhao et al., 2013), and suggest that the rejuvenation function of *AHL15* is conserved in dicotyledonous plant species.

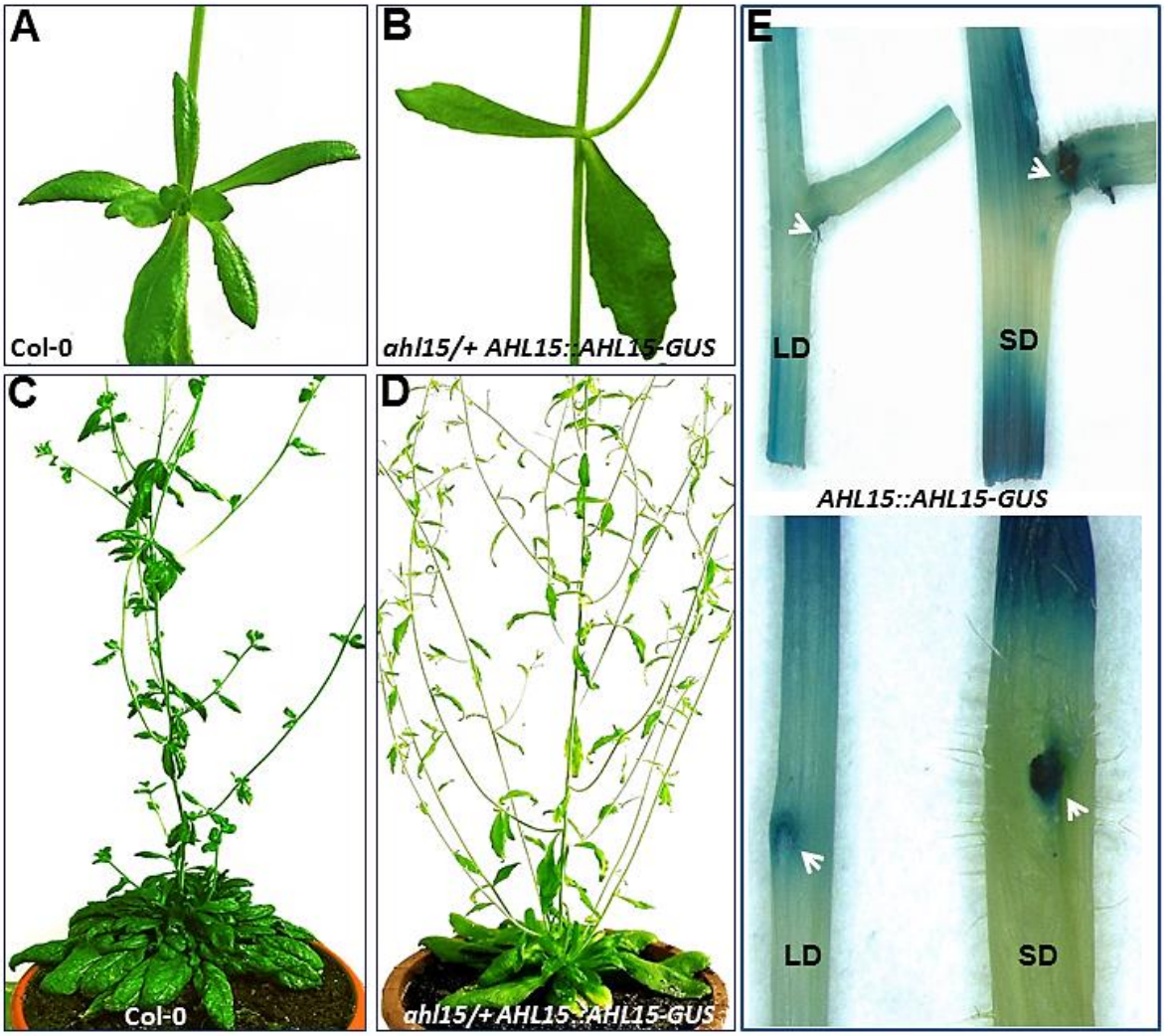

Figure 3 ***AHL*** **genes are essential for SD-induced vegetative axillary meristem activity in** ***Arabidopsis*****.** (A) A lateral inflorescence with an aerial rosette formed on the first inflorescence node of a two-month-old wild-type *Arabidopsis* plant grown under SD. (B) A lateral inflorescence and cauline leaf formed on the first aerial node of a two-month-old *ahl15/+ AHL15::AHL15-GUS* plant grown under SD. (C,D) Mature shoot phenotype of wild-type (C and *ahl15/+ AHL15::AHL15-GUS* (D) plants grown under SD. (E) GUS staining showing a higher level of *AHL15-GUS* expression in the first inflorescence node (top, arrowhead) and axil of a cauline leaf (bottom, arrowhead) of SD grown plants (left) than of LD grown plants (right). Inflorescence stems were harvested three weeks after flowering time.

Ectopic *AHL15/RJV* expression converts monocarpic *Arabidopsis* into a polycarpic woody plant

Arabidopsis is a typical annual monocarpic plant with a growth cycle of approximately 3 months. Following vegetative growth, plants bolt and produce several inflorescences with cauline leaves and flowers. Depending on the number of fruits and seeds produced, the activity of the inflorescence meristems arrests, and the plant senesces(Hensel et al., 1993; Bleecker and Patterson, 1997). Several related species, such as *Arabis alpina*, are perennial polycarpic plants that flower and produce seeds multiple times[8]. In contrast to the monocarpic life style of wild-type *Arabidopsis*, *AHL15* overexpression plants continued to grow vegetatively for several months after the first cycle of flowering and seed set by producing new aerial rosettes (Fig. 4A). These aerial rosettes produced new inflorescences, resulting in enhanced shoot branching (Fig. 3D) and a significant increase in seed yield (Fig. 4B). Removal of the terminated inflorescences with ripened siliques induced the production of new aerial rosettes (Fig. 4C) that again produced inflorescences with cauline leaves and flowers (Fig. 4E). Continuous removal of the terminated inflorescences and continuous supply of fertilizer allowed plants to produce new inflorescences and new seeds following each cutting for the 9 month period that was tested. The same phenotypes were observed in DEX-treated *35S::AHL15-GR* plants. Moreover, DEX-treated *35S::AHL15-GR* plants already produced aerial vegetative growth and new inflorescences while the first batch of siliques was still ripening (Fig. 4F).

Many polycarpic (perennial) plant species are woody, and a continuous ring of xylem, indicative of secondary growth and wood formation, can already be observed in young stems (Gerttula et al., 2015). Inflorescence stems of herbaceous monocarpic species such as *Arabidopsis* show secondary xylem development, but do not form the regular xylem cylinder that precedes wood formation (Fig. 5A,B). In line with their polycarpic behaviour, *35S::AHL15* plants developed a complete xylem ring in their primary inflorescence stems as early as two weeks after the induction of flowering (Fig. 5C) and a solid wood cylinder was established in the main and lateral inflorescences of four-month-old plants (Fig. 5D). The fact that secondary growth can be observed early during inflorescence development, suggests that it is not an indirect effect of the enhanced and prolonged inflorescence development in *AHL15* overexpression plants, but rather, that ectopic *AHL15* expression directly triggers cambium activity resulting in wood development.

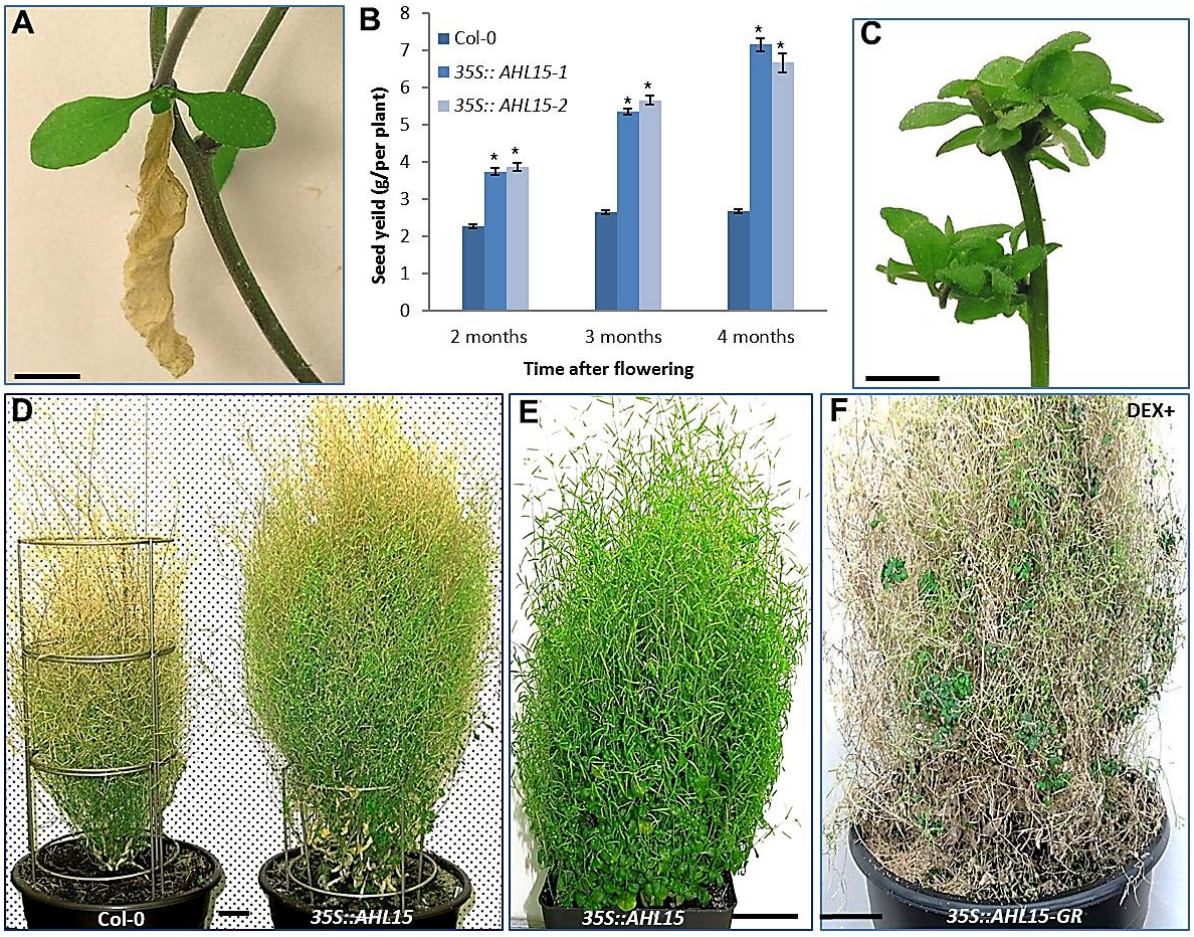

Figure 4 Ectopic *AHL15* expression converts monocarpic *Arabidopsis* into a polycarpic plant. (**A**) Development of an aerial rosette from an axillary meristem on an inflorescence of a four-month-old *35S::AHL15* plant. The senesced cauline leaf indicates that the rosette developed after seed ripening. (B) Comparison of seed yield of wild-type and *35S::AHL15* plants grown under LD for the indicated time. Asterisks indicate a significant difference from wild type (Student's *t*-test, $p < 0.01$), and error bars indicate standard error of the mean (n=6). (C) Efficient production of aerial rosettes in a 5-month-old *35S::AHL15* plant from axillary meristems just below the positions where inflorescences were cut to harvest the seeds. (D) Inflorescence branching of wild-type (left) and *35S::AHL15* (right) plants 3 months after flowering. (E) Efficient production of inflorescences and new seed set in a five-month-old *35S::AHL15* plant after the first seed harvesting. (F) Renewed vegetative growth on aerial branches of a five-month-old *35S::AHL15-GR* plant and sprayed with 20 µM DEX (no seed were harvested yet). Plants in A-F were grown under LD conditions. Size bars indicate 1 cm in A and C and 4 cm in D, E and F.

Arabidopsis AHL15/RJV induces juvenile traits and polycarpy in tobacco

We determined whether heterologous *AHL15* expression could also induce similar developmental changes in a non-related plant species. We introduced the *35S::AHL15-GR* construct into tobacco. Young DEX-treated *35S::AHL15-GR* plants formed small, round juvenile leaves, whereas untreated transgenic plants produced only three juvenile leaves before producing the typically larger and longer adult tobacco leaves (Fig. 6A). This result indicates that *AHL15* expression extends the juvenile phase in tobacco, as in *Arabidopsis*.

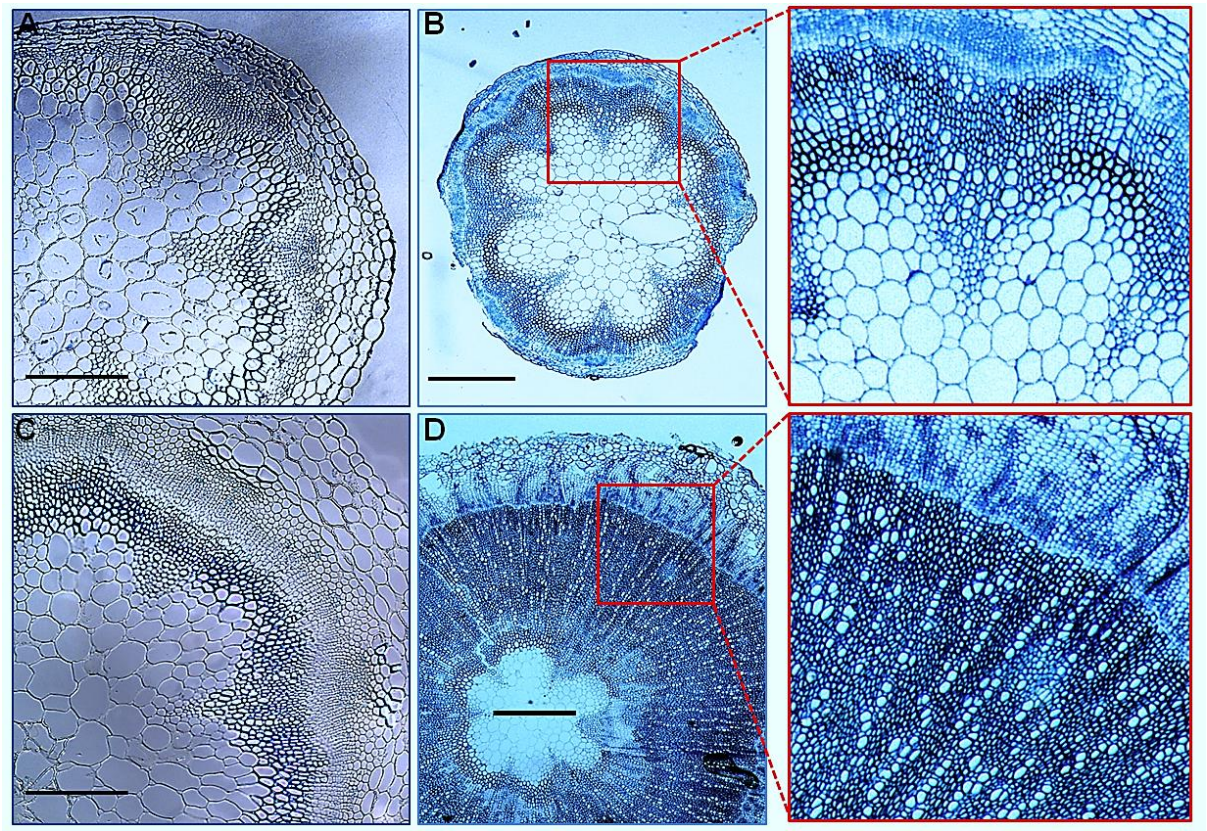

Figure 5 Secondary growth in wild-type and *35S::AHL15 Arabidopsis* inflorescence stems. (A,B) Cross-section of the main inflorescence stem of a two-week-old (A, 4-5 mm above the rosette) or two-month-old (B, 5-7 mm above the rosette) wild-type plant. (C,D) Cross-section of the main inflorescence stem of a 2-week-old (C, 4-5 mm above the rosette) or three-month-old (D, 5-7 mm above the rosette) *35S::AHL15* plant. Cross-sections were stained with toluidine blue. Size bars in a to D indicate respectively 100, 200, 150 and 500 µm.

DEX-treated *35S::AHL15-GR* tobacco plants continued to produce small juvenile leaves for six months before flowering and from axillary meristems during flowering (Fig. 6B), and showed reduced apical dominance, resulting in enhanced shoot branching and enhanced production of leaves and inflorescences (Fig. S4A). Axillary meristems in DEX-treated *35S::AHL15-GR* were also able to resume growth after the first seed set (Fig. 6D), whereas wild-type and non-treated *35S::AHL15-GR* plants arrested growth and senesced after seed set (Fig. 6C). After the second seed batch produced by the now seven month-old DEX treated *35S::AHL15-GR* plants (Fig. 6E) were harvested, the plants were treated with DEX for a third, fourth and fifth cycle, which efficiently induced vegetative growth and subsequent flowering and seed set, allowing the *35S::AHL15-GR* plants to survive for more than 2 years (Fig. S4B). The production of juvenile-like leaves on DEX sprayed axillary meristems of *35S::AHL15-GR* plants (Fig. 6F) indicated that, as in *Arabidopsis*, the polycarpic behaviour of DEX treated *35S::AHL15-GR* tobacco plants was caused by rejuvenation of axillary meristems.

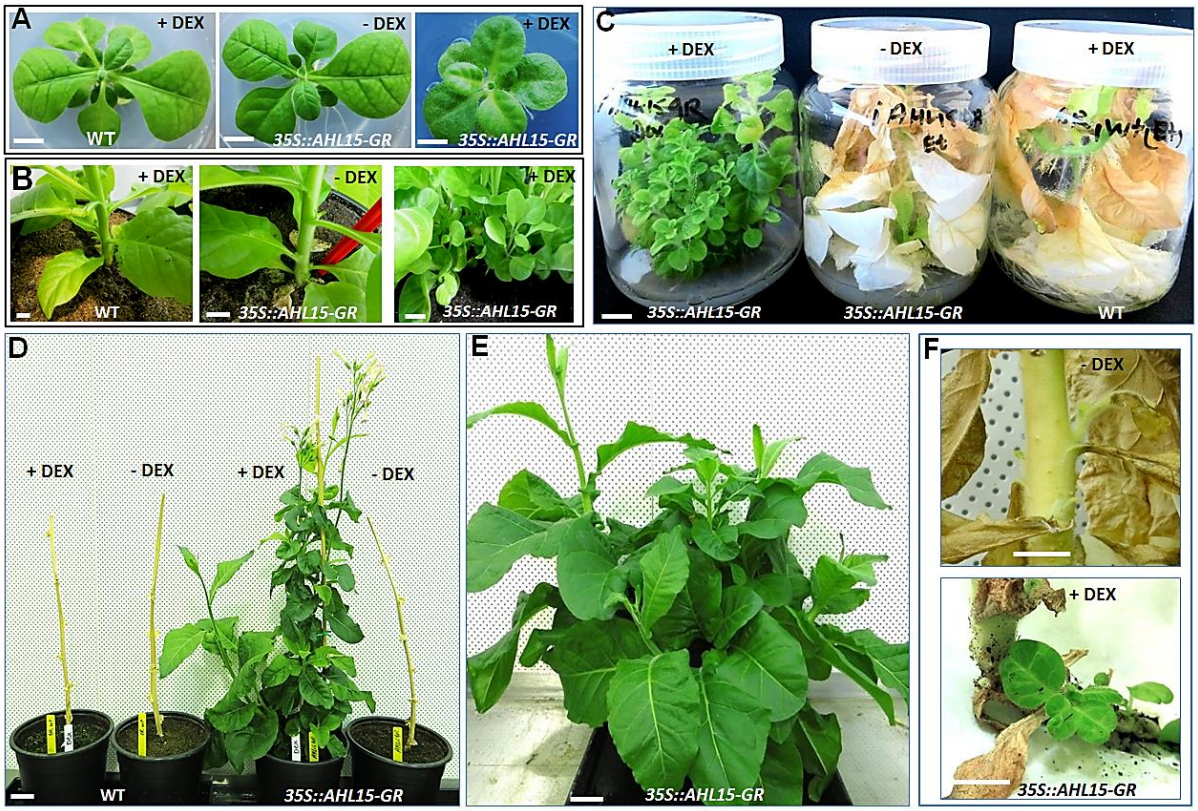

Figure 6 Heterologous *AHL15* expression rejuvenates axillary meristems and induces polycarpy in tobacco. (A) Shoot morphology of axenically grown one-month-old wild-type (left) and *35S::AHL15-GR* (middle and right) plants on media with 10 µM DEX (left and right) or without DEX (middle). (B) Differential activity (formation juvenile-like leaves) of axillary meristems in flowering 30 µM DEX-sprayed wild-type (left) or untreated *35S::AHL15-GR* (middle) plants, versus 30 µM DEX-sprayed *35S::AHL15-GR* plants (right). (C) Enhanced shoot development on axenically grown four-month-old *35S::AHL15-GR* plants (right) on media with DEX (left) versus senesced plants on medium without DEX (middle) or senesced wild-type plants on medium with10 µM DEX (right). (D) Growth response to DEX spraying in five-month-old wild-type (left) and *35S::AHL15-GR* (right) plants. (E) Efficient production of new leaves and subsequently inflorescences in a seven-month-old *35S::AHL15* plant after DEX treatment. (F) Axillary meristem activity before (upper panel) and 10 days after 30 µM DEX treatment (lower panel) in a 1 year-old *35S::AHL15-GR* plant. Size bars indicate 1cm in A, B, C and F and 5 cm in D and E.

AHL15/RJV acts downstream of Ageing (miR156, SPL) and flowering (SOC1, FUL) genes

During the *Arabidopsis* life cycle the gradual decrease in *microRNA156* (*miR156*) expression results in increased expression of the *SQUAMOSA-PROMOTER BINDING PROTEIN-LIKE (SPL) miR156* target genes. *SPL* genes in turn promote the adult developmental program at the shoot apical meristem (SAM), resulting in the transition from juvenile to adult leaf production and eventually from vegetative to reproductive development (Wang et al., 2009a; Wu et al., 2009). The effect of *miR156* and *SPL* genes on AMs, however, has not been described. We therefore investigated the relationship between *miR156/SPL*- and *AHL* in the control of AM maturation. *miR156* promoter-*GUS* fusions were expressed in the basal part of the rosette in flowering *Arabidopsis* plants (Fig. 7A), explaining the enhanced SPL9 expression in *miR156* target mimic (*35S::MIM156*) (Franco-Zorrilla et al., 2007) and *miR156*-insensitive *SPL* lines (*SPL9::rSPL9*, Fig. 7B) (Wu et al., 2009). We observed

reduced cauline leaf formation and branching in *35S::MIM156* and *SPL9::rSPL9* plants, indicating precocious maturation of AMs (Fig. S5A,B), while, reducing *SPL* expression by overexpressing *miR156* (*35S::miR156*) or by *spl9 spl15* loss-of-function led to the production of rosette leaves from the AMs during flowering (Fig. S6), and induced polycarpic behaviour (Fig. 8A and Fig. S7). These results indicated that *miR156* prevents precocious maturation of AMs by suppressing *SPL* gene expression.

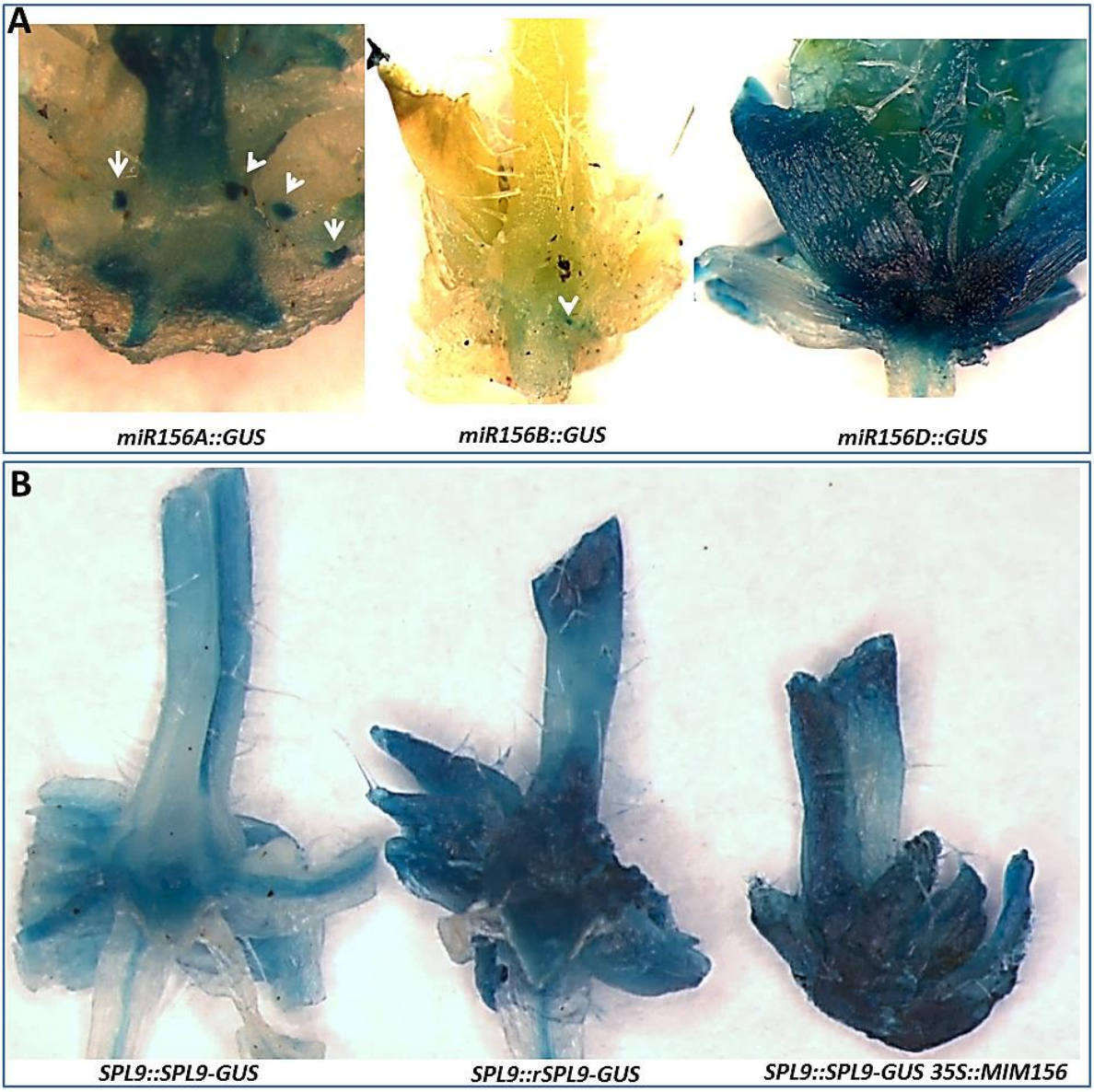

Figure 7 *miR156* reduces SPL9 expression in AMs and the rosette base of flowering *Arabidopsis* plants. (A) Expression pattern of *miR156* promoter-*GUS* gene reporters (*miR156A::GUS*, *miR156B::GUS*, *miR156D::GUS*) in AMs (arrowheads) and the rosette base of *Arabidopsis* plants 1week after flowering. (B) Expression of miR156-sensitive *SPL9::SPL9-GUS* (left) compared to the miR156-resistant SPL9::rSPL9-GUS (middle) in the rosette base of wild-type *Arabidopsis* 1week after flowering, or to *SPL9::SPL9-GUS* in *35S::MIM156* background . Plants were grown under LD.

Interestingly, *AHL15/RJV* overexpression negated the precocious maturation of AMs in *35S::MIM156* and *SPL9::rSPL9* plants (Fig. S5A,B), and dramatically enhanced the polycarpic behaviour of *35S::miR156* plants (Fig. 8A). In addition, *AHL15/RJV* function was required for the aerial rosette leaf formation and polycarpy phenotypes observed in *35S::miR156* and *spl9 spl15* plants (Fig. 8A, Fig. S6 A-D and Fig. S 7). Consistent with these results, *AHL15/RJV* and its paralog *AHL20* were strongly expressed in *35S::miR156* and *spl9 spl15* AMs (Fig. 8B,C) and showed reduced expression in *35S::MIM156* and *SPL9-rSPL9* inflorescence nodes (Fig. 8D). Based on these results, we concluded that *AHL15/RJV* and *AHL20* act downstream of the *SPL* genes. In wild-type plants *AHL* repression by SPLs promotes AM maturation, whereas under conditions where SPL activity is reduced (e.g. in *35S::miR156* or *spl9 spl15* plants) AHLs delay AM maturation, which in the case of *35S::miR156* leads to rejuvenation resulting in aerial rosette phenotypes and polycarpy.

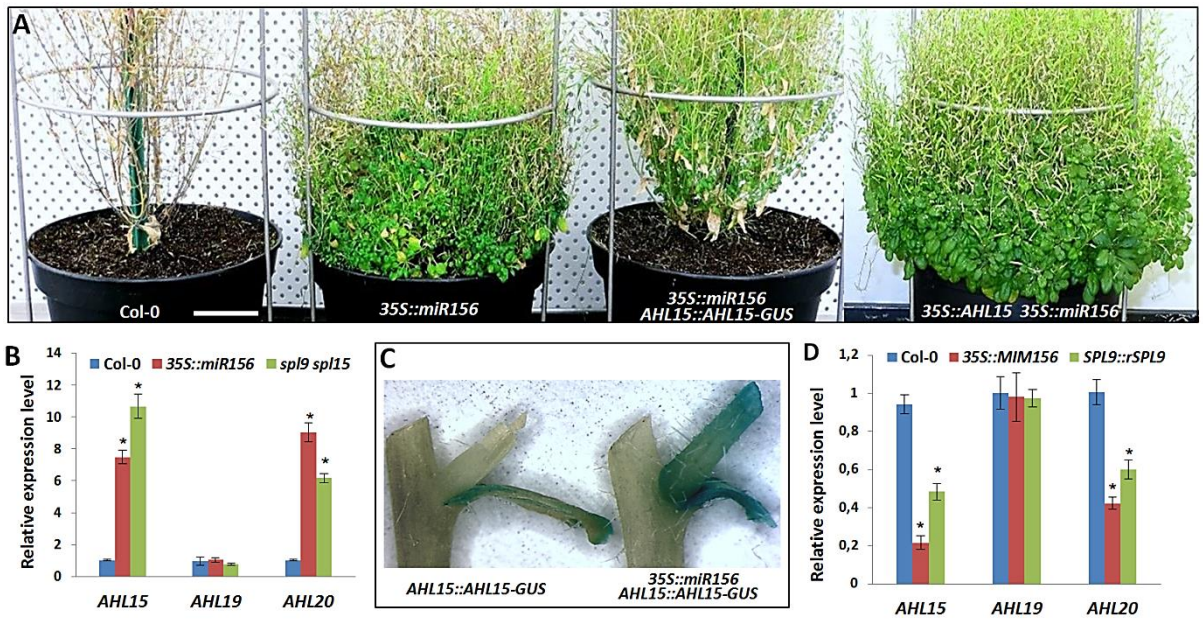

Figure 8 The miR156-regulated SPL pathway contributes to AM maturation by suppressing *AHL* genes expression. (A) Phenotype of four-month-old wild-type (Col-0), *35S::miR156*, *35S::miR156 AHL15::AHL15-GUS*, or *35S::miR156 35S::AHL15* plants, respectively. (B) Quantitative RT-PCR (qPCR) analysis of *AHL15/19/20* expression in inflorescence nodes of wild-type, *35S::mirR156* or *spl9 spl15* plants 2 weeks after flowering. (C) GUS activity showing *AHL15::AHL15-GUS* expression in an inflorescence node of six week-old wild-type and *35S::mirR156* plants. (D) qPCR analysis of *AHL15*/*19*/*20* expression in inflorescence nodes of wild type, *35S::MIM156* or *SPL9::rSPL9* plants 2 weeks after flowering. In B and D asterisks indicate a significant difference in expression level in the mutant compared to wild-type plants (Student's *t*-test, $p < 0.001$) and error bars indicate standard error of the mean of three biological replicates. Plants in A-D were grown under LD conditions. Size bars indicate 5 cm in A.

Previously, a double loss-of-function *Arabidopsis* mutant of the *SUPPRESSOR OF CONSTANS 1* (*SOC1*) and *FRUITFULL* (*FUL*) genes was found to show a perennial lifestyle (Melzer et al., 2008), with similar phenotypes as *35S::AHL15* plants. Interestingly, the *soc1 ful* double mutant in the *ahl* dominant negative loss-of-function mutant background completely lost its perennial features (Fig. 9A), suggesting that AHL function is normally repressed by SOC1 and FUL, and that *AHL* upregulation plays a key role in acquiring the

perennial lifestyle. Expression analysis using qRT-PCR (Fig. 9B) and the *AHL15::AHL15-GUS* reporter (Fig. 9C,D) showed that *AHL15/RJV* and *AHL20* were strongly upregulated in *soc1 ful* inflorescence nodes and lateral inflorescences, thereby corroborating that *AHL* genes are suppressed by SOC1 and FUL. *AHL19* transcription was unchanged in the *soc1 ful*, *35S::miR156* or *spl9 spl15* mutant lines relative to wild type (Fig. 8B and Fig. 9B), indicating that *AHL19* is not regulated by either SPL or SOC1/FUL. Previously, it was been shown that SPL proteins promote *SOC1* and *FUL* expression (Wang et al., 2009a; Yamaguchi et al., 2009) and that SOC1 binds to the *AHL15/RJV* upstream and downstream regions (Immink et al., 2012; Tao et al., 2012). Consistent with these and our findings, we postulate that SPLs promote AM maturation by upregulating *SOC1* (and *FUL*) and that AHLs act downstream of SOC1 (and FUL) as key regulators of AM maturation (Fig. 10).

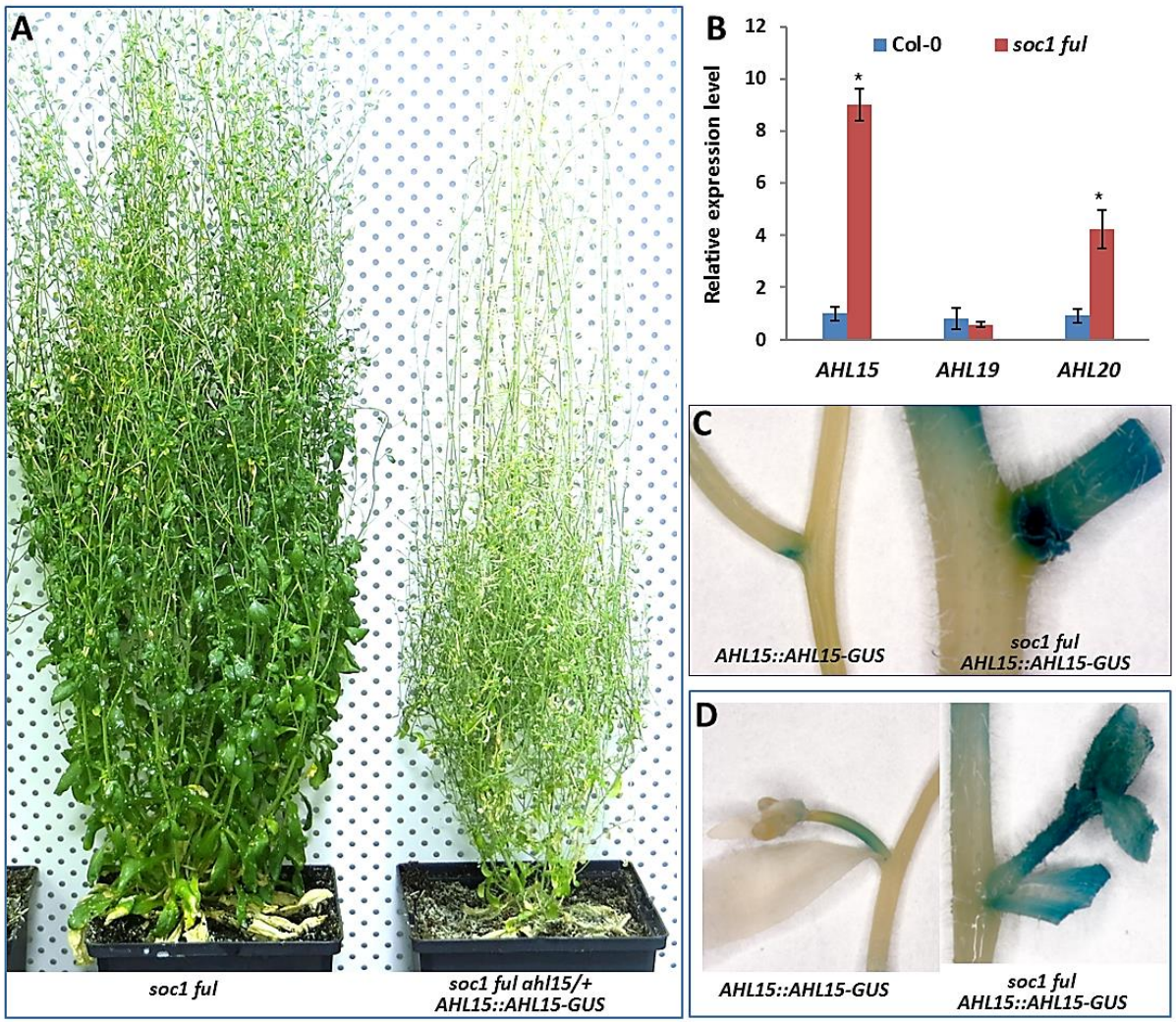

Figure 9 *AHL* genes are essential for the polycarpic behaviour of *Arabidopsis soc1 ful* mutant plants. (A) Comparison of a four-month-old *soc1 ful* mutant with many aerial rosettes (left) and a more wild-type looking *soc1 ful ahl15/+ AHL15::AHL15-GUS* plant (right) both grown in LD. (B) qPCR analysis of *AHL15*/*19*/*20* expression in inflorescence nodes of wild-type (Col-0) and *soc1 ful* plants 2 weeks after flowering. Asterisks indicate a significant difference in expression level in mutant compared to wild-type plants (Student's *t*-test, $p < 0.001$) and error bars indicate the standard error of the mean of three biological replicates. (C and D) GUS activity staining showing *AHL15::AHL15-GUS* expression in an inflorescence node (C) or a lateral inflorescence (D) of wild-type (left) and *soc1 ful* (right) plants at a comparable developmental stage.

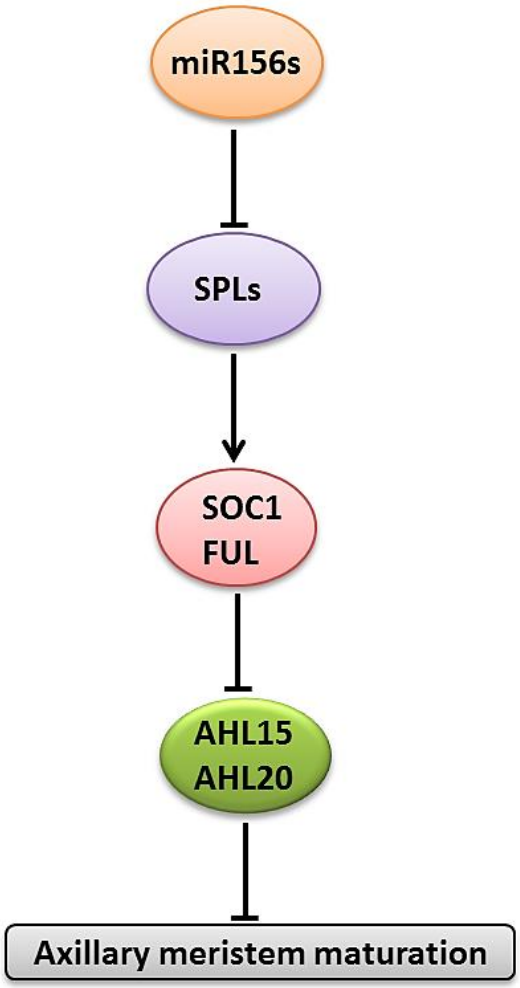

Figure 10 Proposed model for the key role for AHL genes in controlling AM maturation downstream of Ageing (SPL) and flowering (SOC1 and FUL) genes. It is well established that miR156 controls the action of SPL proteins in promoting the floral transition by directly activating the flowering genes *SOC1* and *FUL* (Wang et al., 2009a; Yamaguchi et al., 2009). Here we show that *AHL* genes, of which *AHL15/RJV* has been previously identified as direct downstream target of *SOC1* (Immink et al., 2012a; Tao et al., 2012), are repressed by the SPL-SOC1/FUL pathway, and that they are directly responsible for the delay in flowering and the vegetative growth from axillary meristems observed in the *spl* or *soc ful* loss-of-function or knock-down mutant lines. Enhanced *AHL* expression bypasses the SPL-SOC1/FUL pathway and turns monocarpic *Arabidopsis* into a polycarpic plant by maintaining some axillary meristems in a vegetative state. Arrows indicate gene activation, and blunted lines indicate repression.

Discussion

Flowering plants age through several well-defined developmental phase transitions, starting with the embryonic to juvenile phase change, and ending with the adult vegetative to generative transition, which in annual monocarpic plants preludes senescence and plant death (Amasino, 2009). Here we show that the *Arabidopsis* AT-hook protein *RJV/AHL15* and related paralogs act as master regulators of ageing, as their expression induces meristem rejuvenation, causing annual monocarpic plants such as *Arabidopsis* and tobacco to become

polycarpic, perennial plants. This newly discovered function of AHL proteins is conserved in at least three families of flowering plants (Brassicaceae, Solaneaceae and Fabaceae). Reversion of developmental phase transitions by overexpression of key regulators has been reported before (Lotan et al., 1998; Stone et al., 2001; Boutilier et al., 2002; Zuo et al., 2002), but this is the first time that reversion was observed for all developmental phase transitions. This suggests that AHL15/RJV and its family members play a central role in all these developmental phase transitions, and that regulation of their expression can delay plant development and change a plant's life history. In fact, *Arabidopsis* when grown under SD conditions can adopt polycarpic traits such as aerial rosette, and the enhanced *AHL15* expression in axillary meristems under SD conditions suggests that *AHL15/RJV* is involved in the plant's response to environmental triggers. Moreover, the existence of both mono- and polycarpic species within many plant genera indicates that life history traits changed frequently during evolution (Amasino, 2009). As *AHL* gene families have been identified in monocarpic and polycarpic plant species (Zhao et al., 2014), we hypothesize that *AHL* genes are key evolutionary targets for modulating monocarpic to polycarpic growth.

AHL proteins are DNA-binding proteins, and as in animals they are able to remodel chromatin (Lim et al., 2007; Ng et al., 2009). The mode of action of AHL proteins is largely unknown, and therefore one of the objectives of our future research will be to unravel the molecular mechanisms by which these proteins influence plant developmental phase transitions. One gene family encoding transcription factors involved predominately in plant tissue ageing are the *SPL* genes, which are known to orchestrate the adult developmental program, and are highly upregulated in adult leaves and during flowering (Wu and Poethig, 2006; Wu et al., 2009). The age-related function of *AHL* genes might potentially be mediated by repression of *SPL* gene expression.

Our findings create new possibilities for applications in crop breeding and in agri- and horticultural practices. Monocarpic crops require more fertilizer and herbicides than polycarpic plants, which can have negative effects on productivity and biodiversity(Asbjornsen et al., 2013; Armstrong et al., 2012). Converting monocarpic crop plants with a single harvest of seeds, flowers or fruits into polycarpic plants, permits multiple harvests without the need for sowing and replanting. Such plants do not have to invest resources into a new root system, and since their root system grows deeper, there will be less need for watering and a reduced chemical runoff and soil erosion (Armstrong et al., 2012). Moreover, longer photosynthetic activity and greater root mass in polycarpic plants increase plant productivity (Glover et al., 2010), which holds promise for future environment and food security (Werling et al., 2014). Based on our results, we expect that perennialized crops can be obtained by spatio-temporal enhancement of *AHL* gene expression through CRISPR/Cas9-based technology (Woo et al., 2015).

Methods

Plant material and growth conditions

All *Arabidopsis* mutant- and transgenic lines used in this study are in the Columbia (Col-0) background. The *ahl15* and *ahl19* T-DNA insertion mutants (SALK_040729C and

SALK_070123) and the previously described *spl9-4 spl15-1*, *soc1-6 ful-7*, *35S::miR165*, *35S::MIM156* and *SPL9::rSPL9* lines (Wang et al., 2009a) were obtained from the Nottingham *Arabidopsis* Stock Centre (NASC). The reporter lines *pSPL9::SPL9-GUS*, *pSPL9::rSPL9-GUS* (Yang et al., 2011) and *pmiR156A::GUS*, *pmiR156B::GUS*, and *pmiR156A::GUS* (Yu et al., 2015) have been described previously. Seeds were germinated after three days incubation at 4°C on MA medium (Masson and Paszkowski, 1992) containing 1% sucrose, and 0.7% agar at 21 °C under a 16 hour photoperiod, and seedlings were transferred to soil and grown at 21 °C under 65% relative humidity and long-day (LD: 16 hour photoperiod) or short-day (SD: 12 hours photoperiod) conditions. To score phenotypes such as maintenance of juvenility, rejuvenation, and longevity, Col-0 wild-type and overexpression plants were transferred to larger pots about 3 weeks after flowering and after harvesting ripened siliques. Vegetative phase changes and flowering time were determined under long-day (LD; 16 hours photoperiod and 70% relative humidity at 21°C) or short-day (SD; 12 hours photoperiod and 70% relative humidity at 21°C) conditions. *Nicotiana tabacum* (cv SR1 Petit Havana) plants were grown in medium-sized pots at 25 C° temperature, 75% relative humidity and 16 hours photoperiod. For dexamethasone (DEX, Sigma-Aldrich) treatment, *Arabidopsis* seeds were germinated on MA medium containing 20 µM DEX or soil grown plants were sprayed with 20 µM DEX. Tobacco seeds were germinated on ½ MS medium containing 10 µM DEX, and seedlings or plants were sprayed with 30 µM DEX.

Plasmid construction and plant transformation

The *35S::AHL15* construct was generated by PCR amplification of the full-length *AHL15* cDNA of (AT3G55560) from ecotype Columbia (Col-0) using primers 35S::AHL15-F and -R (Table S1), and the resulting PCR product was cloned as a *Sma*I/*Bgl*II fragment into the *p35S-3'OCS* expression cassette of plasmid pART7, which was subsequently cloned as *Not*I fragment into the binary vector pART27 (Gleave, 1992). To generate the other overexpression constructs, the full-length cDNA clones of *AHL20* (AT4G14465), *AHL27* (AT1G20900), *AHL29* (AT1G76500) from *Arabidopsis* Col-0, *AC129090* from *Medicago trunculata cv* Jemalong, and *Bo-Hook1* (AM057906) from *Brassica oleracea* var *alboglabra* were used to amplify the open reading frames (ORFs) using primers indicated in Table S1. The ORFs were cloned into plasmid pJET1/blunt (GeneJET™ PCR Cloning Kit, #K1221), and subsequently transferred as *Not*I fragments to binary vector pGPTV 35S-FLAG (Becker et al., 1992). To construct *35S::AHL15-GR*, a synthetic *Pst*I-*Xho*I fragment containing the *AHL15-GR* fusion was used to replace the BBM-GR fragment in binary vector pSRS031 (Passarinho et al., 2008). To generate the *AHL15::AHL15-GUS* and *pAHL15::AHL15-tagRFP* translational fusions, a 4 kb fragment containing the promoter and exon-intron sequences of *AHL15* was amplified using PCR primers AHL15-GUS-F and -R (Table S1), and inserted into pDONR207 via a BP reaction (Gateway, Invitrogen). LR reactions were carried out to fuse the 4 kb fragment upstream of GUS or tagRFP in destination vectors pMDC163 (Karimi et al., 2007) or pGD121 (Immink et al., 2012). All binary vectors were introduced into *Agrobacterium tumefaciens* strain AGL1 by electroporation (Den Dulk-Ras

and Hooykaas, 1995) and *Arabidopsis* Col-0 was transformed using the floral dip method (Clough and Bent, 1998).

Tobacco transformation

Round leaf discs were prepared from the lamina of 3rd and 4th leaves of 1-month-old soil grown tobacco plants. The leaf discs were surface sterilized by three washes with sterile water followed by incubation in 10 % glorix for 20 minutes (Baltes et al., 2014), and then again 4 to 5 washes with sterile water. The surface sterilized leaf discs were syringe infiltrated with an overnight acetosyringone (AS)-induced culture of *Agrobacterium tumefaciens* strain AGL1 containing binary vector pSRS031 (grown to OD_{600}= 0.6 in the presence of 100 µM AS) carrying the *35S::AHL15-GR* construct and co-cultivated for 3 days in the dark on co-cultivation medium (CCM). CCM consists of full strength MS medium (Murashige and Skoog, 1962) with 3% (w/v) sucrose (pH 5.8) solidified with 0.8 % (w/v) Diachin agar and supplemented with 2mg/l BAP, 0.2mg/l NAA and 40mg/l AS. After co-cultivation, the explants were transferred to CCM supplemented with 15mg/l phosphinothricin (ppt) for selection and 500mg/l cefotaxime to kill *Agrobacterium*. Regeneration was carried out at 24C° and 16 hours photoperiod. The regenerated transgenic shoots were rooted in big jars containing 100 ml hormone free MS medium with 15mg/l ppt and 500 mg/l cefotaxime. The rooted transgenic plants were transferred to soil and grown in a growth room at 25 °C, 75% relative humidity and a 16 h photoperiod. All the transgenic plants were checked for the presence of the T-DNA insert by PCR on genomic DNA extracted from leaf tissues using the CTAB method (Doyle, 1990).

Histolochemical staining, tissue fixation and microscopy

Histochemical β-glucuronidase (GUS) staining of transgenic lines expressing GUS was performed as described previously (Anandalakshmiet al.,1998). Tissues were stained for 4 hours at 37 °C, followed by rehydration by incubation for 10 minutes in a graded ethanol series (75, 50, and 25 %). GUS stained tissues were observed and photographed using a LEICA MZ12 microscope (Switzerland) equipped with a LEICA DC500 camera.

For scanning electron microscopy (SEM), fresh leaves were fixed in 0.1 M sodium cacodylate buffer (pH 7.2) containing 2.5% glutaraldehyde and 2% formaldehyde. After fixation, samples were dehydrated by a successive ethanol series (25, 50, 70, 95, and 100 %) and subsequently critical-point dried in liquid CO2. Dried specimens were gold-coated and examined using a JEOL SEM-6400 (Japan).

Quantitative real-time PCR (qPCR) analysis

RNA isolation was performed using a NucleoSpin® RNA Plant kit (MACHEREY-NAGEL). For qPCR analysis, 1 µg of total RNA was used for cDNA synthesis with the iScript™ cDNA Synthesis Kit (BioRad). PCR was performed using the SYBR-Green PCR Master mix (SYBR® Premix Ex Taq™, Takara) and a CFX96 thermal cycler (BioRad). The Pfaffl method was used to determine relative expression levels (Pfaffl, 2001). Expression was

normalized using *β-TUBULIN-6*. Three biological replicates were performed, with three technical replicates each. The primers used are described in Table S1.

Acknowledgements

We thank Kim Boutilier for critically reading the manuscript. This work is partially supported by Iranian Ministry of Science, Research, and Technology (MSRT 89100156)

References

Amasino, R. (2009). Floral induction and monocarpic versus polycarpic life histories. Genome Biol. **10**: 228.

Anandalakshmi, R., Pruss, G.J., Ge, X., Marathe, R., Mallory, A.C., Smith, T.H., and Vance, V.B. (1998). A viral suppressor of gene silencing in plants. Proc. Natl. Acad. Sci. **95**: 13079-13084.

Aravind, L. and Landsman, D. (1998). AT-hook motifs identified in a wide variety of DNA-binding proteins. Nucleic Acids Res. **26**: 4413–4421.

Armstrong, O.N., Glover, D., Reganold, J.P., and Cox, C.M. (2012). Plant perennials to save Africa ' s soils. Nature. **489**: 359–361.

Asbjornsen, H., Hernandez-Santana, V., Liebman, M., Bayala, J., Chen, J., Helmers, M., Ong, C.K., and Schulte, L. A. (2013). Targeting perennial vegetation in agricultural landscapes for enhancing ecosystem services. Renew. Agric. Food Syst. **29**: 101–125.

Baltes, N.J., Gil-Humanes, J., Cermak, T., Atkins, P.A, and Voytas, D.F. (2014). DNA replicons for plant genome engineering. Plant Cell **26**: 151–163.

Becker, D., Kemper, E., Schell, J., and Masterson. A. (1992). New plant binary vectors with selectable markers located proximal to the left T-DNA border. Plant Mol. Biol. **20**: 1195–1197.

Bleecker, B. and Patterson, S.E. (1997). Last exit: senescence, abscission, and meristem arrest in *Arabidopsis*. Plant Cell **9**: 1169–79.

Boutilier, K., Offringa, R., Sharma, V.K., Kieft, H., Ouellet, T., Zhang, L., Hattori, J., Liu, C., van Lammeren, A.A.M., Miki, B.L.A., Custers, J.B.M., and van Lookeren, M.M. (2002). Ectopic expression of *BABY BOOM* triggers a conversion from vegetative to embryonic growth. **14**: 1737–1749.

Clough, S.J. and Bent, F. (1998). Floral dip: a simplified method for *Agrobacterium*-mediated transformation of *Arabidopsis thaliana.* Plant J. **16**: 735–743.

Doyle, J.J. (1990). Isolation of plant DNA from fresh tissue. Focus (Madison). **12**: 13–15.

Den Dulk-Ras, A. and Hooykaas P.J.J (1995). Electroporation of *Agrobacterium tumefaciens*. Plant Cell Electroporation Electrofusion Protoc. **55**: 63–72.

Franco-Zorrilla, J.M., Valli, A., Todesco, M., Mateos, I., Puga, M.I., Rubio-Somoza, I., Leyva, A., Weigel, D., García, J.A., and Paz-Ares, J. (2007). Target mimicry provides a new mechanism for regulation of microRNA activity. Nat. Genet. **39**: 1033–1037.

Gerttula, S., Zinkgraf, M., Muday, G.K., Lewis, D.R., Ibatullin, F.M., Brumer, H., Hart, F., Mansfield, S.D., Filkov, V., and Groover, A. (2015). Transcriptional and hormonal regulation of gravitropism of woody stems in populus. Plant Cell **27**: 2800–2813.

Gleave, A.P. (1992). A versatile binary vector system with a T-DNA organisational structure conducive to efficient integration of cloned DNA into the plant genome. Plant Mol. Biol. **20**: 1203-1207.

Glover, J.D., Reganold, J.P., Bell, L.W., Borevitz, J., Brummer, E.C., Buckler. E.S., Cox, C.M., Cox, T.S., Crews, T.E., and Culman, S.W. (2010). Increased food and ecosystem security via perennial grains. Science. **328**: 1638–1639.

Hensel, L.L., Grbić, V., Baumgarten, D., and Bleecker, B. (1993). Developmental and age-related processes that influence the longevity and senescence of photosynthetic tissues in *Arabidopsis*. Plant Cell. **5**: 553–564.

Immink, R.G.H., Posé, D., Ferrario, S., Ott, F., Kaufmann, K., Valentim, F.L., de Folter, S., van der Wal, F., van Dijk, A.D.J., Schmid, M., and Angenent, G.C. (2012). Characterization of SOC1's central role in flowering by the identification of its upstream and downstream regulators. Plant

Physiol. **160**: 433–449.

Jarillo, J.A., Piñeiro, M., Cubas, P., and Martínez-zapater, J.M. (2009). Chromatin remodeling in plant development. **1596**: 1581–1596.

Karimi, M., Depicker, A., and Hilson, P. (2007). Recombinational cloning with plant gateway vectors. Plant Physiol. **145**: 1144–1154.

Kaufmann, K., Pajoro, A., and Angenent, G.C. (2010). Regulation of transcription in plants: mechanisms controlling developmental switches. Nat. Rev. Genet. **11**: 830–842.

Kishi, Y., Fujii, Y., Hirabayashi, Y., and Gotoh, Y. (2012). HMGA regulates the global chromatin state and neurogenic potential in neocortical precursor cells. Nat. Neurosci. **15**: 1127–1133.

Lim, P.O., Kim, Y., Breeze, E., Koo, J.C., Woo, H.R., Ryu, J.S., Park, D.H., Beynon, J., Tabrett, A., Buchanan-Wollaston, V., and Nam, H.G. (2007). Overexpression of a chromatin architecture-controlling AT-hook protein extends leaf longevity and increases the post-harvest storage life of plants. Plant J. **52**: 1140–1153.

Lotan, T., Ohto, M., Yee, K.M., West, M. a, Lo, R., Kwong, R.W., Yamagishi, K., Fischer, R.L., Goldberg, R.B., and Harada, J.J. (1998). *Arabidopsis LEAFY COTYLEDON1* is sufficient to induce embryo development in vegetative cells. Cell. **93**: 1195–1205.

Masson, J., and Paszkowski, J. (1992). The culture response of *Arabidopsis thaliana* protoplasts is determined by the growth conditions of donor plants. Plant J. **2**: 829-833.

Melzer, S., Lens, F., Gennen, J., Vanneste, S., Rohde, A., and Beeckman, T. (2008). Flowering-time genes modulate meristem determinacy and growth form in *Arabidopsis thaliana*. Nat. Genet. **40**: 1489–1492.

Munné-Bosch, S. (2008). Do perennials really senesce? Trends Plant Sci. **13**: 216–20.

Murashige, T., and Skoog., E.F. (1962) A revised medium for rapid growth and bio assays with tobacco tissue cultures. Physiol. Plant. **15:** 473–497.

Ng, K.-H., Yu, H., and Ito, T. (2009). AGAMOUS controls *GIANT KILLER*, a multifunctional chromatin modifier in reproductive organ patterning and differentiation. PLoS Biol. **7**: e1000251.

Passarinho, P., Ketelaar, T., Xing, M., van Arkel, J., Maliepaard, C., Hendriks, M.W., Joosen, R., Lammers, M., Herdies, L., den Boer, B., van der Geest, L., and Boutilier, K. (2008). BABY BOOM target genes provide diverse entry points into cell proliferation and cell growth pathways. Plant Mol. Biol. **68**: 225–237.

Pfaffl, M.W. (2001). A new mathematical model for relative quantification in real-time RT-PCR. Nucleic Acids Res. **29**: e45-e45.

Reeves, R. (2010). Nuclear functions of the HMG proteins. Biochim. Biophys. Acta. Gene Regul. Mech. **1799**: 3–14.

Stone, S.L., Kwong, L.W., Yee, K.M., Pelletier, J., Lepiniec, L., Fischer, R.L., Goldberg, R.B., and Harada, J.J. (2001). *LEAFY COTYLEDON2* encodes a B3 domain transcription factor that induces embryo development. Proc. Natl. Acad. Sci. **98**: 11806–11811.

Street, I.H., Shah, P.K., Smith, A.M., Avery, N., and Neff, M.M. (2008). The AT-hook-containing proteins SOB3/AHL29 and ESC/AHL27 are negative modulators of hypocotyl growth in *Arabidopsis*. Plant J. **54**: 1–14.

Tao, Z., Shen, L., Liu, C., Liu, L., Yan, Y., and Yu, H. (2012). Genome-wide identification of SOC1 and SVP targets during the floral transition in *Arabidopsis*. Plant J. **70**: 549–561.

Telfer, A., Bollman, K.M., and Poethig, R.S. (1997). Phase change and the regulation of trichome distribution in *Arabidopsis thaliana*. Development **124**: 645–654.

Usami, T., Horiguchi, G., Yano, S., and Tsukaya, H. (2009). The more and smaller cells mutants of

Arabidopsis thaliana identify novel roles for *SQUAMOSA PROMOTER BINDING PROTEIN-LIKE* genes in the control of heteroblasty. Development **136**: 955–964.

Wang, J.-W., Czech, B., and Weigel, D. (2009a). miR156-regulated SPL transcription factors define an endogenous flowering pathway in *Arabidopsis thaliana*. Cell **138**: 738–749.

Wang, R., Farrona, S., Vincent, C., Joecker, A., Schoof, H., Turck, F., Alonso-Blanco, C., Coupland, G., and Albani, M.C. (2009b). *PEP1* regulates perennial flowering in *Arabis alpina*. Nature **459**: 423–427.

Weigel, D.N.O. (1995). A developmental switch sufficient for flower initiation in diverse plants. Nature. **377**: 495–500.

Werling, B.P. et al. (2014). Perennial grasslands enhance biodiversity and multiple ecosystem services in bioenergy landscapes. Proc. Natl. Acad. Sci. U. S. A. **111**: 1652–7.

Woo, J.W., Kim, J., Kwon, S. Il, Corvalán, C., Cho, S.W., Kim, H., Kim, S.-G., Kim, S.-T., Choe, S., and Kim, J.-S. (2015). DNA-free genome editing in plants with preassembled CRISPR-Cas9 ribonucleoproteins. Nat. Biotechnol. **33**: 1162–1165.

Wu, G., Park, M.Y., Conway, S.R., Wang, J.-W., Weigel, D., and Poethig, R.S. (2009). The sequential action of miR156 and miR172 regulates developmental timing in *Arabidopsis*. Cell **138**: 750–759.

Wu, G. and Poethig, R.S. (2006). Temporal regulation of shoot development in *Arabidopsis* thaliana by miR156 and its target *SPL3*. Development **133**: 3539–3547.

Xiao, C., Chen, F., Yu, X., Lin, C., and Fu, Y.-F. (2009). Over-expression of an AT-hook gene, *AHL22*, delays flowering and inhibits the elongation of the hypocotyl in *Arabidopsis thaliana*. Plant Mol. Biol. **71**: 39–50.

Xu, Y., Wang, Y., Stroud, H., Gu, X., Sun, B., Gan, E.-S., Ng, K.-H., Jacobsen, S.E., He, Y., and Ito, T. (2013). A matrix protein silences transposons and repeats through interaction with retinoblastoma-associated proteins. Curr. Biol. **23**: 345–350.

Yamaguchi, A., Wu, M.-F., Yang, L., Wu, G., Poethig, R.S., and Wagner, D. (2009). The microRNA-regulated SBP-Box transcription factor *SPL3* is a direct upstream activator of *LEAFY*, *FRUITFULL*, and *APETALA1*. Dev. Cell **17**: 268–278.

Yang, L., Conway, S.R., and Poethig, R.S. (2011). Vegetative phase change is mediated by a leaf-derived signal that represses the transcription of miR156. Development **138**: 245–249.

Yu, N., Niu, Q.-W., Ng, K.-H., and Chua, N.-H. (2015). The role of miR156/SPLs modules in *Arabidopsis* lateral root development. Plant J. **83**: 673–85.

Yun, J., Kim, Y.-S., Jung, J.-H., Seo, P.J., and Park, C.-M. (2012). The AT-hook motif-containing protein AHL22 regulates flowering initiation by modifying *FLOWERING LOCUS T* chromatin in *Arabidopsis*. J. Biol. Chem. **287**: 15307–15316.

Zhao, J., Favero, D.S., Peng, H., and Neff, M.M. (2013). *Arabidopsis thaliana* AHL family modulates hypocotyl growth redundantly by interacting with each other via the PPC/DUF296 domain. Proc. Natl. Acad. Sci. **110**: E4688–E4697

Zhao, J., Favero, D.S., Qiu, J., Roalson, E.H., and Neff, M.M. (2014). Insights into the evolution and diversification of the *AT-hook Motif Nuclear Localized* gene family in land plants. BMC Plant Biol. **14**: 2-19.

Zhou, C.-M., Zhang, T.-Q., Wang, X., Yu, S., Lian, H., Tang, H., Feng, Z.-Y., Zozomova-Lihová, J., and Wang, J.-W. (2013a). Molecular basis of age-dependent vernalization in *Cardamine flexuosa*. Science **340**: 1097–1100.

Zhou, J., Wang, X., Lee, J.-Y., and Lee, J.-Y. (2013b). Cell-to-cell movement of two interacting AT-hook factors in *Arabidopsis* root vascular tissue patterning. Plant Cell **25**: 187–201.

Zuo, J., Niu, Q.-W., Frugis, G., and Chua, N.-H. (2002). The *WUSCHEL* gene promotes vegetative-to-embryonic transition in *Arabidopsis*. Plant J. **30**: 349–359.

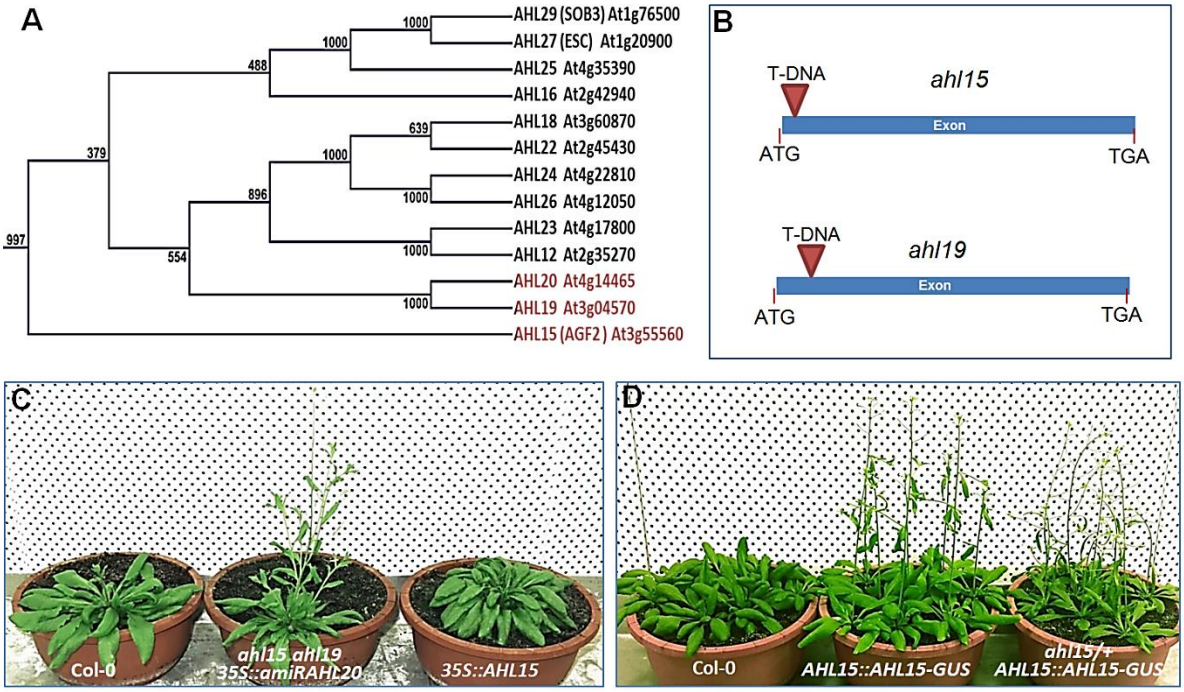

Supplementary figure 1 ***Arabidopsis AHL15*** **and close homologs redundantly regulate flowering time.** (A) Part of the phylogenetic tree of the *Arabidopsis* AHL protein family showing AHL15 and the closest paralogs. (B) Location of the T-DNA insertions in the *ahl15* and *ahl19* loss-of-function mutants. Note that the *AHL15* and *AHL19* genes are intronless. (C) Early flowering phenotype of an *ahl15 ahl19 35S::amiRAHL20* plant and delayed flowering phenotype of a *35S::AHL15* plant, both grown under short days (SD). (D) Early flowering phenotypes of *AHL15::AHL15-GUS* (observed in 25 independent lines) and *ahl15/+ AHL15::AHL15-GUS* (observed in three independent *AHL15::AHL15-GUS* lines crossed with *ahl15*) plants grown under long days (LD).

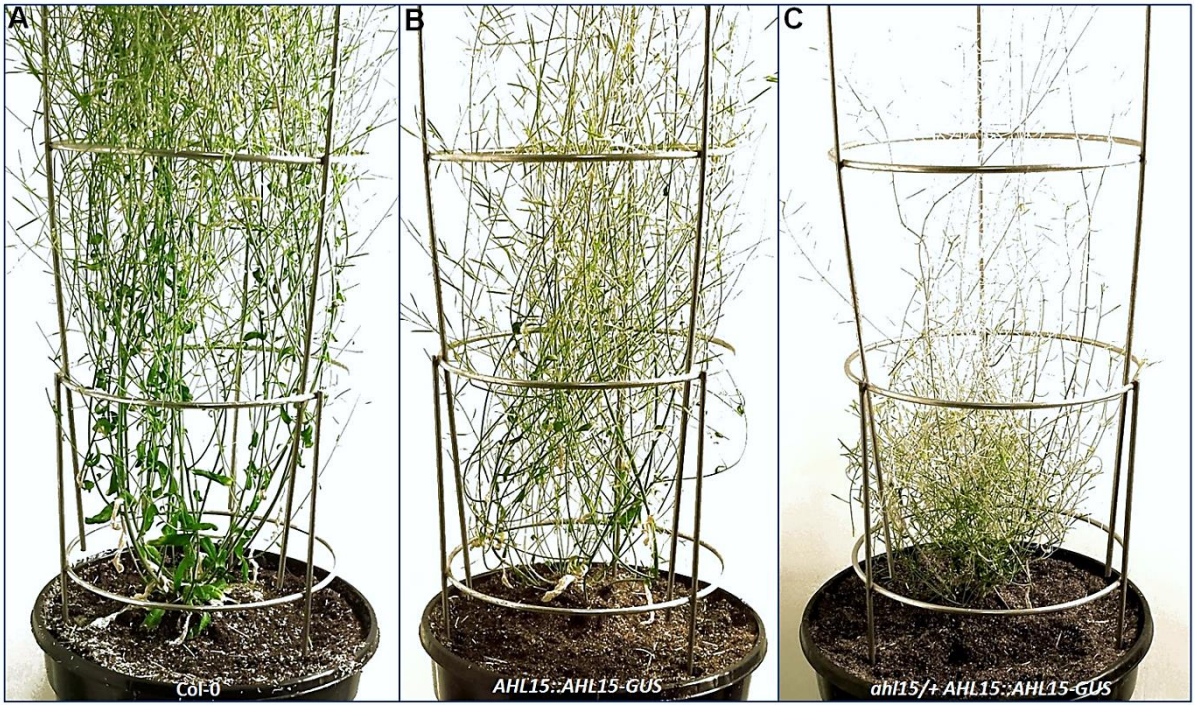

Supplementary figure 2 Early seed set and senescence of *Arabidopsis ahl* loss-of-function mutant plants. Two-month-old wild-type (Col-0) (A), *AHL15::AHL15-GUS* (B), or *ahl15/+ AHL15::AHL15-GUS* (c) *Arabidopsis* plants grown under LD.

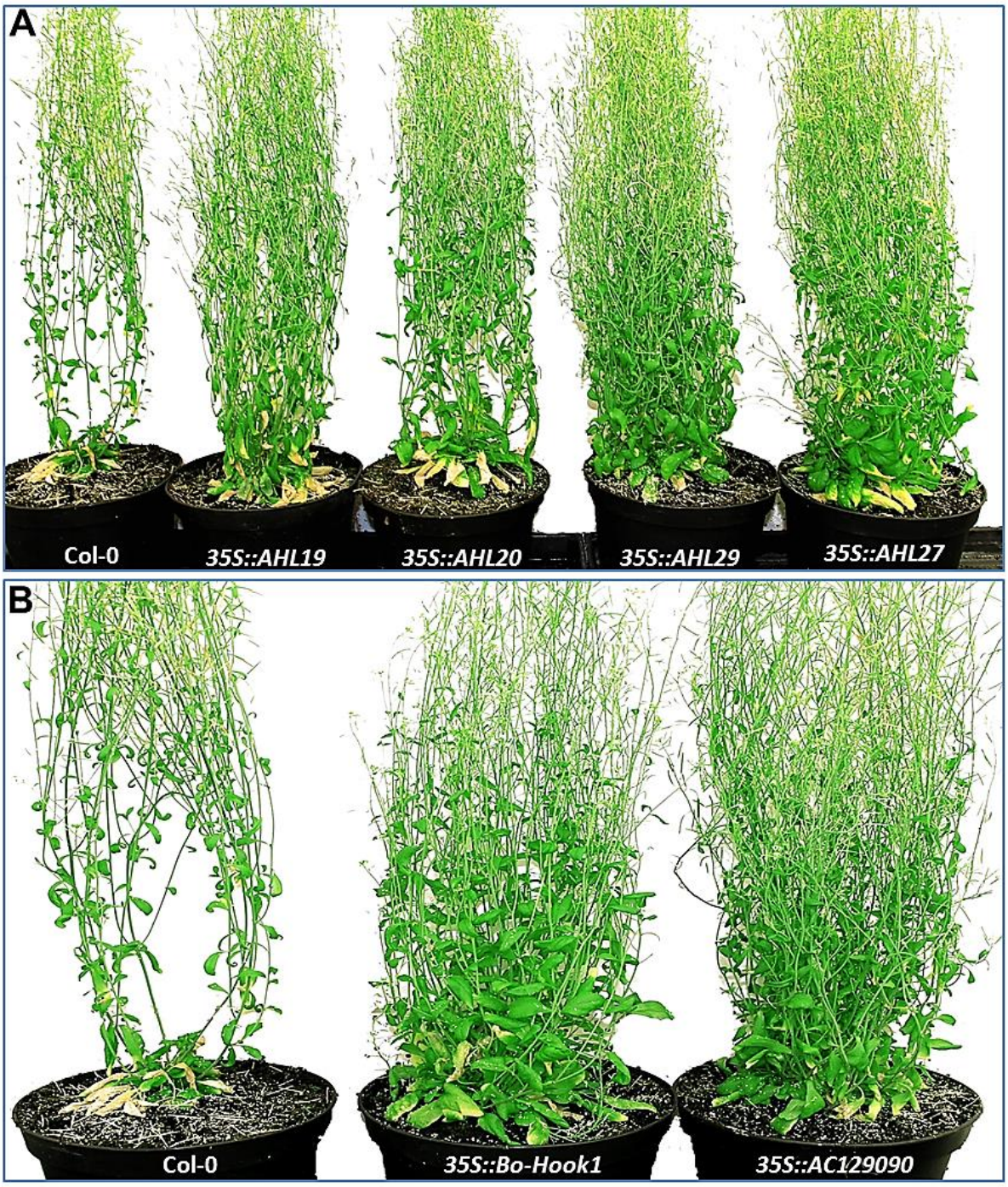

Supplementary figure 3 Overexpression of *Arabidopsis AHL15* paralogs or putative orthologs induces enhanced branching and aerial rosette formation in *Arabidopsis*. (A and B) Wild-type (Col-0) or transgenic *Arabidopsis* plants overexpressing *Arabidopsis AHL19*, *AHL20*, *AHL27* and *AHL29* (A), or the putative *AHL15* orthologs from *Brassica oleracea* (*Bo-Hook1*) or *Medicago trunculata* (*AC129090*) (B). Plants were grown under LD.

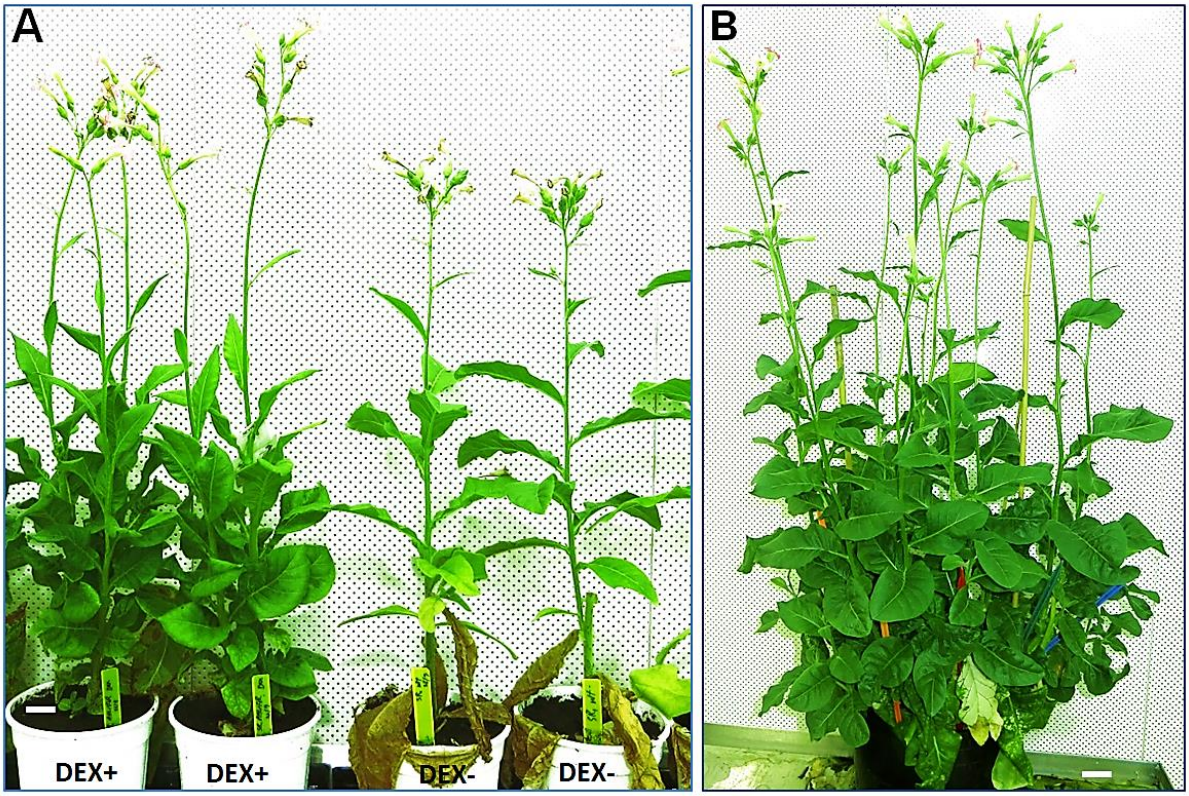

Supplementary figure 4 Induction of polycarpy and reduced senescence in tobacco plants overexpressing *Arabidopsis AHL15*. (A) Induction of axillary meristem activity in flowering *35S::AHL15-GR* tobacco plants sprayed with 30 μM DEX (left). Axillary meristem activity and delayed senescence was not observed in mock treated *35S::AHL15-GR* plants (right). (B) A two-year-old *35S::AHL15-GR* tobacco plant flowers treated with 30 μM DEX, after four previous cycles of DEX-induced rejuvenation and seed production. Size bars indicate 3cm in A and 5 cm in B.

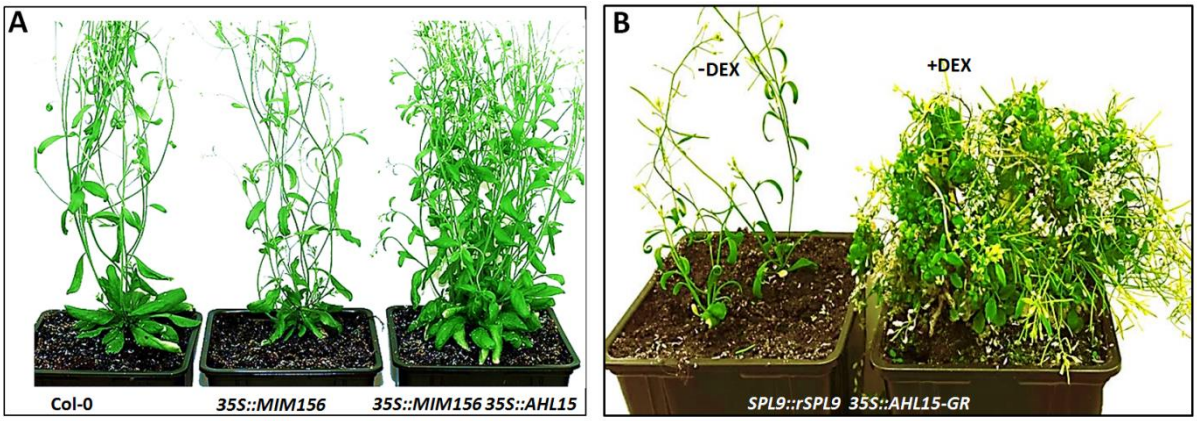

Supplementary figure 5 Ectopic expression of *AHL15* rescues precocious maturation of AMs caused by elevated SPL levels. (A) Mature shoot phenotype of a flowering wild-type plant (left) *35S::MIMR156* plant (middle) and a *35S::MIMR156 35S::AHL15* plant (right). (B) Mature shoot phenotypes of flowering of *35S::AHL15-GR* and *SPL9::rSPL9* double transgenic plants after mock sprayed (-DEX) (left) and sprayed with 20 μM DEX (+DEX) (light). Plants were grown under LD.

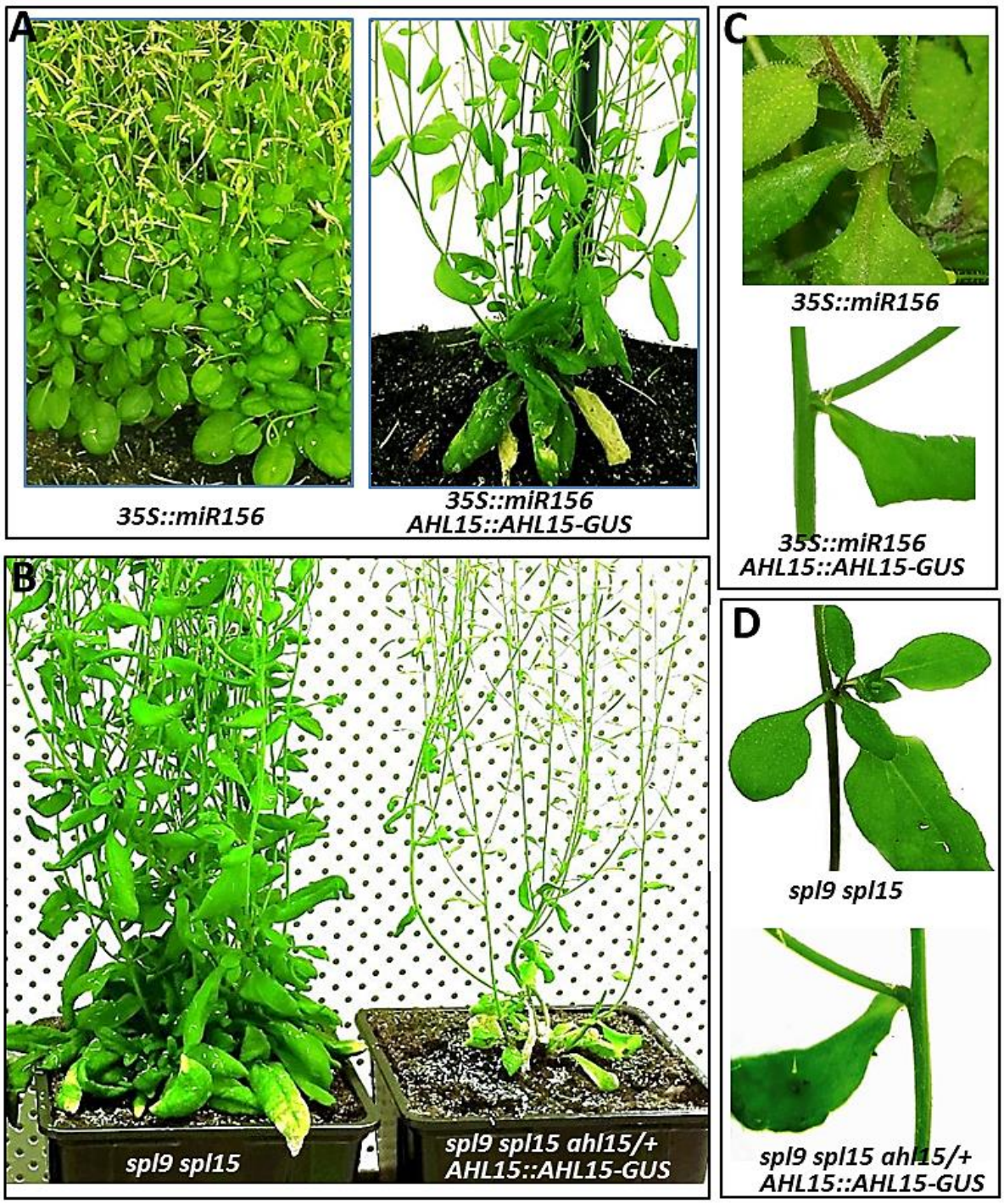

Supplementary figure 6 AHL function is essential for the suppression of AM maturation caused by reduced SPL levels. (A) Mature shoot phenotype of a flowering *35S::miR156* plant (left) and a *35S::miR156 AHL15::AHL15-GUS* plant (right). (B) Mature shoot phenotype of a flowering *spl9 spl15* plant (left) and a *spl9 spl15 ahl15/+ AHL15::AHL15-GUS* plant (right). (C) A lateral inflorescence with and without an aerial rosette on the first inflorescence node of a two-month-old *35S::miR156* (top) and *35S::miR156 AHL15::AHL15-GUS* plant (bottom), respectively. (D) A lateral inflorescence with and without an aerial rosette formed on the first inflorescence node of a two-month-old *spl9 spl15* (top) and *spl9 spl15 ahl15/+ AHL15::AHL15-GUS* plant (bottom), respectively. Plants were grown under LD. For presentation purposes, the original background of images in A (right panel), C and D was replaced by a homogeneous white background.

Supplementary figure 7 AHL function is essential for the polycarpic growth of *spl9 spl15* plants.
Phenotype of 5 month-old *spl9 spl15* (A) and *spl9 spl15 ahl15/+ AHL15::AHL15-GUS* (B) plants. Plants were grown under LD.

Supplementary Table 1: PCR primers used for cloning, genotyping, or qRT-PCR.

Name*	**Sequence (5' to 3')**	**Purpose**
35S::AHL15-F	CCCGGGATGGCGAATCCTTGGTGGGTAG	*35S::AHL15* construct
35S::AHL15-R	GGATCCTCAATACGAAGGAGGAGCACG	
35S::AHL29-F	ATAAGAATGCGGCCGCGACGGTGGTTACGATCAATC	*35S::AHL29* construct
35S::AHL29-R	ATAGTTTAGCGGCCGCCTAAAAGGCTGGTCTTGGTG	
35S::AHL20 –F	ATAAGAATGCGGCCGCGCAAACCCTTGGTGGACGAAC	*35S::AHL20* construct
35S::AHL20-R	ATAGTTTAGCGGCCGCTCAGTAAGGTGGTCTTGCGT	
35S::AHL27-F	ATAAGAATGCGGCCGCGAAGGCGGTTACGAGCAAGG	*35S::AHL27* construct
35S::AHL27-R	ATAGTTTAGCGGCCGCTTAAAAAGGTGGTCTTGAAG	
35S::Bo-Hook-1-F	ATAAGAATGCGGCCGCGCGAATCCTTGGTGGGTAGA	*35S::Bo-Hook-1* construct
35S::Bo-Hook-1-R	ATAGTTTAGCGGCCGCTCAATATGAAGGAGGACCAC	
35S::AC129090-F	ATAAGAATGCGGCCGCTCGAATCGATGGTGGAGTGG	*35S::AC129090* construct
35S::AC129090-R	ATAGTTTAGCGGCCGCTCAATATGGAGGTGGATGTG	
35S::AHL19-F	GGGGACAAGTTTGTACAAAAAAGCAGGCTCGATGGC GAATCCATGGTGGAC	*35S::AHL19* construct
35S::AHL19-R	GGGGACCACTTTGTACAAGAAAGCTGGGTAAACAAG TAGCAACTGACTGG	
AHL15-GUS-F	GGGGACAAGTTTGTACAAAAAAGCAGGCTCGACACT CCTCTGTGCCACATT	*AHL15::AHL15-GUS* construct
AHL15-GUS-R	GGGGACCACTTTGTACAAGAAAGCTGGGTAATACGA AGGAGGAGCACGAG	
SALK_040729-F	GTCGGAGAGCCATCAACACCA	*ahl15* genotyping
SALK_040729-R	CGACGACCCGTAGACCCGGATC	
SAIL_150_B05-F	TGGTTCCTCCACTGAGTCATC	*spl9-4* genotyping
SAIL_150_B05-R	GCTCATTATGACCAGCGAGTC	
SALK_074426-F	TGTTGGTGTCTGAAGTTGCTG	*spl15-1* genotyping
SALK_074426-R	TCCACCGAGTCTTCTTCACTC	
soc1-6 -F	AAAGGATGAGGTTTCAAGCG	*soc1-6* genotyping
soc1-6 -R	ATGTGATTCCACAAAAGGCC	
ful-7-F	GACCCGTTTTCTTCTCCCTC	*ful-7* genotyping
qAHL15-F	AAGAGCAGCCGCTTCAACTA	PCR *AHL15*
qAHL15-R	TGTTGAGCCATTTGATGACC	
qAHL20-F	CAAGGCAGGTTTGAAATCTTATCT	qPCR *AHL120*
qAHL20-R	TAGCGTTAGAGAAAGTAGCAGCAA	
qAHL19-F	CTCTAACGCGACTTACGAGAGATT	qPCR *AHL19*
qAHL19-R	ATATTATACACCGGAAGTCCTTGGT	
qβ-TUBULIN-6-F	TGGGAACTCTGCTCATATCT	qPCR *β-TUBULIN-6*
qβ-TUBULIN-6-R	GAAAGGAATGAG GTTCACTG	

*, F: forward; R: reverse

Chapter 4

Rapid chromatin decondensation by the Arabidopsis AT-Hook domain protein AHL15 leads to long-term repression of the ageing pathway

Omid Karami[1], Christiaan Henkel [2] and Remko Offringa[1]

[1] Plant Developmental Genetics, and [2] Bioinformatics and Genomics, Institute of Biology Leiden, Leiden University, Sylviusweg 72, 2333 BE Leiden, The Netherlands

Abstract

In the previous chapters, we documented that overexpression of the *Arabidopsis* nuclear protein AHL15 leads to reprogramming of somatic cells to embryonic cells and to suppression of plant ageing. Here we show that transient (4 hours) activation of overexpressed AHL15-GR in *Arabidopsis* seedlings has long-term effects on plant development. RNA sequencing analysis detected an extensive reprogramming of the transcriptome 4 hours after AHL15-GR activation, with respectively 540 and 1107 genes showing more than 2-fold up- and down-regulation. AHL15 seemed to act in a transcription level-dependent manner, activating predominantly low expressed genes and repressing mostly highly expressed genes. Rapid decondensation of heterochromatin was observed after AHL15 activation in leaf primordia and axillary meristems, indicating that the global reprogramming of the transcriptome by transient activation of this AT-Hook domain protein might at least in part be caused by extensive modulation of the chromatin configuration. Co-activated or co-repressed genes were often physically linked in small chromosomal clusters, which is in line with regulation at the chromatin level. More detailed analysis of down-regulated genes indicated that AHL15 represses plant ageing by targeting several components of the ageing pathway, including the *SQUAMOSA-PROMOTER BINDING PROTEIN-LIKE* (*SPL*) genes, GA biosynthesis and photosynthesis-dependent sugar production.

Keywords: AHL15, *Arabidopsis*, heterochromatin decondensation, RNA sequencing, transcriptome

Introduction

In flowering plants, ageing is defined by a series of developmental phase transitions that starts with the embryonic to vegetative phase change during germination, and is followed by the juvenile to adult (vegetative) phase change, and the vegetative to reproductive phase change, ultimately culminating in gametogenesis, embryogenesis and seed production. Each developmental phase is characterized by a unique set of morphological traits and the production and growth of specific organs (Huijser and Schmid, 2011). During the past few years, molecular genetic studies have demonstrated that the timing of these developmental phase transitions is orchestrated by specific sets of key regulators, which the SQUAMOSA PROMOTER BINDING PROTEIN-LIKE (SPL) proteins play a central role in promoting the vegetative (juvenile to adult)- and the vegetative to reproductive phase transition. Early during development, high levels of miR156 repress the production of the SPL proteins, thereby maintaining plants in the juvenile phase. A gradual decrease in *miR156* expression during the progression of development leads to increased SPL levels, which promote the progression of development through the subsequent phase transitions (Wu and Poethig, 2006; Xie et al., 2006; Saeteurn K, 2007; Wu et al., 2009; Andrés and Coupland, 2012).

In Chapters 2 and 3 we have shown that the AT-HOOK MOTIF NUCLEAR LOCALIZED protein AHL15 and other members of the plant-specific AHL protein family redundantly repress the ageing pathway by delaying the juvenile to adult and the vegetative to reproductive phase transition. In fact, overexpression of *AHL15* was able to reverse developmental phase transitions, resulting in the hormone-indepenent induction of somatic embryos on immature zygotic embryos or seedlings, and converting the monocarpic annual *Arabidopsis thaliana* into a polycarpic plant. How AHL15 can have such a dramatic effect on developmental phase transitions is one of the key questions to be addressed.

The paradigm for transcription factors is that they are nuclear proteins that bind to upstream regulatory DNA sequences and activate and/or repress transcription of target genes by respectively facilitating or inhibiting the recruitment of RNA polymerase to the transcription start site. By contrast, proteins of the plant-specific AHL family are a specific class of nuclear proteins that unlike most transcription factors, do not bind the major groove of the DNA helix, but instead interact with the narrow minor groove of DNA (Matsushita et al., 2007; Ng et al., 2009; Zhao et al., 2013). AHL proteins contain at least one AT-hook DNA binding motif and a Plant and Prokaryote Conserved (PPC) domain. Based on mutants and protein-protein interaction studies, the AHL family members have been proposed to bind AT-rich DNA regions as hetero-multimeric complexes that recruit other transcription factors through their interacting PPC domains (Zhao et al., 2013). In addition, it has been shown that AHL proteins repress transcription of several key developmental regulatory genes, possibly through modulation of the epigenetic code in the vicinity of its DNA binding regions (Lim et al., 2007; Ng et al., 2009; Yun et al., 2012). Some evidence has been obtained that AHL proteins function by altering the organization of the chromatin structure (Lim et al., 2007; Ng et al., 2009; Yun et al., 2012; Xu et al., 2013). Thus, different modes of transcription regulation by the AHL proteins have been described, but since this plant specific class of nuclear proteins is not well studied, their exact mode of action is still elusive.

Many AT-rich sequences in the DNA function as matrix attachment regions (MARs), which are well known to interact with the nuclear matrix, a fibrillar network of proteins inside the nucleus. Although, MARs are widely distributed in the genome, they are commonly found at the boundaries of transcription units. MARs play important roles in the higher-order organization of chromatin structure, thereby regulating gene expression (Heng et al., 2004; Girod et al., 2007; Chavali et al., 2011; Wilson and Coverley, 2013). The majority of the animal AT-hook motif containing DNA-binding proteins are localized to MARs where they are associated with proteins that modulate chromatin architecture (Fusco and Fedele, 2007). Also for the plant-specific AHL proteins it has been shown that they preferentially bind to the AT-rich DNA sequences of MARs (Morisawa et al., 2000; Fujimoto et al., 2004; Lim et al., 2007; Ng et al., 2009; Xu et al., 2013). However, a correlation between the function of AHL proteins and their localization to MARs has not been documented yet.

Here we observed that short-term activation (4 hours) of *35S::AHL15-GR* seedlings, overexpressing a fusion between AHL15 and the dexamethasone (DEX) responsive domain of the glucocorticoid receptor, resulted in long-term effects on plant development, such as delayed flowering, enhanced branching and the recurrent formation of aerial rosettes, converting monocarpic *Arabidopsis* into a polycarpic plant. In order to understand the AHL15 mode of action, we compared the chromatin configuration and transcriptome of mock- or DEX-treated *35S::AHL15-GR* seedlings by respectively nuclear staining and high throughput next generation sequencing of transcripts (Illumina RNA-Seq) (Mortazavi et al., 2008). Rapid decondensation of heterochromatin was observed after AHL15-GR activation in leaf primordia and axillary meristems, indicating that the observed global reprogramming of the transcriptome by transient activation of this AT-Hook domain protein might at least in part be caused by extensive modulation of the chromatin configuration. More detailed analysis of down-regulated genes indicated that AHL15 represses plant ageing by targeting several components of the ageing pathway, including the *SQUAMOSA-PROMOTER BINDING PROTEIN-LIKE* (*SPL*) genes, GA biosynthesis and photosynthesis-dependent sugar production.

Results

Short-term activation of AHL15-GR has long-term effects on plant development

In Chapter 3 we showed that *Arabidopsis* plants that constitutively express AHL15 (*35S::AHL15*) or plants that express a dexamethasone (DEX) activatable version of AHL15 (*35S::AHL15-GR*) and were subjected to continuous DEX treatment both showed a strong delay in the juvenile-to-adult transition and flowering time. In contrast, *ahl* loss-of-function mutant plants or plants expressing a dominant negative AHL15-GUS fusion showed a premature vegetative phase change and early flowering. Moreover, *AHL15* overexpression induced rejuvenation of axillary meristems, resulting in enhanced branching and in the production of aerial rosettes, converting monocarpic *Arabidopsis* into a polycarpic plant. For typical transcription factors it has been shown that they act transiently, whereas other nuclear factors have a more long-lasting effect on the gene expression profile of a cell, as they act on the chromatin structure by inducing epigenetic changes (Bratzel and Turck,

2015). In order to analyses the mode of action of AHL15, 5-day-old *35S::AHL15-GR* seedlings were submerged in water with 20 µM DEX or without DEX (mock) for 4 and 8 hours, and subsequently DEX was removed by washing the seedlings in water and transferring them to soil. DEX-incubated seedlings developed much slower and the resulting plants showed a significant delay in flowering compared to the plants derived from the mock-treated seedlings (Fig. 1A). DEX-treatment for 8 hours enhanced the phenotypes observed in the 4 hour DEX-treated seedlings and derived plants (not shown). Also, 35-day-old flowering *35S::AHL15-GR* plants that were only sprayed once with 20 µM DEX developed aerial rosettes from their axillary meristems 7-10 days after spraying (Fig. 1B), and new aerial rosettes continued to develop for at least 4 months after spraying (Fig. 1C-E). These data indicates that short-term activation of AHL15 leads to long-term changes in development, which would be in line with a function for AHL15 in chromatin remodeling.

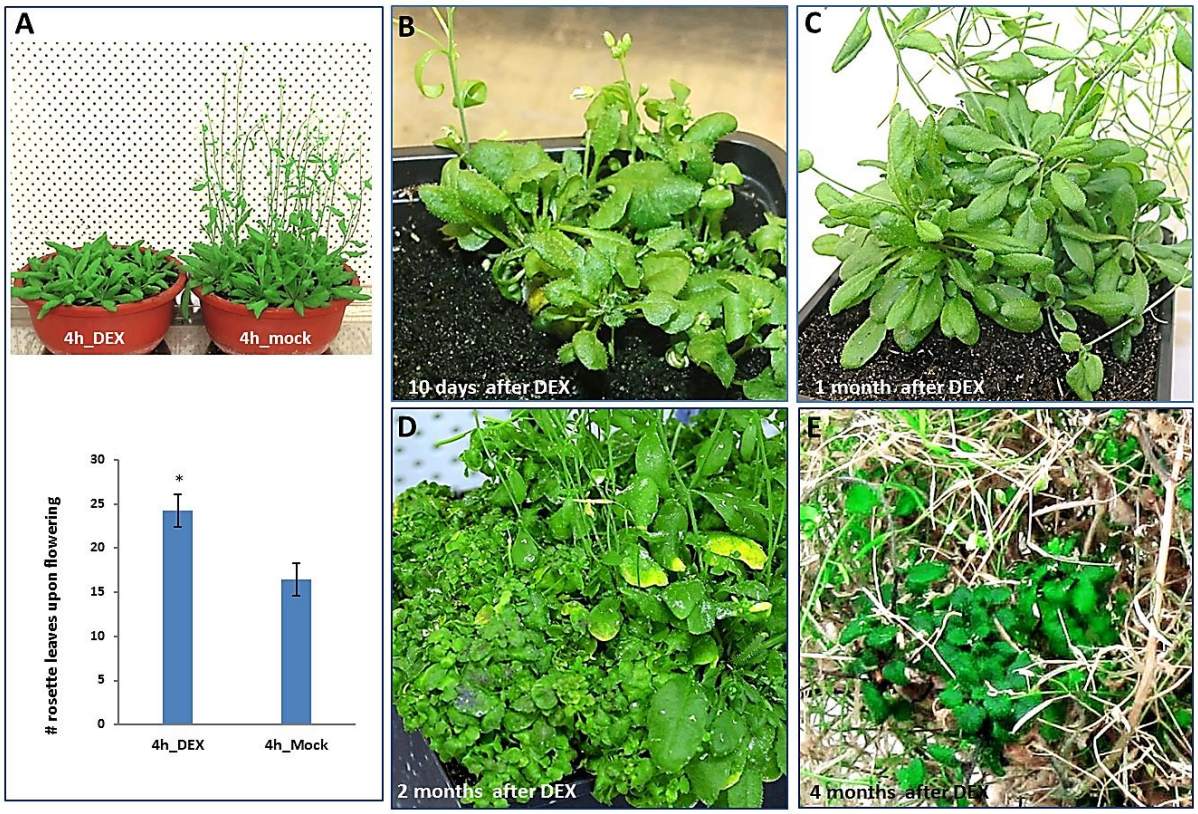

Figure 1 Short term activation of AHL15 has long term effects on plant development. (A) Phenotype (upper panel) and quantification of the number of rosette leaves (lower panel) of 35 day old flowering *35S::AHL15-GR* plants that were grown from 5 day old seedlings that were submerged for 4 hours in water (4h_mock) or in 20 µM DEX solution (4h_DEX). Asterisk in the graph indicates a significant difference between mock- and DEX-treated plants (Student's *t*-test, $p < 0.01$), and error bars indicate standard error of the mean (n =20). (B E) Aerial rosettes developing from axillary meristems in *35S::AHL15-GR* plants 10 days (B), or one (C), two (D) or four months (E) after spraying 1 month old flowering *35S::AHL15-GR* plants with 20 µM DEX solution. Plants were grown under LD.

AHL15 extensively reprograms the *Arabidopsis* transcriptome

In order to uncover the molecular basis of these long term developmental changes induced by AHL15, the genome-wide expression changes were compared between DEX-treated and untreated *35S::AHL15-GR* seedlings. As the major developmental changes induced by AHL15 overexpression were observed in the shoot (Chapter 3, Figure 1), we isolated RNA from the shoot part (i.e. shoot apex, cotyledons and top part of hypocotyl) of 5-day-old *35S::AHL15-GR* seedlings submerged for 4 hours in mock or in 20 µM DEX, or for 8 hours in 20 µM DEX. RNA sequencing was performed on RNA isolated from three biological replicates for each treatment. A slight but significant reduction of *AHL15-GR* expression was observed in DEX-treated seedlings compared to untreated samples (Table 1), suggesting that AHL15 modulates the *35S* promoter activity in this time period.

Table 1. Overview of raw data obtained by Illumina sequencing on RNA isolated from the shoot part of 5-day-old *35S::AHL15-GR* seedlings that were treated with water for 4 hours (4h_mock)) or with 20 µM DEX for 4 or 8 hours (resp. 4h_DEX or 8h_DEX).

Sample #	Treatment	Raw sequencing reads	Expression level of *AHl15* [1]	
1	4h_mock	14285557	678.13	687.06 ± SE
2	4h_mock	17597921	636.59	
3	4h_mock	27463033	746.46	
4	4h_DEX	32465125	519.36	519.70 ± SE *
5	4h_DEX	21100996	526.87	
6	4h_DEX	28328909	512.89	
7	8h_DEX	30340913	519.13	532.90 ± SE *
8	8h_DEX	26594329	538.09	
9	8h_DEX	30496134	541.48	

[1] Normalized Reads Per Kilobase Million (RPKM) values.Right column indicates the average value of the three biological replicates +/- standard error of the mean.
* Significantly different from 4h_mock (Student's *t*-test, $p < 0.001$)

Annotation of the reads using the *Arabidopsis* Information Resource (www.arabidopsis.org) showed that the expression of 22570 genes could be detected in the 4 hours mock samples, which is 83% of the total gene number (Table S1). Statistical analysis showed that 13483 genes were differentially expressed in 4 hours DEX-treated compared to mock treated *35S::AHL15-GR* shoot organs (Table S2). However, only 1663 genes showed a fold change of ≥ 2 (and $P \leq 0.05$) after 4 hours DEX treatment (Fig. 2A, B, Table S3 and S4). Verification of the change in expression for 4 selected genes by qRT-PCR analysis showed a good agreement with the RNA-sequencing results (Table 2).

Comparison of the up- and downregulated gene sets showed a considerable overlap between 4 and 8 hours DEX treatment (Fig. 2A,B). Still, however, the number of up- (Table S5) and down-regulated (Table S6) genes increased significantly after 8 hours DEX treatment (Fig. 2A,B). Several of the genes that did not show a ≥ 2 fold change after 4 hours DEX treatment reached this level after 8 hours treatment (Fig. 2A,B). Conversely, some genes that reached ≥ 2 fold change after 4 hours, did not appear anymore in the ≥ 2 fold gene set after 8

hours (Fig. 2A,B), indicating time-dependent transcriptome changes by AHL15-GR. The latter result would be more in line with a role for AHL15 as a gene-specific transcription factor.

Table 2. Confirmation of RNA-seq data by qRT-PCR analysis.

Locus	Name and short description	Fold change found by RNA Seq	P Value	Fold change detected by qRT-PCR[1]	P Value
AT5G59490	Haloacid dehalogenase-like hydrolase (HAD) superfamily protein	135.5	2.07E-145	78.30 ± 7.80	0.003
AT4G22770	AT hook motif DNA-binding family protein 2	15.19	8.02E-139	9.32 ± 1.45	0.005
AT2G17740	Cysteine/Histidine-rich C1 domain family protein	0.002	1.21E-62	0.008 ± .002	0.0003
AT1G78580	Trehalose-6-phosphate synthase 1	0.35	2.11E-54	0.43 ± 0.06	0.021

[1]Shown is the fold changes ± standard error of the mean (n=3). P value: Student's t-test.

Notably, we found that the down-regulated genes were generally expressed at higher levels in the 4h_mock control sample, whereas the up-regulated genes were expressed at relatively low levels in the 4h_mock control sample (Fig. 2C). This data suggests that AHL15 reverses phase changes by modulating gene activity in a transcription level-dependent manner, repressing genes that are highly expressed and activating genes that are low expressed during a specific developmental phase. Global prediction of the transcriptome changes using gene ontology (GO) examination (Du et al., 2010) (http://bioinfo.cau.edu.cn/agriGO/) and TAIR as reference for the annotation of *Arabidopsis* genes indicated that up- and down-regulated gene sets grouped in many different biological categories (Tables S7 and S8). These results suggested that, beside its action as regulator of individual genes, AHL15 contributes to a more global reprograming of biological processes by inducing global changes in gene transcription.

Whereas most gene families represented in the transcriptome profiles (Table S2) had gene members that were either up- or down-regulated, members of the *CYSTEIN-RICH RECEPTOR-LIKE KINASE* (*CRK*) gene family only showed down-regulation of gene expression by AHL15 (Table 3). Notably, several of the down-regulated *CRKs* by AHL15 are neighboring genes that are located in a tandem arrays on chromosome 4 (Fig, 3A). This triggered us to look into the localization of up- or down-regulated genes, and surprisingly, a high rate (~75%) of co-activation or co-repression of neighboring genes by AHL15 was observed across the genome (Tables S9, and Fig. 3B). These observations suggest that AHL15 modulates gene expression in a chromosomal position- rather than a gene-specific manner.

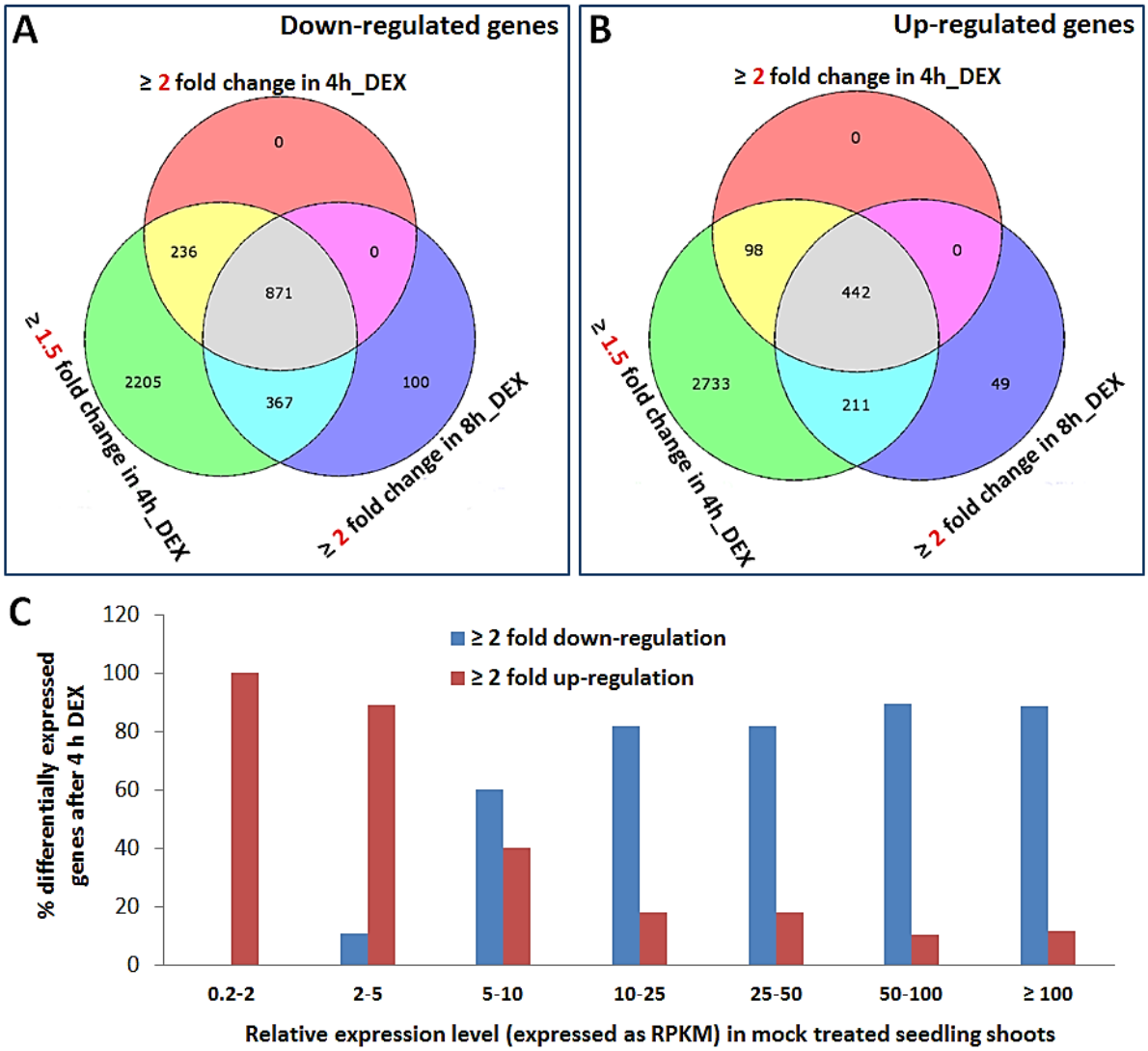

Figure 2 Changes in the transcriptome of *Arabidopsis 35S::AHL15-GR* seedling shoots after DEX treatment. (A, B) Venn diagrams indicating the number of (overlapping) down-regulated (A) or up-regulated (B) genes in *35S::AHL15-GR* seedling shoots with a ≥1.5 fold or ≥2 fold change in gene expression following 4 or 8 hours of DEX treatment. (D) Graph showing the percentage of genes having a specific expression level (in RPKM) in mock treated *35S::AHL15-GR* seedling shoots that are either ≥2 fold up- (red) or ≥2 fold down- (blue) regulated by 4 hours DEX treatment.

Table 3. Members of the *Cysteine-rich receptor-like kinase* gene family were all down-regulated in *35S::AHL15-GR* seedling shoots after 4 hours DEX treatment

Locus	Name and short description	Fold change	P Value
AT4G23180	cysteine-rich RLK (RECEPTOR-like protein kinase) 10	0.34	5.49E-29
AT4G23190	cysteine-rich RLK (RECEPTOR-like protein kinase) 11	0.32	4.58E-39
AT4G23200	cysteine-rich RLK (RECEPTOR-like protein kinase) 12	0.04	1.92E-87
AT4G23210	cysteine-rich RLK (RECEPTOR-like protein kinase) 13	0.08	1.28E-44
AT4G23260	cysteine-rich RLK (RECEPTOR-like protein kinase) 18	0.138	9.12E-165
AT4G23270	cysteine-rich RLK (RECEPTOR-like protein kinase) 19	0.82	0.0098589
AT1G70520	cysteine-rich RLK (RECEPTOR-like protein kinase) 2	0.40	5.80E-33
AT4G23290	cysteine-rich RLK (RECEPTOR-like protein kinase) 21	0.11	6.19E-110
AT4G23300	cysteine-rich RLK (RECEPTOR-like protein kinase) 22	0.17	1.37E-106
AT4G21400	cysteine-rich RLK (RECEPTOR-like protein kinase) 28	0.77	7.47E-05
AT4G21410	cysteine-rich RLK (RECEPTOR-like protein kinase) 29	0.94	0.33050
AT1G70530	cysteine-rich RLK (RECEPTOR-like protein kinase) 3	0.40	7.76E-26
AT4G11460	cysteine-rich RLK (RECEPTOR-like protein kinase) 30	0.31	5.07E-19
AT4G04490	cysteine-rich RLK (RECEPTOR-like protein kinase) 36	0.14	1.29E-53
AT4G04570	cysteine-rich RLK (RECEPTOR-like protein kinase) 40	0.30	4.74E-63
AT4G00970	cysteine-rich RLK (RECEPTOR-like protein kinase) 41	0.09	2.31E-62
AT5G40380	cysteine-rich RLK (RECEPTOR-like protein kinase) 42	0.25	1.70E-23
AT4G23130	cysteine-rich RLK (RECEPTOR-like protein kinase) 5	0.19	5.63E-41

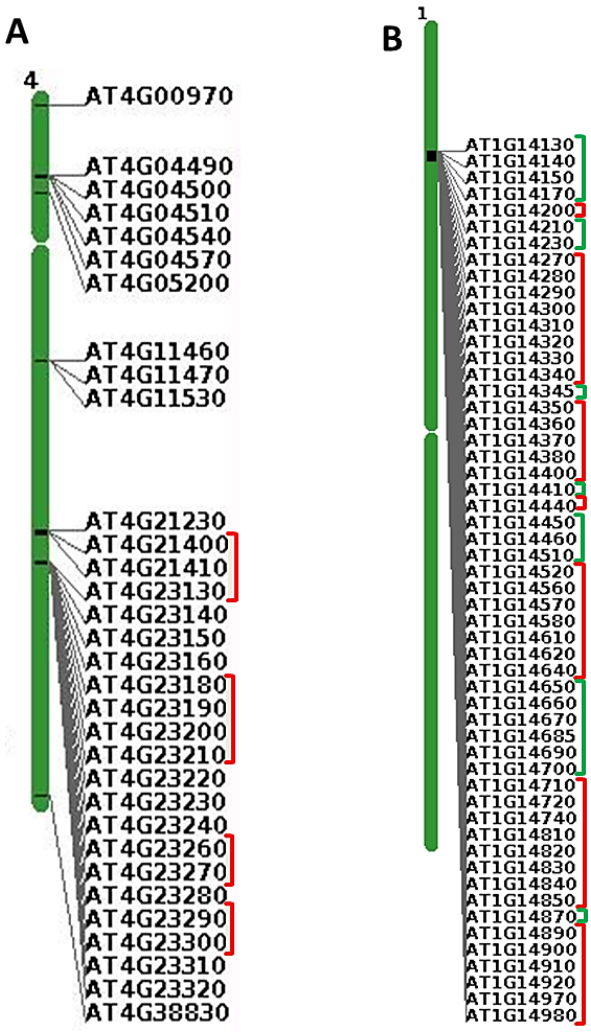

Figure 3 AHL15 modulates gene expression in a chromosomal region-dependent manner. (A) Schematic representation of *Arabidopsis* chromosome 4 showing the tandem arrays of *CRKs* genes on this chromosome. RNA Seq analysis on 5 day old *35S::AHL15-GR* seedlings shoots treated for 4 hours with 20 uM DEX shows that some neighboring *CRK* genes are co-repressed (indicated by the red line). (B) Schematic representation of *Arabidopsis* chromosome 1 showing for one region that neighboring genes are co-repressed (red line) or co-induced (green line) in 5 day old *35S::AHL15-GR* seedling shoots following 4 hours DEX treatment.

AHL15 overexpression results in reduced heterochromatin condensation

Based on previous analysis in animals that AT-hook proteins are able to change the higher order compaction of chromatin organization (Catez et al., 2004; Kishi et al., 2012; Postnikov and Bustin, 2016), we compared the chromatin organization in leaf cells of two week old *35S::AHL15* seedlings with that in wild-type leaf cells. By imaging DAPI stained nuclei or nuclei of leaf cells expressing GFP-tagged histone H2B, a considerable reduction of heterochromatin could be detected in *35S::AHL15* leaf cells compared to wild-type cells (Fig. 4A). This reduction in heterochromatin by AHL15 was even more clearly observed by imaging GFP-H2B in leaf primordia produced from axillary meristems on inflorescences (Fig. 4B). Time-lapse imaging of GFP signals revealed a rapid gradual reduction in heterochromatin condensation in DEX-treated compared to mock-treated *35S::AHL15-GR* leaf primordia (Fig. 4B), indicating that the AHL15-induced heterochromatin opening occurs in a time-dependent manner and within the time frame of the transcriptome analysis. These data support the view that the observed global reprogramming of the transcriptome by AHL15 might be caused by extensive modulation of the chromatin configuration.

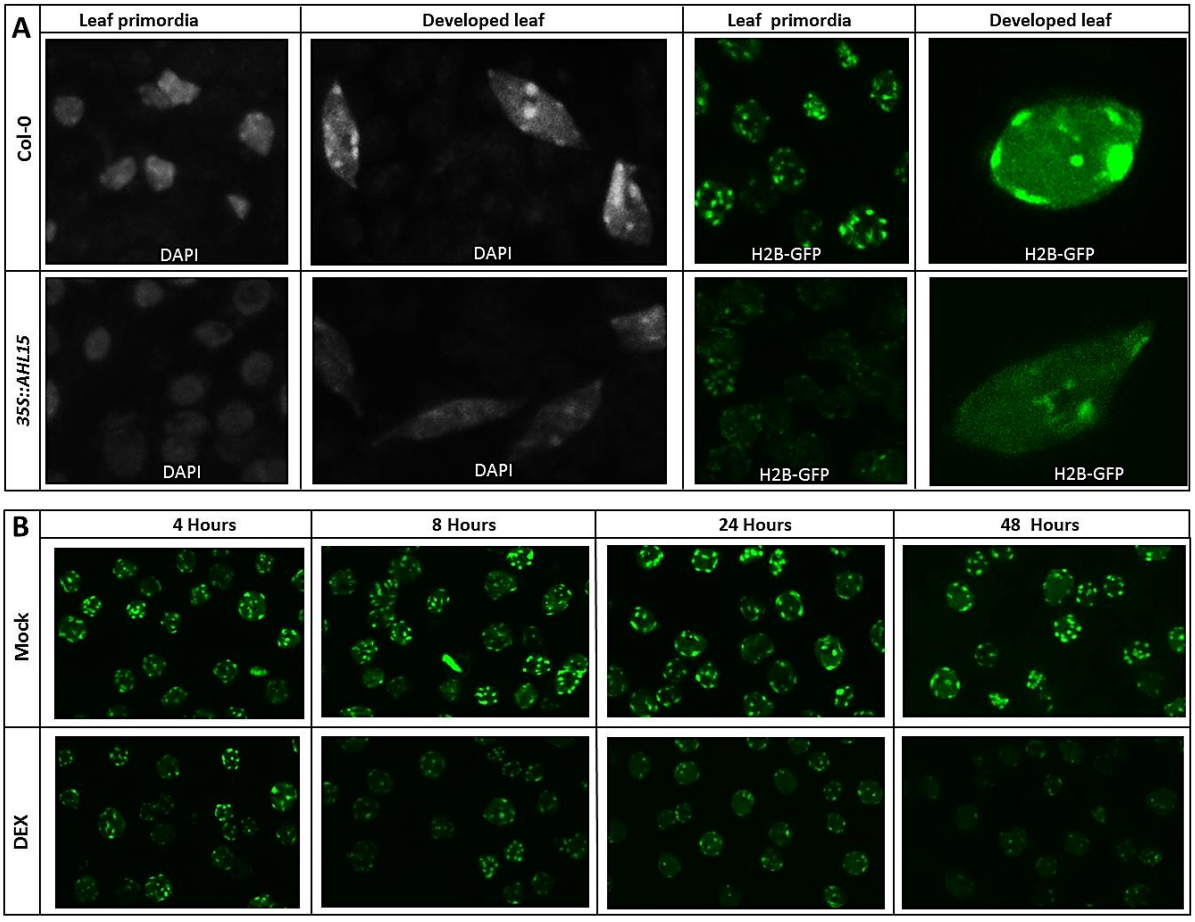

Figure 4 *AHL15* overexpression induces rapid heterochromatin decondensation. (A) Visualization of heterochromatin using DAPI-staining or H2B-GFP labelling of nuclei in leaf primordia or fully developed leaf cells in 2-week-old wild-type (upper row) or *35S::AHL15* (lower row) plants. (B) Heterochromatin labelling by H2B-GFP in nuclei of *35S::AHL15-GR* axillary leaf primordium cells at 4, 8, 24, or 48 hours after mock (upper row) or DEX treatment (lower row).

AHL15 represses ageing genes

Since *AHL15* expression delays and even reverses plant ageing (Chapter 2 and 3), we searched for age regulatory genes among the differentially expressed genes in the transcriptome profiles. The first gene family we looked for were the *SQUAMOSA-PROMOTER BINDING PROTEIN-LIKE* (*SPL*) genes encoding transcription factors that promote the juvenile-to-adult transition in *Arabidopsis* (Wu and Poethig, 2006; Xie et al., 2006; Saeteurn K, 2007; Wu et al., 2009). *SPL* mRNAs are targeted by MicroRNA156 (miR156), and the juvenile to adult transition is attributed to the down-regulation of *miR156* gene expression and the subsequent increase in SPL protein abundance (Wu and Poethig, 2006; Xie et al., 2006; Saeteurn K, 2007; Wu et al., 2009). Our transcriptome data revealed that *SPL4*, *SPL9*, *SPL13* and *SPL15* were significantly down regulated after AHL15-GR activation (Fig 5A), whereas the expression of *SPL2*, *SPL11*, *SPL10* was not significantly changed (Fig 4A). The expression of *SPL3* and *SPL5* was undetectable in the RNA seq-based transcriptome profile (Fig 5A), which could be related to the high levels of degradation of SPL3 and SPL5 mRNAs by miR165 in young seedlings. This RNA seq-based result triggered us to further study the genetic regulation *SPL* genes by AHL15. Quantitative RT-PCR (qPCR) analysis confirmed that the expression of *SPL3*, *SPL9*, and *SPL15* was significantly down-regulated in 4 hour DEX-treated *35S::AHL15-GR* seedlings (Fig. 5B). Time-lapse GUS staining of *pSPL3::GUS-SPL3* plants (Yang et al., 2011) revealed a gradual reduction of *SPL3* expression in response to continuous DEX activation of AHL15-GR (Fig. 5C). These results indicate that the *SPL* genes are gradually suppressed by AHL15.

Consistent with maximum activity of the *SPL* genes in inflorescence stems (Cardon et al., 1999), we analyzed the effect of *AHL15* overexpression on *SPL* expression levels in inflorescence nodes. Compared to wild-type inflorescence nodes, qPCR detected only low expression of *SPL3*, *SPL9* and *SPL15* in *35S::AHL15* inflorescence nodes (Fig. 5D). These results displayed that *AHL15* overexpression strongly suppresses *SPL* genes in the reproductive phase, which is likely to maintain axillary meristems in *35S::AHL15* plants in the vegetative state during flowering, thereby resulting in the production of areal rosettes and enhanced branching (Chapter 3).

To determine whether down-regulation of *SPL* genes by *AHL15* is dependent on *miR156* function, two miR156-insensitive reporters, *pSPL9::rSPL9-GUS* and *pSPL3::GUS-rSPL3* (Yang et al., 2011), were introduced into *35S::AHL15-GR* plants. The expression of *pSPL9::rSPL9-GUS* and *pSPL3::GUS-rSPL3* was significantly down-regulated in DEX-treated *35S::AHL15-GR* seedlings compared with mock-treated seedlings (Fig. 5E). These results indicated that *AHL15* overexpression suppresses *SPL* genes in a miRNA156-independent manner.

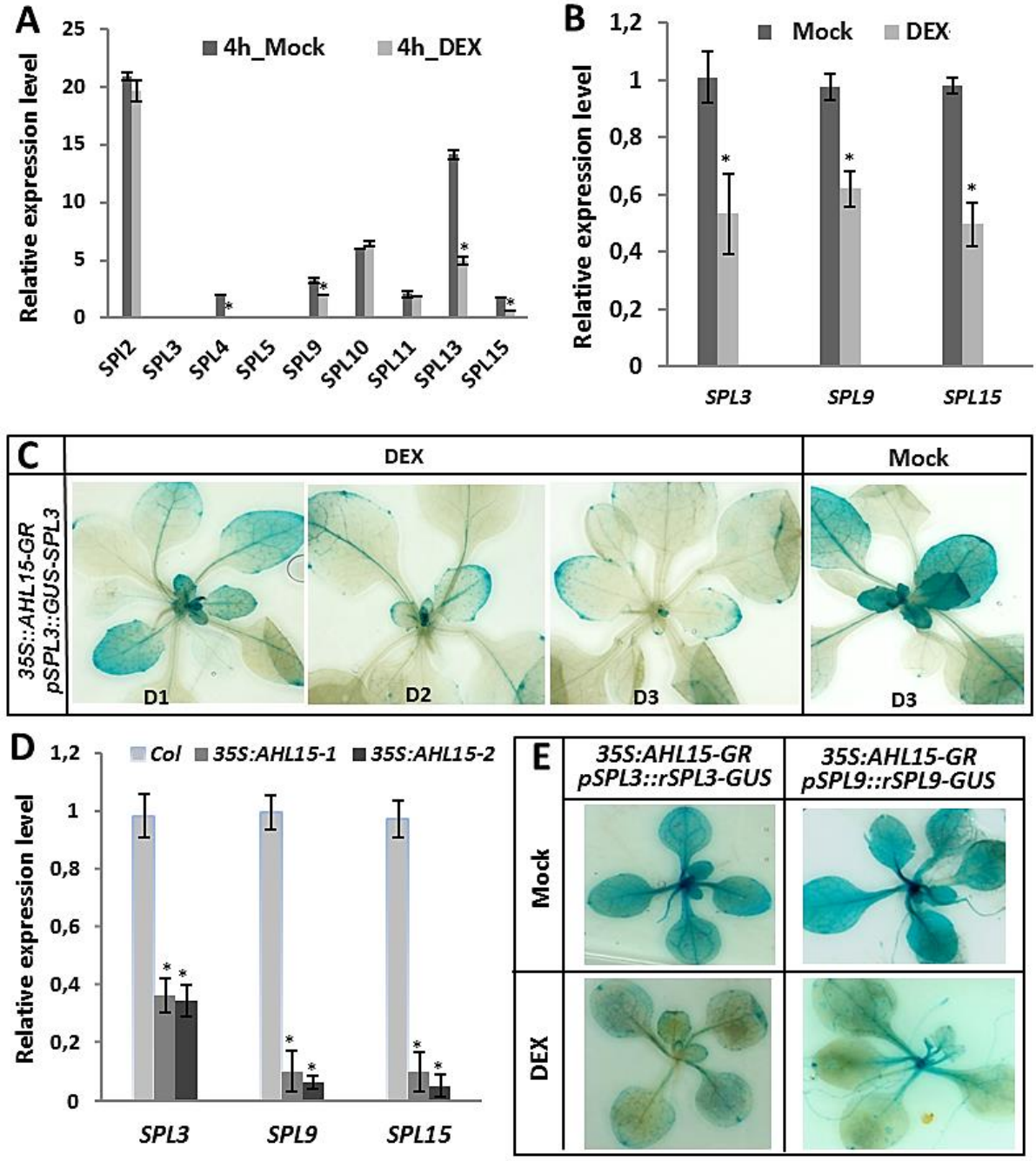

Figure 5 AHL15 represses *SPL* expression in a miRNA-independent manner. (A) The relative expression level (in RPKM) of different *SPL* genes detected by RNA Seq analysis on 5 day old *35S::AHL15-GR* seedlings shoots following 4 hours water (mock) or 20 uM DEX treatment. (B) The relative expression level of *SPL* genes by qPCR analysis on shoot parts of 2 week old *35S::AHL15-GR* seedlings incubated for 1 day on medium without (mock) or with 20 μM DEX (DEX). (C) Histochemical staining for GUS activity on 3 week old *GUS-SPL3 35S::AHL15-GR* seedlings incubated on medium without (mock, right) or with 20 uM DEX (DEX, left) for 1, 2 or 3 days (respectively D1, D2 or D3). (D) Relative expression level of *SPL3*, *SPL9* and *SPL15* by qPCR analysis on the base regions of 1 week old inflorescences of wild-type (Col) or *35S::AHL15* #1 or #2 plants. (E) Histochemical staining for GUS activity on 2 week old water (mock) or 20 uM DEX (DEX) treated *35S::AHL15-GR* plants expressing miR156-resistant -*SPL3-rSPL3-GUS* or *SPL9-rSPL9-GUS* reporters. Asterisks in A, B and D indicate significant difference from mock-treated (A,B) or wild-type (D) plants (Student's *t*-test, $p < 0.01$). Error bars indicate standard error of the mean (n =3).

One of the plant hormones involved in ageing is gibberellic acid (GA), as it promotes the juvenile-to-adult or the vegetative-to-reproductive phase transitions (Telfer et al., 1997; Mutasa-Göttgens and Hedden, 2009; Poethig, 2013). In our transcriptome profile we observed that the GA biosynthesis gene *GIBBERELLIN 20-OXIDASE 2* (*GA20OX2*) was highly down-regulated in 4 hour DEX-treated *35S::AHl15* seedlings (Fig 6A). GA20OX2 is a rate limiting enzyme in the last steps of the GA biosynthetic pathway (Huang et al., 1998; Rieu et al., 2008; Andrés et al., 2014). In line with this down-regulation, meristem rejuvenation in DEX treated flowering *35S::AHL15-GR* plants was remarkably reduced when these plants were treated with GA 3 days after DEX (Fig 6B). We conclude that the repression of GA biosynthesis, next to a decrease in *SPL* gene expression, plays an important role in the AHL15-mediated suppression of phase transitions and axillary meristem rejuvenation.

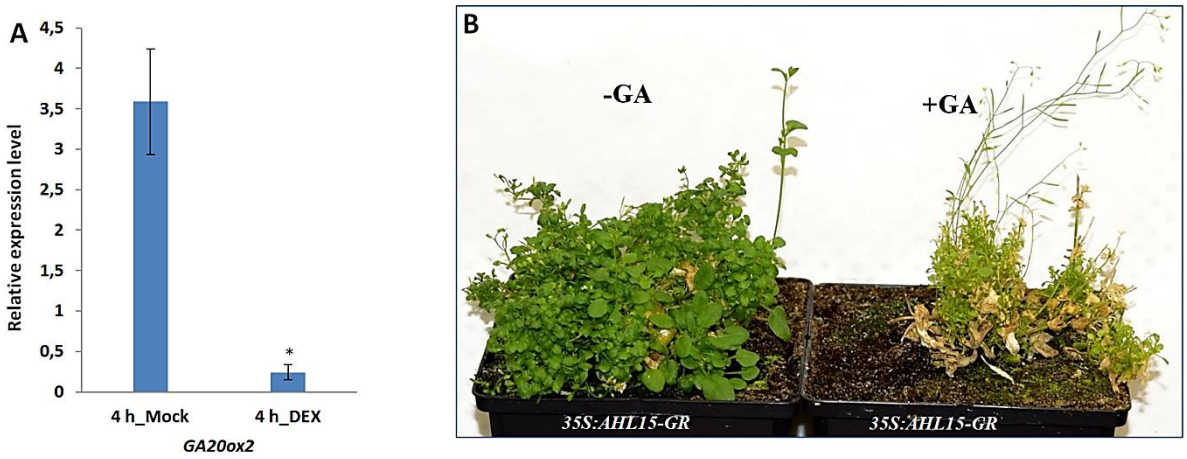

Figure 6 AHL15-induced developmental changes by reduced GA biosynthesis. (A) The relative expression level of the *GA20OX2* gene detected by RNA Seq analysis on 5 day old *35S::AHL15-GR* seedlings submerged for 4 hours in water (4h_mock) or 20 uM DEX solution (4h_DEX). Asterisk indicates significant difference from mock seedlings (Student's *t*-test, $p < 0.001$). Error bars indicate standard error of the mean (n =3). (B) Shoot phenotypes of two month old *35S::AHL15-GR* plants derived from 35 day old DEX sprayed plants that were subsequently sprayed 3 days later with water (-GA) or with 15 µM GA4 (+GA).

Reduced photosynthesis in *35S::AHL15* plants causes sucrose-dependent seedling growth

In the transcriptome profile of DEX-treated *35S::AHL15-GR* seedlings we detected down-regulation of several photosynthesis-related genes (Table 4). The MapMan hierarchical ontology software (Thimm et al., 2004) showed that several of the down regulated genes encode for components of photosystem I and II, such as the light harvesting complexes, and the reaction centers (Fig. 7A, Table 4). These are among the most highly expressed genes in plants, and the fact that they are repressed by AHL15 is in line with the previously proposed transcription level-dependent manner of regulating gene expression by AHL15.

Recent studies suggest that the increasing photosynthesis efficiency and sugar concentration in shoot organs of the developing young plant promote the vegetative phase change (Matsoukas et al., 2013; Yang et al., 2013; Yu et al., 2013). The suppression of

ageing in *35S::AHL15* seedlings could therefore at least in part be caused by a delayed increase in the photosynthesis efficiency. To confirm that *AHL15* overexpression reduces the photosynthesis efficiency and thus the sugar concentration, we germinated wild-type or *35S::AHL15* seedlings on medium with or without sucrose. On medium with sucrose, both wild-type and *35S::AHL15* seedlings developed, albeit that development of *35S::AHL15* seedlings was retarded, as observed previously (Chapter 3). On medium without sugar wild-type seedlings also developed, but generally much slower than sucrose grown seedlings, suggesting that photosynthesis under these *in vitro* conditions is rate limiting (Fig. 7B). In contrast, *35S::AHL15* seeds did germinate on medium without sucrose but seedling development was completely arrested (Fig. 7B). The results indicate that the germinating seedlings lack endogenous sugars, and therefore are completely dependent for their development on externally provided sucrose, most likely due to *AHL15*-mediated repression of photosynthesis during germination.

Table 4. List of photosynthesis-related genes that were down-regulated in *35S::AHL15-GR* seedling shoots after 8 hours DEX induction

Locus	Name and descriptions	Expression level in 4h_water	Fold change	P Value
AT4G10340	light harvesting complex of photosystem II 5	3485	0.37	1.58E-44
AT5G01530	light harvesting complex photosystem II	2405	0.45	3.93E-35
AT3G08940	light harvesting complex photosystem II	1043	0.34	2.54E-37
AT1G15820	light harvesting complex photosystem II subunit 6	2323	0.44	1.29E-32
AT5G54270	light-harvesting chlorophyll B-binding protein 3	3520	0.18	5.28E-78
AT3G47470	light-harvesting chlorophyll-protein complex I subunit A4	3885	0.18	2.13E-93
AT2G34430	light-harvesting chlorophyll-protein complex II subunit B1	2402	0.08	1.22E-118
AT3G54890	photosystem I light harvesting complex gene 1	3839	0.23	2.29E-103
AT1G61520	photosystem I light harvesting complex gene 3	2957	0.39	8.23E-42
AT2G05100	photosystem II light harvesting complex gene 2.1	1773	0.04	2.11E-109
AT2G05070	photosystem II light harvesting complex gene 2.2	1495	0.05	7.91E-101
AT3G27690	photosystem II light harvesting complex gene 2.3	362	0.02	8.19E-97
AT2G34420	photosystem II light harvesting complex gene B1B2	5162	0.36	2.86E-51
AT1G03130	photosystem I subunit D-2	612	0.36	1.03E-32
AT1G31330	photosystem I subunit F	3256	0.41	1.78E-40
AT3G50820	photosystem II subunit O-2	713	0.41	4.87E-38
AT1G08380	photosystem I subunit O	3446	0.37	2.84E-58
AT5G64040	photosystem I reaction center subunit PSI-N, chloroplast	2222	0.37	2.58E-37
AT4G28750	Photosystem I reaction center subunit IV / PsaE protein	1711	0.49	2.94E-26
AT2G30570	photosystem II reaction center W	2243	0.48	5.79E-26

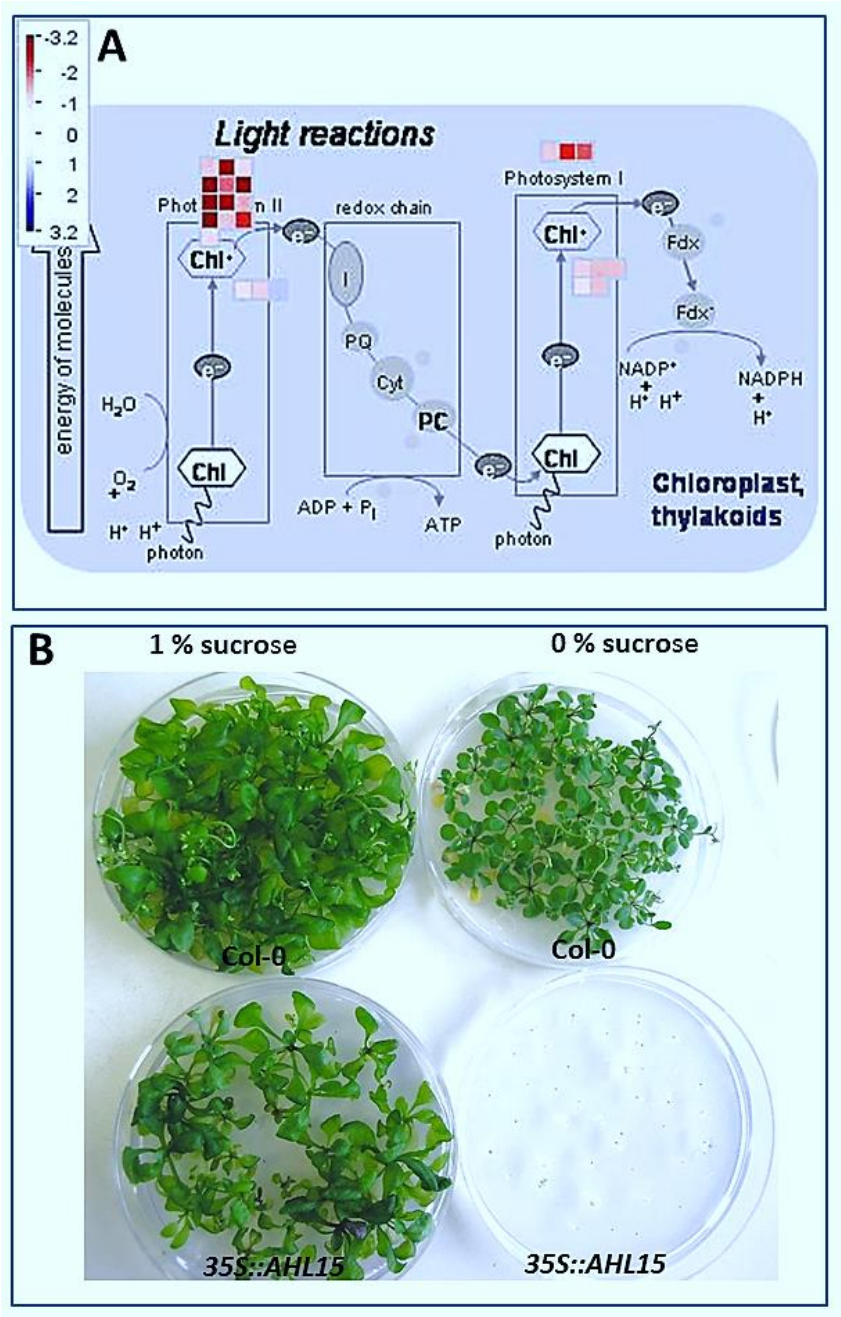

Figure 7 Repression of photosynthesis by AHL15 results in sucrose-dependent seedling growth. (A) A simplified scheme generated by the MAPMAN software (Thimm et al., 2004) showing that the expression of most genes encoding Photosystem I and II components is repressed in *35S::AHL15-GR* seedling shoots following 8 hours of DEX treatment. Blue squares indicate up-regulated genes, red squares indicate down-regulated genes, and gray dots indicate genes for which the expression did not change. (B) Phenotypes of 4 week old wild-type (Col-0, top) and *35S::AHL15* plants (bottom) germinated and grown on medium containing 1% sucrose (left) or no sucrose (right).

Discussion

The *Arabidopsis* AT-hook motif nuclear-localized protein AHL15 delays phase transitions during plant development. In fact, overexpression of this protein can even reverse these phase transitions, resulting in the 2,4-D-independent induction of somatic embryos on cotyledons of immature zygotic embryos or seedlings, or in the appearance of juvenile aerial rosettes from axillary meristems of flowering plants. In addition to these initial results (Chapters 2 and 3 of this thesis), we observed that short transient activation of a constitutively expressed AHL15-GR fusion led to long-term effects on plant developmental timing and ageing. Activation of AHL15-GR by DEX treatment of seedlings resulted in a significant delay of development and flowering for up to a month after treatment, whereas spraying flowering plants with DEX resulted in the development of aerial rosettes from axillary meristems for up to 4 months after treatment. These results suggested that AHL15 establishes a long-term molecular memory, which made us wonder about the mode of action of this plant-specific class of nuclear DNA binding proteins.

Genome-wide analysis of transcriptome changes following transient activation of AHL15-GR showed that AHL15 modulates the expression level of a large number of genes participating in various biological processes. Some genes were induced after 4 hours but showed basal expression levels again after 8 hours, suggesting the direct transient activation of target genes that is typical for normal transcription factors. On the other hand, the large number of genes with a changed expression profile suggested a more global reprogramming of cellular processes. Previous studies have demonstrated that the dynamics of higher-order chromatin organization plays a critical role in both the global regulation of the transcriptome (Ho and Crabtree, 2010; Li and Reinberg, 2011; Pombo and Dillon, 2015) and the establishment of long-term molecular memory (He and Amasino, 2005; Jarillo et al., 2009; Harmston and Lenhard, 2013).

An additional result supporting a regional rather than single gene regulation mode was the observation that neighboring genes are co-activated or co-suppressed by AHL15. Previous analyses of genome-wide gene expression datasets using bioinformatics approaches have shown that neighboring genes in *Arabidopsis* are more co-expressed than random gene pairs (Williams and Bowles, 2004; Zhan et al., 2006; Chen et al., 2010; Wada et al., 2012; Yeaman, 2013; Kundu et al., 2017). Several mechanisms have been proposed to explain this phenomenon, such as gene duplications, shared promoters or common transcription factor binding motifs, but chromatin architecture has always been considered as the major source of co-expression of neighboring genes (Grob et al., 2014; Pombo and Dillon, 2015; Quintero-cadena and Sternberg, 2016). A recent genome-wide data analysis has excluded that co-regulation of neighboring genes in *Arabidopsis* is caused by gene duplications or the presence of common promoter motifs in neighboring genes (Kundu et al., 2017). Instead, co-regulation could be clearly correlated with local rearrangement of chromatin configuration (Kundu et al., 2017). Therefore, we suggest that the co-activation or co-repression of neighboring genes across genome by AHL15 is most likely also caused by extensive modulation of the chromatin configuration.

In animals, the contribution of higher-order chromatin organization to ageing processes has been well documented (Moraes, 2014; Chandra and Kirschner, 2016; Gorbunova and

Seluanov, 2016). In contrast, the role of global organization of chromatin architecture in plant Ageing is not described yet. *Arabidopsis* adult leaves display a visible increase of chromatin compaction compared to juvenile leaves (Exner and Hennig, 2008), but the actual involvement of this chromatin compaction in the juvenile-to-adult transition has not been reported yet. Our results suggest that the global changes in gene expression after 4 hours of DEX-induced AHL15-GR activation coincide with rapid de-condensation of heterochromatin, thereby clearly linking plant ageing or tissue rejuvenation to respectively an increase or a reduction in the heterochromatin. Our results suggest that the extensive reprogramming of the transcriptome and the observed establishment of a long-term molecular memory following AHL15-GR activation might at least in part be caused by an extensive reorganization of the chromatin configuration.

Previously, it has been shown that the juvenile-to-adult vegetative transition is mediated mainly by SPL proteins, which are central components of the ageing pathway in several plant species (Wu and Poethig, 2006; Xie et al., 2006; Saeteurn K, 2007; Wang et al., 2011; Zhang et al., 2011; Fu et al., 2012; Xie et al., 2012). *SPL* genes are well known targets of miR156 (Wu and Poethig, 2006; Xie et al., 2006;; Wu et al., 2009), and a steep decline in miR156 levels over 1-2 weeks of shoot development results in an increase in SPL protein levels (Xu et al., 2016). This pushes plant development to the adult vegetative phase, and from there to the induction of flowering. Our expression- and genetic analyses showed that AHL15 represses the expression of several *SPL* genes, independent of miR156. In both *Arabidopsis* wild-type and *AHL15* overexpression plants this delays both the juvenile to adult and the vegetative to reproductive phase transitions. However, we also found evidence that AHL15 represses *GA20ox2*, a rate limiting enzyme in GA biosynthesis pathway (Huang et al., 1998; Rieu et al., 2008; Andrés et al., 2014). In several plant species GA was shown to promote the vegetative phase transition (Telfer et al., 1997; Park et al., 2017). Moreover, we found that AHL15 represses several genes encoding components of the photosynthesis machinery. Recent studies have shown that the gradual increase in the sugar levels as a result of enhanced photosynthetic efficiency or an increase in leaf numbers promotes the juvenile-to-adult transition in *Arabidopsis*, tobacco, and tomato (Matsoukas et al., 2013; Yang et al., 2013; Yu et al., 2013). In contrast, a mutation in the *Arabidopsis CAO* gene that causes a low photosynthetic efficiency, was found to prolong the juvenile vegetative phase (Espine et al., 1999; Yu et al., 2013). By combining all our findings we propose a model (Fig. 8) whereby AHL15 represses the *Arabidopsis* ageing pathway by inducing changes in higher-order chromatin organization that lead to repression of *SPL* genes, GA biosynthesis, and photosynthesis-mediated sugar production. Unfortunately, how AHL15 alters the chromatin structure remains unclear. Detailed studies on the chromatin configuration by new approaches such as chromosome conformation capture technologies (Dekker et al., 2013), and comparative analysis of the putative binding sites of AHL15 with our transcriptome data are directions of future research that might provide more insight into the mode of action of this plant-specific AT-motif protein.

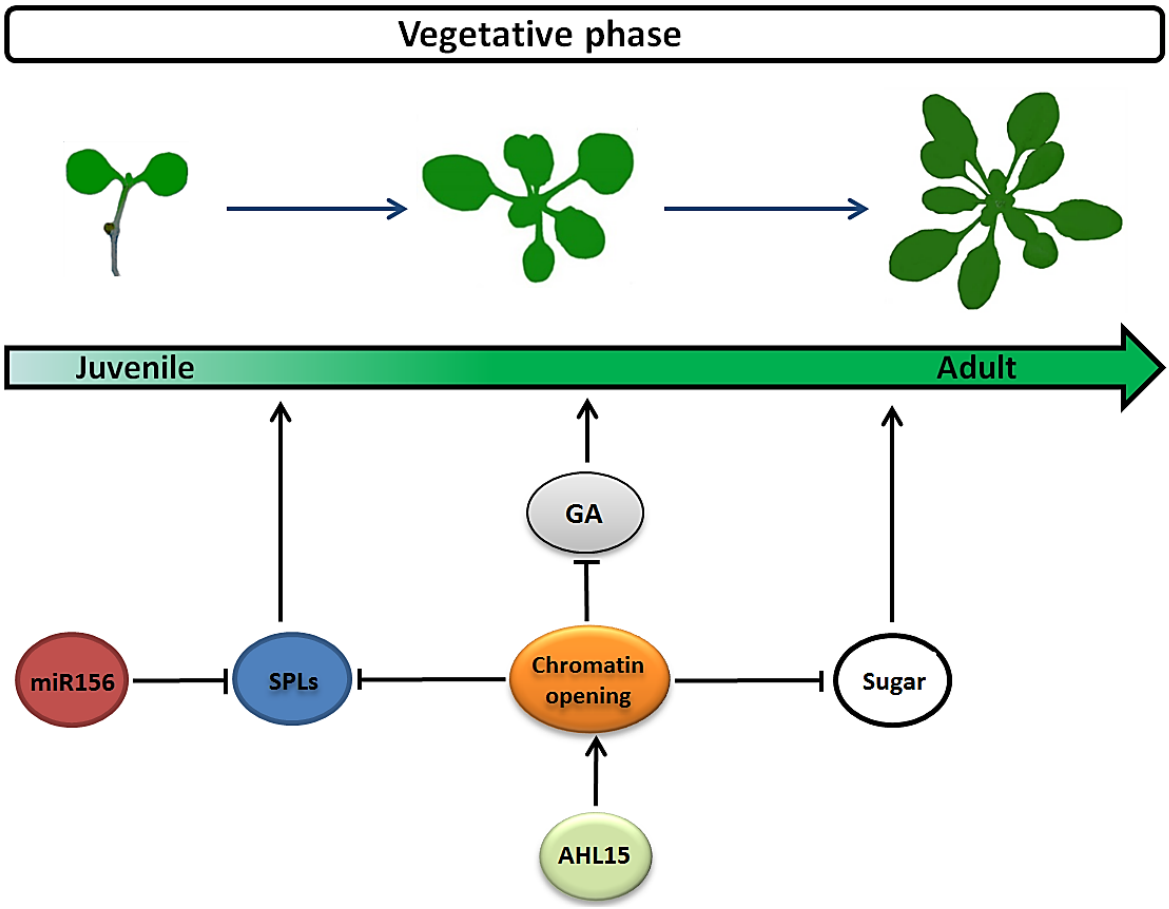

Figure 8 Model for suppression of plant ageing by AHL15. Large-scale chromatin opening by AHL15 leads to repression of key age promoting factors such as the *SPL* genes, gibberellin (GA) biosynthesis, and photosynthesis leading to sugar production. Arrows indicate activation or induction, and blunted lines indicate repression. Note that AHL15-mediated SPL suppression is independent of miR156.

Methods

Plant material and RNA isolation and sequencing

The *Arabidopsis thaliana* (Col-0) plant line harboring the *35S::AHL15-GR* construct is described in Chapter 3. The reporter lines *pSPL3::GUS-SPL3*, *pSPL3::rSPL3-GUS*, *pSPL9::rSPL9-GUS* (Yang et al., 2011) and *H2B::H2B-GFP* (Fang and Spector, 2005) have been described previously. Seeds were surface sterilized (30 sec 70% ethanol, 10 minutes 1% chlorine, followed by washes in sterile water) and germinated after three days incubation at 4°C on MA medium (Masson and Paszkowski, 1992) containing 1% or no sucrose, and 0.7% agar at 21 °C and a 16 hours photoperiod. Following germination, 14 days old seedlings were transferred to soil and grown at 21 °C, 65% relative humidity, and long-day (LD: 16 hours photoperiod) condition.

For the transcriptome analysis (specifically), MA plates with 5 day old seedlings were flooded with water containing 1 ml ethanol per liter (mock), or with water to which dexamethasone (DEX, Sigma-Aldrich) dissolved in 1 ml ethanol was added to a final

concentration of 20 µM. After 4 and 8 hours treatment, the shoot part of seedlings, including the shoot apex and cotyledons, was carefully separated from the hypocotyl and immediately frozen in liquid nitrogen and stored at -80 °C for RNA isolation.
Total RNA was extracted using a Qiagen RNeasy Plant Mini Kit, and the quality of the isolated RNA was validated using a nanodrop spectrophotometer (NanoDrop, ND-1000, Life Science). The isolated RNAs were reverse transcribed and sequenced on an Illumina HiSeq 2000 (100 nucleotides single reads). Three biological replicates were performed.
To test the effect of GA on AHL15-GR activation, 35 day old flowering *35S::AHL15-GR* plants were first sprayed with 20 µM DEX, followed 3 days later by spraying with 15 µM GA4 (Sigma-Aldrich).

Quantification of expression levels and differential expression analysis

The quality control of all sequencing samples was carried out using FASTQC (version 0.10.1: http://www.bioinformatics.babraham.ac.uk/projects/fastqc/. Reference sequences and annotations for the *Arabidopsis* genome (TAIR10) were obtained from www.arabidopsis.org. To obtain expression levels the reads were aligned to the *Arabidopsis* genome sequence using Tophat2 (version 2.0.10) (Kim et al., 2013), using Bowtie2 (version 2.1.0) (Langmead and Salzberg, 2012) as the short read aligner at 'very sensitive' settings. Secondary alignments, i.e. alignments that meet Tophat's criteria but are less likely to be correct than simultaneously reported primary alignments, were removed from the BAM files using SAMtools (version 0.1.18) (Li et al., 2009). Fragment alignment counts per transcript were determined from SAM alignment files using the Python package HTSeq-count (version 0.5.3p9) (Anders et al., 2014) with 'strict' settings to exclude reads aligning ambiguously with respect to annotated gene structures. Counts were summarized at the level of annotated genes, resulting in between 12.992.327 and 29.972.677 aligned fragments per sample. Read counts per annotated gene were normalized across all samples using the DESeq-like robust scaling factor (Anders and Huber, 2010) on reads per kilobase per million mapped reads (RPKM) values. For 13496 genes which had an expression value ≥ 10 in at least two samples, differential expression statistics were calculated using the R package edgeR (version 3.2.4) (Robinson et al., 2010).

Gene ontology term analysis

Gene ontology (GO) term analysis for identification of enriched functional categories was performed using the agriGO single enrichment analysis tool (Du et al., 2010) (http://bioinformatics. cau.edu.cn/easygo/) with TAIR10 GO annotations. The MapMan software (Thimm et al., 2004) (http://mapman.gabipd.org/) was used to visualize pathways containing multiple genes with significant changes in expression.

Quantitative real-time PCR analysis

RNA isolation was performed using a RevertAidTM Kit (Thermo Scientific). For qRT-PCR (qPCR), 1 µg of total RNA was used for cDNA synthesis with the iScript™ cDNA Synthesis

Kit (BioRad). PCR was performed using the SYBR-Green PCR Master mix and amplification was run on a CFX96 thermal cycler (BioRad). The Pfaffl method was used to determine relative expression levels (Pfaffl, 2001). Expression was normalized using the *β-TUBULIN-6* gene. Three biological replicates were performed, with three technical replicates each. The primers used are described in Table 5.

Table 5: Sequences of DNA primers used for qRT-PCR (from 5' to 3')

Name*	Sequence (5' to 3')	Purpose
q AT5G59490-F	TTCGAGAAAGCCTTCGACAT	qRT-PCR AT5G59490
q AT5G59490-R	ATAACTCGGGGAATGCCTCT	
q AT4G22770-F	TGCAGCCACTCCTATTCAAGT	qRT-PCR AT4G22770
q AT4G22770-R	GAAGGAAAAGACGGTGTCCAT	
q AT2G17740-F	GTCTGTGCCTGAGACCATGA	qRT-PCR AT2G17740
q AT2G17740-R	CTTCAGCAACGCATGAATGT	
q AT1G78580-F	GAAACTCAAGACGTCCTTCACCAG	qRT-PCR AT1G78580
q AT1G78580-R	TCTAGCATTGGTGCGAGTACGAC	
qSPL3-F	CTCATGTTCGGATCTCTGGTC	qRT-PCR *SPL3*
qSPL3-R	TTTCCGCCTTCTCTCGTTGTG	
qSPL9-F	AACAATACATGGCGAGCTTCTT	qRT-PCR *SPL9*
qSPL9-R	ATTGCCGTGCCACTACTTATCT	
qSPL15-F	AATCCAGTTAGGGAAACCCATC	qRT-PCR *SPL15*
qSPL15-R	GAGTCGAAACCAGAAGATGGTC	

*, F: forward; R: reverse

Histological staining and microscopy

Histochemical β-glucuronidase (GUS) staining of transgenic lines expressing GUS was performed as described previously (Anandalakshmi et al., 1998). Tissues were stained for 4 hours at 37°C, followed by rehydration by incubation for 10 minutes in a graded ethanol series (75, 50 and 25%). GUS stained tissues were observed and photographed using a LEICA MZ12 microscopy (Switzerland) equipped with a LEICA DC500 camera.

DAPI staining of nuclei was performed as described previously (Zanten et al., 2011). Samples were fixed in ice-cold Carnoys fixative (1:3 acetic acid:ethanol), then treated with enzymatic cell wall degrading solution containing 0.5% cellulose Onozuka R10 (Duchefa)), 0.25% macerozyme R10 (Duchefa), and 0.1% Triton X-100 for 1 h 30 min at room temperature. The samples were mounted with Vectashield (Vector laboratories) supplemented with 2 μg/ml 4′,6-diamidino-2-phenylindole (DAPI) before microscopic observation.

The heterochromatin phenotypes of the DAPI-stained leaf cells were recorded using a confocal laser scanning microscope (ZEISS-003-18533) using a 405 laser, a 350 nm LP excitation filter and a 425-475 nm BP emission filter. The H2B-GFP fusion protein was visualized using the same laser scanning microscope with a 534 laser, a 488 nm LP excitation filter and a 500-525 nm BP emission filters.

References

Anandalakshmi, R., Pruss, G. J., Ge, X., Marathe, R., Mallory, A. C., Smith, T. H., and Vance, V.B. (1998). A viral suppressor of gene silencing in plants. Proc. Natl. Acad. Sci. **95**: 13079-13084.

Anders, S. and Huber, W. (2010). Differential expression analysis for sequence count data. Genome Biol. **11**: R106.

Anders, S., Pyl, P.T., and Huber, W. (2014). HTSeq – A Python framework to work with high-throughput sequencing data. Bioinformatics **31**: 0–5.

Andrés, F. and Coupland, G. (2012). The genetic basis of flowering responses to seasonal cues. Nat. Rev. Genet. **13**: 627–639.

Andrés, F., Porri, A., Torti, S., Mateos, J., Romera-Branchat, M., García-Martínez, J.L., Fornara, F., Gregis, V., Kater, M.M., and Coupland, G. (2014). SHORT VEGETATIVE PHASE reduces gibberellin biosynthesis at the *Arabidopsis* shoot apex to regulate the floral transition. Proc. Natl. Acad. Sci. **111**: E2760-9.

Bratzel, F. and Turck, F. (2015). Molecular memories in the regulation of seasonal flowering: from competence to cessation. Genome Biol. **16**: 192.

Cardon, G., Höhmann, S., Klein, J., Nettesheim, K., Saedler, H., and Huijser, P. (1999). Molecular characterisation of the *Arabidopsis SBP-box* genes. Gene **237**: 91–104.

Catez, F., Yang, H., Tracey, K.J., Reeves, R., Misteli, T., and Bustin, M. (2004). Network of dynamic interactions between histone H1 and high-mobility-group proteins in chromatin. Mol. Cell. Biol.: 4321–4328.

Chandra, T. and Kirschner, K. (2016). Chromosome organisation during ageing and senescence. Curr. Opin. Cell Biol. **40**: 161–167.

Chavali, P.L., Funa, K., and Chavali, S. (2011). Cis-regulation of microRNA expression by scaffold/matrix-attachment regions. Nucleic Acids Res. **39**: 6908–6918.

Chen, W., Meaux, J. De, and Lercher, M.J. (2010). Co-expression of neighbouring genes in *Arabidopsis*: separating chromatin effects from direct interactions. BMC Genomics **11**: 2–8.

Dekker, J., Marti-Renom, M. A., and Mirny, L.A. (2013). Exploring the three-dimensional organization of genomes: interpreting chromatin interaction data. Nat. Rev. Genet. **14**: 390–403.

Du, Z., Zhou, X., Ling, Y., Zhang, Z., and Su, Z. (2010). agriGO: a GO analysis toolkit for the agricultural community. Nucleic Acids Res. **38**: 64–70.

Espineda, C.E., Linford, A.S., Devine, D., and Brusslan, J.A. (1999). The *AtCAO* gene, encoding chlorophyll a oxygenase, is required for chlorophyll b synthesis in *Arabidopsis thaliana*. Proc. Natl. Acad. Sci. **96**: 10507–10511.

Exner, V. and Hennig, L. (2008). Chromatin rearrangements in development. Curr. Opin. Plant Biol.: 64–69.

Fang, Y. and Spector, D.L. (2005). Centromere positioning and dynamics in living *Arabidopsis* plants. Genetics **16**: 5710–5718.

Fu, C., Sunkar, R., Zhou, C., Shen, H., Zhang, J.-Y., Matts, J., Wolf, J., Mann, D.G.J., Stewart, C.N., Tang, Y., and Wang, Z.-Y. (2012). Overexpression of *miR156* in switchgrass (*Panicum virgatum* L.) results in various morphological alterations and leads to improved biomass production. Plant Biotechnol. J. **10**: 443–452.

Fujimoto, S., Matsunaga, S., Yonemura, M., Uchiyama, S., Azuma, T., and Fukui, K. (2004).

Identification of a novel plant MAR DNA binding protein localized on chromosomal surfaces. Plant Mol. Biol. **56**: 225–239.

Fusco, A. and Fedele, M. (2007). Roles of HMGA proteins in cancer. Nat. Rev. Cancer **7**: 899–910.

Girod, P., Nguyen, D., Calabrese, D., Puttini, S., Martinet, D., Regamey, A., Saugy, D., Beckmann, J.S., Bucher, P., and Mermod, N. (2007). Genome-wide prediction of matrix attachment regions that increase gene expression in mammalian cells. Nat. Methods **4**: 747–753.

Gorbunova, V., and Seluanov, A. (2016). DNA double strand break repair , aging and the chromatin connection. In Mutation Research - Fundamental and Molecular Mechanisms of Mutagenesis (Elsevier B.V.), pp. 2–6.

Grob, S., Schmid, M.W., and Grossniklaus, U. (2014). Article Hi-C analysis in *Arabidopsis* identifies the KNOT , a atructure with similarities to the flamenco locus of drosophila. Mol. Cell **55**: 678–693.

Harmston, N. and Lenhard, B. (2013). Chromatin and epigenetic features of long-range gene regulation. Nucleic Acids Res. **41**: 7185–7199.

He, Y. and Amasino, R.M. (2005). Role of chromatin modification in flowering-time control. Trends Plant Sci. **10**: 30–35.

Heng, H.H.Q., Goetze, S., Ye, C.J., Liu, G., Stevens, J.B., Bremer, S.W., Wykes, S.M., Bode, J., and Krawetz, S. (2004). Chromatin loops are selectively anchored using scaffold/matrix-attachment regions. J. Cell Sci. **117**: 999–1008.

Ho, L. and Crabtree, G.R. (2010). Chromatin remodelling during development. Nature **463**: 474–484.

Huang, S., Raman, A.S., Ream, J.E., Fujiwara, H., Cerny, R.E., and Brown, S.M. (1998). Overexpression of *20-Oxidase* confers a gibberellin- overproduction phenotype in *Arabidopsis*. Plant Physiol. **118**: 773–781.

Huijser, P. and Schmid, M. (2011). The control of developmental phase transitions in plants. Development **138**: 4117–4129.

Jarillo, J.A., Piñeiro, M., Cubas, P., and Martínez-zapater, J. (2009). Chromatin remodeling in plant development. Int. J. Dev. Biol. **1596**: 1581–1596.

Kim, D., Pertea, G., Trapnell, C., Pimentel, H., Kelley, R., and Salzberg, S.L. (2013). TopHat2: accurate alignment of transcriptomes in the presence of insertions, deletions and gene fusions. Genome Biol. **14**: R36.

Kishi, Y., Fujii, Y., Hirabayashi, Y., and Gotoh, Y. (2012). HMGA regulates the global chromatin state and neurogenic potential in neocortical precursor cells. Nat. Neurosci. **15**: 1127–1133.

Kundu, S., Pendle, A., Irish, V.F., Shaw, P., Reimeg, J., Emanuelsson, O., Nakayama, N., and Sundstr, J.F. (2017). Genome-wide identification of physically clustered genes suggests chromatin-level co-regulation in male reproductive development in *Arabidopsis thaliana*. Nucleic Acids Res. **45**: 3253–3265.

Langmead, B. and Salzberg, S.L. (2012). Fast gapped-read alignment with Bowtie 2. Nat. Methods **9**: 357–359.

Li, G., and Reinberg, D. (2011). Chromatin higher-order structures and gene regulation. Curr Opin Genet Dev. **21**: 49–64.

Li, H., Handsaker, B., Wysoker, A., Fennell, T., Ruan, J., Homer, N., Marth, G., Abecasis, G., and Durbin, R. (2009). The Sequence alignment/map format and SAMtools. Bioinformatics **25**: 2078–2089.

Lim, P.O., Kim, Y., Breeze, E., Koo, J.C., Woo, H.R., Ryu, J.S., Park, D.H., Beynon, J., Tabrett, A.,

Buchanan-Wollaston, V., and Nam, H.G. (2007). Overexpression of a chromatin architecture-controlling AT-hook protein extends leaf longevity and increases the post-harvest storage life of plants. Plant J. **52**: 1140–1153.

Masson, J., and Paszkowski, J. (1992). The culture response of *Arabidopsis thaliana* protoplasts is determined by the growth conditions of donor plants. Plant J. **2**: 829–833.

Matsoukas, I.G., Massiah, A.J., and Thomas, B. (2013). Starch metabolism and antiflorigenic signals modulate the juvenile-to-adult phase transition in *Arabidopsis*. Plant. Cell Environ. **36**: 1802–1811.

Matsushita, A., Furumoto, T., Ishida, S., and Takahashi, Y. (2007). AGF1, an AT-hook protein, is necessary for the negative feedback of *AtGA3ox1* encoding GA 3-oxidase. Plant Physiol. **143**: 1152–1162.

Moraes, S. (2014). Gerontology & geriatric changes in chromatin structure along aging. Gerontol. Geriatr. Res. **3**: 1000157.

Morisawa, G., Han-Yama, A., Moda, I., Tamai, A., Iwabuchi, M., and Meshi, T. (2000). *AHM1*, a novel type of nuclear matrix-localized, MAR binding protein with a single AT hook and a J domain-homologous region. Plant Cell **12**: 1903–1916.

Mortazavi, A., Williams, B.A., Mccue, K., Schaeffer, L., and Wold, B. (2008). Mapping and quantifying mammalian transcriptomes by RNA-Seq. Nat. Methods **5**: 1–8.

Mutasa-Göttgens, E. and Hedden, P. (2009). Gibberellin as a factor in floral regulatory networks. J. Exp. Bot. **60**: 1979–1989.

Ng, K.-H., Yu, H., and Ito, T. (2009). AGAMOUS controls *GIANT KILLER*, a multifunctional chromatin modifier in reproductive organ patterning and differentiation. PLoS Biol. **7**: e1000251.

Park, J., Oh, D., Dassanayake, M., Nguyen, K.T., Ogas, J., and Choi, G. (2017). Gibberellin signaling requires chromatin remodeler PICKLE to promote vegetative growth and phase transitions. Plant Physiol. **173**: 1463–1474.

Pfaffl, M.W. (2001). A new mathematical model for relative quantification in real-time RT-PCR. Nucleic Acids Res. **29**: e45--e45.

Poethig, R.S. (2013). Vegetative phase change and shoot maturation in plants. Curr. Top. Dev. Biol. **105**: 125–152.

Pombo, A. and Dillon, N. (2015). Three-dimensional genome architecture: players and mechanisms. Nat. Rev. Mol. Cell Biol. **16**: 245–257.

Postnikov, Y. V and Bustin, M. (2016). Functional interplay between histone H1 and HMG proteins in chromatin. Biochim. Biophys. Acta **1859**: 462–467.

Quintero-cadena, P. and Sternberg, P.W. (2016). Enhancer sharing promotes neighborhoods of transcriptional regulation across eukaryotes. G3 **6**: 4167–4174.

Rieu, I., Ruiz-Rivero, O., Fernandez-Garcia, N., Griffiths, J., Powers, S.J., Gong, F., Linhartova, T., Eriksson, S., Nilsson, O., Thomas, S.G., Phillips, A.L., and Hedden, P. (2008). The gibberellin biosynthetic genes *AtGA20ox1* and *AtGA20ox2* act, partially redundantly, to promote growth and development throughout the *Arabidopsis* life cycle. Plant J. **53**: 488–504.

Robinson, M.D., McCarthy, D.J., and Smyth, G.K. (2010). edgeR: a Bioconductor package for differential expression analysis of digital gene expression data. Bioinformatics **26**: 139–140.

Saeteurn, K. H.S., and huck, G.C.A. (2007). The heterochronic maize mutant *Corngrass1* results from overexpression of a tandem microRNA. Nat. Genet. **39**: 544–549.

Telfer, A., Bollman, K.M., and Poethig, R.S. (1997). Phase change and the regulation of trichome

distribution in *Arabidopsis thaliana*. Development **124**: 645–654.

Thimm, O., Bläsing, O., Gibon, Y., Nagel, A., Meyer, S., Krüger, P., Selbig, J., Müller, L. a., Rhee, S.Y., and Stitt, M. (2004). Mapman: a user-driven tool to display genomics data sets onto diagrams of metabolic pathways and other biological processes. Plant J. **37**: 914–939.

Wada, M., Takahashi, H., Nakamura, K., Hirai, M.Y., Ohta, D., and Kanaya, S. (2012). Prediction of operon-like gene clusters in the *Arabidopsis thaliana* genome based on co-expression analysis of neighboring genes. Gene **503**: 56–64.

Wang, J.-W., Park, M.Y., Wang, L.-J., Koo, Y., Chen, X.-Y., Weigel, D., and Poethig, R.S. (2011). miRNA control of vegetative phase change in trees. PLoS Genet. **7**: e1002012.

Williams, E.J.B. and Bowles, D.J. (2004). Coexpression of neighboring Genes in the genome of *Arabidopsis thaliana*. Genome Res. **14**: 1060–1067.

Wilson, R.H.C. and Coverley, D. (2013). Relationship between DNA replication and the nuclear matrix. Genes Cells **18**: 17–31.

Wu, G., Park, M.Y., Conway, S.R., Wang, J.-W., Weigel, D., and Poethig, R.S. (2009). The sequential action of miR156 and miR172 regulates developmental timing in *Arabidopsis*. Cell **138**: 750–759.

Wu, G. and Poethig, R.S. (2006). Temporal regulation of shoot development in *Arabidopsis thaliana* by miR156 and its target *SPL3*. Development **133**: 3539–3547.

Xie, K., Shen, J., Hou, X., Yao, J., Li, X., Xiao, J., and Xiong, L. (2012). Gradual increase of miR156 regulates temporal expression changes of numerous genes during leaf development in rice. Plant Physiol. **158**: 1382–1394.

Xie, K., Wu, C., and Xiong, L. (2006). Genomic organization, differential expression, and interaction of *SQUAMOSA Promoter-Binding-Like* transcription factors and *microRNA156* in rice. Plant Physiol. **142**: 280–293.

Xu, M., Hu, T., Zhao, J., Park, M.-Y., Earley, K.W., Wu, G., Yang, L., and Poethig, R.S. (2016). Developmental functions of miR156-regulated *SQUAMOSA PROMOTER BINDING PROTEIN-LIKE* (*SPL*) genes in *Arabidopsis thaliana*. PLoS Genet. **12**: e1006263.

Xu, Y., Wang, Y., Stroud, H., Gu, X., Sun, B., Gan, E.-S., Ng, K.-H., Jacobsen, S.E., He, Y., and Ito, T. (2013). A matrix protein silences transposons and repeats through interaction with retinoblastoma-associated proteins. Curr. Biol. **23**: 345–350.

Yang, L., Conway, S.R., and Poethig, R.S. (2011). Vegetative phase change is mediated by a leaf-derived signal that represses the transcription of *miR156*. Development **138**: 245–249.

Yang, L., Xu, M., Koo, Y., He, J., and Poethig, R.S. (2013). Sugar promotes vegetative phase change in *Arabidopsis thaliana* by repressing the expression of *MIR156A* and *MIR156C*. Elife **2**: e00260.

Yeaman, S. (2013). Genomic rearrangements and the evolution of clusters of locally adaptive loci. Proc. Natl. Acad. Sci.

Yu, S., Cao, L., Zhou, C.-M., Zhang, T.-Q., Lian, H., Sun, Y., Wu, J., Huang, J., Wang, G., and Wang, J.-W. (2013). Sugar is an endogenous cue for juvenile-to-adult phase transition in plants. Elife **2**: e00269.

Yun, J., Kim, Y.-S., Jung, J.-H., Seo, P.J., and Park, C.-M. (2012). The AT-hook motif-containing protein AHL22 regulates flowering initiation by modifying *FLOWERING LOCUS T* chromatin in *Arabidopsis*. J. Biol. Chem. **287**: 15307–16.

Zanten, M. Van, Koini, M.A., Geyer, R., Liu, Y., Brambilla, V., and Bartels, D. (2011). Seed maturation in *Arabidopsis thaliana* is characterized by nuclear size reduction and increased chromatin condensation. Proc. Natl. Acad. Sci. **108**: 1–6.

Zhan, S., Horrocks, J., and Lukens, L.N. (2006). Islands of co-expressed neighbouring genes in *Arabidopsis thaliana* suggest higher-order chromosome domains. Plant J. **45**: 347–357.

Zhang, X., Zou, Z., Zhang, J., Zhang, Y., Han, Q., Hu, T., Xu, X., Liu, H., Li, H., and Ye, Z. (2011). Over-expression of *sly-miR156a* in tomato results in multiple vegetative and reproductive trait alterations and partial phenocopy of the *sft* mutant. FEBS Lett. **585**: 435–439.

Zhao, J., Favero, D.S., Peng, H., and Neff, M.M. (2013). *Arabidopsis thaliana* AHL family modulates hypocotyl growth redundantly by interacting with each other via the PPC/DUF296 domain. Proc. Natl. Acad. Sci. **110**: 4688–4697.

Summary

Just like other multicellular organisms, plants undergo several distinct developmental phase transitions, starting with embryogenesis, and subsequently progressing from the juvenile vegetative and the adult vegetative to the adult reproductive and finally to the gametophyte phase. Recent genetic and molecular biology studies have shown that the correct timing of plant developmental transitions is regulated by orchestration of gene expression in response to various environmental cues, triggering multiple regulatory pathways. Despite these shared developmental transitions, flowering plants display a wide range of life spans, varying from a few weeks for some annual species up to several thousand years for some perennial species, such as the sequoia trees. Related to their life span, plants have evolved two opposing growth habits. Many species are monocarpic, meaning that their life cycle is completed after flowering and producing offspring, even under optimal growth conditions. By contrast, polycarpic plants flower and reproduce more than once during their life history and are able to survive multiple successful offspring production events. The molecular basis of these two main growth habits in flowering plants is still largely unknown.

Developmental phase transitions have been shown to coincide with large scale remodeling of the chromatin structure. In plants, several candidate chromatin-remodelling proteins have been shown to play an important role in the regulation of plant developmental processes, among which the AT-HOOK MOTIF CONTAINING NUCLEAR LOCALIZED (AHL) proteins. The *Arabidopsis* genome encodes 29 AHL family members, containing either one or two AT-hook motifs and a PPC (Plant and Prokaryote Conserved) domain, that possibly act through remodeling of the chromatin structure. Molecular genetic studies in *Arabidopsis* have revealed that AHL proteins are involved in multiple aspects of pant growth and development, including flowering time, flower development, hypocotyl growth, and vascular tissue differentiation. The main objective of this PhD research was to understand the biological function of the *AHL15* gene and its homologs with a focus on yet unidentified roles in plant embryogenesis and -Ageing.

Chapter 1 reviews the current advances in understanding the molecular mechanisms regulating plant developmental phase transitions and the underlying differences between the mono-and polycarpic growth habit, with a focus on how the interaction between cellular factors and environmental cues mediate the plant developmental transitions and -life histories. In plants, embryogenesis usually takes place when haploid gametes meet to create a diploid zygote. However, somatic cells can be reprogrammed to totipotent embryonic cells that are able to form differentiated embryos in a process called somatic embryogenesis (SE). C**hapter 1** also discusses the involvement of plant hormones and some key transcription factors in the initiation of somatic embryos under *in vitro* conditions.

Chapter 2 focuses on the role of *AHL15* and its close homologs, *AHL19* and *AHL20* in SE and zygotic embryogenesis (ZE). In *Arabidopsis*, SE is usually induced by exogenous application of the synthetic auxin, 2,4-dichlorophenoxyacetic acid (2,4-D). Alternatively, SE can be induced by overexpression of certain transcription factor genes such as *BABY BOOM* (*BBM*). In this chapter, we show than *AHL15* overexpression induces SE on *Arabidopsis* seedlings in the absence of hormonal treatment. By contrast, *ahl15* loss-of-function mutants

show reduced somatic embryo induction in response to 2,4-D treatment or overexpression of the SE-inducing *BABY BOOM* (*BBM*) transcription factor. The *AHL15* gene is bound and transcriptionally-regulated by BBM during SE. During zygotic embryogenesis, *AHL15* is expressed in early embryos, where it is required for proper patterning and for development beyond the heart stage. Morphological and cellular analyses showed that a significant number of plants derived from *35S::AHL15* SEs are polyploid. Chromatin staining with fluorescent reporters suggested that AHL15 induces chromatin decondensation, which might lead to chromosome missegregation and thus to the occurrence of polyploid cells. Using centromere-specific markers, we demonstrated that polyploidisation is caused by endomitotic events, which specifically occur during the initiation of SE. Our findings indicate that *AHL15* is an important driver of plant cell totipotency acquisition, and based on our results, we propose that opening of the chromatin structure is required for the acquisition of embryonic competency in somatic plant cells.

In flowering plants, Ageing is defined by a series of developmental phase transitions that start with vegetative growth, followed by flowering and culminating in seed production. Tissue senescence and plant death follow seed production in monocarpic plants, while polycarpic plants prolong their life span by maintaining a number of vegetative axillary meristems, thereby allowing subsequent cycles of vegetative and reproductive development. **Chapter 3** describes the role of *AHL15* and its close homologs, *AHL19* and *AHL20*, in vegetative phase change and life history strategy. Here we show that the *AHL15* gene is a suppressor of developmental phase transitions. We therefore renamed *AHL15* to *REJUVENATOR* (*RJV*). Loss-of-function of *RJV* in *Arabidopsis* resulted in precocious appearance of adult vegetative traits and early flowering, whereas *RJV* overexpression prolonged the juvenile phase and delayed flowering in *Arabidopsis* and tobacco. We also show that RJV is a suppressor of axillary meristem maturation, with effects on plant shoot architecture and longevity. Expression of a dominant-negative *RJV-GUS* gene fusion accelerated axillary meristem maturation, whereas constitutive expression of *RJV* kept juvenile traits on axillary meristems during flowering and converted monocarpic *Arabidopsis* and tobacco plants into polycarpic plants with enhanced seed and biomass production. Our results show that *RJV* acts downstream of Ageing (*miR156*, *SPL*) and flowering (*SOC1*, *FUL*) genes as a molecular switch between monocarpic and polycarpic life history strategy.

In **Chapters 2 and 3**, we documented that overexpression of the *Arabidopsis* nuclear protein AHL15 leads to reprogramming of somatic cells to embryonic cells and to suppression of plant ageing. In **Chapter 4** we show that transient (4 hours) activation of overexpressed RJV-GR in *Arabidopsis* seedlings has long-term effects on plant development. RNA sequencing analysis detected an extensive reprogramming of the transcriptome 4 hours after RJV-GR activation, with respectively 540 and 1107 genes showing more than 2-fold up- and down-regulation. RJV seemed to act in a transcription level-dependent manner, activating predominantly low expressed genes and repressing mostly highly expressed genes. Rapid decondensation of heterochromatin was observed after RJV activation in leaf primordia and axillary meristems, indicating that the global reprogramming of the transcriptome by transient activation of this AT-Hook domain protein might at least in part be caused by extensive modulation of the chromatin configuration. Co-activated or co-repressed genes were often found to be physically linked in small chromosomal clusters, which is in

line with regulation at the chromatin level. More detailed analysis of down-regulated genes indicated that RJV represses plant ageing by targeting several components of the ageing pathway, including the *SQUAMOSA-PROMOTER BINDING PROTEIN-LIKE* (*SPL*) genes, GA biosynthesis and photosynthesis-dependent sugar production. Our findings provide new insights in understanding plant age regulation, but further investigations are needed to test the relevance of these finding.

Samenvatting

Net andere multi-cellulaire organismen ondergaan planten gedurende hun leven verschillende fasen in hun ontwikkeling, beginnend met embryogenese, gevolgd door de juveniel vegetatieve- en de volwassen vegetatieve fase, en eindigend met de volwassen reproductieve- en uiteindelijk de gametofytfase. Recente genetische en moleculaire biologische studies hebben aangetoond dat de correcte timing van de overgang van de ene naar de andere fase in plantontwikkeling gereguleerd wordt door veranderingen in genexpressie in reactie op diverse omgevingsfactoren, die meerdere signaaltransductieroutes aanzetten. Ondanks dat deze faseovergangen in ontwikkeling bij alle bloeiende planten te vinden zijn, kunnen plantensoorten wat levensduur betreft enorm van elkaar verschillen, variërend van een paar weken voor een aantal eenjarige soorten, tot enkele duizenden jaren voor sommige meerjarige soorten, zoals de sequoia bomen. De grote verschillen in levensduur zijn gekoppeld aan twee tegengestelde groeistrategieën in bloeiende planten. Veel soorten zijn monocarp, zij bloeien eenmalig en eindigen hun levenscyclus met de vorming van nakomeling, zelfs onder optimale groeicondities. Polycarpe planten daarentegen bloeien meerdere keren tijdens hun levensloop, en produceren daardoor meerdere keren nakomelingen. De moleculaire basis van deze twee groeistrategieën in bloeiende planten is nog grotendeels onbekend.

De faseovergangen in de ontwikkeling gaan gepaard met het grootschalig remodelleren van de chromatinestructuur. In planten zijn verschillende kandidaat chromatine-remodellerende eiwitten gevonden die een belangrijke rol spelen bij het reguleren van ontwikkelingsprocessen, waaronder de AT-HOOK MOTIF CONTAINING NUCLEAR LOCALIZED (AHL) eiwitten. Het *Arabidopsis* genoom codeert voor 29 leden van de AHL eiwitfamilie. Deze eiwitten bevatten één of twee geconserveerde AT-Hook motieven en een PPC (Plant and Prokaryote Conserved) domein. Ze zijn zeer waarschijnlijk betrokken bij het remodelleren van de chromatinestructuur. Moleculair genetische studies in *Arabidopsis* hebben aangetoond dat AHL eiwitten betrokken zijn bij meerdere aspecten van plantengroei en -ontwikkeling, waaronder bloeitijd, bloemontwikkeling, hypocotylgroei en differentiatie van vasculaire weefsels. Het hoofddoel van dit promotieonderzoek was om de biologische functie van het *AHL15* gen en zijn homologen te begrijpen, met een focus op de nog niet geïdentificeerde rol in embryogenese en veroudering bij planten.

Hoofdstuk 1 beschrijft de huidige kennis over de moleculaire mechanismen die de faseovergangen in de ontwikkeling van planten reguleren, en de onderliggende verschillen tussen de mono- en polycarpe groeistrategie, met de nadruk op de interactie tussen cellulaire en omgevingsfactoren die de overgangen in de ontwikkeling van planten en hun levensloop bepalen. In planten vindt embryogenese gewoonlijk plaats wanneer haploïde gameten versmelten om een diploïde zygote te vormen. Somatische plantencellen kunnen echter opnieuw geprogrammeerd worden tot totipotente embryonale stamcellen, die gedifferentieerde embryo's kunnen vormen via een proces dat somatische embryogenese (SE) wordt genoemd. **Hoofdstuk 1** bespreekt ook de betrokkenheid van plantenhormonen en een aantal belangrijke transcriptiefactoren bij de initiatie van SE onder *in vitro* omstandigheden.

Hoofdstuk 2 richt zich op de rol van *AHL15* en de homologen *AHL19* en *AHL20* in SE en zygotische embryogenese (ZE). In *Arabidopsis* kan SE worden geïnduceerd door het extern

toedienen van het synthetische auxine-analoog 2,4-dichloorfenoxyazijnzuur (2,4-D), of door overexpressie van bepaalde transcriptiefactorgenen, zoals *BABY BOOM* (*BBM*). In dit hoofdstuk laten we zien dat ook overexpressie van *AHL15* SE op *Arabidopsis* zaailingen kan induceren in afwezigheid van 2,4-D. Daarentegen vertonen *ahl15*-verlies-van-functie-mutanten verminderde SE-inductie in reactie op 2,4-D-behandeling of bij overexpressie van de SE-inducerende BABY BOOM (BBM) transcriptiefactor. Ook laten we zien dat het *AHL15* gen wordt gebonden door en dat de transcriptie wordt op gereguleerd door BBM tijdens SE. Tijdens ZE komt *AHL15* tot expressie in het vroeg globulaire embryo, waar het nodig is voor een goede patroonvorming en de ontwikkeling naar het hartstadium. Morfologische en cellulaire analyses tonen aan dat een significant aantal planten afkomstig van *35S :: AHL15* SEs polyploïde zijn. Chromatinekleuring met fluorescerende reporters suggereert dat *AHL15* overexpressie chromatine-decondensatie induceert, wat vervolgens kan leiden tot chromosoommissegregatie en dus tot het ontstaan van polyploïde cellen. Centromeer-specifieke markers laten zien dat polyploïdisatie zeer waarschijnlijk veroorzaakt wordt door endomitotische gebeurtenissen die zich specifiek voordoen tijdens de initiatie van SE. Onze bevindingen wijzen erop dat AHL15 een belangrijke regulator is van de totipotentie van plantencellen, en op basis van onze resultaten stellen we voor dat het openen van de chromatinstructuur nodig is voor het verkrijgen van embryonale competentie in somatische plantencellen.

In bloeiende planten wordt veroudering bepaald door een reeks overgangen in ontwikkelingsfasen, beginnend met vegetatieve groei, gevolgd door bloei en eindigend in zaadproductie. In monocarpe planten wordt zaadproductie gevolgd door het afsterven van weefsels, uiteindelijk leidend tot de dood van de plant. Daarentegen zijn polycarpe planten in staat hun levensduur te verlengen door een aantal vegetatieve axillaire meristemen te handhaven, die een volgende cyclus van vegetatieve- en reproductieve ontwikkeling mogelijk maken. **Hoofdstuk 3** beschrijft de rol van *AHL15* en zijn directe homologen, *AHL19* en *AHL20*, in de vegetatieve fase verandering en levensloopstrategie van planten. We laten zien dat het *AHL15* gen de overgangen van de ene naar de andere ontwikkelingsfase onderdrukt, en dat overexpressie van het gen deze overgangen zelfs kan omkeren. Op basis hiervan is het *AHL15* gen omgedoopt tot *REJUVENATOR* (*RJV*). Verlies van functie van *RJV* resulteert in *Arabidopsis* in het vroeg verschijnen van volwassen vegetatieve eigenschappen en vroege bloei, terwijl *RJV* overexpressie de juveniele fase verlengt en de bloei vertraagt in *Arabidopsis* en tabak. We tonen ook aan dat *RJV* de veroudering van axillaire meristemen onderdrukt, wat gevolgen heeft voor de architectuur en levensduur van planten. Expressie van een dominant-negatieve *RJV-GUS* genfusie zorgt voor versnelde rijping van axillaire meristemen, terwijl constitutieve overexpressie van *RJV* leidt tot het behoud van de juveniele eigenschappen van axillair meristemen tijdens bloei, en ook de monocarpe planten *Arabidopsis*- en tabak kan veranderen in polycarpe planten met verhoogde zaad- en biomassa productie. Onze resultaten laten zien dat *RJV* als een centrale moleculaire schakelaar tussen de monocarpe en polycarpe levensloopstrategie werkt, gecontroleerd door verouderings- (*miR156*, *SPL*) en bloei- (*SOC1*, *FUL*) genen.

In de **hoofdstukken 2 en 3** hebben we beschreven dat overexpressie van het *Arabidopsis* kerneiwit AHL15 leidt tot herprogrammering van somatische cellen naar embryonale cellen, en dat het de veroudering in planten onderdrukt. In **hoofdstuk 4** laten we zien dat korte (4

uur) activatie van een tot overexpressie gebracht RJV-GR fusie-eiwit in *Arabidopsis*-zaailingen lange termijn effecten heeft op de ontwikkeling van planten. Met behulp van RNA sequencing analyse kan al 4 uur na RJV-GR activering een uitgebreide herprogrammering van het transcriptoom worden aangetoond, waarbij respectievelijk 540 en 1107 genen meer dan tweemaal verhoogd en verlaagd tot expressie komen. RJV lijkt op een transcriptie-afhankelijke manier te werken, waarbij overwegend laag tot expressie komende genen geactiveerd, en hoog tot expressie komende genen onderdrukt worden. Na RJV-GR activering wordt snelle decondensatie van heterochromatine waargenomen in bladprimordia en axillaire meristemen, wat aangeeft dat de globale herprogrammering van het transcriptoom door tijdelijke activatie van dit AT-Hook eiwit ten minste gedeeltelijk wordt veroorzaakt door uitgebreide modulatie van de chromatine structuur. Genen die gezamenlijk geactiveerd of onderdrukt worden, blijken vaak fysiek gekoppeld in kleine chromosomale clusters te liggen, wat overeenkomt met de regulering op chromatineniveau. Meer gedetailleerde analyse van de onderdrukte genen toont aan dat RJV verschillende verouderingsprocessen onderdrukt, waaronder de *SQUAMOSA-PROMOTER BINDING PROTEIN-LIKE* (*SPL*) en gibberelline biosynthese genen, en de fotosynthese-afhankelijke productie van suikers. Onze bevindingen bieden nieuwe inzichten in het begrijpen van de regulering van veroudering in planten, maar verder onderzoek is nodig om de relevantie van deze bevinding te testen.

Curriculum vitae

Omid Karami was born on September 23, 1977, in Divandareh (Iran). After graduating from the Andishe high school at Saghez (Iran) in 1997, he studied agricultural engineering and plant breeding at the Faculty of Agriculture, of the University of Tehran (Tehran, Iran), where he obtained his BSc degree in 2001. He continued his studies at Faculty of Agriculture of Bu-Ali Sina University (Hamedan, Iran), where he received his MSc degree in plant biotechnology in 2004. For his master project, he studied somatic embryogenesis in carnation (*Dianthus caryophyllus*). From 2004 on, he became a full time faculty member of the teaching and research staff at the Plant Biotechnology Department at Bu-Ali Sina University (Hamedan, Iran) for 5 years. In this position, he taught subjects such as plant micropropagation, and plant growth regulation. Besides teaching, he studied *in vitro* regeneration of carnation, oleaster (*Elaeagnus angustifolia*) and strawberry (*Fragaria ananassa*). In 2010, he was awarded a PhD scholarship by the Iranian Ministry of Science, Research, and Technology, and in the same year he started his PhD research under the supervision of Prof. Dr. Remko Offringa (Plant Developmental Genetics) at the Institute of Biology Leiden (IBL) of Leiden University (The Netherlands). For his PhD research, he focused on the functional analysis of *AT-HOOK MOTIF CONTAINING NUCLEAR LOCALIZED* genes, as is described in this thesis. From 2015 until now he worked as researcher on Generade- and IBL-funded projects concerning tulip bulb regeneration and auxin-induced somatic embryogenesis in *Arabidopsis thaliana*. In September 2017, he will start as a post-doc in the group of Prof. Dr. Remko Offringa on the NWO-funded Building Blocks of Life project "The Interplay Between Stress and Auxin during in vitro Embryogenesis".